Signaling oligogalacturonides and transduction signal in cell adhesion

Cyril Grandjean

UNIVERSITÉ de Picardie Jules Verne

Thèse de Doctorat

Mention – Biologie
Spécialité – Biologie cellulaire

présentée à ***l'Ecole Doctorale en Sciences Technologie et Santé (ED 585)***

de l'Université de Picardie Jules Verne

par

Cyril Grandjean

pour obtenir le grade de Docteur de l'Université de Picardie Jules Verne

Signaling Oligogalacturonides and transduction signal in cell adhesion

Oligogalacturonides signalisant et transduction du signal dans l'adhésion cellulaire

Soutenue le 18 mars 2022, après avis des rapporteurs, devant le jury d'examen :

M. J.- C Mollet, Professor, Université de Rouen	**Rapporteur**
M. F. Monéger, Directeur de Recherche CNRS, INRAE, Lyon	**Rapportrice**
M. F. Mesnard, Professeur, Université Picardie Jules Verne, Amiens	**Président**
M^{me}. C. Hervé, Chargé de Recherches CNRS, Roscoff	**Examinatrice**
M. S. Verger, Assistant Professor, Umeå Plant Science Centre	**Examinateur**
M^{me}. S. Bouton, Maître de Conférences, UPJV, Amiens	**Co-Directrice de thèse**
M. G. Mouille, Directeur de Recherches, INRAE, Versailles	**Directeur de thèse**

INRAE ijpb Région Hauts-de-France


UNIVERSITÉ
de Picardie
Jules Verne


INRAE


ijpb


Région
Hauts-de-France

Acknowledgments/Remerciements

Premièrement je tiens à remercier tous les membres du jury, M. Jean-Claude Mollet, Mme Françoise Monéger, M. Francois Mesnard, Mme Cécile Hervé et M. Stéphane Verger d'avoir accepté de juger mon travail de thèse.

Je remercie bien évidemment mon directeur de thèse Grégory Mouille, mon MENTOR. Merci de m'avoir fait confiance pour cette thèse, de m'avoir parfaitement intégré dans l'équipe, de m'avoir laissé tenter tout ce que je souhaitais en autonomie, ce qui m'a permis de grandir en tant que scientifique. Merci pour toute ces discussions scientifiques/ou non qui n'ont fait que galvaniser mon envie de persévérer dans le sujet. Merci de m'avoir toujours soutenu à ta façon « tu es nul, c'est cool et peut être un jour un, c'est bien … » (Que j'apprécie au passage), qui m'ont permis de me surpasser et de te surprendre par moment. Merci de m'avoir transmis tant de connaissances et j'espère un jour en avoir autant que toi (le chemin et encore long). Merci d'avoir fait en sorte que notre cohésion directeur/doctorant se soit si bien passé. Bien que certaines personnes pensent que nous avons un lien de parenté, ce n'est pas le cas mais en tout cas ce fut un honneur de bosser à tes cotés. En espérant qu'on ait l'occasion que cela se reproduise sous forme d'une collaboration !! En tout cas merci pour tout.

Je remercie bien chaleureusement ma co-directrice de thèse Sophie Bouton. Cela fait presque 5 ans que l'on travaille ensemble, depuis le master. C'est en grande partie grâce à toi que j'ai réussi à décrocher cette thèse et rien que pour ça je t'en serais toujours reconnaissant. Merci de m'avoir fait grandir en tant que scientifique. Merci pour toute ta bienveillance, tes nombreux conseils, et la rigueur que tu m'as transmise. Mais surtout merci d'avoir toujours été là pour moi, de m'avoir soutenu dans les moments les plus difficiles (tu sais de quoi je parle). Merci d'avoir toujours cru en moi, pour la confiance que tu m'as accordée, et la patience que tu as eu à mon égard et je suis si fière d'avoir eu l'opportunité de travailler avec toi. Alors pour tout ça un grand merci !

Je remercie Jérôme Pelloux (BIOPI) de m'avoir permis d'intégrer son laboratoire pour mon stage de master et de m'avoir encore accordé sa confiance pour ma thèse. Merci de m'avoir parfaitement intégré à ton équipe, pour toutes tes discussions, ta sympathie et ta franchise.

Un grand merci à Monsieur Salem (IJPB), car sans toi mon khouya, rien n'aurait été possible. Toutes les manips que l'on a réalisées ensemble, toute ces découvertes, ces moments de joie. Ce fut plus qu'un honneur de bosser avec toi. Merci pour la connaissance que tu m'as transmise,

pour toute ces discussion FOOT toutes plus intéressantes les unes que les autres. C'était un « On refait le match chaque lundi ». Merci d'avoir rendu ma thèse aussi agréable qu'elle a pu l'être et pour les valeurs que tu m'as transmises. Chaque journée jamais l'un sans l'autre, tout ça va beaucoup me manquer mais j'en garderai un très bon souvenir.

Un grand Merci à Aline Voxeur (IJPB), (THE QUEEN of OGs) de m'avoir transmis un maximum de ta connaissance sur les OGs et sur la masse, merci de m'avoir consacré tout ce temps. Merci, de m'avoir transmis cette passion pour l'identification des molécules ou la découverte d'un nouveau pic et le fait de considérer cela comme un jeu. Merci pour toutes ces discussions scientifiques, toutes plus enrichissantes les unes que les autres. Merci pour toutes les idées que tu m'as données et ton aide pour les manips réalisées ensemble. Je suis si fier de ce qu'on a accompli, rien n'aurait été possible sans toi.

Je tiens à remercier particulièrement Stéphanie Boutet (IJPB), pour toute ta bienveillance, tes précieux conseils et la connaissance que tu m'as transmise, ta patience à mon égard et nos longues discussions scientifiques ou non. Merci d'avoir toujours été là pour moi et de m'avoir toujours soutenu dans les moments difficiles. Ce fut un réel plaisir d'interagir avec toi.

Un grand merci à Julien Sechet, pour ton aide indispensable au début de ma thèse, pour avoir pris le temps de répondre à mes 1000000 questions. Pour toutes ces soirées FOOT partagées, mais aussi pour m'avoir fait comprendre qu'il faut toujours être zen dans n'importe quelle situation, « NO stress ». Enfin merci pour ton soutien indispensable, et comme dirait Joan merci Mon ami.

Merci également aux membres de la plateforme OV-CHIMIE (IJPB), Gilles Clément, Sylvie Citerne, Frédérique Tellier, François Perreau. Merci de m'avoir transmis tant de connaissances dans vos différents domaines d'expertise, votre rigueur scientifique, mais aussi pour toutes les manips ou tests que l'on a réalisés, et pour vos anecdotes scientifiques, ou non. Merci pour votre accueil et votre bienveillance, tous ces fous rires et on retiendra notamment le AVEC OU SANS MOUSSE. Ce fut un réel plaisir de partager chaque journée en votre compagnie.

Un grand merci à Rawen Ben Malek, pour tous les moments partagés, ces fous rires, depuis ton arrivée au labo. Pour tout le soutien qu'on s'est accordé entre doctorants et les réflexions scientifiques accompagnées de quelques bières à n'en plus finir. Nos hypothèses aussi

complexes les unes que les autres mais qui aboutissent finalement. Je suis très heureux de te compter parmi mes amis, en te souhaitant GOOD LUCK pour la suite.

Je tiens à remercier particulièrement Thibaut Geneste. Merci de m'avoir toujours soutenu, conseillé, surtout en BM, depuis le début de la thèse. Merci de m'avoir fait les traductions anglais/français lorsque je ne comprenais rien quand on était en collocation ! Toute ces anecdotes, fous rires, les parties de jeux de cartes mémorables, les discussions, j'en garde forcément un bon souvenir. Bonne chance à toi aussi pour la suite et peut être qu'on aura l'occasion de collaborer un jour.

Je remercie particulièrement Adrien Lemaire et Josip Safran, pour votre aide et tout le temps que vous avez consacré pour me transmettre toutes les caractéristiques de la technique de production de protéine en système hétérologue. Ce fut un réel plaisir d'interagir avec vous !

Un grand merci à tous les Membres de BIOPI avec qui j'ai pu interagir : Fabien, Valérie, Olivier, Karine, Catherine, Camille, Wafae, Pauline, Solène, pour votre accueil, pour toute votre bienveillance, vos conseils, votre joie de vivre, pour les discussions que j'ai pu avoir avec vous, ce fut un réel plaisir.

Un grand merci à tous les Membres de l'IJPB, CR, IR, IE, techniciens, doctorants, post doctorants que j'ai pu côtoyer, pour leurs conseils, leur aide et les échanges aussi enrichissant les uns que les autres.

Merci également aux membres de la plateforme du CRRBM (Amiens) : Stéphanie Guénin, Laurent Gutierrez, Hervé Demailly, avec qui j'ai eu le plaisir d'interagir et ou de travailler. Merci pour votre expertise et vos précieux conseils.

Merci également à Mme Marie Dufresne et M. François Mesnard qui ont participé à mes comités de thèse. Merci pour vos conseils, vos idées, qui m'ont servi pour accomplir ma thèse.

Enfin un grand merci à mes amis, ma famille, ma sœur et mes parents pour leur soutien inconditionnel et d'avoir fait office de cobaye pour mes différentes présentations.

RESUME EN FRANÇAIS

INTRODUCTION

La matrice extracellulaire (MEC) est constituée de différents polymères. Cette MEC fournit un support mécanique et une barrière biophysique à la plante. Cette barrière joue un rôle majeur dans l'interaction cellule/cellule et plante/environnement. La MEC est constituée de compartiments enchevêtrés : cuticule, lamelle moyenne et paroi cellulaire. Ces compartiments sont constitués de différents polymères lipidiques et glycaniques, de protéines structurelles et de protéines fonctionnelles. La structure des polymères et la nature des protéines qui composent la MEC diffèrent en fonction du niveau ou de l'emplacement de la couche dans la matrice et du stade de développement des cellules. La MEC peut également réagir à divers stimuli, tels que les agents pathogènes ou l'environnement.

La paroi cellulaire est constituée de différents polysaccharides tels que des microfibrilles de cellulose qui sont imbriquées dans une matrice d'hémicelluloses, de pectines et de protéines. Cette paroi à la particularité d'apporter souplesse et maintien structurel de base, tout en assurant la protection de la cellule. En outre, les polymères de cette paroi peuvent être réticulés par des liaisons non covalentes et covalentes contribuant à l'insolubilité et à la résistance de la paroi cellulaire plus globalement aux propriétés physicochimiques de cette paroi. Les réticulations qui relient entre eux les polymères sont par exemple des liaisons covalentes ou hydrogènes.

Au sein de la paroi, les pectines sont les composants majoritaires. Les pectines sont constituées de 4 domaines distincts : les homogalacturonanes (HG) (65 %), les HGs substitués tels que les rhamnogalacturonanes II (RG-II) (10 %), les xylogalacturonanes (XGA) (5 à 7 %) dont le squelette est ramifié par des unités de sucre simples ou de courtes chaînes et enfin les rhamnogalacturonanes I (RG-I) (20 à 35 %). Ces derniers représentent le seul domaine pectique ayant un squelette hétéropolymérique constitué alternativement de résidus de L-rhamnose et d'acide D-Galacturonique, substitués par diverses chaînes latérales de sucres neutres. Ainsi, en raison de leur diversité, les pectines sont composées de 17 monosaccharides différents et nécessitent au moins 67 transférases différentes chez *Arabidopsis thaliana*, notamment des glycosyl-, méthyl- et acétyltransférases. Par ailleurs, au cours de la croissance et du développement des plantes, la paroi cellulaire est soumise à divers événements de remodelage. Ces événements affectent notamment la structure des homogalacturonanes, le principal composant des pectines. Ce remodelage est réalisé par l'action d'enzymes spécifiques, les pectines méthylesterases et leurs inhibiteurs (PME/PMEI), qui contrôlent le degré de méthyl

estérification et les pectines acétylestérases (PAE), qui affectent le degré d'acétylation. Enfin, les polygalacturonases et pectates lyases (PG, PLL) impactent le degré de polymérisation en générant des oligogalacturonnanes (OGs). La particularité des OG réside, notamment, dans le fait qu'ils peuvent déclencher différentes voies de signalisation, une fois associés à des récepteurs de la paroi cellulaire (e.g. WAKs), eux-mêmes associés à des kinases qui médient différentes réponses.

L'adhésion cellulaire est un phénomène essentiel au développement et dans la réponse à certains stress. Depuis le début du siècle, de nombreuses études ont mis en évidence l'implication de gènes, directement ou indirectement, dans l'adhésion cellulaire. Ces études nous procurent des indices sur la façon dont l'adhésion cellulaire peut être régulée au cours du développement. Cependant, le mécanisme par lequel la plante contrôle et maintient l'adhésion cellulaire en réponse aux modifications de la paroi cellulaire n'est pas encore entièrement compris. Le mutant d'Arabidopsis *quasimodo2* est affecté dans un gène codant une pectine méthyltransferase, il présente des défauts d'adhésion cellulaire ainsi qu'une quantité réduite d'homogalacturonanes. L'analyse d'un de ses suppresseurs *esmeralda1*, affecté dans un gène codant une O-fucosyltransferase putative, suggère que le défaut d'adhésion cellulaire de *qua2* peut être contourné par la modification d'une voie de signalisation, sans restaurer la quantité des HG. Certains éléments nous indiquent qu'*esmeralda* aurait un impact dans la médiation du signal pectique sans modifier la quantité d'HGs. En effet *esmeralda* semble restaurer l'expression du gène *FAD-LINKED OXIDOREDUCTASE* (*FADLox*), un gène connu pour répondre aux pectines et dont l'expression est augmentée chez *quasimodo*. Sur la base de ces connaissances, il a été proposé que la mutation *quasimodo* puisse conduire à la libération d'un signal, tel que des oligogalacturonides, qui sont connus pour avoir une affinité avec les récepteurs pariétaux WAK, et médiais la séparation cellulaire une fois perçus. Les récepteurs pariétaux des OGs de type WAK présentent des sites potentiels d'O-fucosylation. Par analogie avec les facteurs Notch chez les animaux, l'absence d'O-fucosylation dans le mutant *esmeralda* pourrait conduire à l'inhibition de l'interaction du récepteur avec les OGs empêchant ainsi l'induction de la signalisation et conduisant à la séparation cellulaire. Ainsi, la compréhension des modifications pariétales et des signaux médiés par *esmeralda* chez *quasimodo* semble utile pour identifier les différentes cibles de cette voie impliquée dans l'adhésion cellulaire des plantes.

La stratégie de cette thèse se décline en 2 parties. Le premier objectif est d'identifier les modifications et signaux pectiques médiés par ESMERALDA permettant le contrôle de

l'adhésion cellulaire pendant le développement de la plante. Par ailleurs nous chercherons à déterminer les acteurs pariétaux intermédiaires responsables de ces modifications. Le second objectif de notre étude est d'identifier des OGs et tester leur impact sur le contrôle de l'adhésion cellulaire. Les acteurs responsables de ce contrôle ont fait l'objet d'une étude plus approfondi.

CHAPITRE 1 : MODIFICATIONS PARIÉTALES ET IDENTIFICATIONS DE NOUVEAUX ACTEURS CONDUISANT À LA RESTAURATION DE L'ADHÉSION PAR LA MUTATION *ESMERALDA*.

Ce travail a été réalisé sur la plante modèle *Arabidopsis thaliana* et plus particulièrement sur l'hypocotyle étiolé des différents mutants *esmd1, qua2 et esmd1/qua2.* Nous avons choisi de caractériser différentes composantes de la matrice extra cellulaire et ainsi mettre en évidence les différences entre *esmeralda* chez *quasimodo*.

Nous avons tout d'abord choisi d'analyser les OGs endogènes par LC/MS après une extraction à l'éthanol 70°C. Parmi les différents OG identifiés, nous n'avons observé une différence de quantité, mais pas d'identité, entre les génotypes. Il semble que chaque OG est présent en plus faible quantité dans *qua2* par rapport au sauvage. Certains OGs sont en quantité significativement réduite chez *qua2* par rapport à Col0 mais restaurée par la mutation *esmd1*. Cette restauration concerne notamment deux OG methylés, le $GalA_4Me$ et le $GalA_4Me_2$ et le trimère non substitué. La question qui se pose donc maintenant est de savoir si cette diminution de la quantité d'OGs endogènes dans *qua2* est liée à la diminution de la quantité de pectine et/ou à un profil de substitution (Methylesterification, Acetylation, et Hydratation) modifié.

Pour analyser la structure fine des pectines nous avons utilisé une endo-PG commerciale d'*Aspergillus acculeatus* appliquée sur une paroi cellulaire sèche d'hypocotyles cultivés à l'obscurité pendant 4 jours. Les fragments libérés ont été analysés par LC-MS. Chez l'ensemble des génotypes étudiés, nous avons identifié 96 Fragment de HGs dont un monomère et 4 xylogalacturonanes, allant d'un DP1 à DP14, avec différentes « signatures » de méthylation, d'acétylation, d'oxydation et déshydratation. Ainsi nous avons pu révéler que la digestibilité des pectines de *quasimodo* était affectée et que la mutation *esmeralda* restaurait cette digestibilité. Ainsi dans le double mutant *esmd1/qua2*, on constate une restauration du « pattern » des pectines : méthylation, méthylation/acétylation, acétylation et hydratation.

Pour mieux comprendre comment ces modifications des pectines sont mises en œuvre par la plante, nous avons réalisé une analyse par RTqPCR de tous les gènes *PAE, PME* et *PMEI*.

L'analyse transcriptionelle réalisée sur les différents génotypes a permis de mettre en évidence 6 dérégulations de gènes, codant des enzymes de modification des pectines, induites par les différentes mutations. Ainsi nous avons mis en évidence une surexpression des gènes *PME 41* et *PME53* dans *qua2*. L'augmentation de l'expression de ces *PME* peut expliquer la forte diminution des OG méthylés dans *qua2*. A l'inverse, la diminution de l'expression de *PAE7* et *PAE12* dans *qua2*, peut expliquer l'augmentation des motifs acétylés méthylés et acétylés. Par ailleurs nous avons pu observer que l'expression des gènes *PMEI4* et *PME35* sont réprimés dans le double mutant et *esmeralda* par rapport à *qua2*. Ces sous-expressions peuvent participer à la restauration du pattern méthylé médiée par la mutation *esmeralda*.

L'analyse des monosaccharides de la paroi a mis en évidence une diminution significative d'acide galacturonique chez *qua2* par rapport à Col0 et *esmd1*. De plus la quantité d'arabinose est augmentée alors que celle de xylose est diminuée chez *qua2* par rapport au sauvage. Ces variations sont restaurées par la mutation *esmeralda*. Ces résultats mettent en évidence un défaut en pectines et xyloglucanes chez *qua2*, semblant être modulé par la mutation *esmeralda*. Pour mieux appréhender la nature des XGs chez *qua2*, une empreinte enzymatique des xyloglucanes a été réalisée et nous a permis de mettre en évidence que 2 fragments de XGs sont diminués chez *qua2* et sont restaurées par *esmeralda*, les XXG et les XXXG. Nous savons que les xyloglucanes jouent un rôle important dans l'entrelacement des microfibrilles de cellulose et dans la régulation de l'extension de la paroi cellulaire. Cependant nos résultats préliminaires nécessitent d'être approfondis afin de pouvoir conclure sur leur implication dans ce modèle d'adhésion cellulaire.

Enfin, il a été démontré récemment que *quasimodo* possède une cuticule plus perméable alors qu'elle ne présente pas de modification de structure. Ainsi, nous avons voulu savoir si la mutation *esmeralda* provoquait des changements au niveau de la cuticule. Pour ce faire nous avons réalisé une coloration au bleu de toluidine. On constate que la coloration bleue est intense chez *qua2* et absente chez Col0. Par ailleurs, nous avons observé que la mutation *esmeralda* chez le mutant *qua2* modifie la coloration de cette cuticule en rose. On peut supposer que ce changement de coloration de la cuticule est lié à la restauration du phénotype d'adhésion cellulaire chez le double mutant.

En conclusion nos resultats suggèrent que la restauration du phénotype d'adhésion cellulaire par la mutation *esmeralda* chez *quasimodo* implique des changements au niveau de la paroi : modifications i) de digestibilité et du pattern des HGs, ii) de la quantité de monosaccharides, iii) de la cuticule. Par ailleurs de nouveaux acteurs intermédiaires sous le contrôle *d'Esmeralda*

ont été identifiés tels que des gènes de remodelage des pectines. Enfin les modifications de pattern pectique et transcriptionelle médiés par la mutation *esmeralda* conduirait à la génération d'une quantité d'OGs endogènes éllicitrice pouvant correspondre à un signal contribuant au maintien et au contrôle de l'adhésion.

CHAPITRE 2 : L'ACIDE GALUCTURONIQUE INDUIT LA RESTAURATION DE L'ADHÉSION CELLULAIRE VIA LA RÉTICULATION DES EXTENSINES

En raison de leur potentiel éliciteur, les OGs sont les candidats les plus prometteurs comme molécule signal dans la voie de transduction médiée par ESMERALDA. Lors de notre analyse d'OGs libres endogènes, nous avons identifié deux monomères dont la quantité est significativement plus faible chez *quasimodo* par rapport au contrôle, le GalU et le GalUox. C'est particulièrement vrai pour l'acide Galacturonique dont la quantité est diminuée de 83 %. Par ailleurs, nous avons pu mettre en évidence une inversion de la balance GalU/GalUox chez *quasimodo* par rapport au sauvage. Cela se traduit par une quantité de GalUox plus élevée que de GalU chez ce mutant. Ainsi pour rétablir la balance GalU/GalUox nous avons appliqué du GalU sur des plantules *qua2*. Grace à des observations empiriques telle que la coloration au rouge de ruthénium et des données quantitatives comme la tortuosité et la longueur des hypocotyles nous avons pu observer une restauration à la fois du phénotype d'adhésion et de la croissance de l'hypocotyle grâce à l'apport de GalU.

Afin de déterminer si cette restauration est liée à un effet métabolique et/ou signalisant du GalU, nous avons analysé la structure fine des pectines du mutant *qua2* traité au GalU. Ainsi l'empreinte enzymatique réalisée sur de la paroi lavée et séchée d'hypocotyles n'a révélé aucune différence dans les spécificités de « pattern » des HGs chez *qua2* à la suite du traitement. L'analyse de la fraction non digérée (enzyme inactivée + tampon) de ces mêmes échantillons a permis de mettre en évidence la présence d'OGs potentiellement piégés dans la paroi. Fait intéressant, nous avons révélé une accumulation de GalUox « piégé » dans la paroi chez *quasimodo* dans cette fraction non digérée par rapport au sauvage. De plus cette accumulation a été largement augmentée par l'application de GalU. Nous avons identifié par RTqPCR 4 candidats potentiels responsables de cette oxydation du GalU, il s'agit des oxydases *OGOX4 OGOX3, BBE3, BBE5.* Des membres de cette famille ont déjà montré une activité oxydase sur des oligogalacturonides. Ces gènes semblent être surexprimés dans *qua2*, traité ou non avec le

GalU. Ainsi nous avons décidé d'appliquer du GalUox sur *qua2* pour déterminer s'il était responsable de cette restauration. Aucun changement n'a été observé. Nous avons donc testé le second composé résultant de cette oxydation : le peroxyde d'hydrogène (H_2O_2). A notre grande surprise nous avons pu observer les mêmes effets qu'avec l'acide Galacturonique à savoir une restauration de l'adhésion cellulaire. Certaines études ont démontré que les extensines sont des protéines pouvant être réticulées ensemble via leur résidu tyrosine grâce à l'action de peroxydases en présence d'H_2O_2. Une coloration au bleu de Coomassie, pour marquer les protéines et donc les extensines, a été réalisée sur des plantules traitées ou non avec de l'H_2O_2 ou du GalU. Nous avons montré que les 2 traitements sont capables d'augmenter le marquage au bleu de Comassie entre les cellules. Cela suggère que l'H_2O_2 appliqué et/ou produit est utilisée pour réticuler les protéines de la paroi cellulaire. Enfin une hydrolyse à l'HCl couplée à une analyse LC/MS a permis de mettre en évidence que le taux de réticulation des extensines chez les mutants *qua2* traités au GalU était nettement augmentée. Par ailleurs une analyse LC/MS des différentes hormones a permis d'identifier que deux hormones sont significativement augmentées par le traitement au GalU, l'auxine et l'acide salicylique.

Ainsi pour conclure nous avons mis en évidence un mécanisme permettant la restauration de l'adhesion chez *quasimodo.* Celui-ci consiste à transformer le GalU en GalUox pour ainsi utiliser l'H_2O_2 formé afin de réticuler ses protéines pariétales par le biais de peroxydase. Néanmoins en raison de la plus faible teneur en HGs et/ou de néo-synthèse de HGs, chez *quasimodo*, ce mécanisme n'est pas suffisant pour permettre l'adhésion cellulaire. L'addition de GalU dans le milieu de culture des plantes favorise ce mécanisme et permet donc la restauration de l'adhésion. Par ailleurs, les faibles variations de pattern pectique observées dans la condition *qua2* traité suggère que ce mécanisme initié à partir de l'ajout du GalU ne passe par un processus de recyclage intégrant le GalU dans les homogacturonanes .

CONCLUSION ET PERSPECTIVES

Au travers de notre étude nous avons pu révéler que la mutation *esmeralda* dans un fond génétique *qua2* ou sauvage, contrôle l'expression de certains gènes de remodelage des pectines. Cela conduit à une restauration du pattern pectique et permet la restauration de la quantité d'OGs endogènes dans le fond génétique *qua2*. Cela confirme entre autres le lien entre ESMERALDA et la signature pectique et/ou les OGs endogènes. Ainsi différentes perspectives s'offrent à nous pour identifier d'autres acteurs intermédiaires de la voie de transduction du signal médié par ESMERALDA et conduisant au contrôle de certaines HGME. Pour se faire

différentes constructions PME/PMEI/PAE::LUC vont être introduites dans les fonds génétiques (*emsd ; esmd1/qua2; qua2*) en fonction de leur niveau d'expression. Ainsi nous pourrons procéder à une mutagenèse de ces lignées et rechercher des mutants dont l'expression est revenue au niveau d'expression observé dans le fond génétique de type sauvage. Celle-ci sera réalisée grâce à une technique de criblage utilisant une phénobox associée à une caméra mesurant la chemiluminescence (générée par l'action de la luciférase sur la luciférine). Cette approche révélera les acteurs impliqués dans la cascade de transduction du signal médiée par ESMD ou QUASIMODO. Par ailleurs une analyse plus approfondie de différentes enzymes de type HGME produites en système hétérologue va permettre de déterminer l'impact de ces protéines candidates sur les patterns pectiques de nos différents mutants après leur application exogène. Enfin, des fractions enrichies des OGs endogènes identifiés vont être étudiées afin de déterminer leur effet éliciteur dans le cadre de l'adhésion cellulaire.

Au travers de notre étude nous avons aussi pu mettre en évidence l'action spécifique du monosaccharide GalU conduisant à la restauration de l'adhésion cellulaire chez *quasimodo* au travers d'un processus non métabolique. L'oxydation du GalU en GalUox permet la production l'H_2O_2 utilisé pour réticuler les protéines pariétales par le biais de peroxydase. Ceci suggère aussi, qu'un simple monomère peut avoir un impact sur le développement et l'adhésion. Par ailleurs certains éléments de cette boucle nécessitent d'être approfondi. Nous avons identifié des gènes candidats pour l'oxydation de GalU et deux des protéines codées par ces gènes ont été produites en système hétérologue. De plus, la génération de double mutant *qua2/ogox ou bbe* candidats est en cours. Ces deux analyses permettront de confirmer ou non les candidats potentiels responsables de l'oxydation du GalU dans un fond *qua2*. Par ailleurs des plantes mutantes *qua2/prx71* sont aussi en cours d'analyse phénotypique. Ce gène candidat codant la peroxydase PRX71 est connue pour être surexprimée chez *qua2* et pourrait être le parfait candidat à l'origine de la réticulation des extensines. Plusieurs études confirment que *qua2* surexprime 2 extensines, EXT3 et 4. Nous ne pouvons pas cependant exclure que d'autres extensines puissent être sujettes à une surexpression suite à l'application de GalU ou d'H_2O_2. Par exemple, les extensines EXT 17 et 18 possèdent un nombre de site tyrosine plus élevé que les 2 précédentes. Ainsi, une analyse du transcriptome et du métabolisme semble nécessaire afin de déterminer les différentes voies qu'implique cette restauration de l'adhésion chez *qua2*. Enfin l'étude d'autres mutants possédant des défauts d'adhésion permettrait d'établir un lien solide entre la réticulation des extensines issu d'un processus d'oxydation et la restauration de

l'adhésion. Des résultats préliminaires obtenus semblent soutenir ce phénomène notamment avec l'étude du mutant *qua1* codant pour une galacturonosyltransferase.

A) THE EXTRA CELLULAR MATRIX

The extracellular matrix (ECM) is made up of different polymers (**Figure A-1**) . This ECM provides mechanical support and biophysical barrier. This barrier plays a major role in cell/communication and plant/environment interaction. ECM is made of entangled compartments: cuticle, middle lamella, and cell wall. These compartments are made of different lipidic and glycanic polymers, structural proteins, and functional proteins. The structure of polymers and the nature of the proteins that composed the ECM differs according to the different layer, level or location in the matrix and the developing cell stages. ECM can also react to various stimuli, such as pathogens or the environment (Caffall & Mohnen, 2009; Carpita & Gibeaut, 1993).

1) PRIMARY CELL WALL

In general, the plant cell wall can be represented as an assembly of several layers consisting essentially of polysaccharides and proteins. Their proportions vary according to the species, but also according to the types of cell wall (Keegstra, 2010). The primary cell wall has the particularity of providing flexibility and basic structural support, while ensuring the protection of the cell. This cell wall is made up of different polysaccharides such as cellulose microfibrils which will be nested in a matrix of hemicelluloses, pectins, and proteins (Carpita & Gibeaut, 1993).

a) Cellulose

About 15-40 % of the plant's primary cell wall is made up of cellulose (Caffall & Mohnen, 2009). As illustrated in (**Figure A-2**), cellulose consists of a backbone of glucose, (A) 2000 to 25000 residues, linked in β (1→4), assembled into crystalline microfibrils (B) by hydrogen bonds and non-covalent hydrophobic interactions, which ensure a rigid structure (Harris & DeBolt, 2008). The length of the cellulose chains, as well as the degree of crystallization, can vary, but the chemical structure of cellulose remains the same in the cell walls of different

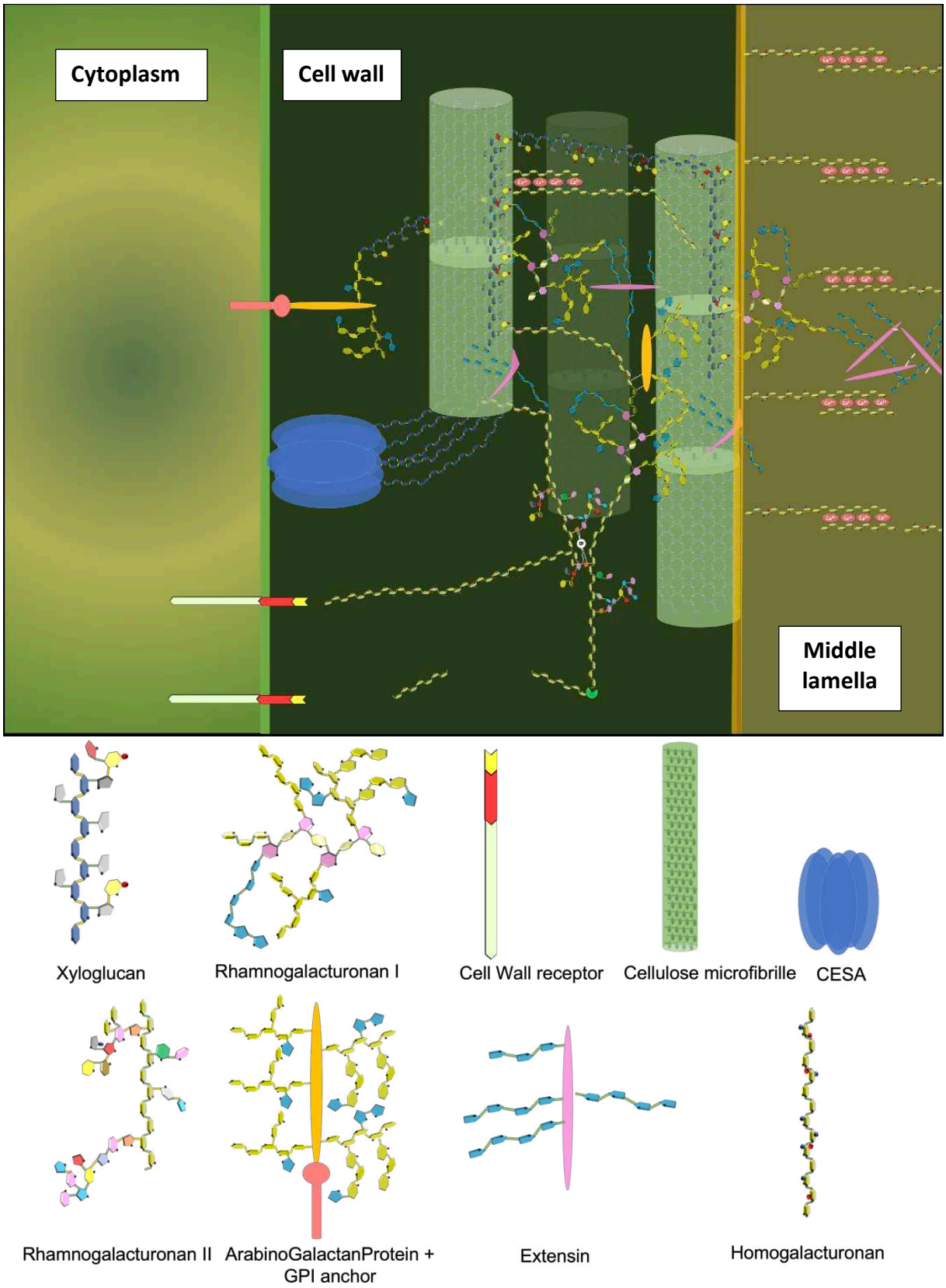

Figure A-1 **Structural representation of Matrix Extra Cellular**

plants, organs, and tissues (Burton et al., 2010). Cellulose microfibrils are produced by a plasma membrane-localized protein complex called Cellulose Synthase Complex (CSC) using UDP-glucose (uridine diphosphate-glucose) as a precursor (Cosgrove, 2005). The Cellulose Synthases (CESA) are assembled in a rosette: each rosette is made up of six sub-units, and each sub-unit is made up of six CESA. Microfibrils are formed by the spontaneous clustering and crystallization of several cellulose chains. The microfibrils are 3 to 5 nm wide, and several micrometers long, which is enough to wrap around the cell several times (Cosgrove, 2005; Somerville, 2006).

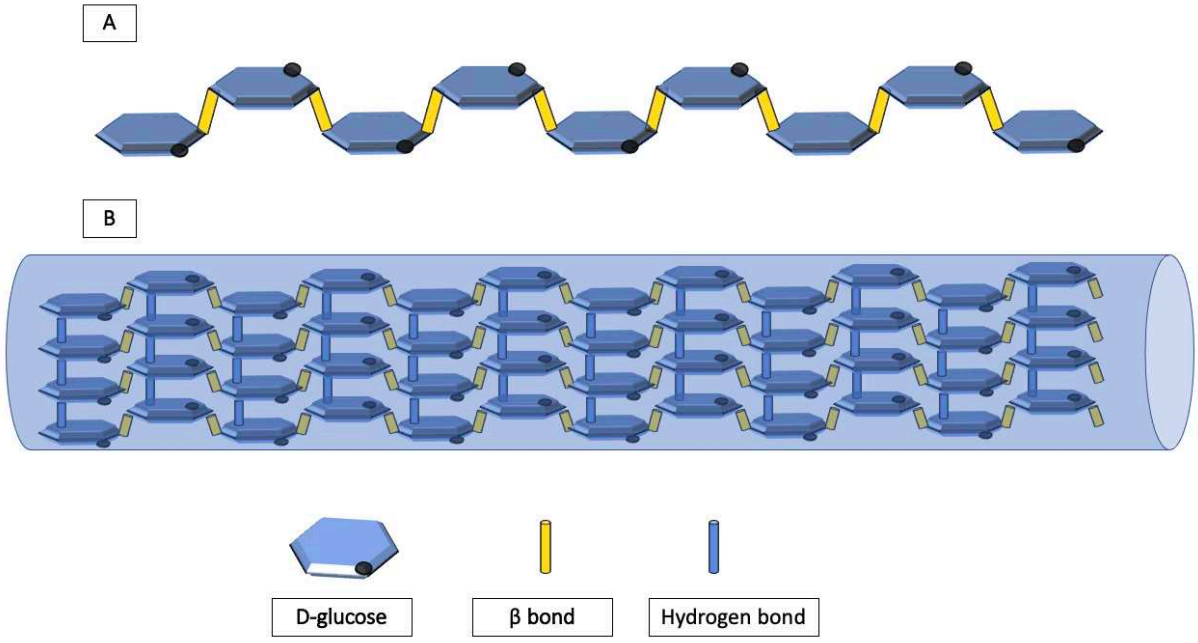

Figure A-2 **Structural representation of cellulose Chain (A) and microfibrils (B)**

b) Hemicellulose

The hemicelluloses are xyloglucans, xylans (including glucuronoxylan, arabinoxylan, and glucuronoarabinoxylan), mannans (which include glucomannan, galactomannan, and galactoglucomannan) (Cosgrove, 1997; O'Neill & York, 2018). Xyloglucans are the most abundant hemicelluloses which consist of a β (1→ 4) D-glucose chain like cellulose with 50 and 75 % residues substituted by α (1→ 6) D-xylose residues, by β (1 → 2) D-galactose residues, which can be acetylated to O-6 (Pauly et al., 2013) and can, in turn, be substituted by α (1 → 2) L-fucose residues **(Figure A-3**) (Fry et al., 1993). Moreover, xyloglucans structure can be specific depending on the tissue. In *Arabidopsis thaliana* root hair, (Maria J. Peña et al.,

2012) identified xyloglucan sidechain containing β-d-galactosyluronic acid linked to (1→2)-α-d-xylose. The galacturonic residue can be also substituted by α-(1→2)-L-fucosyl

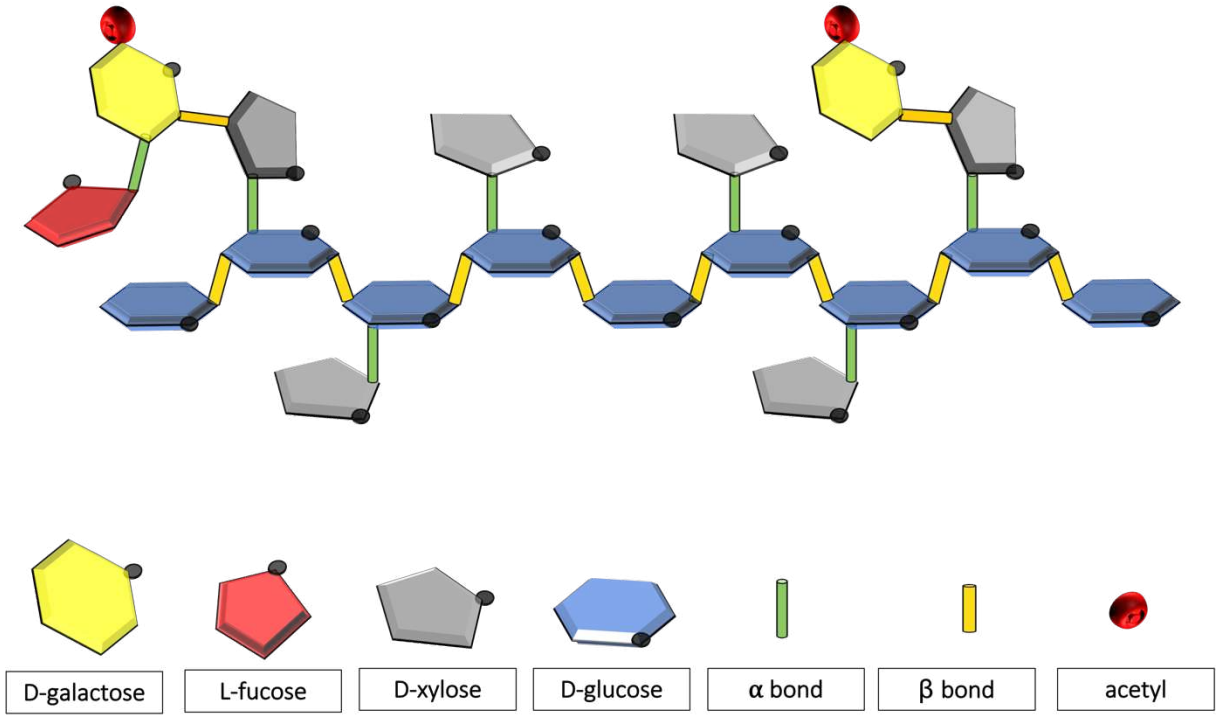

Figure A-3 **Structural representation of Xyloglucan**

The hemicelluloses are synthesized in the Golgi apparatus, thanks to glycosyltransferases allowing the production of the β-glucan backbone and the addition of sidechains. The synthesis of the β-1,4-glucan backbone is carried out by members of the subfamily of cellulose synthase-like (CSL) (Cocuron et al., 2007). The addition of α-D-xylose residues at O-6 of the backbone glucose residues is mediated by xyloglucan α-1,6-xylosyltransferase. The substitution at O-2 of the xylose side chains in xyloglucan by β-d-Gal residues is mediated by two glycosyltransferases, MUR3 and XLT2 in Arabidopsis. Indeed, *mur3* and *xlt2* mutants present a defect in galactosylation of xylose residues (Jensen et al., 2012; Madson et al., 2003). The addition of the terminal α-L-fucosyl residues at O-2 of the Gal residues in xyloglucan is catalyzed by xyloglucan fucosyltransferase (FUT1) (Perrin et al., 2003). Finally, the acetylation of D-galactose residue may be mediated by different members of the *TRICHOME BIREFRINGENCE LIKE (*TBL) family like AXY4 and ESK1, or O-acetyltransferase REDUCED WALL ACETYLATION (RWA) (Gille et al., 2011; Sinclair et al., 2020; Zhong et al., 2018). After the formation of glycan chains, polysaccharides are then transported to the

plasma membrane by vesicles derived from Golgi. These vesicles fuse with the membrane, releasing the polysaccharides towards the cell wall.

c) Pectin

Pectin is present in both the middle lamella and primary cell wall. Pectins are made up of 4 distinct domains, mainly made up of a backbone of α (1→ 4) D-galacturonic acid residues including homogalacturonans (HGs) (65 %), or HGs substituted like rhamnogalacturonans II (RG-II) (10 %) and xylogalacturonans (XGA) (5 to 7 %), this backbone is branched by single sugar units or short side chains (Mohnen, 2008). Rhamnogalacturonans I (RG-I) (20 to 35 %) is the only pectic domain having a heteropolymeric backbone made up alternately of residues of L-rhamnose and of D-galacturonic acid, which can be substituted by various neutral sugar sidechains (Mohnen, 2008). Pectins are made up of 17 different monosaccharides (Vincken et al., 2003) and require at least 67 different transferases in *A. thaliana*, including glycosyl-, methyl-, and acetyltransferases (Mohnen, 2008). Due to its charged nature, pectin seems to be involved in the regulation of ionic transport and porosity of cell walls, thus controlling the permeability of the cell wall. Furthermore, pectins are considered to be involved in various structural and signaling functions in plant development and organogenesis (Saffer, 2018).

i. Homogalacturonan

Homogalacturonans (HG) (**Figure A-4A**) are synthesized in the Golgi apparatus as linear chains of D-galacturonic acid residues linked by α-(1→ 4) bonds and generally have a length of 60-100 GalA residues (Mohnen, 2008; Sénéchal et al., 2014). The carboxyl groups of HGs can be methylesterified; this modification aims to block the acid group and therefore may reduce their ability to form gels (Cosgrove, 2005). HG can be acetylated in the O-2 or O-3 position (Höfte & Voxeur, 2017). The degree of methylation (DM) and acetylation (DA) impact the physicochemical properties of pectins. Indeed, HGs (DM < 50 %) form a gel in the presence of calcium ions (**Figure A-4B**) (Pelloux et al., 2007). Conversely, high DA is a limiting factor for gelling properties (Vriesmann & Petkowicz, 2013). Homogalacturonans are remodeled during plant development or in response to various stresses. Recently the role of nanofilament of homogalacturonan was highlighted using super-resolution three-dimensional direct stochastic optical reconstruction microscopy (3D-dSTORM) and cryo–scanning electron microscopy (cryo-SEM). Nanofilaments of homogalacturonan in the cell wall seem to shift between crystalline and anisotropic phases according to their DM, in cotyledon pavement cell.

This structural shift may lead to changes in cell wall shape that stand independently of turgor pressure (Haas et al., 2020).

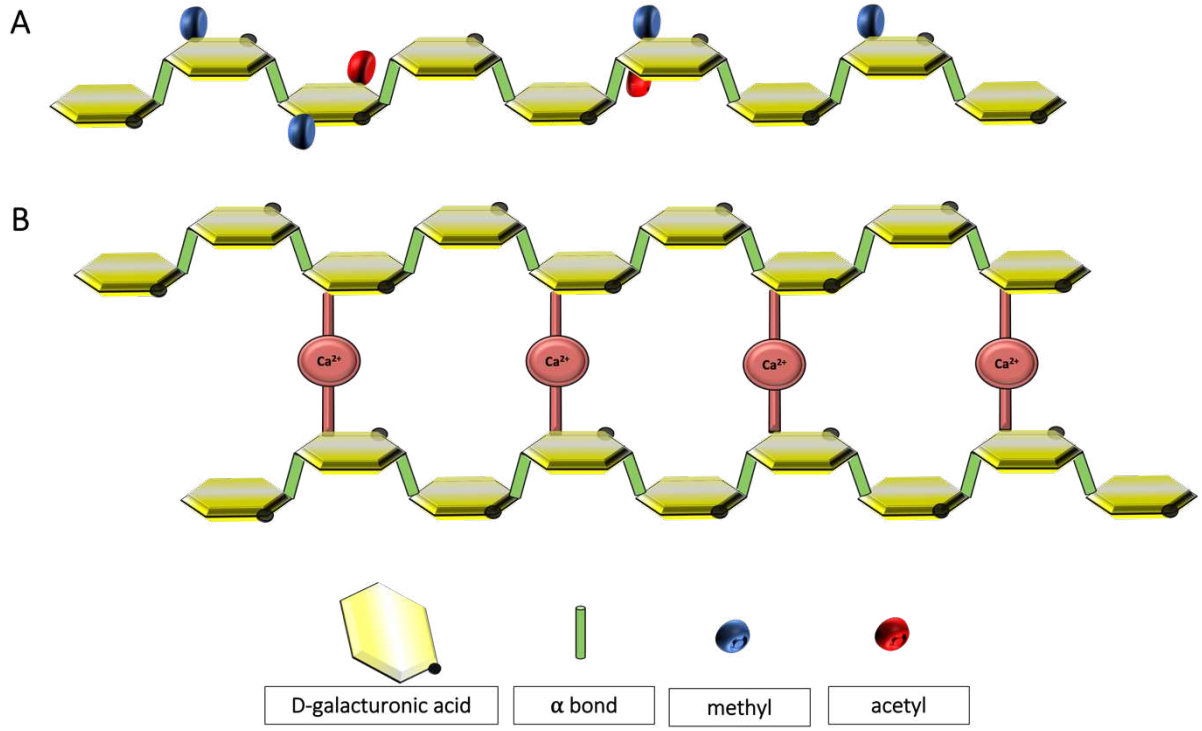

Figure A-4 **(A) Structural representation of homogalacturonans, (B) Structural representation of homogalacturonans crosslink with calcium ions**

ii. Xylogalacturonan

Among the various pectic polysaccharides mentioned, xylogalacturonans (XGA) represent a minor component of the pectic domains (**Figure A-5**). They consist of a chain of α (1→ 4) D-galacturonic acid substituted in position O-3 by side chains of β-(1→3)-xylose (Mohnen, 2008). No specific function has been attributed to XGA, but the abundance of this polymer would affect the physical properties of the pectic matrix. Thus, calcium-dependent interactions between HG chains would be prevented if the chains are substituted with xylose. How this could affect the biology of the plant remains unclear. However, XGAs have been determined as poorly digestible by endo-polygalacturonases (PG) (Jensen et al., 2008).

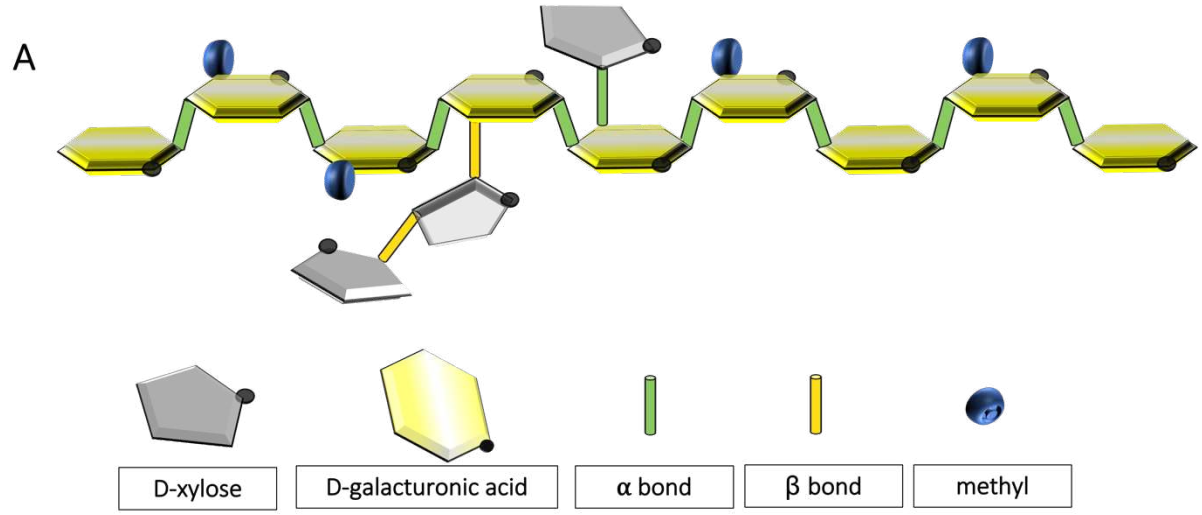

Figure A-5 **Structural representation of Xylogalacturonan.**

iii. Rhamnogalacturonan II

Type II rhamnogalacturonan (RG-II) (**Figure A-6**) is a complex pectin domain that consists of a backbone of at least 8 α (1 → 4) D-galacturonic acid and have 4 types of side chains A to D. Two features distinguish RG-II from other plant polysaccharides. First, RG-II is composed of 12 different monomers linked to each other by up to 20 different glycosidic linkages. Secondly, RG-II is the only polysaccharide known to contain both apiose and aceric acid (Bar-Peled et al., 2012). In the presence of boron, RGII spontaneously dimerized *via* borate diester (Ishii et al., 1999). This crosslinking may impact porosity and cell wall thickness (Cosgrove, 2005). Several studies have shown that mutations affecting the formation of nucleotide sugars involved in RG-II synthesis severely impact plant growth and development (Dumont et al., 2014, 2016; Sechet et al., 2018; Voxeur et al., 2011).

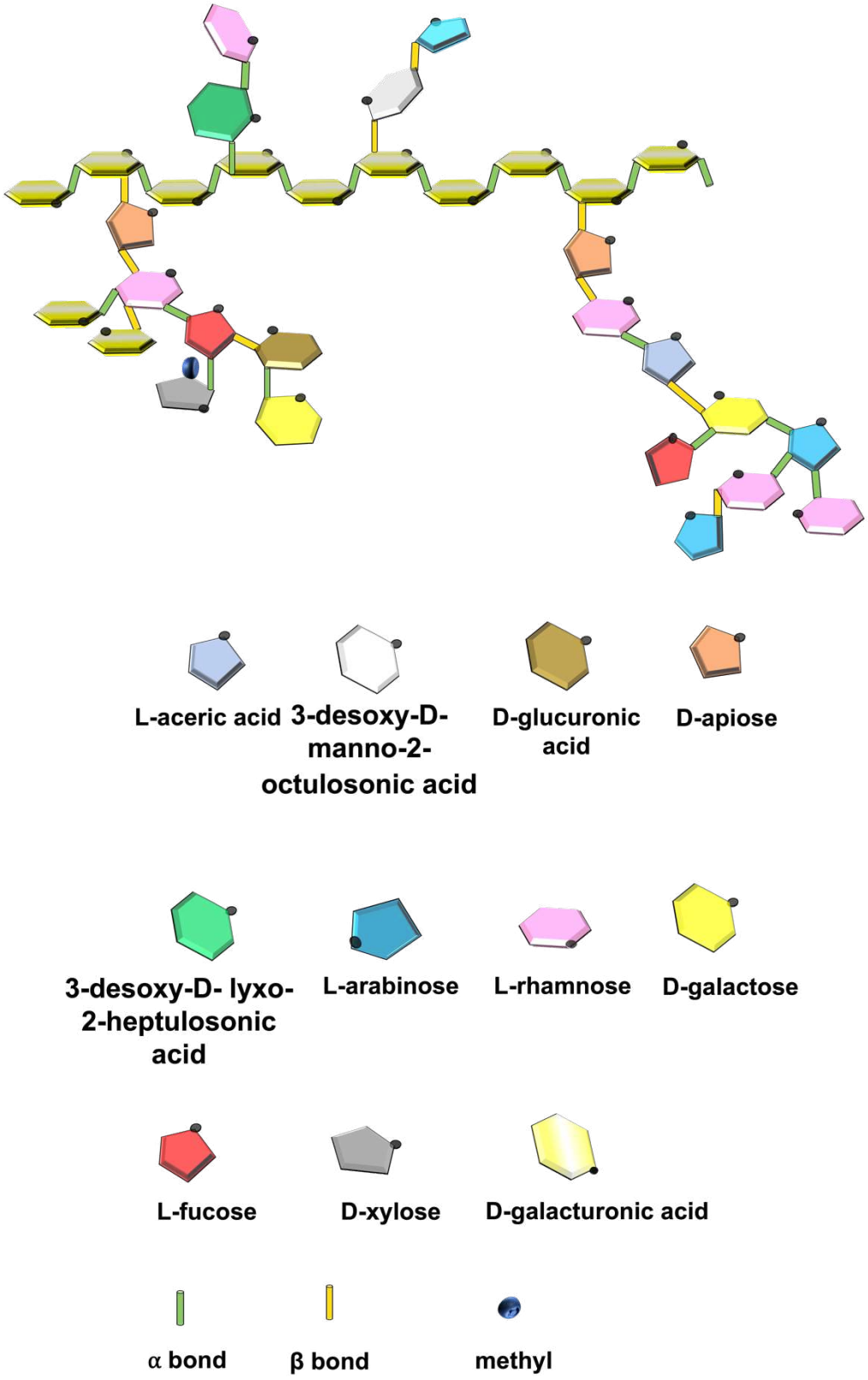

Figure A-6 **Structural representation of Rhamnogalacturonan II.**

iv. Rhamnogalacturonan I

The RG-I backbone (**Figure A-7**) is composed of alternating residues [→ 4) -α-D-galacturonic acid -(1→ 2) -α-L-rhamnose (1 →], up to 100 repeats. Between 20 % and 80 % of all rhamnose residues in the RG-I backbone are substituted with a side chain (Ridley et al., 2001). The proportion, length, and degree of branching of side chains vary depending on the monomer residues and the type of plant, organs, and tissues. GalA residues in the RGI are not presumed to be methylesterified,

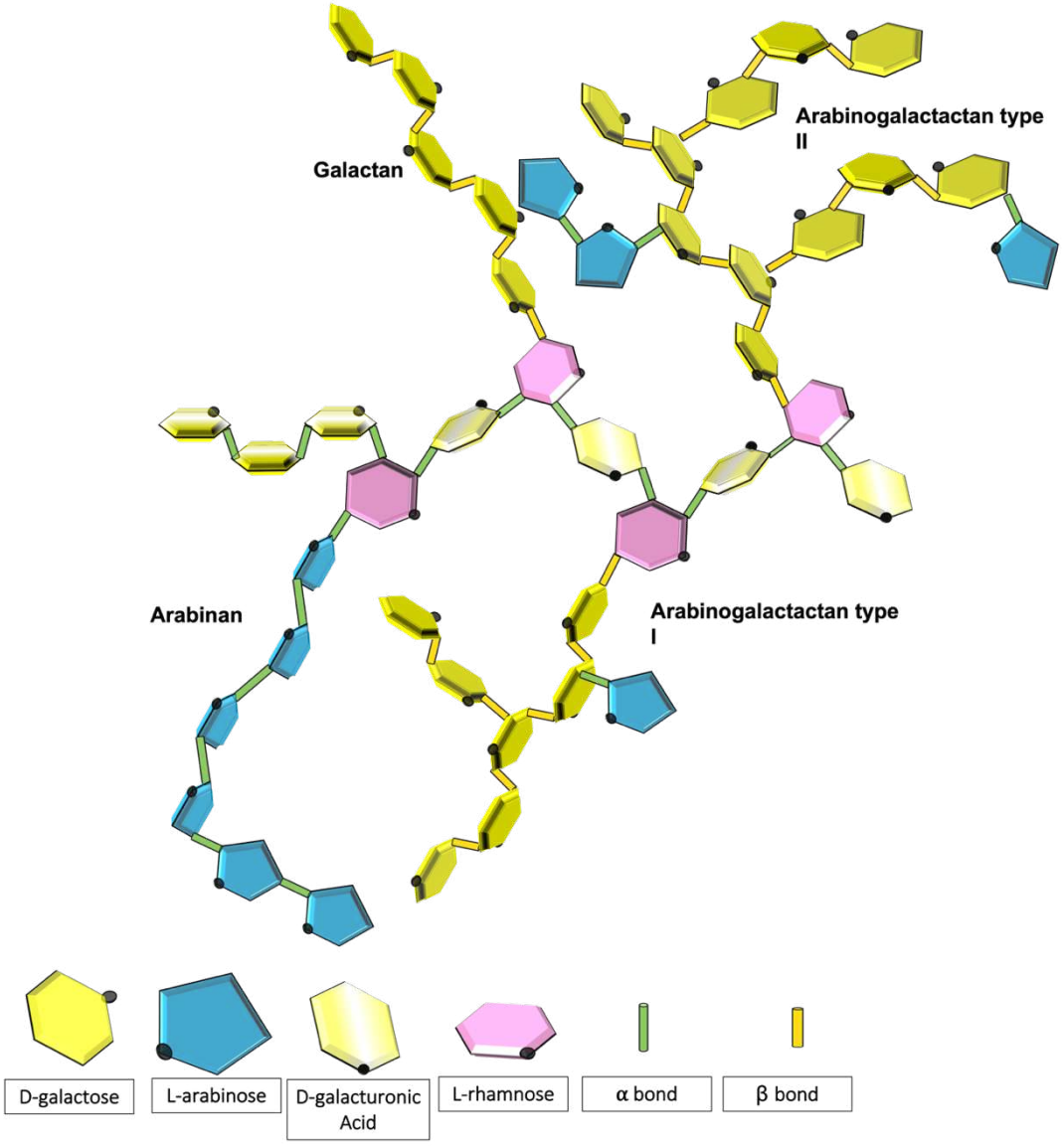

Figure A-7 **Structural representation of Rhamnogalacturonan I.**

Different side chains may occur on this pectic domain. The length and proportion of arabinan, galactan, arabinogalactan type I and arabinogalactan type II side chains are plant- and tissue-specific.

residues in RG-I can be substituted at the O-4 positions with a neutral sugar chain. Side chains vary in size, from a single residue to chains up to 50 or more residue, and can be divided into arabinans, galactans, and arabinogalactans type I and II (Voragen et al., 2009).

The synthesis of pectins takes place in the Golgi apparatus, catalyzed by glycosyltransferases (GT), that transfer glycosyl residues from nucleotide-sugars onto oligosaccharide or polysaccharide acceptors. GT also transfers the recycled nucleotide sugars from the cell wall from salvage pathways by sequential reactions involving sugar kinases and UDP-sugar pyrophosphorylases (Atmodjo et al., 2013) and those synthesized by the metabolism of photosynthesis (Bar-Peled & O'Neill, 2011). Atmodjo et coll. (2013) proposed two biosynthetic pathways for pectin synthesis in the Golgi system: i) consecutive glycosyltransferase (GT) model which adds glycosyl residues one by one, or ii) domain synthesis model for which pectin blocks are separately synthesized and subsequently fused. Recently, the hypothesis turned to a combination of both models (Hoffmann et al., 2021). To build the pectic complex polymers, about 67 different transferases are required (Mohnen, 2008). Finally, polysaccharides are packaged in transport vesicles, so that they can be exported to the plasma membrane (Monhen, 2008). Indeed, mobile Secretory Vesicle Compartments (SVCs) marked by the late trafficking protein SECRETORY CARRIER MEMBRANE PROTEIN 2 (SCAMP2) have been demonstrated to contain pectins (Toyooka et al., 2009).

The most well-characterized GT implicated in HGs biosynthesis is the GAlacturonosylTransferas 1 (GAUT1) encoding galacturonosyltransferase of the GT8 Cazy family, which catalyzes the transfer of GalA from UDP-GalA to an oligo-GalA acceptor (Sterling et al., 2006). Furthermore, it has been shown that GAUT1 functions in a protein complex with GAUT7, by the concomitant loss of its transmembrane domain, and its anchoring in the Golgi apparatus by covalent and noncovalent interactions with GAUT7. GAUT7 does not possess detectable GalA transferase activity (Atmodjo et al., 2011, 2013). Mutation in *QUA1/GAUT8* another putative galacturonosyl-transferase GT8 leads to dwarfism, cell adhesion defect, and decrease in GalA content related to a defect in HG synthesis (Bouton et al., 2002). HG can also be xylosylated to form xylogalacturonan by the membrane-associated protein XYLOGALACTURONAN-DEFICIENT1 (Jensen et al., 2008). Four genes encoding RG-II xylosyltransferase, belonging to the GT77 family, have been described (J. Egelund et al., 2006; N. Egelund, 2008; X. L. Liu et al., 2011). Three members of this family, *RGXT1–3*, have shown enzymatic activity, transferring D-xylose to L-fucose *in vitro* assays (J. Egelund et al.,

2006; N. Egelund, 2008). Among the 4 RG-II xylosyltransferases, only *mgp4* mutant presents visible phenotypes in both RG-II structure and pollen tube growth (Liu et al., 2011). Concerning RG-I, recently (Takenaka et al., 2018) identified and characterized in the glycosyltransferase family (GT106) four rhamnosyltransferases *(RRT1-4),* which transfer the rhamnose residue from UDP-β-L-rhamnose to RG-I oligosaccharides. The loss of function of *RRT1* led to a decrease of the amount of RG-I in the seed coat mucilage. Among the different members of the GT92 family, 3 genes *GALS1, GALS2,* and *GALS3* were shown to encode an RG-I β-(1→4)-D-galactosyl-transferase (Madrid Liwanag et al., 2013). The three mutants *gals1, gals2,* and *gals3*, showed a decrease in galactose content but did not display any morphological phenotypes. In contrast, overexpression of *GALS1* results in 50 % higher β-1,4-galactan content. ARAD1 a putative arabinosyltransferase impacts the cell wall arabinan content (Harholt et al., 2006). *Arad1* displays a defect in α-(1→5)-L-arabinose suggesting that *ARAD1* encodes a putative RG-I α-(1→5)-L-arabinosyltransferase. In addition, ARAD1 was demonstrated to form a complex with ARAD2 (Harholt et al., 2012).

During synthesis, some pectic glycosyl residues are modified by methyltransferases (MT) that catalyzed esterification, O-methylation, or acetyltransferase that catalyzed acetylation (Anderson, 2016). The donor for these modifications appears to be S-adenosyl-methionine (SAM) and acetyl-CoA respectively. Methylesterification of galacturonic acid in HG is achieved by the methyltransferases in the Golgi apparatus (Du et al., 2020; Mouille et al., 2007). Fully methylesterified HGs are then exported to the cell wall (Sénéchal et al., 2014). In *A. thaliana* mutations in genes encoding pectic methyltransferase can lead to dramatic phenotypes. For example, *qua2* mutants show dwarfism, cell adhesion defect phenotype, and less HG in their cell walls (Mouille et al., 2007). Recently QUA2 protein has been shown to have a methyltransferase (MT) activity on PGA substrate (Du et al., 2020). In contrast, a mutation in *QUA3,* coding a putative MT, did not lead to any phenotype but the *qua3RNAi* transgenic lines displayed less pectin methylation as well as altered composition and assembly of cell wall polysaccharides (Miao et al., 2011). *Cgr3* knockout mutants and plants overexpressing *CGR3* display respectively a decrease and increase of HG methylesterification (Held et al., 2011). In contrast to the methyltransferase, no specific protein has been shown to have an acetyltransferase activity on pectin. However, some candidates have been investigated, like the TRICHOME BIREFRINGENCE LIKE (TBL) family, and maybe involved in the O-acetylation of pectin in Arabidopsis. Indeed, the degree of acetylation of the pectin rhamnogalacturonan-I (RG-I) in *tbl10* mutant was reduced by 50 % (Showalter & Basu, 2016; Stranne et al., 2018).

d) Structural proteins

Extracellular proteins can cover different functions in the cell wall. Among these cell wall proteins, structural proteins are necessary to maintain the integrity of the cell wall. Structural proteins are hydroxyproline-rich glycoproteins (HRGPs), implicated in diverse aspects such as plant growth, development, and stress responses (Showalter and Basu, 2016). This family regroups 3 members: highly glycosylated soluble arabinogalactan proteins (AGPs), moderately glycosylated insoluble extensins (EXTs), and lightly glycosylated proline-rich proteins (PRPs). Here we will focus on AGP and EXT.

i. AGPs

AGPs are known to be more glycosylated than EXTs. They are characterized by an abundance of Hyp, Ala, Ser, and Thr residues and by the occurrence of Ala-Pro, Pro-Ala, Ser-Pro, Thr-Pro, Val-Pro, and Gly-Pro dipeptide repeats (Showalter and Basu, 2016). Interestingly AGP can be associated with a glycosylphosphatidylinositol anchor (GPI) at the hydrophobic C-terminal extremity which allows the incorporation of AGPs to the plasma membrane (Borner et al., 2003). Glycan chains of type II arabinogalactans (AGII) and short arabinans are branched to the protein backbone *via* Hyp residues. AG type II structures also contain glucuronate or 4-methyl-glucuronate linked to galactose in β-(1 → 6) as well as terminal modifications by L-rhamnose and L-fucose (Seifert, 2020). AGPs are also known to crosslink by calcium on glucuronic acid (GlcA) residue (Zhang et al., 2020) or hemicellulose and pectin with the APAP1 domain (Tan et al., 2013). Different studies investigated mutants in AGP glycosylation genes revealing the role of their side chain in plant growth and development (Showalter and Basu, 2016). For example, a mutation in *galt31a* gene encoding a β-(1 → 6)-galactosyltransferase caused the arrest of embryo development at the globular stage (Geshi et al., 2013). Knockout mutants for β-(1→6)-glucuronosyl transferases *glcat14a* showed enhanced cell elongation rates in dark-grown hypocotyls and light-grown roots during seedling growth (Dilokpimol & Geshi, 2014). Finally, α-(1 → 2)-fucosylation of type II AG might be mediated by 2 members of family GT34 called FUT4 and FUT6. *fut4 fut6* double mutant showed a strong reduction in type II AG linked fucose, and oversensitivity to 150 mM NaCl (Liang et al., 2013; Tryfona et al., 2014). AGP function is still unclear, and their structural heterogeneity suggests that they could cover several functions in root development, cell wall integrity, or adhesion (Showalter et al., 2010).

ii. Extensins

EXTs are characterized by the repetitive sequence Ser-Hyp-Hyp-Hyp-Hyp, which can be substituted by a β-D-galactose on Ser residues and the arabinosylation of most hydroxyproline residues (X. Liu et al., 2016). The glycosylation wrapping the protein stabilizes the structure, prevents enzymatic degradation, and enhances the extensins crosslink (Chen et al., 2015). The hydrophilic glycosylated pentapeptide is interspersed with hydrophobic motifs containing Tyr residues. These residues are modified by peroxidases to form intramolecular isodityrosine crosslinks or intermolecular di-isodityrosine (Fry, 1982; Held et al., 2004).

Crosslink might be crucial in response to stress and the adhesion (Mishler-Elmore et al., 2021; Sala et al., 2019). Some EXTs seem to be required in the new wall assembly such as *ext3*, a lethal homozygous mutant, which presents broken and misplaced walls (Hall & Cannon, 2002). During their biosynthesis, these proteins undergo extensive posttranslational modifications, which include proline hydroxylation modification of HRGPs, catalyzed by prolyl 4-hydroxylases (P4Hs), and glycosylation (Tiainen et al., 2005; Velasquez et al., 2011). Briefly, nine genes have been identified to be involved in EXT glycosylation highlighting their different role. SERINE GALACTOSYLTRANSFERASE 1 (SGT1), is responsible for adding single galactose residues to Ser residues in Ser-Hyp-Hyp-Hyp-Hyp sequences (Saito et al., 2014). HPAT1, HPAT2, and HPAT3 encode hydroxyproline O-β-arabinosyltransferases, which add single arabinose residue to Hyp residues. Loss-of-function mutations in HPAT-encoding genes cause pleiotropic phenotypes that include enhanced hypocotyl elongation, defects in cell wall thickening, early flowering, early senescence, and impaired pollen tube growth (Ogawa-Ohnishi et al., 2013). Three other genes, named REDUCED RESIDUAL ARABINOSE (RRA1, RRA2, RRA3), encode arabinosyltransferases adding the second arabinose residue in a β-(1→2)-linkage. Mutants *rra1 and rra2*, have been shown to reduce the cell wall arabinose content (Egelund et al., 2007). Another gene, XYLOGLUCANASE113, encodes the arabinosyltransferase which adds the third arabinose residue in a β-(1→2)-linkage (Gille et al., 2009). Finally, ARABINOSE DEFICIENT (ExAD), encodes the arabinosyltransferase that adds the fourth arabinose in an α-(1→3)-linkage (Velasquez et al., 2012; Møller et al., 2017).

2) CUTICLE

The cuticle is the outermost layer of epidermal cells. The cuticle is a complex structure composed of insoluble cutin and solvent-soluble organic lipids, called waxes. Although

generally viewed separately from the cell wall polysaccharides, waxes are physically linked to the polysaccharide forming a continuum with the cell wall (Fernández et al., 2016; Segado et al., 2016; Yeats & Rose, 2013). The polymers of cutin are mainly biosynthesized in the chloroplast. It contains esterified and oxygenated fatty acids, small amounts of glycerol and phenylpropanoids. Cuticular waxes are mainly composed of various primary and secondary alkanes, alcohols, aldehydes, ketones, and esters derived from very long chain fatty acids (Zeisler-Diehl et al., 2018). Based on histochemical staining cuticle is often organized into two parts: an underlying layer of cutin in which polysaccharides of the wall are entangled called "cuticular layer" and an outer layer rich in cutin and waxes called "cuticle proper". Waxes can either be incorporated into the cutin matrix (intracuticular waxes) or deposited on the surface (epicuticular waxes), in the form of a film or crystals (Yeats and Rose, 2013).

3) MIDDLE LAMELLA

Middle lamella (ML) is a 50 nm thick layer that is sandwiched between the primary cell walls of neighboring cells and suggested to glue adjacent cells together. Thus, ML may be intimately linked to the control of adhesion through a strict regulation of cell separation in response to development and environmental stimuli (Matar & Catesson, 1988; Waldron & Brett, 2007). The ML is formed of homogalacturonans pectin containing vesicles that fuse not as a solid structure, but as a network that gradually fills any gaps until a cell wall layer is formed. Based on the study of growing tissue stained by PATAg (periodic acid–thio carbohydrazide silver proteinate). The ML is only recognizable once the cell plate has expanded sufficiently to connect with the parental cell wall and cell wall polysaccharides are deposited on both sides of the mature cross-wall (Matar & Catesson, 1988). In young and growing plant tissues the ML is primarily composed of pectic polysaccharides with small amounts of protein. Cellulose and hemicellulose are absent from the ML (Jarvis et al., 2003; Moore & Staehelin, 1988). Immuno-histochemistry of polysaccharides and structural proteins provide a detailed composition of the middle lamella. The use of antibodies such as JIM5 (specific to partially esterified HG), JIM7 (esterified HG), LM7 (non-blockwise partially esterified HG), and PAM1 (blockwise partially esterified HG) showed that in the mature ML pectins are partially esterified HG, and potentially subject to reticulation by Ca^{2+} to stiffer the pectic material (Knox, 1992). Another feature of the chemical composition of the ML located in cell junctions is the presence of hydroxyproline-rich glycoproteins (HRGPs) (Burlat et al., 2001). RG-I detection was investigated on different plant models and tissue, RG-I was found to be restricted to the ML lining junctions in some

plants, with labeling associated with the expanding portion of the middle lamella (Moore & Staehelin, 1988) and in other studies, it's labeled in both cases (Moore et al., 1986). This suggests that the quality of the middle lamella is highly dependent on tissue and plant species (Jones et al., 1997). The crosslink between polymers remains an important feature to cell adhesion mediated by ML, this part is more described in the part B)2). Today, we still know very little things about the middle lamella, and many types of research, using modelization coupled with different acquisition techniques, are carried out to understand the mechanical properties of this layer connected to the cell wall.

4) CROSSLINKING OF THE EXTRACELLULAR MATRIX

Individual cell wall polymers are crosslinked by non-covalent and covalent bonds contributing to the insolubility and strength of the cell wall. A crosslink is a chemical bond covalent or hydrogen bond for example, that joins together separate polymers. Crosslinks appear at different times and in different contexts, depending on the stage of development, the type of tissue (Fry, 2010). Understanding these interactions and in which condition they occur can provide a better view of the parietal organization during plant development but also a better interpretation of the different mechanisms governing cell adhesion *via* a complex polysaccharide network (Waldron et al., 2007; Fry., 2011).

a) Inter-polysaccharides bonds

The main components in the cell walls representing the backbone of the cell wall are the cellulose microfibrils. Xyloglucans, on the other hand, play an important role in the interlacing of cellulose microfibrils and are involved in the regulation of cell wall extension. It has been shown for a long time that XG interacts with cellulose forming a non-covalent association mediated by hydrogen bonds (Valent & Albersheim, 1974). This was confirmed by a later study, eventually leading to the concept that xyloglucan extensively coats cellulose surfaces and tethers microfibrils together (Pauly et al., 1999). A study showed that the Xyl/Glc ratio affects the binding of XGs to cellulose, the less the XGs are substituted, the highest the binding yields is. Moreover, the terminal fucose residue of XGs differentially affects the binding, depending on the crystallinity of cellulose, suggesting that the surface status of native cellulose microfibrils affects the XG/Cellulose interaction (Chambat et al., 2005). To illustrate the

importance of this interaction, it has been shown that the microtubule distribution, the cellulose content, and biosynthesis are altered in etiolated hypocotyls *xxt1 xxt2* Arabidopsis xyloglucan mutant. This indicates that loss of xyloglucan affects the mechanic and the stability of the microtubule cytoskeleton (Xiao et al., 2016a). Other polysaccharides can compete with the xyloglucan/cellulose bond. It has been shown that pectin and xyloglucan could be crosslinked by a non-ester covalent bond. A co-elution of xyloglucan with anionic pectin fractions was observed on Anions Exchange Chromatography from cell suspension cultures. Besides, the complex was also extracted with 6 M NaOH, suggesting an alkali-stable bond between xyloglucan and pectin (Popper & Fry, 2005). Moreover, *in vitro* xyloglucans and pectins can bind simultaneously to the surface of cellulose. However, when the proportion of xyloglucan is high relative to pectin, this would induce very low adsorption of pectin. Conversely, a low concentration of xyloglucan would lead to higher adsorption of pectin especially the arabinan and galactan side chains with cellulose. This suggests that pectin may play a dual role depending on the amount of xyloglucan in the primary cell wall (Zykwinska et al., 2007, Zykwinska et al., 2008; Zykwinska et al., 2005). Later on, NMR analysis demonstrated direct cellulose−pectin spatial contacts, that are the most present, in contrast to a limited number of cross-links between xyloglucan and cellulose (Dick-Pérez et al., 2011; Wang et al., 2012). Moreover, a partially depectinated cell wall in which 40 % of homogalacturonan is extracted retains some cellulose-pectin crosslinks (Wang et al., 2015). Biochemical and *in vitro* binding assays demonstrated that xylan chains are attached to RG-I chains by a covalent bond and mediate adsorption to cellulose microfibrils in mucilage. Furthermore, *mum1-5* mutant presents a defect in ratio Rha-Xyl in mucilage that influences the weak adsorption to cellulose (Ralet et al., 2016). MS / MS analysis showed residues of galacturonic acid after digestion substituted by residues of hexose in plum and pear. These hexoses have been identified as cellobiose residues indicating HGs-cellodextrins could be linked by a covalent bond (Nunes et al., 2012). Using “epitope detection chromatography” (Cornuault et al., 2014) showed a co-elution of pectin-xyloglucan complexes, but differences in intensity were found between Arabidopsis root and shoot extracts, indicating that crosslink varies throughout distinct tissue.

b) Protein-polysaccharide bonds

Previously, we have described the main crosslinking that could occur in the extracellular matrix by a covalent or non-covalent bond between cellulose, hemicellulose, and pectin which allows a durable and rigid structure that can withstand extreme turgor pressure and may participate in

the maintenance of cell adhesion. However, the extracellular matrix also contains structural proteins, such as glycoproteins rich in hydroxyproline (HRGP) including extensins and arabinogalactan proteins (AGPs) which are crosslinked with polysaccharides and participate in the maintenance of cell adhesion (Showalter and Basu, 2016). It has been shown that some AG type II are covalently attached to hemicellulosic and pectic polysaccharides.

AG Type II links the protein part of AGP through a Gal-GlcA-Rha element to RG-I. Arabinoxylan can appear attached to either a rhamnosyl residue in the RG-I domain or directly to an arabinosyl residue in the AG domain. This complex is called APAP1 (Tan et al. 2013). Moreover, this cross-link is still present after aqueous KOH extraction from the *Abies sibirica* foliage. Xylans, AGPs, RG-I, and glucan were co-fractionated even after the removal of homogalacturonans by polygalacturonase digestion (Makarova & Shakhmatov, 2021). HG-AGP interaction was also observed on the carrot model. After extraction from carrot cell wall, AGP was precipitated by Yariv reagent and separated with copper ion. Different AGP fractions rich and poor in GalA fragments were identified by HPAEC and MALDI-TOF MS. Even after digestion with pectin methyl esterase and polygalacturonase, highlighting the potential interaction between type II AG chain of AGPs linked to the pectic GalA *via* ester linkages (Immerzeel et al., 2006). Furthermore, *in vitro* AGP31 interacts with galactans of rhamnogalacturonan I through its C-terminal PAC (PRP-AGP containing Cys) domain as well as with PGA through probably a His stretch domain (Hijazi et al., 2012, 2014). Another potential linkage between extensin and pectin was also observed (Nunez et al., 2009). Extensin and pectin were used to construct multilayer structures. AFM analysis of the final structure showed that the polymers are intimately mixed and confirms a rearrangement during the adsorption step. This interaction can be linked to the balance of charges between the two polymers, basic extensins form an ionic bond with acidic pectins. However, this interaction depends on the degree of methylesterification of HGs, and the weak charge of the extensin due to their lysine content (Valent & Albersheim, 1974). This result could correlate with what is observed on the graft union model in Arabidopsis. The analysis of 17 epitopes, belonging to different cell wall components, showed that only three were present abundantly in extracellularly deposited material and in bead-like structures un/low-methylesterified HG and extensins. The results also indicated a possibility of ionic interaction between the two polymers, pectins and extensins, due to their chemical nature, which can result in the formation of a network that led to adhesion (Sala et al., 2019).

c) Pectin-pectin bonds

As discussed above, pectins are implicated in several crosslinks with various cell wall components. Pectins are also known to have the capacity to crosslink together through different domains and different bonds. The most well-known is the crosslink of two de-methylesterified HGs chain HGs-HGs by Ca^{2+} known as Egg-Box. Ca^{2+}-mediated gel formation may be crucial for maintaining the integrity of cell walls, both within and between cell layers and across the middle lamella (Grant et al., 1973; Willats et al., 2001). It was proposed that blocks of 7–14 methyl free α-D-GalA residues may be required for stable association with calcium (Daas et al., 2001). Other pectin domains present important crosslinks which could lead to dramatic phenotypes if they are not present in quantity. RG-IIs can be crosslinked in presence of borate forming a borate diol ester. The borate diester is linked in O-3 and O-2 to apiosyl residues of the A side chain (Ishii et al., 1999; O'neill et al., 2001). Moreover, RG-IIs are an integral part of HGs, its borate-diol esters can cross-link two HG chains (**Figure A-8**) (Ishii et al., 2001). Some cations such as Ca^{2+} promote dimer formation *in vitro* in a concentration- and pH-dependent manner (Ishii et al., 1999) and stabilize them. Recently it has been shown that in the Golgi GDP-L-galactose transporter (GGLT1)-silenced transgenic line, the amount of L-galactose in side-chain A of RG-II is reduced by up to 50 %. This led to a reduction in the extent of RG-II cross-linking in the cell walls resulting in a dwarf phenotype, which is rescued by growth in the presence of boric acid (Sechet et al., 2018).

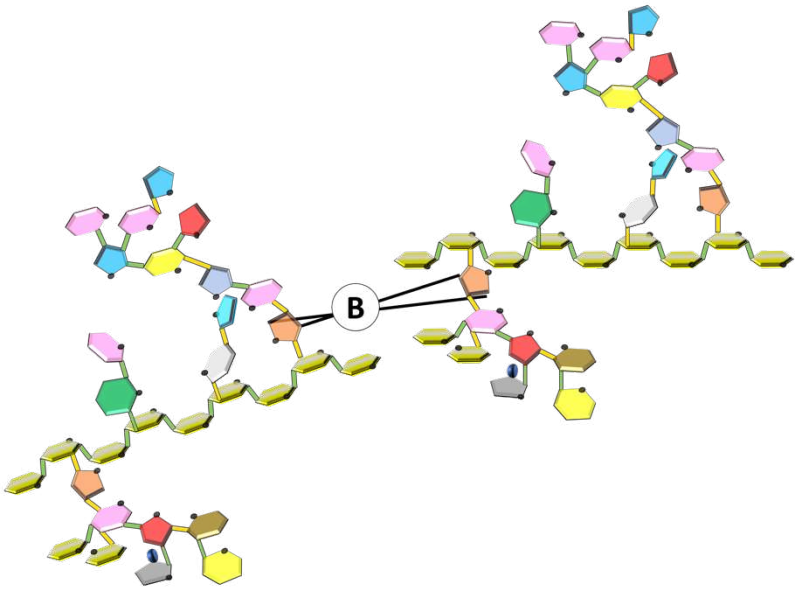

Figure A-8 **Structural representation of Rhamnogalacturonan II borate-diol esters crosslink.**

d) Hydroxyproline Rich GlycoProteins (HRGP)

Hydroxyproline rich proteins, such as extensin or AGP, are cell wall structural proteins and can be subject to different crosslinking. EXT crosslinking is mediated by covalent crosslinking of Tyr residues (**Figure A-9**). These Tyr residues are part of crosslinking modules/motifs that are regularly spaced along the backbone of classical EXTs. The first evidence was the discovery, in cell wall hydrolysates, of cross-linked amino acids isodityrosine (Idt) (Fry, 1982). This crosslinked was proposed to be intermolecular. However, a later study demonstrates that isodityrosine was only detected as EXT intramolecular crosslinks (Epstein & Lamport, 1984). Brady et coll. (1998) identified, in the cell wall of cell culture a trimer of tyrosine named Pulcherosine, composed of isodityrosine and tyrosine oxidatively coupled to tyrosine. *In vitro* studies that use synthetic glycoproteins, allowed the identification of additional and novel crosslinks within the EXT
network as tetramer called Di-Isodityrosine (Held et al., 2004).

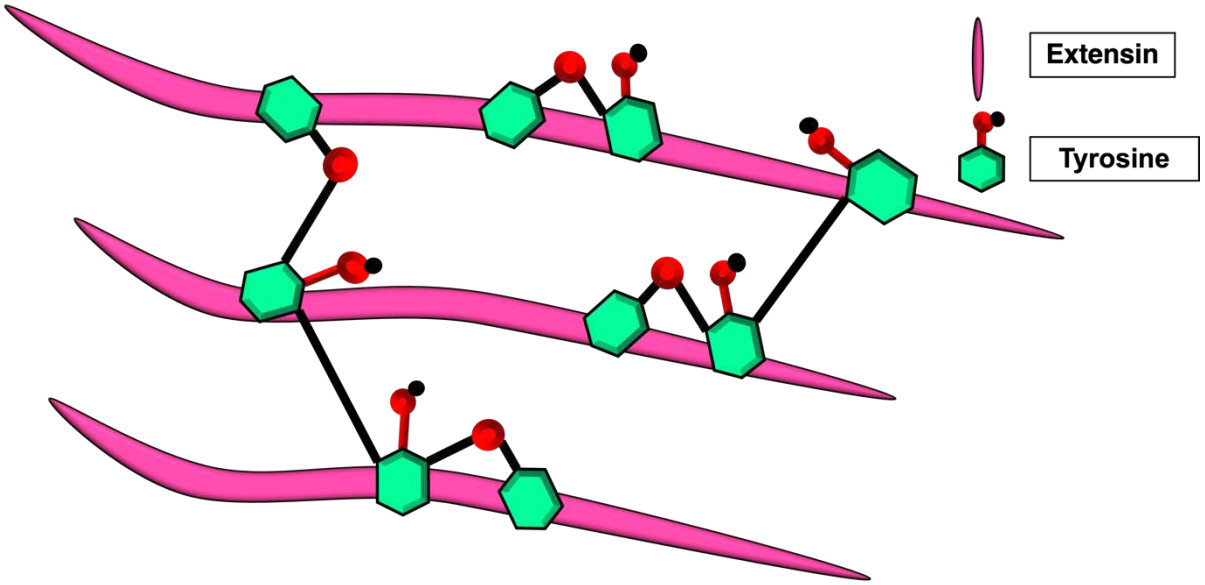

Figure A-9 **Structural representation of tyrosine inter and intramolecular crosslink of extensin.**

The involvement of arabinosylation in the crosslinking of EXTs was studied by measuring the initial crosslinking rate and the degree of crosslinking of partially or fully desarabinosylated EXTs, using an *in vitro* cross-linking test followed by chromatography by gel permeation. EXT arabinosylation is required for EXT crosslinking *in vitro* and the fourth Ara on the Hyp-Ara4 chains, appeared crucial for the initial rate and extent of EXT cross-linking *in vitro* by peroxidase (Chen et al., 2015). Another family of cell wall proteins contributes to reticulation and is involved in different physiological events. It has been shown that AGPs can be β-linked by calcium on glucuronic acid (GlcA) residue. A triple mutant AG β-glucuronyltransferases showed a strong reduction in glucuronidation. The AG mutant *glcat14* had lower *in vitro* calcium-binding capacity, severely limited growth, and could be suppressed by increasing the concentration of calcium in the growth medium (Lopez-Hernandez et al., 2020).

B) MODULATION & CONTROL OF CELL ADHESION DURING PLANT GROWTH AND DEVELOPMENT

1) Key actors identified

Cell adhesion is a phenomenon essential to the development, constantly solicited for maintenance through crosslinks and the control of cell wall remodeling in organ and tissue and at the cell level. Previously we described what could be the different polymers interactions occurring in the plant cell wall that could maintain the structure of the cell wall and consequently the cell adhesion. Now the question is how cell adhesion is controlled? Since the beginning of the century, some genes have been demonstrated to be linked directly or indirectly to cell adhesion and give us some clues on how this phenomenon is regulated during development.

a) Pectin methyltransferases

To date, in Arabidopsis, only a few mutants show cell adhesion phenotype. One of them, the mutants in a gene encoding a pectin methyltransferase, particularly the allelic mutants *quasimodo2 (qua2)* (Mouille et al., 2007, Du et al., 2020) and *tumorous shoot development2 (tsd2)* (Krupková et al., 2007), display strong cell adhesion phenotype (**Figure B-1**). Both share common features such as shorter hypocotyls with cell adhesion defects at the epidermal cells level of the hypocotyl, and a decrease in the amount of uronic acid, without modification of the total cell wall methanol content (Mouille et al., 2007; Du et al., 2020). Conversely, QUA3 a putative pectin methyl transferase only seems to affect the methylesterification of pectin without exhibiting any cell adhesion defect (Miao et al., 2011). Starting from this basis, we could think that cell adhesion defects would be linked to a decrease in the quantity of pectin. This could have sense, knowing that middle lamella is enriched in pectin (Daher & Braybrook, 2015). However, recently it was shown that *qua2* and *tds2* are also affected in cellulose content, microtubules synthesis, organization contributing to the instability of the cell adhesion, and cell integrity (Du et al., 2020; Kirui et al., 2021). In another context, QUA2 seems to play a key role in the modulation of C/N balance (Gao et al., 2008). Another QUA2 allele, *oversensitive to sugar1 (osu1)*, is more sensitive to carbon/nitrogen imbalance perception (Gao et al., 2008). Otherwise, in rice, a mutation in a putative OsQUA2 ortholog gene leads to a reduction in the DM of HGs and exhibits an excessive rate of sucrose related to a decrease in its transport (Xu

et al., 2017). Finally, *qua2* displays cuticle permeability without presenting any changes in cuticle structure. The cuticle permeability in *qua2* appeared to be dependent on the reduction of epidermal cell adhesion rather than on the direct effect of altered cuticle ultrastructure or cutin composition (Lorrai et al., 2021). Surprisingly, *qua2* appeared resistant to *Botrytis cinerea* (Verger, 2014; Lorrai et al., 2021), correlated with an increase of expression of the class III peroxidase AtPRX71 that contributes to their elevated ROS levels and reduced growth. Loss of AtPRX71 partially suppresses it (Lorrai et al., 2021; Raggi et al., 2015). *qua2* also exhibits altered border-like cells. Indeed border-like cells in *qua2* are released as isolated cells separated from each other, and not as a layer (Durand et al., 2009). These observations allow us to establish that QUASIMODO2 is intimately linked to cell adhesion through various processes and not only pectin defect.

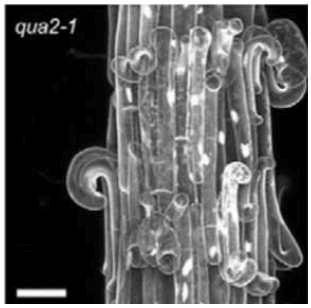

Figure B-1 **Picture of *quasimodo2* mutant hypocotyl according to (Verger et al., 2016)**

b) Glycosyltransferases

i. Galacturonosyltransferase

Other functions seem to be involved in the control of cell adhesion. Some mutants in glycosyl transferases such as QUASIMODO1 / GAUT8, exhibit a dwarf phenotype, cell adhesion phenotype, a decrease in the amount of GalA, and an abnormal “border like cells” release (Bouton et al., 2002; Durand et al., 2009; Singh et al., 2005). It was proposed that QUA1/GAUT8 and QUA2 could interact in HG synthesis (Mouille et al., 2007). Another glycosyltransferase seems to be involved in cell adhesion. EPC1, has a possible role in the metabolism of a UDP-sugar which could be incorporated into a cell wall component. The *epc1* mutant exhibits a dramatically reduced growth, defects in vascular formation, and presents reduced cell–cell adhesion in hypocotyl and cotyledon tissues (Singh et al., 2005).

ii. O-Fucosyltransferase

Another gene family has been identified to be linked with cell adhesion. The mutant in a gene encoding a putative O-fucosyltransferase GT65, *friable1,* displays a cell adhesion phenotype, spontaneous organ breakage and defective ectopic organ fusion. Unlike other cell adhesion mutants, *frb1* mutants do not have a reduced content of pectins in the cell wall. Instead, *frb1* affects the relative amounts of galactosyl, fucosyl, and O-acetyl residues of xyloglucans. Furthermore, *frb1* mutants display over expression of cell wall-related genes such as *PME41* & *EXT4* which are also up-regulated in *qua2* (Du et al., 2020; Neumetzler et al., 2012).

Recently, two studies proposed that 3 members of the Cazy family (GT106), phylogenetically linked to FRIABLE1 are rhamnosyltransferases (Takenaka et al., 2018; Wachananawat et al., 2020). Indeed, the RG-I rhamnosyltransferase activity was demonstrated using oligosaccharides GR8-PA as acceptor substrate. The corresponding mutant was showing altered mucilage release in seeds.

Because of the lack of cell adhesion mutants in Arabidopsis, our group decided to screen for suppressors of the cell adhesion phenotype of *quasimodo2* mutants to identify new genes involved in the control of cell adhesion.

Interestingly, most of the mutants described above can be restored genetically by a mutation in this gene (Verger et al., 2016). Indeed *qua2/esmd1, frb1/qua2/esmd1, frb1/esmd1* mutants present a restoration of cell adhesion (**Figure B-2**). *ESMERALDA1* encodes a putative O-fucosyltransferase (cazy family GT65), which was hypothesized to play a role in the O-fucosylation of the EPIDERMAL GROWTH FACTOR (EGF) like the domain of the cell wall receptor, Wall Associated Kinase (WAK). O-fucosylation is necessary to promote the interaction between proteins. In animals, Notch receptors interact with ligands through their epidermal growth factor. Defects in O-glycosylation affect Notch-ligand interaction and the trafficking of Notch receptor (Takeuchi & Yano, 2014). The system can also be limited by additional glycosylation of the fucose that changes the affinity of the protein (Lei et al., 2003). Based on this knowledge, it was proposed that *qua2* may lead to the release of a signal, such as oligogalacturonides which are known to have an affinity with WAKs (Kohorn et al., 2014), and mediates the cell separation once perceived. In *frb1*, the absence of WAKs fucosylation may lead to a modification such as inhibition of protein-protein interaction even in the absence of a cell wall signal and induced the loss of adhesion. Finally, the absence of O-fucosylation in *esmd1* may lead to the inhibition of the receptor interaction preventing the induction of signaling leading to cell separation (Verger et al., 2016). This hypothesis makes sense when we

know that in addition to restoring the *qua2* phenotype, *esmd1* mutation decreases FADlox gene expression, known to respond to the pectic signal (Denoux et al., 2008), and this without restoring the defect in *qua2* pectin content (Verger et al., 2016). Furthermore, recently it was shown that another member of the ESMERALDA family, AtOFT1 is required in pollen tube penetration through the stigma/style. Indeed, *oft1* mutant is defected in pollen tubes penetration leading to a reduction in seed set and pollen transmission, thus strengthening the role of O-fucosylation (Smith et al., 2018). However, (Kohorn et al., 2021) investigated the WAK1-5 locus deletion allele in *qua2/esmd1*. The WAK deletion did not affect the ability of *esmd1* to suppress cell adhesion defect, suggesting their post-translational modification is not a required component or not mediated by ESMD1. Then, the signal mediated by ESMERALDA may occur through another cell wall receptor or enhance the interaction between 2 receptors including the WAKs.

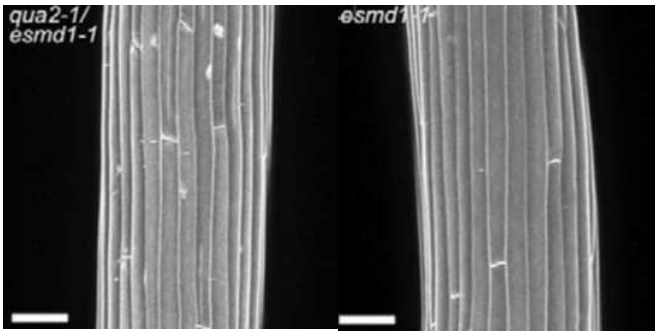

Figure B-2 **Picture of *quasimodo2/esmeralada1* and *esmeralda1* mutants hypocotyl according to (Verger et al., 2016)**

c) Other actors

In recent years, new players involved in the control of cell adhesion have been identified. Some of them have been defined as either new cell adhesion suppressors or proteins interacting with QUA1 or QUA2 or full-fledged players. Arabidopsis mutant displaying cell adhesion phenotype *elmo1* was isolated by (Kohorn, et al., 2021). *ELMO1* encodes a Golgi membrane bound protein that has no predicted enzymatic domains (DUF 1068). Apart from cell adhesion defects, the *elmo1* mutant did not exhibit significant cell wall modification. In addition, another member containing the DUF 1068 domain has been characterized and named NKS1 or ELMO4 (B. D. Kohorn, Zorensky, et al., 2021; Lathe et al., 2021). NKS1 protein is localized in the Golgi apparatus and loss of the protein results in changes in the structure and function of Golgi. *nks1* mutant exhibited reduced growth, a defect in cell adhesion, and a decrease in cell wall

pectin. Thus, it has been suggested that NKS1 interacts on the same pathway with QUA1 and QUA2 and impacts their Golgi trafficking (Lathe et al., 2021).

Besides, a new suppressor of another QUA2 allele mutant, *qua2-4*, was also isolated and identified as SABRE (SAB), which encodes a previously described plasma membrane protein required for longitudinal cellular expansion that organizes the tubulin cytoskeleton (Aeschbacher et al., 1995; Pietra et al., 2013). In contrast to *esmd1, sab* and *qua2-4/sab1* mutations increase pectin content, upregulate the expression of pectin methylesterases and extensins, and reduce cell surface area (Kohorn, et al., 2021).

Another actor, *RUBY*, encodes a member of the Auxiliary Activity 5 (AA5) family of Carbohydrate-Active Enzymes (Gal/glyoxal oxidases). RUBY has been described as Gal oxidase that strengthens pectin cohesion within the middle lamella and is required for mucilage integrity, through oxidation of RG-I Gal sidechains (Šola et al., 2019).

In plant cells, actin filaments indirectly affect cell shape by determining the transport properties of organelles and molecules that modulate the mechanical properties of the wall. In plants, the ARP2/3 complex activates the polymerization of branched F-actin and promotes actin nucleation from the side of existing actin filaments (Li et al., 2003). ARPC4 encodes a putative core subunit that controls the assembly and steady-state levels of the complex ARP2/3. *arpc4* dark-grown plants present reduced hypocotyl length like other *arp2/3* mutants. *arpc4* pavement cells had a slightly simpler shape compared with the wild type, and cell-to-cell adhesion is affected in both cotyledons and dark-grown hypocotyls (Kotchoni et al., 2009). Finally, the transcription factor *ZHOUPI* (*ZOU*) has been identified as a member of the signaling pathways that coordinate the separation of the embryo from the endosperm and the concomitant breakdown of the endosperm. Interestingly, *zou* mutant embryos have defects in cuticle formation and epidermal cell adhesion (Yang et al., 2008).

Cell adhesion is also investigated on mechanical aspects (Verger et al., 2018). These investigations provide more information on the different actors or signals which contribute to defining what governs mechanically the growth orientation, organization, plant cell morphogenesis, and the tension between two adjacent cells. (Verger et al., 2018) demonstrated the importance of epidermal continuity for mechano-perception, and this by modulating turgor pressure in the growth media which could rescue cell-adhesion defects in *qua1* possibly through a tension-adhesion mechanism connected to cortical microtubules. Finally, all these data highlighted the complex mechanism of cell adhesion which requires more studies. Thus, investigating new actors or signals remains fundamental to define the different feedback loops

which control the cell adhesion and how the different actors modulate the cell wall component leading to the cell adhesion.

2) Pectin remodeling: a fundamental mechanism in the control of adhesion

a) The different actors of remodeling: the HomoGalacturonan Remodeling Enzymes (HGME)

Enzymes modifying the pattern of HGs such as PME, PAE, PMEI, PG, and PLL are called HGME for Homo-Galacturonan-Modifying-Enzymes These enzymes have distinct activities leading to HGs remodeling depending on organs, tissues, or external environment (Sénéchal et al., 2014). Here we will be described what are the mode of action of these enzymes, their impact on development, their implication in the response to various stresses, and the actors influencing their mode of action.

i. Pectin methylesterases and their inhibitor

Pectin methylesterases (PMEs) in *Arabidopsis thaliana* belong to a multigene family (66 members). PMEs hydrolyze the C6 methylester groups of GalA residues. It leads to the production of methanol and free carboxyl groups that induces the acidification of the wall (Pelloux et al., 2007). There are 2 groups of PMEs. The 21 PMEs in group 1 (Type II) have a PME catalytic domain (Pfam01095) in the C terminal position preceded by a signal peptide and/or a transmembrane domain at the N-terminal position. The 45 group 2 (Type I) PMEs differ at the level of the PRO domain which corresponds to a N-terminal extension similar to the PMEI domain (Pfam04043) (Sénéchal et al., 2014). The secretion of type I PMEs to the cell wall may differ from the type II. Indeed, those PMEs would require correct targeting *via* the PRO domain for the export of mature PMEs to the apoplast (Bosh M & Hepler P K., 2005; Giovane et al., 2004). Type-II PMEs without the PRO-region have a similar structure as the PME of phytopathogenic organisms, such as fungi and bacteria (Pelloux et al., 2007).
The activity of PME is tightly regulated by inhibitory proteins, Pectin Methylesterase Inhibitor (PMEIs, 71 members) which control the degree of methylesterification (DM) of HGs, during interactions with pathogens or plant development and growth (Giovane et al., 2004; Lionetti et al., 2012). Protein inhibitors of plant PMEs (PMEIs) can form a stoichiometric 1:1 complex

with PMEs, leading to an inhibition of PME activity. Arabidopsis *PME3* and *PMEI7* were shown to have overlapping expression patterns in etiolated hypocotyls, acidic pH promotes the interaction of the proteins, thus impairing PME activity (Sénéchal et al., 2017). Therefore, variation of the DM affects cell wall physicochemical properties including cell wall rheology (Braybrook & Peaucelle, 2013), cell growth (Wolf et al., 2012), and cell adhesion (Francis et al., 2006). But the mechanism through which that phenomenon occurs remains obscure.

Several factors like pH, substrate, type of PME, as well as ionic environment will determine the mechanism of action of the PME. Three mechanisms of action have been described (**Figure B-3**): (i) "a single chain mechanism", where PME removes all continuous methylesters of a chain before dissociating from the substrate (Aragunde et al., 2018; Hocq et al., 2021). (ii) "a multiple attack mechanism", in which PME catalyzes the release of a limited number of methylesters on several HG chains. These two modes of action both produce de-methylesterified HG, which may allow the association of HG chains in egg box structures and increase the susceptibility to endogenous polygalacturonases. The resulting modified pattern of esterification plays a significant role in the mechanical property of the cell wall. (iii) "a multi-chain mechanism", where PMEs remove a single methylester before dissociating from GalA chains. This mode of action leads to a random de-methylesterification, which can lead to the degradation of partially de-methylesterified HGs by PGs and PLLs and the release of methylesterified oligosaccharides. Recently it was observed that pH variation leads to a modification of the mode of action. AtPME2 can go from full processivity (at pH 8), creating large blocks of unmethylated galacturonic acid, to low processivity (at pH 5). This relates to differences in the electrostatic potential of the protein (Hocq et al., 2021).

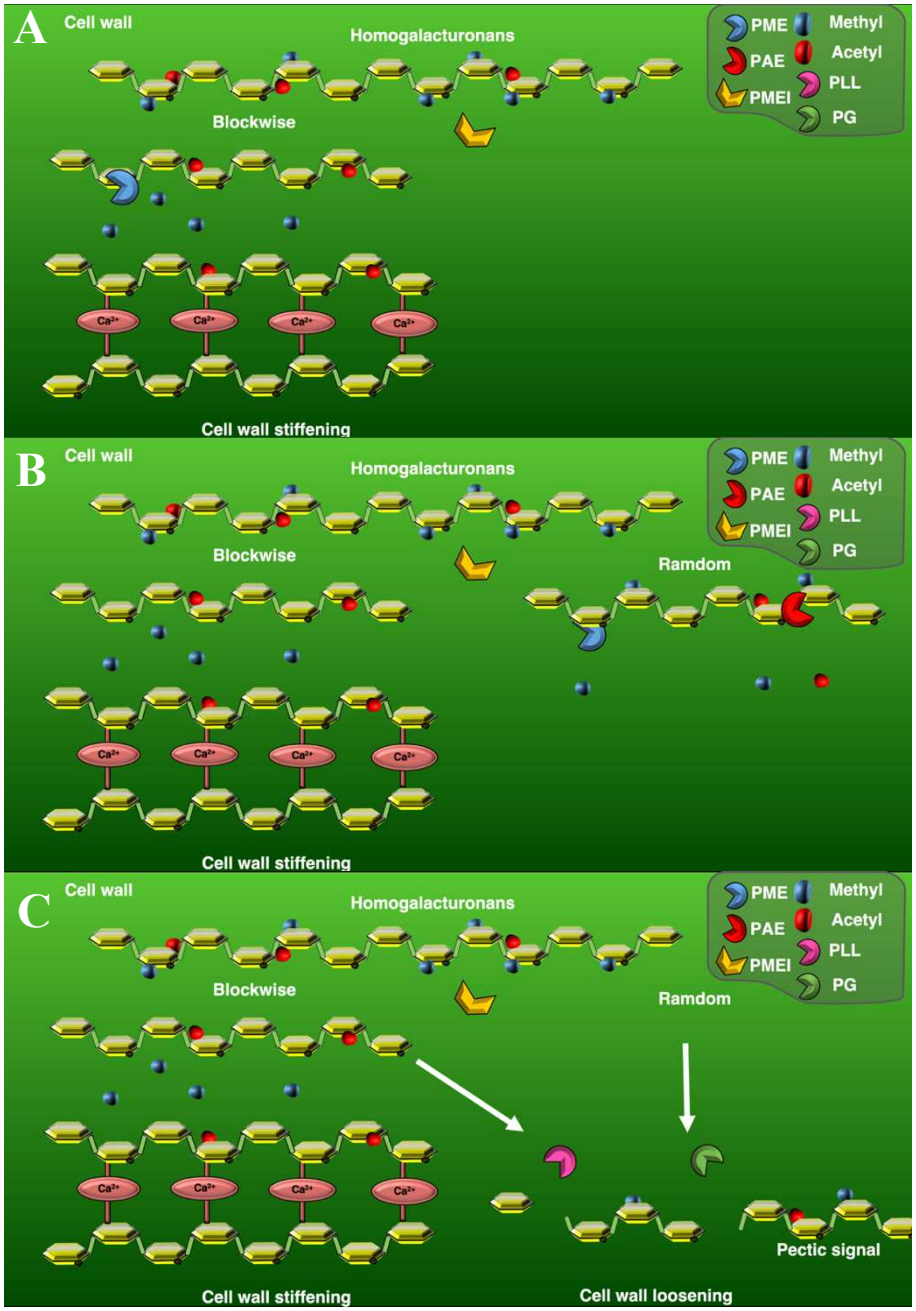

Figure B-3 **Representation of Homogalacturonans remodeling**

Blockwise de-methylesterification, PME removes all continuous methylesters of HGs backbone. This corresponds to "single chain mechanism "or "multiple attack mechanism" favorizing the eggs box formation (A). Random de-methylesterification, PMEs remove a single methylester. This corresponds to "multi-chain mechanism" (B). In both case PAE can remove acetyl. Finally, after radom or blockwise de-methylesterification PG and PLL can hydrolyzed the HGs to generate pectic signal and this corresponds to cell wall loosening.

ii. Pectin acetylesterases

Pectin acetyl-esterases (PAEs) belong to a multigene family (12 members), they have been characterized in plants, bacteria, and fungi (Sénéchal et al., 2014). PAEs hydrolyze the acetyl ester groups present on HG and RG-I at the O-2 or O-3 position. This modulation of the degree of acetylation allows modification of the morphology and plasticity of plant tissues (Orfila et al., 2012). The GalA of the HG backbone may be mono-acetylated at the O2 or O3 position but not di-acetylated (Ralet et al., 2005). In the HG backbone, the simultaneous presence of acetyl and methyl groups on the same Gal-A residues is observed infrequently but might influence either PME or PAE activities (Ralet et al., 2005). Pectin acetyl-esterase cleaves the ester bond between a glycosyl carbon and an acetyl group, thus releasing acetate from polysaccharides. The protein sequence of PAE contains a PAE domain (PfamPF03283) which corresponds to the catalytic part of the protein. Some have a signal peptide, others do not, yet none have a transmembrane domain (Philippe et al., 2017).

Few studies have been performed on the specificity of their substrate or how they act on pectin (de Souza et al., 2014; Gou et al., 2012). Acetylation can prevent HG degradation by endo-PGs (Bonnin et al., 2002), and influence cell wall viscosity (Gou et al., 2012) In contrast, deacetylation promotes gelation of HGs in sugar beet (Ralet et al., 2003). *In vitro,* the presence of acetyl groups along the HG chains strongly hinders the dimerization of pectin chains through the formation of egg-boxes, and this effect was also related to inhibition of PME activity (Ralet et al., 2003). Therefore, a synergistic effect between PME and PAE is likely to occur at the cell wall to mediate either egg box formation or degradation of HG by PGs and PLLs.

iii. Polygalacturonases

Polygalacturonases (PGs) belong to the Cazy family of glycoside hydrolases 28. This family includes endo- (EC 3.2.1.15) and exo-polygalacturonases (EC 3.2.1.67), 7 exopolygalacturonosidases (EC 3.2.1.82), rhamnogalacturonases (EC 3.2.1.171), endoxylogalacturonan hydrolases (EC 3.2.1.) and rhamnogalacturonans α-1-rhamnopyranohydrolases (EC 3.2.1.40). The GH28 family has 68 isoforms. PGs have been identified in plants, herbivorous insects, bacteria, fungi, and nematodes (Yang et al., 2018). PGs cleave the α (1-4) bonds by hydrolysis linear homopolymers of HG. Usually, their activity increases proportionally to the decrease in the DM of HG. Degradation of HGs by PGs produces oligogalacturonides (OGs) with varying degrees of polymerization. In plants, endo-PGs

particularly prefer HG with a chain region containing more than four consecutive de-methylesterified GalA residues between methylesterified GalA. Their action leads to the release of OGs. On the other hand, exo-PGs only act on the terminal positions of the HG chains and thus release monomers (Brummell & Harpster, 2001; Verlent et al., 2005).

PG activity is also inhibited by PG inhibitors (PGIP), produced by plants to inhibit the PG activity of pathogens (de Lorenzo & Ferrari, 2002; Federici et al., 2001). Plant-based PGIPs act in two modes of action: by forming a PG-PGIP complex (Federici et al., 2001; Spadoni et al., 2006) and/or by binding of PGIPs to HGs, to prevent pathogen PGs from accessing their substrate (de Lorenzo & Ferrari, 2002; N. Liu et al., 2017) but also to prevent the action of plants endo-PGs.

iv. Pectate/pectin-Lyases

PLLs belong to the polysaccharide lyase 1 (PL1) Cazy family and contain 26 isoforms. They are found in plants, bacteria, fungi, and nematodes. PLLs include pectate lyases and pectin lyases. PLLs cleave, by β-elimination, the α-1,4 bond of the methylesterified or unmethylesterified GalA units, giving rise to an unsaturated C4-C5 bond at the non-reducing end of the newly formed oligogalacturonide. Pectate lyases (PLs) have specificity for un-methylesterified or slightly methylesterified HGs; moreover, they require Ca^{2+} for their activity. Conversely, PectiN Lyases (PNL) only degrade highly methylesterified HGs and do not require Ca^{2+}. PLs have both endo (EC 4.2.2.2) and exo (EC 4.2.2.9) activities, while only endo activity (EC 4.2.2.10) has been found in PNL (Sinitsyna et al., 2007).

b) The role of HGME during the plant development

Homo-Galacturonan-Modifying-Enzymes (HGMEs) play an important role in pectin remodeling and cell wall disassembly and are therefore involved in many physiological processes including pollen germination, pollen tube growth, pollen separation cell, germination, root development, stem elongation, leaf polarity growth, leaf abscission, lateral root emergence, intercellular space formation, and fruit dehiscence (Francis et al., 2006; Guénin et al., 2011; Hongo et al., 2012; Pelletier et al., 2010). These biological processes are closely related to the control of cell separation that occurs at different times and in different places during plant development. Various models are used to observe these phenomena of cell wall remodeling:

dark-grown hypocotyl, pollen tube, or root system growth. Pectin methylesterases and their inhibitor

i. Pectin methylesterases and their inhibitor

The *PME QUARTET1* gene (*QRT1*) contributes to the release of pollen grains from tetrads during floral development (Francis et al., 2006). Moreover, an earlier study showed that *qrt1* mutation led to the production of pollen tetrad in which microspores fail to separate during pollen development (Rhee & Somerville, 1998). A similar phenotype results in failure of microspore separation during pollen development for PG mutants *qrt3* (Rhee et al., 2003). It was suggested that both PME and PG activity are necessary to separate the tetrads and that PME QUARTET1 would act in tandem with PG QUARTET3 to degrade de-methylesterified HG in the primary wall of the pollen mother cell (Francis et al., 2006). This analysis indicates that PG mediated, PME dependent, pectin degradation is a key event in cell separation during development. In another context, the role of PMEs seems to be decisive for the mechanical properties of the plant. AtPME35 is responsible for the de-methylesterification of pectins and participates in the regulation of the mechanical strength of the supporting tissue in the stems of Arabidopsis. Indeed, the *pme35* mutant exhibited a decrease in PME activity, accompanied by a deformation of the stem (Hongo et al., 2012). PME isoforms in *A.thaliana* play a role in root and hypocotyl elongation. The overexpression of *PME3* showed an increase in root elongation (Hewezi et al., 2008), while the *pme3* mutant exhibits a lower level of GalA and lower PME activity. The change in the level of activity led to modified pectin DM and affected development *via* an increase in the length of the hypocotyl and the number of adventitious roots emerging from the hypocotyls (Guénin et al., 2011). *PME17* was strongly co-expressed and processed with a subtilisin-like serine protease *SBT3.5* to release a mature apoplastic isoform of PME involved in root development and response to various stresses (Sénéchal et al., 2015). In another context, the exogenous application of H_2O_2 increases the rice cell expansion and root diameter by enhancing the PME activity leading to reduce the level of methylesterification (Xiong et al., 2015). PMEs also act on other processes such as mucilage secretion or embryonic development. Thus, *PME6* is abundant during mucilage secretion and acts on the morphology of the embryo and the extrusion of the mucilage (Levesque-Tremblay et al., 2015). In addition, *PME58* is specifically expressed in secretory mucilage cells and plays a role in the structure and organization of the mucilage (Turbant et al., 2016).

The control of DM by the PMEIs plays a key role in the regulation of growth and the development of organs. A PMEI from Arabidopsis, *AtPMEI4*, is involved in regulating hypocotyl growth (Pelletier et al., 2010). Growth acceleration of dark-grown hypocotyls requires significant cell wall remodeling, which is associated with transcriptional upregulation of pectin-modifying genes. A study on hypocotyl grown in the dark demonstrates that growth acceleration was delayed by 3 H and 5 H in pPMEI4::GFP and p35S::PMEI4:GFP transgenic lines respectively, suggesting that the PME inhibitor controlling pectin de-methylesterification is essential for the timing of the growth acceleration, but not for the growth process itself (Pelletier et al., 2010). PMEIs also alter the rheology of the cell wall, as shown by the overexpression of *PMEI3* which prevents normal primordia formation in inflorescence meristems, suggesting that the de-methylesterification is necessary for the normal organ outgrowth (Peaucelle et al., 2008). Furthermore, two over-expressors have been used to follow changes in mechanical anisotropy during dark-grown hypocotyl elongation. Interestingly in *PME5oe* and *PMEI3oe* lines, the overall stiffness of the cell wall was reduced and increased respectively, and in both lines, the mechanical asymmetry was broken (Peaucelle et al., 2015). In addition, the overexpression of *PMEI5* had dramatic effects on plant growth, including a drastic reduction of dark-grown hypocotyl length (Wolf et al., 2012). Conversely, a *pmei4* mutant with elevated PME activity in Arabidopsis root cell walls, showed an increase in root length suggesting a correlation between increased de-methylesterification and increased growth (Sénéchal et al., 2015). It should be noted that compensation phenomena between isoforms within gene families encoding PMEs and PMEIs or PGs may occur (Hocq et al., 2017; Hocq et al., 2021). We still have very little information on how most PMEs and PMEIs are specifically regulated. However, their role as an actor of plant development remains fundamental.

ii. Pectin acetylesterases

As the de DM, the acetylation of pectins affects the development. PAE8 and PAE9 have been characterized and shown pectin acetyl-esterase *in vitro* activity on acetylated pectin. Lack of function of both genes leads to reduced inflorescence growth and an increase by 20 % the amount of acetate in the wall, and 40 % in the double mutant, suggesting a distinct preference substrate for both PAE (de Souza et al., 2014). High deacetylation affects the biophysical and physiological properties of the cell wall polysaccharides leading to some drastic effects. Indeed, overexpressing *Populus trichocarpa PAE1* in *Nicotiana tabacum* decreased the level of acetyl esters of pectin but not of xylan, resulting in a defect in cellular elongation of floral styles and

filaments, the germination of pollen grains, and the growth of pollen tubes (Gou et al.,2012). Moreover, the effects of acetylation on mechanical properties were investigated. A mung bean (*Vigna radiat*) pectin acetyl esterase heterologously expressed in tubers of *Solanum tuberosum* led to a 39 % decrease in the degree of acetylation (DA) of the tuber cell wall (Orfila et al., 2012). This team also investigates the effect of de-acetylation of cell wall polymers and tuber mechanical properties. The tuber tissue was subjected to uniaxial mechanical compression and the results suggested that de-acetylation contributed to stiffer tuber tissue and cell wall matrix (Orfila et al., 2012).

iii. Polygalacturonases

PGs have been implicated as positive regulators of cell separation, fruit ripening, abscission, cell growth, and dehiscence. PG is required for organ separation by cell separation *via* dissolution of the middle lamella which corresponds to cell adhesion disruption. In the case of PG, QUARTET2 (QRT2) and QUARTET3 (QRT3) are necessary for the separation of pollen grains (Rhee et al., 2003; Sun et al., 2010), and QUARTET2, with ARABIDOPSIS DEHISCENCE ZONE POLYGALACTURONASE1 and 2 (ADPG1 and ADPG2) are also involved in the dehiscence of anthers (Ogawa-Ohnishi et al., 2013). PGs have been reported to play a central role in the modifications of the HG network associated with fruit abscission (Swain & Smith, 2011). PGs are also involved in silique dehiscence in Arabidopsis and Brassica (Sander et al., 2001) and silique development accompanied by an increase in PME activity which reinforces the interconnected roles of PME and PG (Louvet et al., 2011). POLYGALACTURONASE INVOLVED IN EXPANSION (PGX1) and (PGX2) function in cell expansion; overexpressing them result in enhanced hypocotyl length and rosette leaf area ((Xiao et al., 2014, 2017). In addition, plants either overexpressing or lacking *PGX1* display alterations in total polygalacturonase activity, pectin molecular mass, and higher proportions of flowers with extra petals suggesting a key role in floral organ patterning (Xiao et al. 2014). PGX2 seems to be implicated in the mechanical properties of the stem in overexpressed lines (Xiao et al. 2017). Different from the two previously characterized PGX, PGX3 functions in seed germination and contributes to the elongation of etiolated hypocotyl and root in young seedlings (Rui et al., 2017). Furthermore, this gene also contributes to normal stomatal development. Some cell adhesion defect phenotypes correlated with PG mutation or overexpression were demonstrated like in rice and apple. The overexpression of a PG1 subunit, *OsBURP16*, decreased cell adhesion and overexpression of *PG* in apple caused premature leaf

shedding due to reduced adhesion in the abscission zone (Atkinson et al., 2012; H. Liu et al., 2014). Recently a couple of studies show the importance of PGs membership in the maintenance of cell adhesion. Indeed, a PG of *Arabidopsis*, *PGLR* is strongly expressed in secondary root initiation. On the other hand, the exogenous application of this enzyme caused a dramatic cell adhesion defect on hypocotyl dark -grown (Tabi et al., 2021 Cell Wall Meeting). These discoveries highlight the potential link between the role of HGME in controlling adhesion during development.

iv. Oxidases

Berberine-bridge enzyme-like (BBE-like) proteins are present in plants, fungi, and bacteria. The *Arabidopsis thaliana* genome has recently been shown to contain genes encoding 28 BBE-like proteins while exhibiting four distinct active site compositions (Daniel et al., 2016). Among the BBE type enzymes, some of them are present in reactions such as the oxidation of mono and polysaccharides. Recently, at least four BBE-like enzymes in Arabidopsis have been shown to be OG oxidases (OGOX1–4). Oxidized OGs exhibit a reduced ability to activate immune responses and are less hydrolyzable by fungal polygalacturonases. Moreover, one of them OGOX, displays maximal activity on OGs with a degree of polymerization >4 (Benedetti et al., 2018).

c) The role of HGMEs in response to stress

During the development, the plant will be subjected to various stresses which will affect its growth and its nutrition. In this context, the cell wall represents the first physical barrier of the plant having a key role in its response to various stresses. We can distinguish abiotic and biotic stresses. The abiotic stresses encompass various unfavorable environmental conditions, such as drought, salinity, temperature, nutrient deficiencies (le Gall et al., 2015). Conversely, biotic stresses are caused by infectious living organisms such as parasitic plants, bacteria, viruses, fungi, or nematodes ((Mitsumasu et al., 2015). Both types of stress will decrease productivity and affect plant survival. Therefore, the plant will put in place a set of morphological, physiological, and biochemical mechanisms that will allow it to avoid and/or tolerate these different stresses. The mechanisms of pectins modifications through transcriptional regulation of *HGMEs* in response to stress will be different for each pest or symbiotic relationship or changes in environmental conditions. The expression pattern of *HGMEs* also differs according to plant species, ecotype (or cultivar), and plant phenology (Sénéchal et al., 2014). The several

examples below represent a non-exhaustive list of the different roles of HGMEs in response to different stresses.

Firstly, parasites like nematodes, parasitic plants, aphids, secrete a mix of enzymes that digest the cell wall, which facilitate penetration and migration. In response, the plant will modulate the *HGMEs* expression to avoid it or adapt to it. It is known that there are common features in the infestation pattern of *Phelipanche ramosa* and nematodes (Mitsumasu et al. 2015). Indeed, it has been shown that the PME3 protein increases the sensitivity of *A. thaliana* during its interaction with the nematode *Heterodera schachtii* by binding to an effector, the Cellulose Binding Protein (CBP) which would induce modifications in the host cell wall and thus facilitate the first stages of installation of the parasite (Hewezi et al., 2008). Furthermore, infection with *Pectobacterium carotovorum* and *Botrytis cinerea* induces in Arabidopsis a rapid expression of *PME3* that acts as a susceptibility factor required for the initial colonization of the host tissues (Alessandro Raiola et al., 2018). In contrast, it has been demonstrated that *PME3* is important in the interaction between *P.ramosa* and Arabidopsis. The infested *pme3* mutant, compared to the infested wild type, showed earlier sensibility to the parasite and pectin remodeling (12 H pre-infestation), correlated with an increase in the expression of *HGMEs* genes including for example *PME18* and *PAE7*, the latter remaining induced 14 days after infestation. This result correlates with a modification of the methylesterification pattern in the presence of the parasite in post-infestation. It suggests *PME3* protein may play a role in the resistance to *P. ramosa* (Grandjean, unpublished data 2018). In addition, Orobanche sp. is known to secrete PMEs and their activity is correlated with the localization of low esterified HG in the cell wall and the middle lamella at the site of contact between host and parasitic cells, probably to promote cell separation of the host plant by cleavage of pectin by pathogen hydrolases enzymes and facilitate the haustoria development (Losner-Goshen et al., 1997). These experiments show the potential implication of one PME in response to different pathogens that do not lead to the same effects, highlight the versatility of one PME isoform. Recently it has been shown that *PME17* expression and activity participate in the activation of defense responses mediated by jasmonic acid (JA) and ethylene (ET), such as *PLANTDEFENSIN1.2 (PDF1.2)* a marker for the JA–ET signaling pathway, against *B. cinerea*. In addition, *PME17* performs a blockwise pectin de-methylesterification leading to pectin precipitation due to calcium-mediated egg-box formation and contributing to a stiffer pectic material (del Corpo et al., 2020).

Other HGMEs take a part in the maintenance of cell wall integrity and plant immunity, such as PMEI. The infestation by aphids, during the early stage of the plant-pathogen interaction, would induce an increase in the total PME activity, associated with a decrease in the degree of methylesterification of HG. In contrast, the exogenous inhibition of PME activity led to a significant alteration of the aphid preference, suggesting a crucial role of PMEI in response to the infestation. Indeed, *pmei13* mutants are more susceptible to *Myzus persicae* in terms of attachment preference and feeding (Silva-Sanzana et al., 2019). This crucial role was highlighted also upon the infestation with *B. cinerea*. *PMEI10, PMEI11* and *PMEI12* expression is required and triggered through different hormonal pathways and stimuli upon the *B. cinerea* infestation. Loss of function increased the infestation, thus strengthening the role of PMEI as mediator of CW integrity maintenance in plant immunity (Lionetti et al., 2017).
Polygalacturonase-inhibiting proteins (PGIPs) are known to act and reduce the aggressive potential of pathogen PGs. PGIPs activity influences PGs to form more long-chain oligogalacturonides that can induce defense responses, thereby indirectly contributing to the plant defense (de Lorenzo & Ferrari, 2002). For example, confrontation of bean plants with *Colletotrichum lindemuthianum,* causes a rapid accumulation of *PGIP* transcripts that correlates with the appearance of a hypersensitive response (HR) in incompatible interactions. A later *PGIP* transcription, correlating with the appearance of lesions, occurs in compatible interactions (Nuss et al., 1996). Resistance mediated by PGIP was demonstrated against PG from *V. dahliae* and *F. oxysporum* in cotton and Arabidospsis. On one hand, the *GhPGIP1* silenced gene cotton was susceptible to VdPG1 and FovPG1, on another hand the overexpression of *GhPGIP1* conferred resistance in Arabidopsis (Liu et al., 2017).

In the context of abiotic stress, HGMEs are also involved in plant response and cell wall remodeling. Recently, it was shown that the *PME34* gene is highly expressed in guard cells in response to the abscisic acid signal. Furthermore, *pme34* mutant exhibits a heat-sensitive phenotype related to a defect in the control of stomatal movement. Thus, PME34 seems to be required to regulate the mechanism of opening and closing of stomata in response to a given stimulus such as heat stress (Huang et al., 2017). Transgenic Arabidopsis, overexpressing a pepper *PME* inhibitor protein (*CaPMEI1*), exhibits enhanced tolerance to various stress including drought stress, during post-germination growth (An et al., 2008). Some genes have been identified as positive actors in salt stress tolerance. *PME31* expression is upregulated under salt stress conditions in Arabidopsis. Conversely, loss of function revealed a hypersensitive phenotype concomitant with the decrease in transcript levels of several stress-

related genes (Yan et al., 2018). Finally, a study demonstrated that *PMEI3* expression varies depending on the type of stress. Indeed, *PMEI3* is induced by cold but repressed by salt stress, suggesting distinct roles of genes in stress tolerance (Y. E. Chen et al., 2018)

d) The role of hormones and transcription factors in the regulation of *HGMEs* expression in the modulation of plant development and cell adhesion

During plant development, it is well known that several *HGMEs* gene expressions are modulated, directly or indirectly, by hormonal signaling and some transcription factors. Hormones linked to the transcription factors play a major role in different processes of organogenesis, cell adhesion, cell separation, and plant development. Auxin is a well-known player implicated in the event of cell separation (Kumpf et al., 2013). One study revealed that application of indole-3-acetic acid (IAA) on shoot apex of auxin-transporter *pin1* mutant, leads to rescued organ outgrowth. AFM analysis and immunolabeling of de-methylesterified homogalacturonan with monoclonal antibody 2F4 revealed that the restoration is due to reduced tissue stiffness concomitantly with pectins de-methylesterification in subepidermal tissues (Braybrook & Peaucelle, 2013). Conversely, blocking the de-methylesterification of pectin in the *PMEI3* overexpressor inhibits IAA-induced organ formation and tissue softening. This suggests that de-methylesterification of pectin triggered by an auxin signal is necessary to reduce tissue stiffness and lead to proper organ formation **(**Braybrook and Peaucelle., 2013). Treatment of Arabidopsis roots with exogenous auxin results in changes in cellular processes, including triggering lateral root formation. During the first 12 hours following auxin treatment, it has been observed an up-regulation of *PL* genes *PLA1* and *PLA2*, temporally coordinate with the lateral root formation (Laskowski et al., 2006)**.** It was suggested that those genes may participate in the degradation of the middle lamella rich in pectin, allowing the separation of the cells. In another context, different exogenous applications were performed on *quasimodo2* mutant to observe if the cell adhesion defect is related to auxin. While the different auxins NAA (Naphthaleneacetic acid) and IAA (Indole-3 acetic acid) induced a clear inhibition of the hypocotyl elongation, it did not restore the cell adhesion defect of *qua2-1*. NPA (1-N-Naphthylphthalamic), however, was, able to restore cell adhesion on the dark-grown hypocotyl, in a dose-effect manner. This nicely shows that inhibition of auxin transport is implicated in the phenotype of the *quasimodo2* mutants and so to cell adhesion (Verger, Thesis 2014). Other hormones are involved in the transcriptional regulation of *HGME*s such as brassinosteroids

(BR). BR has been shown genetically or by exogenous application to regulate some developmental and physiological processes in plants, through a BRI receptor kinase signaling pathway that controls the transcription factor BZR. BZR probably promotes homeostasis between remodeling and biosynthesis in the plant cell wall (Wolf et al., 2012). Transcriptional analysis of the mutant lines of the Arabidopsis transcription factor BZR1 showed that PME2 and PME3 are targets of BZR1 (Sun et al., 2010). (Qu et al., 2011) showed in Arabidopsis wild-type seedlings, that PME activity is increased both under chilling stress and treatment with 24-epi-brassinolide (eBL). This correlates with the upregulation of *PME41* expression. Moreover, this study demonstrated that *bzr1-1D* mutant exhibits an increase of PME activity under chilling stress associated with up-regulation of *PME41*. Thus, it was suggested that BRs signaling pathway may control the PME activity under chilling stress by regulating notably *PME41* expression and this contributes to chilling tolerance. Abscisic acid (ABA) can also participate in the modulation of pectin structure. The *sitiens* tomato exhibits an ABA defect and an alteration in the ultrastructure of the extracellular matrix including an increased rate of methylesterification of HGs that correlate with the release of original oligosaccharides when infected by Botrytis. These features participate in the resistance during inoculation with *Botrytis cinerea* (Curvers et al., 2010).

The expression of genes controlling pectin architecture is also controlled by transcription factors (TFs). Transcription factors are activators or repressors of transcriptional complex which act by binding to regulatory sequences upstream of genes to be transcribed. Thus, by modeling the expression of HGMEs, TFs will impact the cell wall *via* pectin remodeling. For example, Arabidopsis mutant*, stomatal carpenter 1 (scap1)*, develops irregularly shaped guard cells and cannot control the stomatal aperture. The loss of *scap1* led to downregulated *PME6* expression, whereas pectin methylesterases inhibitor expression was enhanced (Negi et al., 2013). *PME5* expression seems to be regulated through a dual role of transcription factor BELLRINGER (BLR) required in the establishment and maintenance of phyllotaxis. BLR transcription factor restricts *PME5* expression in primordia initiation pattern and conversely, BLR activates *PME5* in the internode, promoting the post-meristematic maintenance of phyllotaxis (Peaucelle et al., 2011). A hormonal transcription factor of the AUXIN RESPONSE FACTOR family, ETTIN (ETT), plays a crucial role in tissue patterning gynoecium in Arabidopsis by regulating *HGMEs* expression. Among several genes (Simonini et al., 2017), *PME5* and *PMEI3* are potentially regulated by ETT. Indeed, in the *ett-22* mutant, *PME5* expression is repressed, correlated with decreased PME activity leading to a significantly stiffer

gynoecium cell wall and altered valve development. In parallel, overexpression of *PMEI3* impacts the valve development as in *ett-22* (Andres-Robin et al., 2018). In another process, PMEIs are under the control of some TFs to regulate the DM of pectins. *PECTIN METHYLESTERASE INHIBITOR6 (PMEI6)* is specifically expressed in seed coat epidermal cells. *pmei6* mutant displays a delay in mucilage release. PMEI6 appears to be modulated by GLABRA2 and LEUNIG HOMOLOG/MUCILAGE MODIFIED1, as the expression of *PMEI6* is strongly reduced in *gl2* and *luh/mum1* mutant (Saez-Aguayo et al., 2013). In addition, transcription factor MYB52 has been identified as a negative regulator of pectin de-methylesterification in seed coat mucilage due to its control of *PMEI6* and *PMEI14* expression. In *myb52*, both gene expressions are downregulated, resulting in an increase of PME activity (Shi et al., 2018). Taking together these data highlights that the control of the methylesterification of HGs, through a transcriptional regulation network, is an essential step in seed coat mucilage formation.

In later plant development processes, the regulation of *PG* and *PL* expression by TF or TF related to hormones could be associated with cell separation. Lateral root development is related to INFLORESCENCE DEFICIENT IN ABSCISSION (IDA) which is a key regulator of cell separation. The expression of *IDA* is induced by AUXIN RESPONSE FACTOR7. It has been shown that after receiving a signal from IDA, the leucine-rich repeat receptor-like kinase HAESA triggers the expression of *PGLR* and *PGAZAT* and promotes the cell separation for the lateral root development (Kumpf et al., 2013). The root cap model represents a perfect example of the control of cell separation linked to adhesion. The root cap biological function is to cover the end of the root and protect it from the environment. Border-like cells (BLC) are the cells separated from the rest of the cap and released from its edge as a layer of living cells. The transcription factors BEARSKIN1/2 have been identified to bind to the *ROOT CAP POLYGALACTURONASE (RCPG)* promotor, and the activation of *RCPG* accelerates cell detachment at the root cap. Moreover, the *rcpg* and *brn* loss of function mutants, result in uncomplete cell layer detachment (Kamiya et al., 2016). Parallelly, in the same year, it has been shown that NIN-LIKE PROTEIN7 (NLP7) transcription factor controls the release of BLC. The loss of function of NLP7 leads to decreased levels of pectin and cellulose and among others, regulates the expression of a *PL* (At1g65570) and TF *BEARSKIN1&2*, resulting in BLC being released as single cells instead of an entire layer (Karve et al., 2016). Interestingly, *qua2* et *qua1* exhibited the same phenotype (Durand et al., 2009) but the expressions of *QUA1* and *QUA2* were not modulated in *nlp7* (Karve et al., 2016). Some investigations demonstrate an important link between ethylene signaling and pectin degradation. In sugarcane, it has been shown that

the RAV transcription factor, from the ethylene response factors superfamily, and endo-polygalacturonase (EPG1), has similar transcriptional patterns suggesting a key role at the initial steps of pectin degradation during aerenchyma formation. Moreover, the *EPG1* promotor contains a binding site for the transcription factor RAV, confirmed by transactivation assays leading to is repression (Tavares et al., 2019). Furthermore, apple fruit softening has been associated with an up-regulation of *POLYGALACTURONASE1 (PG1)* in both ethylene treatment and cold treatment. By a transient assay, it was shown ETHYLENE-INSENSITIVE3-like and COLD BINDING FACTOR (CBF) transcription factors were able to transactivate PG1. This highlighted a potential separate or synergic role of ethylene and cold treatment modulating PG expression in fruit softening (Tacken et al., 2010).

3) OLIGOGALACTURONIDS: CELL WALL MESSENGERS WITH MULTIPLE FUNCTIONS

Various cell wall-derived oligosaccharides are generated during plant development or in response to various environmental stimuli. This set of oligosaccharides can be defined as OliGosaccharidomes (OGomes) (Voxeur, INRA communication 2019). Among the different oligosaccharides, we will focus on oligogalacturonides (OGs). OGs are pectin fragments released following the action of different HGMEs such as PME or PAE. Their action will allow the hydrolysis of homogalacturonans by PG or PL and thus will generate OGs (Hocq et al., 2017). The particularity of OGs lies in the fact that they can trigger different signaling pathways, once associated with cell wall receptors, themselves associated with kinases that mediate different responses (Kohorn et al., 2014). For this reason, OGs are now considered as endogenous elicitors that activate the immunity of the plant, referred also to as damage-associated molecular patterns (DAMPs), and may also be involved in various developmental processes (Ferrari et al., 2013). Understanding how OGs are perceived, and the resulting signal transduced seems necessary to elucidate their role *in vivo.*

e) Sensor of the cell wall integrity mediating the transduction signal induced by Oligogalacturonids

Once OGs are released, they can bind to cell wall receptors that will mediate the signal through their kinase domain. The most well know receptor which presents an affinity with OGs, or pectins, are the Wall-associated kinases (WAK). *WAKs* expression is activated by various

environmental stimuli which seem to be required for cell expansion but also in the response to pathogens (Ferrari et al., 2013; B. D. Kohorn et al., 2014). In Arabidopsis, 5 different *WAKs* genes have been identified. The characterization of WAK structure was firstly determined by protease treatment of protoplasts and reveals that the kinase domain of WAKs was cytoplasmic while the epidermal growth factor (EGF) domain and pectin binding domain are placed in the extracellular space (He et al., 1996; B. D. Kohorn, 2016). Then WAKs were defined by their affinity for the cross-linked pectin fraction of the cell wall (He et al., 1996). This result correlates with an experiment performed on WAK1 protein that could only bind to different pectin fragments under Ca^{2+} treatment (Decreux and Messiaen., 2005). This is supported also by the finding that WAKs bind de-esterified pectins with higher affinity than those that are esterified (B. D. Kohorn et al., 2009). However, an experiment suggests that WAK's affinity with OGs is possible (Denoux et al., 2008). Even if WAK1 expression is induced in Arabidopsis seedlings by OGs, interestingly, none of the WAKs is transcriptionally upregulated by FLAGELLIN22 a microbe-associated molecular pattern (MAMP) (Denoux et al., 2008). Besides, OGs and FLG22 trigger a rapid response characterized by the activation at the early stage of many defenses signaling pathways in the processes associated with jasmonic acid and salicylic acid (SA) (Ferrari et al., 2007; Zipfel et al., 2004) and induce the phosphorylation of two protein kinases activated MPK3 and MPK6 (Denoux et al., 2008). A study on *wak2-1* showed a reduction in the activation of MPK3. Furthermore, plants expressing the WAK2cTAP in a *mapk3* background had more severe growth defects than WAK2cTAP expressed in WT background, supporting the concept that MPK3 is required for downstream WAK2 signaling (Kohorn et al., 2009). In contrast, a *mpk6* mutant can suppress the effects of this dominant *WAK2* mutation, suggesting distinct responses of MPK3 and MPK6. Arabidopsis also contains 21 other receptor-like proteins, named WAK-Like, whose extracellular domains show little sequence similarity to the WAKs except for the presence of both conserved and degenerate EGF repeats, and their kinases are similar (Verica & He, 2002). Recently, a study characterized WAKL and their potential signal mediation through hormonal signals. *AtWAKL10* expression could be induced by exogenous ABA, JA, and SA, and the loss-of-function showed precocious senescence (Li et al., 2021). Otherwise, other receptors were identified and revealed their role in signaling pathways that control developmental mechanisms, response to the environment, and are members of the leucine-rich receptor kinase family, including THE1, FER, HERK, ANX, and RLP44. For example, HERKULE, FERONIA and RLP44 were identified to be linked to BRs signaling pathway and required for cell elongation (Guo et al., 2009; Wolf & Höfte, 2014).

f) OGs responses

Several studies provide further evidence of the pleiotropic role exerted by these oligosaccharides on plants. Besides, the phytopathogenic interaction and various exogenous applications demonstrate their elicitation capacity and thus confirmed their role as essential elicitors in response to stress. Eliciting effect of the OGs was observed on several types of tissues or plant processes. Induction of tomato fruit ripening by induction of ethylene was found to be mediated by OGs in the size range of DP 4 to DP6 (Simpson et al., 1998). Tests carried out on shoots of celosia (*Celosia argentea* L.) by (Suzuki et al., 2002) showed that their growth was improved in the presence of polygalacturonic acid of DP 8. It has been demonstrated in cell suspensions of Arabidopsis that the application of pectin egg-box induces extracellular alkalinization and enhances their binding to Wall Associated Kinase 1 (WAK1) (Cabrera et al., 2008). Induction by oligomers of chitosan and egg box was studied in Arabidopsis cells (Cabrera et al., 2010). This study made it possible to demonstrate a combined emergency signal, comprising a signal linked to the degradation of the cell wall and another concerning the presence of pathogens. This combined signal is much stronger when the components chitosan oligomers and egg box are associated compared to the components tested individually (Cabrera et al., 2010). The role of trimers was demonstrated by inhibiting growth in Arabidopsis after application. Treatment with trimers or longer OG improves the resistance to the necrotrophic pathogen *P. carotovorum* in Arabidopsis 24 H post-infection. In fact, the expression of *WAK1* receptor was significantly upregulated by the trimers and even more by the long-OG mixture (Davidsson et al., 2017; Sinclair et al., 2020). In another study, it has been shown that trimer is a trigger signal for elongation in the dark (Branca et al., 1998; Sinclair et al., 2017). In another context (Branca et al., 1988) demonstrated an antagonistic response between OG and IAA. This study showed that auxin-induced elongation in pea stem segments is competitively inhibited by OGs. OGs can also inhibit auxin-induced root formation in tobacco (Bellincampi et al., 1993). Another antagonist action was revealed in tobacco. The OG-induced activation of stomatal mitosis was reduced by exogenously added indole-3- acetic acid (IAA). Oligogalacturonides also enhanced wall thickness. OGs are also involved in the response to pathogens. Thus, a study highlighted that two OGs are linked to the infestation of *B.cinerea*. Firstly, $GalA_2Ox$ is accumulated at the late stages of the infection suggesting the OG oxidase action in post-infection. Secondly, a semi-purified fraction enriched in GalA4MeAc-H_2O activates the plant's defense mechanisms against an attack by *Botrytis cinerea* (Voxeur et al., 2019).

Objectives

Previous studies performed in our lab did suggest that the maintenance of cell adhesion is controlled through a loop that includes various mechanisms: **cell wall signaling, signal transduction and cell wall remodeling**. Our goal here was to identify actors involved in these three steps.

Plant material and growth condition

The *Arabidopsis thaliana* line used for these experiments is the Columbia ecotype (Col0). The mutant *qua2-1* is a mutant resulting from EMS mutagenesis. It results of SNPs at position +2389 (C to T) of the *QUASIMODO2* gene (At1g78240) encoding a pectin methyltransferase (Du et al., 2020), causing a stop codon in exon 7 (Mouille et al., 2007). The mutant *esmd1-1* is an EMS mutant and results of SNPs at position +1363 (G to A) of the *ESMERALDA1* gene (At2g01480) encoding a putative o-fucosyltransferase. This modification of the coding sequence causes the modification of an amino acid at position 455th of the protein ESMARALDA1 (Alanine to Threonine). The last mutant used is the double mutant *qua2-1/esmd1-1* (Verger et al., 2016).

The *Arabidopsis thaliana* seeds were sterilized for 5 minutes with a solution of 0.1 % bayrochlore in ethanol (96 °), under agitation. The solution is then removed and replaced with 96 ° ethanol for a few seconds to remove the remains of the first solution. Seeds are left to dry under a laminar flow hood overnight.

The *Arabidopsis thaliana* seedlings (150 seeds/genotypes) were grown in the dark at 21 °C on a solid medium Duchefa (1.1 g/L supplemented with $CaNO_3$ 0.328 g/L, and 7.5 g/L of agar) at pH 5.7. This medium was only used for the endogenous OGs analysis. Otherwise, the *Arabidopsis thaliana seedlings* were grown on liquid medium H_2O ultra-pure, supplemented with 0.5 g/L of MES (Duchefa M1503.0100) buffered at pH 5.7 by adding KOH 0.04 M to stabilize it. For treated conditions, the liquid medium final concentration used was 500 µM of galacturonic acid, hydrogen peroxide, or glucuronic acid. To synchronize the germination, seeds were cold treated for 48 h. Seeds were exposed to light for 4 h and then the plates were wrapped in 2 layers of aluminum foil and cultivated for 92 h. To not disturb the dark grown condition, all cultures were harvested in a dark room under green light.

Cell adhesion visualization and Tortuosity quantification

50 dark grown etiolated seedlings per genotype were stained with 0.5mg/ml ruthenium red for 2 min (Verger et *al.,* 2016) after removing the liquid medium. Samples were washed twice with water. Images of 4 or 5 hypocotyls were acquired for each condition using an AXIOZOOM V16 ZEISS.

Tortuosity quantifications were performed according to the following procedure. Pictures are converted in Image J software by splitting the channels and keeping the green one. Then the picture is open in Photoscape X to improve the sharpness of the object's image (*Sharpness 100*

% & 0 Gain to improve the shape). Pictures were converted in Image J software following the process: Conversion 8bit, Threshold filter Huang, to get a binary image, analyze particle to get the contour of the shape. Then binary images are analyzed using code of MATLAB software according to (Driscoll et al., 2012; Preetham Manjunatha, 2022). The parameter we used to determine the cell adhesion defect was tortuosity. Tortuosity is a property of a curve that is meandering, around the shape here.

Cuticle visualization

Etiolated seedlings were staining with solution [0.05 % (w/v) Toluidine Blue + 0.4 % (v/v) Tween-20] for 2 minutes. The staining solution was poured off and plates were immediately rinsed gently by flooding under a running tap until the water stream was no longer visibly blue (1-2 minutes). For imaging, samples were placed on a solid agar medium. Images were acquired using an AXIOZOOM V16 ZEISS.

Crosslinked protein staining

Staining was performed as described by (Mellersh et al., 2002) & (Asselbergh et al., 2007). Two biological replicates of about 10 four days dark-grown seedlings were harvested and directly placed in ethanol 96 % for 1 h at 80 °C to fix the sample. Samples were placed in 1 % SDS at 80 °C for 24 h and stained with 0.1 % Coomassie Blue in 40 % ethanol/10 % acetic acid for 30 min and subsequently washed 3 times in 40 % ethanol/10 % acetic acid. Pictures were performed with AXIOZOOM V16 ZEISS.

Endogenous OGs extraction

4 biological replicates of 150 four days old dark-grown seedlings per genotype were dissected in a dark room to keep only the hypocotyl. Note that each biological replicate is spaced a minimum of one week and up to one month. Then, hypocotyls were separated by 50 per tube and directly placed in liquid nitrogen. 300 µl of ethanol 70 ° were added to each tube and placed in a thermomixer at 80 °C for one hour. OGs extracted containing in ethanol were pooled in the same tube and dried in a speed vacuum concentrator at room temperature. The obtained pellet was re-suspended by pipetting in 100 µL of ultra-pure water and centrifugate a 13000 rpm for 10 min. The soluble fraction was transferred in a vial and 10 µl was injected for MS analysis explained in “OG characterization and quantification”.

Enzymatic fingerprinting of pectins and xyloglucans

The fine structure of pectins was determined using the following strategy. First, 4 biological replicates of approximately 300 seedlings cultivated in the dark over 4 days were harvested in a dark room and placed directly in 1ml of ethanol 96 °C. Note that each biological replicate is spaced a minimum of one week and up to one month. Tubes were placed in a thermomixer for 30 min. After discarded the ethanol, the first step is repeated for 20 min. The ethanol is removed and replaced by 1ml of acetone and then placed in a thermomixer for 20 min at 25 °C, this step is repeated 2 times. The hypocotyls were dried in a speed vacuum concentrator at room temperature overnight. Then dry weight was measured for each sample between 1 & 2 mg. Samples were digested with 2,6 U/per sample of *Aspergillus acuelatus* endo-polygalacturonase M2 or Endo-cellulase (Megazyme, Bray, Ireland) in 50 mM ammonium acetate buffer pH 5 at 37 °C for 18 h. Then a heating at about 80 °C for 5 min was done to inactivate the enzyme. Samples were centrifuged a 13000 rpm for 10 min, then the digested fraction was transferred in vial and 10 µl was injected for MS analysis.

OGs characterization and quantification by LC/HRMS analysis

The endogenous OGs and the OGs released from the digestion were analyzed using the protocol according to (Voxeur et *al.,* 2019), using High-performance size-exclusion chromatography (HP-SEC). Chromatographic separation was performed on an ACQUITY UPLC Protein BEH SEC Column (125Å, 1.7 µm, 4.6 mm X 300 mm, Waters Corporation, Milford, MA, USA) coupled with guard Column BEH SEC Column (125Å, 1.7 µm, 4.6 mm X 30 mm). Elution was performed in 50 mM ammonium formate, formic acid 0.1 % at a flow rate of 400 µl/min and a column oven temperature of 40 °C. The injection volume was set to 10 µl. ESI MS-detection was performed in negative mode with the end plate offset set voltage to 500 V, capillary voltage to 4000 V, Nebulizer 40 psi, dry gas 8 l/min and dry temperature 180 °C. Compass 1.8 software (Bruker Daltonics) was used to acquire the data. Mzmine 2.53 software was used to analyzed data according to (Pluskal et al., 2010). The integration process applied is the following: The mass detection with a filter noise level set to 500. The ADAP Chromatogram Builder was used (Myer et al., 2017) with the following parameters: Range: 6 - 9,60 min, min group size of scan 10, group intensity threshold 1500, min highest peak 1000, and m/z tolerance 0.01 or 10 ppm. The chromatogram peaks were deconvoluted (by Baseline cut-off with the baseline level at 300). Chromatograms were deisotoped (with an m/z tolerance 0.01 or 5 ppm, retention time

tolerance 0.1, maximum charge of 2 and representative isotope the most intense). Then peaks were aligned (with an m/z tolerance 0.01 or 5 ppm, retention time tolerance 0.1, and the same weight for m/z and retention time 1). Finally, a gap-filled peak finder was performed (with an m/z tolerance 0.01 or 5 ppm, retention time tolerance of 0.1 and an intensity tolerance of 20 %). The peak area was exported at the end.

RNA extraction and RT-QPCR analysis

5 biological replicates of approximately 150 seedlings cultivated in the dark over 4 days were harvested in a dark room. Note that each biological replicate is spaced by a minimum of one week and up to 5 months. The dark grown seedlings are dried for 5 sec on absorbent paper placed in a tube and then frozen in liquid nitrogen. After grinding the hypocotyls, total RNA isolation was carried out with the RNeasy plant mini kit (Qiagen) according to the manufacturer's instruction and with the on-column DNA digestion using Rnase-Free DNase (Qiagen). The amount of total RNA obtained is assayed using NanoDrop. The purity of the RNAs is estimated by measuring the ratio of the absorbances at (A260 nm / A280 nm) and (A260 nm / A230 nm). The ribosomal ARN 28S was also checking by gel electrophoresis. 2 µg of total RNA was synthesized using Reverted H minus enzyme, according to the manufacturer's instructions Thermofisher. The device used for these experiments is the Light Cycler® 480 System (ROCHE). Each reaction is carried out in microplates (384 wells) filled by the TECAN robot. 2 technical replicates were carried out for each biological replicate. For this a mix is prepared for each cDNA sample tested. It contains 960 µL of SYBR green Master Mix (ROCHE), 520 µL of autoclaved ultra-pure water and 20 µL of cDNA sample (obtained from 2 µg of RNA). The robot will dispense in each well 2 µL of primers (sense and anti-sense primers, 2.5 µM) and 7.2 µL of the previous mix. The plate is heat-sealed with a Clear Seal film (Thermo Fisher) then centrifuged at 1350 rpm for 30 sec before being placed in the Light Cycler® 480. For each RT-qPCR experiment, the best 2 stably expressed references of 8 genes used in this study were selected using GENORM software. They were used as internal controls to calculate the relative expression of target genes.

Clathrin (At5g46630, -FW-5'GTTTGGGAGAAGAGCGGTTA-3' and -REV-5'CTGATGTCACTGAACCTGAACTG-3')

APT1 (At1g27450, -FW- 5'GAGACATTTTGCGTGGGATT 3'

and -REV-5'ATTTTAAGTGGAACA-3').

The normalized relative expression was determined according to the method described in (Taylor et al., 2019). The mean CP values for targeted and references genes from each samples' technical replicates were calculated (1). The average of biological replicates in the control group (Col0) for targeted and references genes was determined (2). Then the relative difference (ΔCP) was assessed and corresponds to subtraction (1)-(2) for each sample within each targeted or reference gene. The relative quantities were calculated from 1+PCR efficiency (E)^(ΔCP). The normalized relative expression (equivalent to ΔΔCP after log transformation) per sample were calculated by dividing the relative quantity of given genes targeted/sample by the geometric mean of the relative quantities of two or more reference genes. The average normalized expression of the samples is computed for each biological group and then perform statistical analysis based on the log-transformed normalized expression per sample.

Gene name	Forward primer sequence	Reverse primer sequence
PME53 (At5g19730)	5'-TTTGTATCTTGGGAGGGCATGGG-3'	5'-ACTGCCCATAGAACACCGTCATC-3'
PME41 (At4g02330)	5'-TACATCGCCGAACTTCGTTGCC-3'	5'-GCTTCTCTGGTCCAGCGGTATTTC-3'
PME35 (At3g59010)	5'-CCGCCATGGGAGATGGATTCATAG-3'	5'-AGTTTGGTCCGGCACTGTTCAC-3'
PMEi4 (At4g25250)	5'-AAACGGCATGCAACTCAACAAC-3'	5'-CGGACTTGATGGTGGAGGAATAGG-3'
PAE7 (At4g19410)	5'-ATGCGAGCATTGTCACCGGTTC-3'	5'- CCGACTGCTTTCGCAATTCTCG-3'
PAE12 (At3g05910)	(Phillipe et al., Unpublished)	(Phillipe et al., Unpublished)
BBE24 (AT5G44380	5'AGATTCAGTACTCGGTGACTTGGC-3'	5'ACACGTAAGGTCCCGCAACTTC-3'

BBE5 (AT1G26400)	5'-TGGTTGGACGCAAAGGAAACAGAG-3'	5'-ACACGTAAGGTCCCGCAACTTC-3'
OGOX2 (AT4G20840)	5'- AGATTCAGTACTCGGTGACTTGGC-3'	-5'-ACACGTAAGGTCCCGCAACTTC-3'
OGOX1 (AT4G20830)	5'-CGGTTGATCCCGGGAATTTCTTC-3'	5'-TCAGGCAACAACATTCCCTTCTC-3'
OGOX3 (AT1G11770)	5'- AGCATCGGTTGTGGCTCTCTTC-3'	5'- ACCAAGCTCCGGGAATTCTTTGG-3'
OGOX4 (AT1G01980)	5'-ACCCGGGCACTGATGTTGAAAG-3'	-5'- TCACGAAAGGAGCCATGTAGCTG-3'
BBE11 (AT1G30730)	5'- ACTTTAGTCAACGGTGCAAAGCC-3'	5'- ACCCGCCAAGATTCATCCCAATG-3'
EXT3 (AT1G21310)	5'- CACCACCACCAAAGAAACATTACG-3'	5'- AGAGTAGTGCTTAACCGGAGGAG-3'
EXT4 (AT1G76930)	5'- ACTACTCACCTCCACACCAACC-3'	5'- GTGTATCGTCGTCGACTCCATTAG-3'

Tableau 1 List of primers used for qPCR

Analysis of monosaccharides

The monosaccharides of the cell wall were analyzed with the protocol according to (Clement et al., 2018). Four biological replicates of approximately 300 seedlings cultivated in the dark over 4 days were harvested in a dark room and placed directly in the 96 ° ethanol for 1 h at 80 ° C to fix the sample. After removing the ethanol, the first step is repeated for 20 minutes. 1 ml of acetone is added and the tubes are placed in a thermomixer for 20 min at 25 ° C., this step is repeated twice. The cell walls are then dried in a high vacuum concentrator at room temperature overnight. 1 mg dry cell wall previously weighed is resuspended in 400 L of TFA (2 M, freshly prepared), and incubate at 120 ° C for 1 h in a heat block in 1.5 mL screwcap tubes. Then samples were centrifugated for 10 min. The supernatant was transferred and dried in a speed vacuum concentrator at room temperature.

Derivatization: after adding 10 µl of 20 mg/ml methoxamine in pyridine to the samples, the reaction was performed for 90 min at 28 °C under continuous shaking in an Eppendorf thermomixer. 50 µl of N-methyl-N-trimethylsilyl-trifluoroacetamide (MSTFA) (Sigma M7891-10x1 mL) were then added and the reaction continued for 30 min at 37 °C. After cooling, 45 µl were transferred to an Agilent vial for injection.

Data processing: Raw Agilent datafiles were converted in NetCDF format and analyzed with AMDIS http://chemdata.nist.gov/mass-spc/amdis/. A home retention indices/ mass spectra library built from the NIST, Golm, http://gmd.mpimp-golm.mpg.de/ and Fiehn databases and standard compounds were used for metabolites identification. Peak areas were also determined with the Targetlynx software (Waters) after conversion of the NetCDF file in masslynx format. AMDIS, Target Lynx in splitless and split 30 modes were compiled in one single Excel file for comparison. After blank mean subtraction, peak areas were normalized to Ribitol and dry weight.

Absolute quantification: A response coefficient was determined for 4 ng each of a set of monosaccharides, respectively to the same amount of ribitol. This factor was used to give an estimation of the absolute concentration of the metabolite in what we may call a "one point calibration".

Cloning and Protein expression

The coding sequence of *PME53, PAE7 &12* without their signal peptide and codon optimization was synthetized and cloning by PROTEOGENIX company (Oberhausbergen, France, http://www.proteogenix.fr) into pPICZαB α-factor (Invitrogen) with EcoRI and NotI restriction enzymes (marque des enzymes) Otherwise, for the other genes (PME 41, 35 & PMEI 4, FADlox) the cloning protocol was performed according to (Lemaire et *al.,* 2019) with the appropriate primers. After E. coli TOP10 (Invitrogen) transformation, recombinant plasmids were linearized with PmeI NEW England Biolabs enzyme and were inserted into X-33 P. *pastoris* (Invitrogen) for protein expression. The culture media were prepared according to the protocol from the Pichia Protein Expression Kit (Invitrogen). The transformed *P. pastoris* strain was grown overnight at 30 °C in baffled flasks in 10 ml of buffered glycerol–complex medium. Cells were then collected by centrifugation and resuspended to an OD600 of 1.0 in 100 ml of buffered methanol complex medium. A final concentration of 0.5 % (v/v) methanol was maintained every 24 h for induction. Supernatants are recovered after centrifugation (1 500×g, 8 min, 4 °C) and filtered with GD/X0.45 µm PES filter Media (Whatman, Maidstone, United Kingdom). 50 mL were concentrated to 500 µL with an Amicon Ultra Centrifugal filter with a

10 or 3 kDa cut-off (Merck Millipore, Burlington, Massachusetts, United States). Buffer exchange of concentrated protein was performed using PD Spintrap G-25 column (GE Healthcare). The buffer used was H_2O buffered to pH 5.7 with MES.

Phenotypic effects of PME41, PME35, PME53, PMEI4 enzymes on Col0 and *qua2-1/esmd1-1*

20 µL supernatant containing the enzyme was applied at 48 h after the start of the culture on 2 biological replicates of approximately 50 seedlings cultivated in the dark over 4 days. Enzyme effects on cell adhesion were phenotyping by ruthenium red staining.

Enzymatic fingerprinting of PME41, PAE7 & 12 enzymes on Col0 and *qua2-1*

40 µl of washed supernatant containing the enzyme was applied at 48 h after the start of the culture on 3 biological replicates of approximately 300 seedlings cultivated in the dark over 4 days. Samples were harvested in a dark room and placed directly in 1 ml of ethanol 70 °C. Tubes were placed in a thermomixer for 1h. After removing the ethanol, the first step is repeated for 20 minutes with ethanol 96 °C. 1 ml of acetone is added and the tubes are placed in a thermomixer for 20 min at 25 ° C, this step is repeated twice. The cell walls are then dried in a high vacuum concentrator at room temperature overnight. Dry weight was measured for each sample between 1 & 2 mg. Samples were digested with 2,6 U/per sample of *Aspergillus acuelatus* endo-polygalacturonase M2 (Megazyme, Bray, Ireland) in 50 mM ammonium acetate buffer pH 5 at 37 °C for 18 h. Then a heating at 80 °C of 5 min was done to inactivate the enzyme. Samples were centrifuged a 13000 rpm for 10 min, then the digested fraction was transferred in vial and 10 µl was injected for MS analysis. The control used for this experiment was the empty vector pPICZαB α-factor supernatant.

Protein deglycosylation

For enzymatic deglycosylation, proteins concentrated were treated with peptide-N-glycosidase F (PNGase) at 37 °C for 1 h according to the supplier's instructions (New England Biolabs) and then analyzed by SDS-PAGE and Western blot.

SDS PAGE and Western Blot analysis

The recombinant proteins are separated by SDS-PAGE (sodium dodecyl sulfate-polyacrylamide gel electrophoresis). The separation gel 12 % is composed of 30 % acrylamide / bis-acrylamide (37.5 / 1; v / v; volume / volume), 1M Tris HCl pH 8.8, 10 % SDS, 10 % ammonium persulfate (APS) and TEMED (N, *N*, *N*′, *N*′-tétramethylethylenediamine). 20 µl of concentrated protein were loaded with 5 µl of loading buffer 5 X (Tris HCl 250 mM pH 6,8, SDS 10 %, Glycerol 30 % [v/v], *β-mercaptoethanol* (*β*-ME)10 mM, Bromophenol blue 0.05 % [p/v]) and denaturated at 95 °C 10 min. After running the gel, the transfer of the proteins from the SDS-PAGE gel onto the PVDF membrane is carried out using electrophoresis in a semi-dry transfer cell (Transfert-Blot® TurboTM Transfert System, Bio-Rad), and using different buffers: a cathode buffer (25 mM of Tris pH 9.4, 40 mM of Glycine, 10% ethanol), an anode buffer I (300 mM of Tris pH 10.4, 10 % ethanol) and an anode buffer II (25 mM of Tris pH 10.4, ethanol 10 %). The SDS-PAGE gel is incubated for 15 min. in the cathode buffer. In parallel, the PVDF membrane cut to the size of the gel is incubated with gentle agitation for 15 sec in ethanol, then 2 min in MilliQ water, and finally 5 min in anode buffer II. Then the gel and the membrane are positioned on the plate of the transfer cell, between several layers of Whatman® paper (Sigma-Aldrich®, Merck) of the size of the gel, soaked in the different buffers.

Western blots were performed following this protocol. Different solutions were prepared before the binding (10 X TBS (200 mM of Tris pH 7.4 and 1.50 M of NaCl), TBS+Tween20 (1 X TBS and 0.5 % of Tween®20, Sigma -Aldrich®, Merck)). The PVDF membrane is incubated for 30 min in 4 % milk in TBS+Tween20 buffer to saturate the membrane. Then the membrane was washed for a few seconds with the TBS+Tween20. Antibody I anti-c-myc or anti-his (sigma A5598) diluted to 1/4000 in a solution of 0.5 % milk in TBST binding the membrane is incubated for 1h30 min. Antibody II anti-rabbit peroxidase (sigma A0545) diluted to 1/4000 in a solution of 0.5 % milk in TBST binding the membrane, is incubated for 2h. It is then washed for 15 min with TBS+Tween20, then 5 min in TBS+Tween20, and finally 5 min with water. The membrane is then air-dried on absorbent paper and revealed. The revelation was performed according to the protocol ECL™ Select Western Blotting Detection Reagent (GE health care). Detection was assessed with iBright Imaging Systems Thermo Fisher for 30 sec to 10 min acquisition.

Cross link quantification

First, 3 biological replicates of about 300 days-old dark grown etiolated seedlings were harvested in a dark room and placed directly in 1 ml of ethanol 96 °C. Note that each biological replicate is spaced a minimum of one week and up to one month. Tubes were placed in a thermomixer at 80 °C for one hour. After discarded the ethanol, the first step is repeated for 20 min. The ethanol is removed and replaced by 1ml of acetone and then placed in a thermomixer for 20 min at 25 °C, this step is repeated 2 times. The hypocotyls were dried in a speed vacuum concentrator at room temperature overnight. Then the dry weight was measured for each sample between 4.5 & 5.5 mg. Then hydrolysis with Hydroxy Chloride acid 6N was performed in a pyrex tube for 24 H at 120 °C. Hydrolysates were filtered on glass paper and dried in a speed vacuum concentrator at room temperature overnight. Samples were resuspended in 100 µl in a solution of acetonitrile diluted by half with ultra-pure water.

Chromatographic separation was carried out on a MACHEREY NAGEL Nucleoshell RP 18plus column (125Å, 2.7 m, 2 mm X 100 mm), coupled to a Nucleoshell RP 18 plus guard column (125Å, 2.7 m, 2 mm X 4 mm). The elution was carried out with a gradient of water with 0.1% formic acid and acetonitrile with 0.1% formic acid, with a flow rate of 400 µl / min and a column oven temperature of 40 ° C.

The injection volume was set at 5 µl. ESI MS and MSMS detections are performed in positive and negative mode with the following ionization conditions: end plate offset voltage at 350 V, capillary voltage at 4500 V, nebulizer gas flow at 30 psi and drying time at 6 l / min for a source temperature of 250 ° C.

For the MS mode, the acquisitions are carried out over a mass range going from m / z 70 to m / z 800 mass unit with a scan speed of 1 Hz.

For ESI MSMS mode in DDA (Data-dependent acquisition) mode, a scan speed is set at 1 Hz to optimize the sensitivity and the mass range from m / z 70 am / z 800 mass units with the programming of the Reference ions for the choice of MSMS in DDA (132.1395, 361.1364, 182.1076, 540.1971, 719.2550) over a collision energy range for fragmentation in the collision cell ranging from 20 to 100 eV depending on the masses selected.

HyStar 4.1 SR2 and DataAnalysis 4.4 software (Bruker Daltonics) was used for data acquisition, internal calibration from sodium formate cluster (Calibration by an HPC equation with a positive mass delta of 1.5 ppm and a negative mass delta of 0.7 ppm) and data visualization.

For the annotation of the fragmentation profiles of each "feature" the Sirius software (https://bio.informatik.uni-jena.de/sirius/) (Dührkop et al., 2021) is used with the CSI identification module: FinderID ref 3 for research in international LCMSMS databases available online (PubChem, Plantcyc, Natural Products, KEGG, GNPS)

Mucilage staining

The mucilage of mature dry seeds was extracted by gentle shaking seeds in water for 30 min. After removing the water, seeds were stained with 0.5 mg/ml ruthenium red for 2 min. After removing the ruthenium red, seeds were rinsed twice. The same protocol was performed with 50 mM EDTA replacing water at the first step.

Hormone extraction and quantification

For each sample, 10mg of dry powder of cell wal 4 day-old dark grown seedlings were extracted with 0.8 mL of acetone/water/acetic acid (80/19/1 v:v:v). Salicylic acid, indole-3-acetic acid-stable labeled isotopes used as internal standards were prepared as described in (Le Roux et al., 2014). 1ng of each standard was added to the sample. The extract was vigorously shaken for 1min, sonicated for 1 min at 25 Hz, shaken for 10 minutes at 10°C in a Thermomixer (Eppendorf®, and then centrifuged (8,000g, 10 °C, 10 min.). The supernatants were collected, and the pellets were re-extracted twice with 0.4 mL of the same extraction solution, then vigorously shaken (1 min) and sonicated (1 min; 25 Hz). After the centrifugations, the three supernatants were pooled and dried (Final Volume 1.6 mL).

Each dry extract was dissolved in 100 µL of acetonitrile/water (50/50 v/v), filtered, and analyzed using a Waters Acquity ultra-performance liquid chromatograph coupled to a Waters Xevo Triple quadrupole mass spectrometer TQS (UPLC-ESI-MS/MS). The compounds were separated on a reverse-phase column (Uptisphere C18 UP3HDO, 100*2.1 mm*3µm particle size; Interchim, France) using a flow rate of 0.4 mL min^{-1} and a binary gradient: (A) acetic acid 0.1 % in water (v/v) and (B) acetonitrile with 0.1 % acetic acid, the column temperature was 40 °C, for salicylic acid, indole-3-acetic acid and oxIAA we used the following binary gradient (time, % A): (0 min., 98 %), (3 min., 70 %), (7.5 min., 50 %), (8.5 min., 5 %), (9.6 min., 0%), (13.2 min., 98 %), (15.7 min., 98 %), Mass spectrometry was conducted in electrospray and Multiple Reaction Monitoring scanning mode (MRM mode), in positive ion mode for the indole-3-acetic acid and in negative ion mode for the other hormones. Relevant instrumental parameters were set as follows: capillary 1.5 kV (negative mode), source block and desolvation

gas temperatures 130 °C and 500 °C, respectively. Nitrogen was used to assist the cone and desolvation (150 L h^{-1} and 800 L h^{-1}, respectively), argon was used as the collision gas at a flow of 0.18 mL min^{-1}.

Statistical analysis

The Software used was Grapdprism 9.

I performed the Shapiro-Wilk and Agostino and Pearson tests to know if the samples follow a normal distribution. If not, the multiple comparison test applied is a non-parametric Krustall Wallis or Mann-Whitney test for single comparison. If the samples follow a normal distribution, a Brown-Forsythe test of variance homogeneity test is then applied or a fisher test (for simple comparisons). The ANOVA one way or 2-way analysis of variance was applied if the normality and homogeneity test was valid, followed by a Tukey multiple comparison. For simple comparison a T-test was used.

RESULTS

A) CHAPTER 1: CELL WALL MODIFICATIONS AND IDENTIFICATION OF NEW ACTORS LEADING TO THE RESTORATION OF ADHESION BY THE ESMERALDA MUTATION.

PART I

This work was carried out on the model plant *Arabidopsis thaliana* and more particularly on the etiolated hypocotyl which is an adequate model to study the mechanisms of cell adhesion but also of the cell wall remodeling. Indeed, the growth of hypocotyls is only subject to cell elongation processes and does not present a cell differentiation process. Thus, each plant studied starts its growth with the same initial number of cells. These characteristics, therefore, offer us a perfect model to answer the various questions we ask ourselves about cell adhesion and the mechanisms that govern it during plant growth.

Recently, it has been shown that cell adhesion can be restored genetically. As a reminder, the *esmeralda* mutation restores cell adhesion in *quasimodo* background without modifying the amount of pectin but probably by modifying a signal leading to a restoration of the level of expression of a gene known to respond to this signal (Denoux et al., 2008). This suggests that a signal would be perceived and generate signal transduction leading to a different control of the quality of cell adhesion. The first part of our work consisted in identifying the potential signals modified by the *esmeralda* mutation in *quasimodo*. In addition, it is also a question of defining the modifications of the cell wall and in particular the modifications of the pectic pattern mediated by the *esmeralda* mutation in *quasimodo*. Finally, identify new actor in this modified signal transduction will help us to understand their involvement in cell adhesion. This allowed us to improve our knowledge of the signaling pathway occurring in *quasimodo* and *esmeralda* mutants, which is an integral part of the control of cell adhesion in plants.

1) Does the endogenous OGs are signals in cell adhesion?

In the Arabidopsis cell adhesion model, OGs appeared to be the best candidates to mediate different signals (Verger et al., 2016) through their perception by cell wall receptors (Kohorn & Kohorn, 2012). Thus, deciphering the diversity of OGs produced *in planta*, also called endogenous OGs, and understanding their role in the context of cell adhesion seems necessary. We performed an ethanol extraction, on dark grown hypocotyls. Endogenous OGs were analyzed by high-performance size exclusion chromatography (HP-SEC) - MS-based (Voxeur et al., 2019). Each endogenous OG identified by the simple MS method was fragmented to confirm its identity. We have identified 7 different OGs from DP 2 to DP 5 decorated with different methylation or oxidation status. Among the different OGs identified **(Figure A-1)** we observed a difference in their quantity but not in their identity between all the genotypes. The similar esterification pattern of the identified endogenous OGs implies that the susceptibility to the endogenous cell wall located PGs that generate OGS is unchanged in the various genotype. Some of these OGs have already been characterized as potential elicitors. For example, the trimer of GalA is considered as triggering a dark grown signal (Sinclair et al., 2017) and the $GalA_2ox$ is an OG accumulated in the later stages of infection by *B. cinerea* (Voxeur et al., 2019). Almost all extracted OG seems to be less present in *qua2*. We observe a 50% to 33% decrease in *qua2* compared to the WT, depending of the considered OG. The average quantity of most of the OGs seems partly or fully restored by the *esmd1* mutation or even more abundant in the double mutant than in the WT. Only the $GalA_2Ox$ is unaffected by the *esmd1*. But, statistically, only the $GalA_4Me$ and $GalA_4Me_2$, are significantly more present in *esmd1* and in the double mutant, compared to *qua2* **(Figure A-1).** Since Verger et coll., (2016) showed that overexpression of the *FAD LOX* gene in *qua2*, known to respond to pectic signal, is restored to WT level of expression by the *esmd1* mutation. The restoration of the pattern of free OGs in *qua2/esmd1* suggests that the digestibility of the pectins is restored. Since the digestibility of the pectin is the direct consequence of the pattern of methylation of the pectin and/or the action of various polygalacturonases we decided to explore the methylation pattern of the homogalacturonans in these various backgrounds.

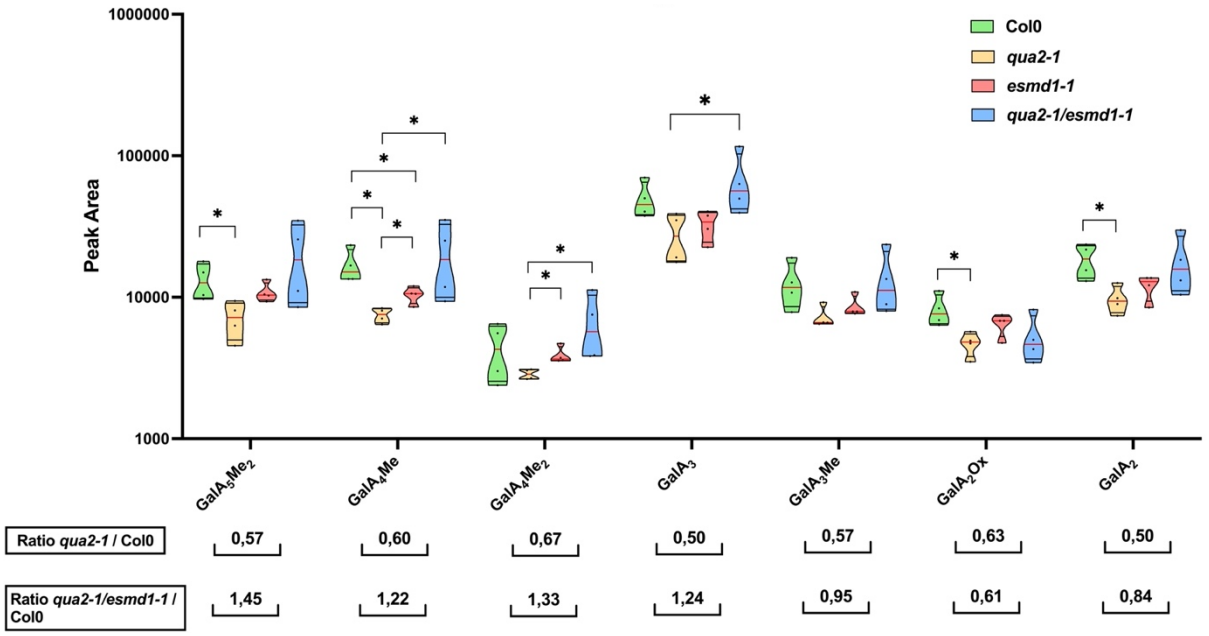

Figure A-1 **Endogenous OGs.**

Truncated violin plot of peak area of endogenous OGs of 150 4-day-old dark grown dissected hypocotyls of Col-0, *qua2-1, qua2-1/esmd1-1 and esmd1-1*. Oligogalacturonides (OGs) are named as follow $GalA_xMe_y$. The number x in subscripts indicates the degree of polymerization, and y the number of methylation or oxidation. GalA: galacturonic acid; Me: methyl ester group Ox: oxidation.

Red line represents the median, black line the quartiles, black dot represents biological replicate (n = 4 biological replicates per genotype).

In (A) *, $P < 0.05$, Mann & Whitney test

2) Does the *esmeralda* mutation change the digestibility of pectin?

It has been shown that only the amount of HG was lower in *qua2* and that the methylesterification degree was unchanged in *qua2* (Mouille et al.,2007, Du et al., 2020 and Verger et al., 2016). None of these features are restored in *qua2/esmd1*. Since we observed changes in the amount and pattern of endogenous OGs in *qua2* and *qua2/esmd1,* we decided to explore what could be the pectins modifications occurring in these mutants, more precisely we explore the pattern of esterification of the HGs. To achieve this, we digested the cell wall of four-day-old dark grown hypocotyls with commercial endo-PG of *Aspergillus aculeatus*. We performed a digestion for 24 hours. The fragments released were analyzed by LC-HRMS. We identified 96 HGs fragments including one monomer and 4 oligoxylogalacturonans, ranging from DP1 to DP14, with distinct methylation, acetylation, dehydration and oxidation (**Chapter 1 Supp data Figure A-7**). The first feature observed is that the total quantity of HGs fragments released (**Figure A-2A**), is strongly lower in the *qua2* compared to the wild type and *esmd1*. This could be correlated with the mutant pectin defect demonstrated by several studies (Mouille et al., 2007; Verger et al., 2016; Du et al., 2020). Considering that the double mutant possesses the same pectin defect as *qua2* (Verger et al., 2016), this result could be related to the poorer digestibility of *qua2* pectin due to potential pectin patterns modified by the mutation. The double mutant partially restores the quantity of the digested fragments and therefore the digestibility of Homogalacturonans.

The fragments identified were grouped and divided into 7 different groups according to their substitution and hydration status. This is the reflect of the Homogalacturans pattern. *quasimodo2* presents a relative quantity of released methylated and methylated-dehydrated fragments less abundant than in the WT (**Figure A-2C**). Their relative contents are divided by two compared to the wild type or *esmd1*. When all the other classes are 1.5 to 4 times more abundant. This fingerprint analysis reveals a not yet described pectin modification in *quasimodo*. This suggests that *qua2* mutation encoding a pectin methyltransferase led to decrease of the methyl-esterification of the polygalacturonase susceptible HG. The characterization of the double mutant *emsd1/qua2* suggest that *esmd1* does partly restore the relative content of fagmenst released by PG digestion (**Figure A-2C**) without fully restoring its digestibility (**Figure A-2A**) undistinguishable from the WT pattern. Since it was shown that *qua2* does not alter the total rate of methylation (Mouille et al., 2007; Du et al., 2020). Here,

qua2 mutation seems to alter the pattern of methylation. This may occur by modifying PMEs expression leading to altered digestibility, which that maybe restored by *esmeralda* mutation, this hypothesis will be further explored later on in this manuscript.

Interestingly, we also identified some xylogalacturonan fragments (**Figure A-2B**). This is not aberrant as we know that xylogalacturonans (XGA) are pectic domains interspaced into homogalacturonans and have been already identified by digestion with *Aspergillus aculeatus* exo-PG or *Aspergillus niger* endo-PG (Beldman et al., 1996; Beldman et al., 2003.) The Gal_3Xyl and Gal_3Xyl_2 appear more present in *qua2* and the double mutant, meaning an intrinsic characteristic of *qua2* unaffected by the mutation *esmd1*. XGAs have been immunolocalized in cell detachment regions on a root cap model (Willats et al., 2004). Thus, XGA increase could be related to the cell detachment in *qua2*. An immunolocalization with LM8 antibody could confirm this hypothesis.

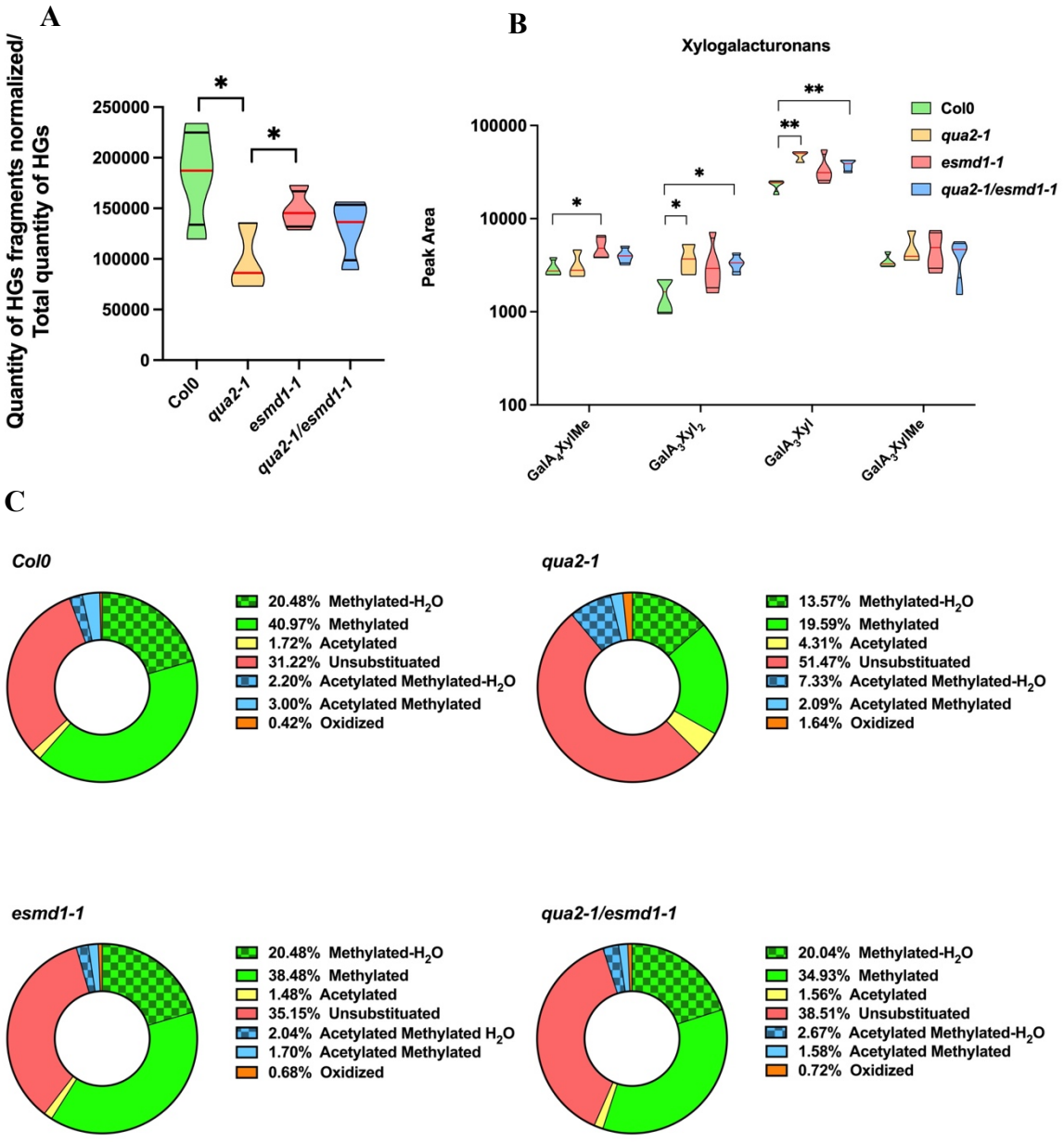

Figure A-2 **Fine structure of homogalacturonans.**

(A) Truncated violin plot of the quantity of HGs fragments & monomers released by PG *Aspergillus aculeatus* digestion of dried cell wall seedlings 4 days dark grown of Col-0, *qua2-1, qua2-1/esmd1-1 and esmd1-1*. The quantity was calculated for 1ug of dried cell wall and normalized by the GalA released by TFA hydrolysis. The quantity of GalA hydrolyzed for 1mg of dried cell wall of same samples was analyzed by GC/MS (Extra data) and subtracted to the equivalent quantity of rhamnose to get the quantity of HGs. HGs fragments were quantified by LC/MSMS according to (Voxeur et al., 2019). *Red line represents the median, black line the quartiles (n ≥ 4 biological replicates per genotype).*

(B) Truncated violin plot of peak area of xylogalacturonans released by PG *Aspergillus aculeatus* of dried cell wall seedlings 4 days dark grown of Col-0, qua2-1, qua2-1/esmd1-1 and esmd1-1. XGs fragments were quantified by LC/MSMS according to (Voxeur et al., 2019). *Red line represents the median, black line the quartiles, black dot represents biological replicate (n ≥ 4 biological replicates per genotype).*

In (A) and (B) *, $P < 0.05$, **, $P < 0.001$, T-Test.

(C) Relative content of HGs fragments family released by PG digestion of dried cell wall of 4-day-old dark grown of seedlings Col-0, *qua2-1, qua2-1/esmd1-1 and esmd1-1(n ≥ 4 biological replicates per genotype).*

3) Which class of HG substitution is affected in *esmeralda* mediate cell adhesion?

If now we focus on the abundance of each class of HGs fragments released instead of their proportion (**Figure A-3**). We do observe that 3 classes of HGs fragments are more abundant in *qua2* compared to col0: the acetylated, the acetylated methylated dehydrated and the oxidized. Four classes are less abundant: the methylated dehydrated, the methylated and the acetylated methylated. The proportion of 5 of them is restored or affected in the double mutant: the methylated dehydrated, the methylated, the acetylated methylated dehydrated, oxidized and the acetylated. It suggest that the *esmd* mutation does impact the pattern of substitution of the HGs that accumulate or decrease in the mutant background *qua2*.

One should point out is that the pattern of substitution of the HG is also modified in the single mutant *esmd*. The digestion of its cell wall released less acetylated dehydrated, acetylated methylated and oxidized fragments than the WT.

In conclusion, the pattern of substitution of the HGs in the various mutants is modified. This can partially explain the differences observed in the quality of the endogenous OGs observed in the various genotypes. We now wish to identify what are the actors responsible for the variability of the substitution of the pectin backbone. But before trying to identify the key responsible enzymes, we should look in more detail at the fine composition of various classes of HGs fragments listed here.

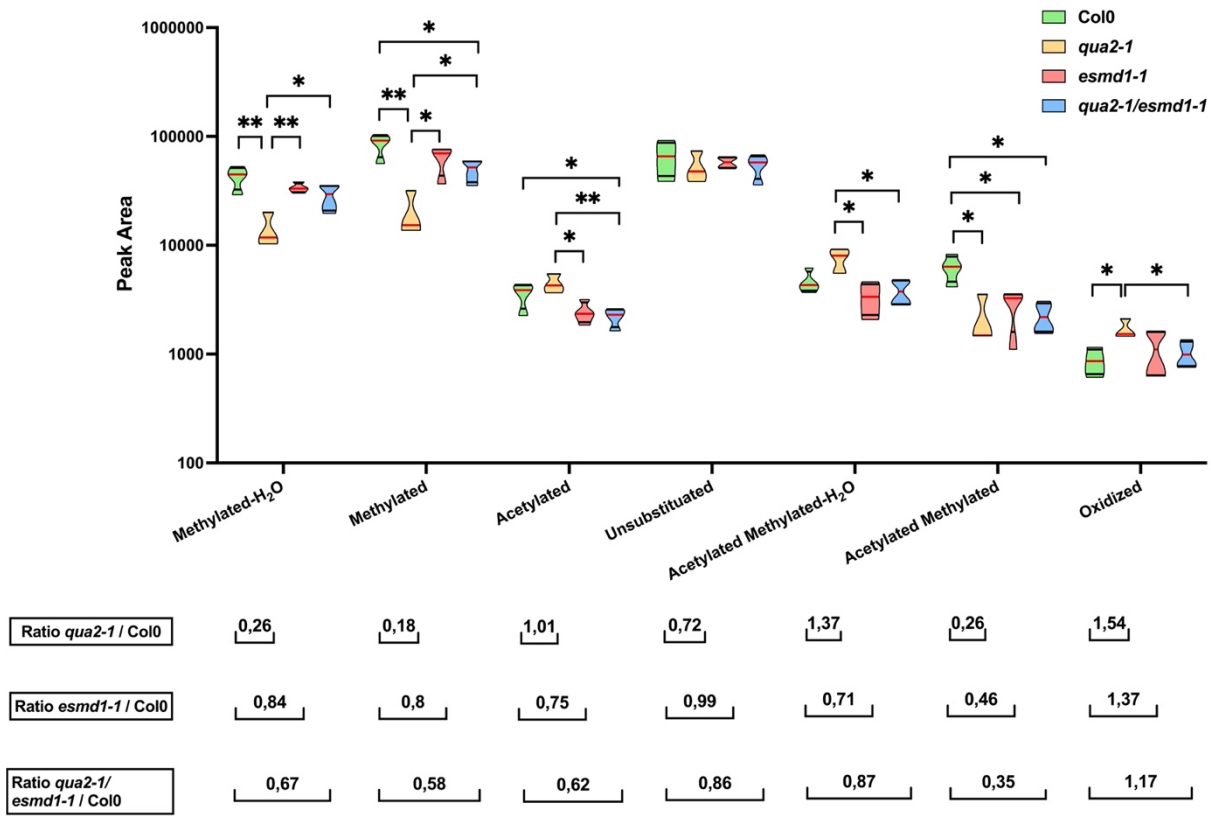

Figure A-3 **Sums of the quantity of the different of HGs fragments.**

Truncated violin plot of sums of the quantity of the classes of HGs fragments released by PG *Aspergillus aculeatus* digestion of dried cell wall of 4-day-old dark grown seedlings of Col-0, *qua2-1, qua2-1/esmd1-1 and esmd1-1*. HGs fragments were quantified by LC/MS according to (Voxeur et al., 2019). *Red line represents the median, black line the quartiles, (n ≥ 4 biological replicates per genotype).* *, $P < 0.05$, **, $P < 0.001$, T-Test.

4) Homogalacturonans fragments linked to cell adhesion

We have therefore observed a restoration of pectin digestibility by the *esmeralda* mutation in *quasimodo*. This restored digestibility suggests a restoration of the pattern of substitution of the HGs. To explore that in detail we compared the quantity of the 92 HGs fragments released by the digestion with Aspergillus PG.

Thus, the heat map (**Figure A-4A**) presents the quantity of 46 HGs fragments significantly different between the WT and *quasimodo* mutant. 31 are more abundant in the WT compared to the mutant. 22 are only methylated with a degree of polymerization between DP 3 and DP 12 and a methylation signature ranging from 1 to 5. Four of these HGs fragments are dehydrated, suggesting an action of endogenous PLs. This type of fragment was observed in

the study carried out by Voxeur et al., (2019). Moreover, 10 acetylated methylated HGs fragments ranging from DP 7 to DP 11 are also more abundant in the wild type. These fragments are moderately methylated (between 2 and 5) and monoacetylated, and only one of them is dehydrated. Conversely, 12 fragments more abundant in *quasimodo* are all methylated acetylated dehydrated DP 7 to DP 12. These HGs fragments have the particularity to be highly methylated (5 to 10) and acetylated (1 to 3). And they are all dehydrated. Finally, the only one oxidized fragment identified in our analysis a dimer of GalA ($GalA_2Ox$) is significantly less present in the wild type. Thus, according to the proportion HGs fragments (**Figure A-2C**) observed previously, we can confirm that the methylated pattern is greatly modified in *qua2* compared to the wild type. This does not result from a decrease in the amount of methylesterification of the cell wall (Du et al., 2020; Mouille et al., 2007) but rather correlates with the modification of the pattern of methylation of the homogalacturonan. Moreover, the increase in the methylated acetylated-H_2O quantity observed in *qua2* (**Figure A-3**) comes from highly methylated acetylated-H_2O fragments. A previous study carried out by Voxeur et coll. (2019) demonstrates that this kind of fragments can activate the plants defense mechanisms against the attack by *Botrytis cinerea*.

According to the digestibility the quantity, and the proportions (**Figure A-2A, A-2C, A-3**) of the different HGs patterns, we were able to observe that *esmeralda* does not seem different from the wild type with globally equivalent proportions. Nevertheless, we wanted to know if some specific HGs signatures are different between them. We identified 22 fragments significantly different between *esmeralda* and Col0 (**Figure A-4B**). Among them, 18 are more abundant in the WT: i) 3 poorly methylated fragments ranging from a DP3 to 5 significantly and ii) 15 methylated acetylated fragments dehydrated (4) or not (11). This suggests that the *esmeralda* mutation probably induces a high PAE activity or poor acetylation of HGs. Finally, 4 fragments with a degree of polymerization ranging from DP12 to 14 and a high degree of methylation are significantly less abundant in the WT.

Finally, we decided to explore comparing the quantity of HGs fragments significantly different between quasimodo and the double mutant (**Figure A-4C**). We observe that 39 methylated HGs fragments are differentially accumulated between the two genotypes. Their DP varies from DP3 to DP14 and can be either weakly or highly methylated and dehydrated or not. Among the 39 methylated HG fragments, 18 are specific of the *esmeralda* mutation. The 21 others show a similar increase in the wild type (**List in Chapter 1 Supp data Figure A-6**). Furthermore, the 9 methylated acetylated -H_2O and oxidized HGs fragments significantly more abundant in *qua2* compared to the WT are still significantly more abundant compared to the double mutant.

Interstingly, the *esmeralda* mutation decrease an acetylated pattern in the *qua2* background. This suggests a greater activity of PAE that decrease and restore acetylated and methyl acetylated-H_2O pattern respectively. This is in agreement with what was observed in *esmd* compared to the WT. Briefly, to summarize, *esmd1* in *qua2* background restores methylated, acetylated methylated-H_2O, acetylated, and oxidized pectic patterns, probably by modulating the expression of some homogalacturonan remodeling enzymes and oxidase. This may allow having a pattern more favorable to proper crosslink in *qua2*. It can be suggested that this modulation of the pectic pattern may allow more cross-linkable micro-domains inter-spaced on the homogalacturonan domain and enhance the restoration of adhesion. Moreover, these changes in pectin digestibility by *esmd1/qua2* correlate with the increase of the eliciting quantity of endogenous OGs observed in (**Figure A-1**) that may correlate to this restoration.

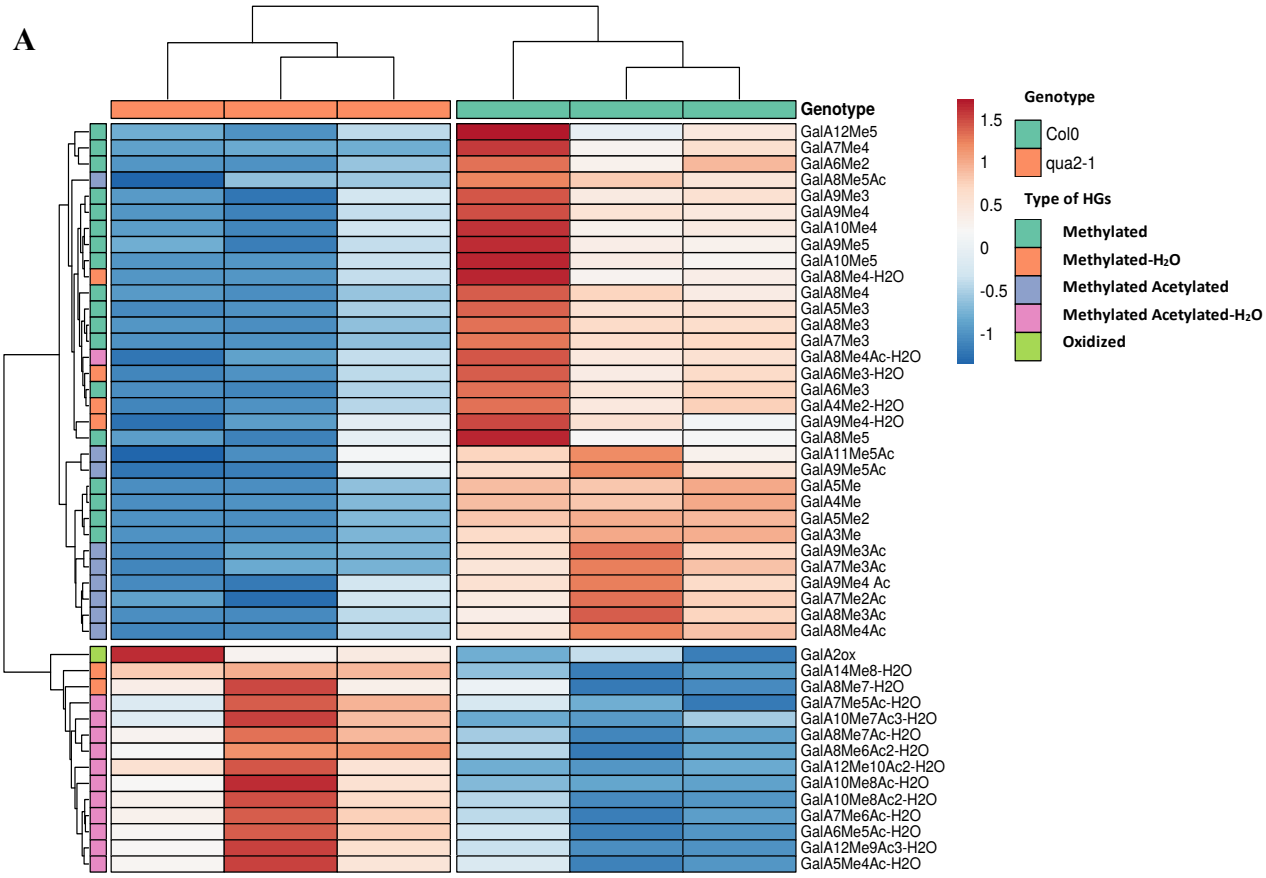

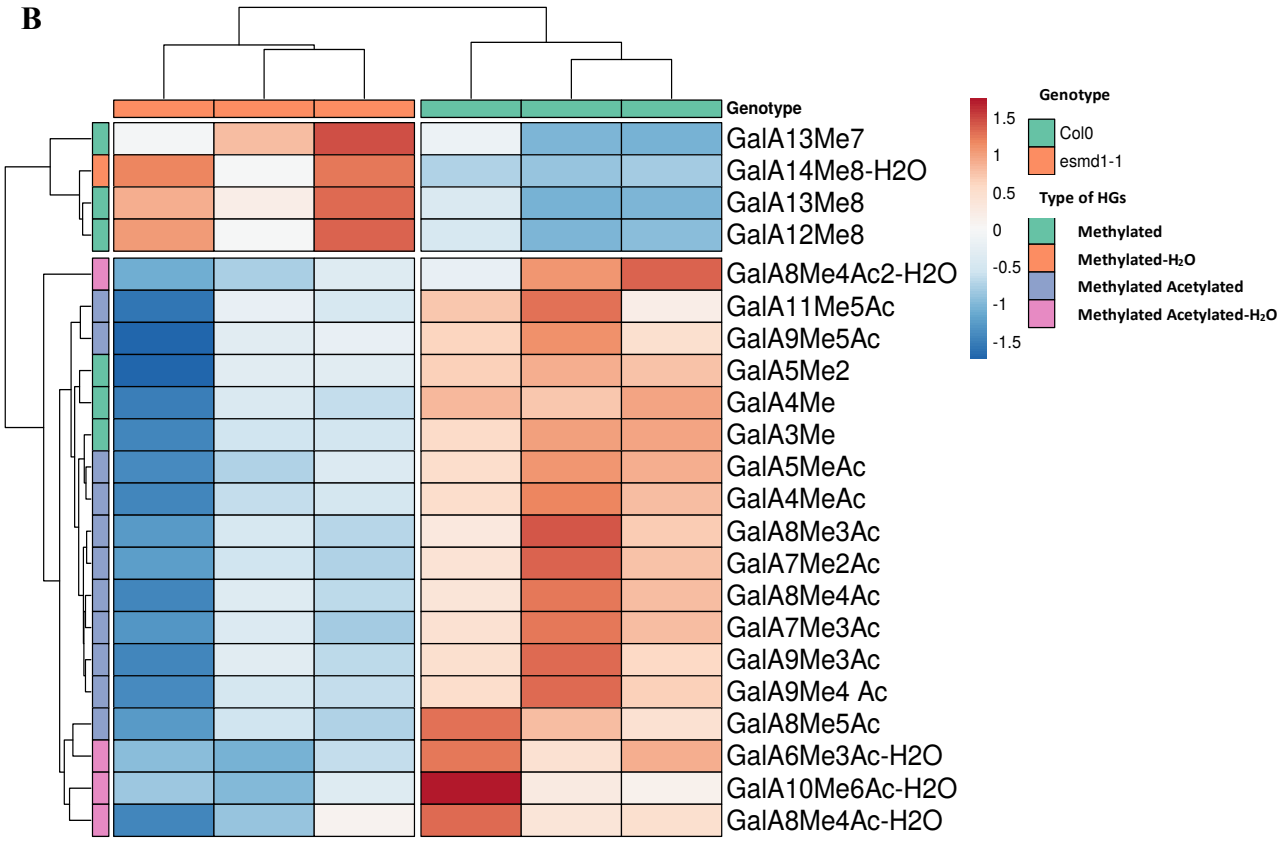
B
Genotype
GalA13Me7
GalA14Me8-H2O
GalA13Me8
GalA12Me8
GalA8Me4Ac2-H2O
GalA11Me5Ac
GalA9Me5Ac
GalA5Me2
GalA4Me
GalA3Me
GalA5MeAc
GalA4MeAc
GalA8Me3Ac
GalA7Me2Ac
GalA8Me4Ac
GalA7Me3Ac
GalA9Me3Ac
GalA9Me4 Ac
GalA8Me5Ac
GalA6Me3Ac-H2O
GalA10Me6Ac-H2O
GalA8Me4Ac-H2O
1.5
1
0.5
0
-0.5
-1
-1.5
Genotype
Col0
esmd1-1
Type of HGs
Methylated
Methylated-H2O
Methylated Acetylated
Methylated Acetylated-H2O

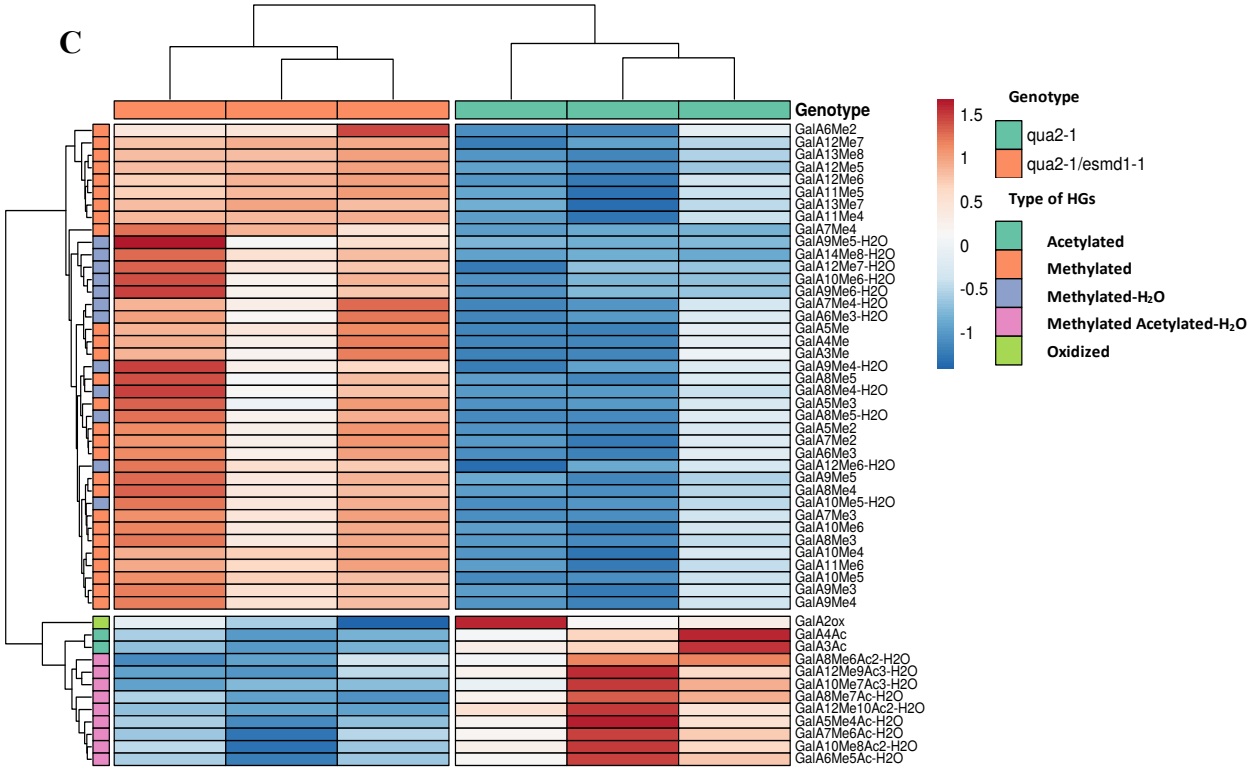

Figure A-4 **HGs fragments released significantly different**

(A) Heatmap of all of the HGs fragments released by *PG Aspergillus aculeatus* significantly different between Col0 and *qua2-1* (46 rows) for 3 samples (columns). Annotation labels refer to HGs fragments structure. Rows are centered; unit variance scaling is applied to rows. Both rows and columns are clustered using McQuitty distance and maximum linkage

(B) Heatmap of all of the HGs fragments released by *PG Aspergillus aculeatus* significantly different between Col0 and *esmd1-1* (22 rows) for 3 samples (columns)

(C) Heatmap of all of the HGs fragments released by *PG Aspergillus aculeatus* significantly different between *qua2-1* and *qua2-1/esmd1-1* (51 rows) for 3 samples (columns).

For (A), (B), and (C) *(n = 3 biological replicates per genotype),*

5) Who is responsible for changing the pectic pattern?

To better understand how these pectins modifications are implemented by the plant, we made an RTqPCR analysis of all PAE, PME and PMEI genes. We analyzed the expression of these genes on dark grown 4-days seedlings. The expression was analyzed over 2 consecutive years, to verify the stability of the expression of the selected genes.

Only genes whose expression varies significantly in genotypes are presented. Their relative expression levels are normalized according to 2 housekeeping genes and reported to the expression of the wild type (Taylor et al., 2019).

Here we can observe (**Figure A-5**) that *PME41* is the most overexpressed gene in *qua2* compared to wild type and *esmd1*. In the double mutant, the *PME41* level of expression is divided by 2, probably reflecting an effect of the *esmd1* mutation. *PME53* is also overexpressed in *qua2* compared to Col0. *esmd1* mutation including the double mutant does not differ from the level of expression of the wild type. *PME35* expression is significantly repressed in *esmeralda* compared to the wild type and *qua2,* while the double mutant tends to under-express it in an insignificant way. *PMEI4* is also found to be significantly under-expressed in *esmeralda* compared to Col0 and *qua2*. In the same manner, the double mutant under-expressed PMEI4 compared to *qua2*. Regarding *PAE*, 2 genes have the same expression profile with a significant tendency for *PAE12*, under-expressed in *qua2* compared to *esmeralda*. *PAE7* tends to be under-expressed in *quasimodo* but not significantly. Furthermore, in the double mutant the expression of these 2 genes returns to similar levels of Col0. Together, gene deregulations observed in *quasimodo* correlate with the pectic pattern differences observed on the enzymatic fingerprint. Indeed, the overexpression of *PME 41 and PME53* genes in *qua2* (**Figure A-5)** may explain the strong decrease in methylated OGs (**Figure A-3 and A-4).** *PME53* is a type II PME and *PME41* is a type I PME (Sénéchal et al., 2014). *PME41* is regulated by brassinosteroid under chilling stress or implicated in pathogen response (Lionetti et al., 2012; Qu et al., 2011). Parallelly, the studies carried out by (Raggi et al., 2015; Verger et al., 2016) highlighted that *qua2* is a stressed mutant, overexpressing the pectin response gene *FADlox* (Denoux et al., 2008) and the peroxidase *PRX71*. Here we suggest, the combined action of *PME41 & PME53* related to their higher expression, generates a particular pectin pattern more susceptible to PG degradation. These features may participate in the stressed phenotype and the loss of adhesion of *qua2*. Conversely, the decrease in the expression of *PAE7* and *PAE12* (**Figure A-5**), may explain the increase of the acetylated methylated and acetylated patterns (**Figure A-3 and -A-4**). Moreover, acetylation may prevent HG degradation by endo-PGs (Bonnin et al., 2003)

correlated with a decreased expression level of PAE in *qua2*. Nonetheless, we cannot omit that the transcription of *PMEI4* and *PME35* genes is repressed in the double mutant and *esmeralda* compared to *qua2*. This under-expression may participate in the control of cell adhesion or different processes restored by the *esmeralda* mutation. It has been shown that *PMEI4* controls pectin de-methyl-esterification for the timing of the growth acceleration, but not the growth process itself (Pelletier et al., 2010). Hypothetically, the growth restored by *esmd in qua* (Verger et al., 2016) may correlate with the repression of *PMEI4* observed, suggesting a growth process already triggered in these mutants. Conversely in the case of *qua2* and considering it has reduced hypocotyl length (Du et al., 2020; Mouille et al., 2007; Verger et al., 2016) we can assimilate the overexpression of *PMEI4* to a growth acceleration untriggered or unfunctional. Another explanation, *PMEI4* controls some PMEs and the decrease of *PMEI4* expression mediated by *esmd1* is necessary to restore the right pattern of methylation. Otherwise, *PME35* is responsible for the de-methyl-esterification of pectins and participates in the regulation of the mechanical resistance of the supporting tissue in the stems of Arabidopsis (Hongo et al., 2012). The underexpression of this gene by *esmd1* and the double mutant may also correlate with the restoration of the methylation pattern.

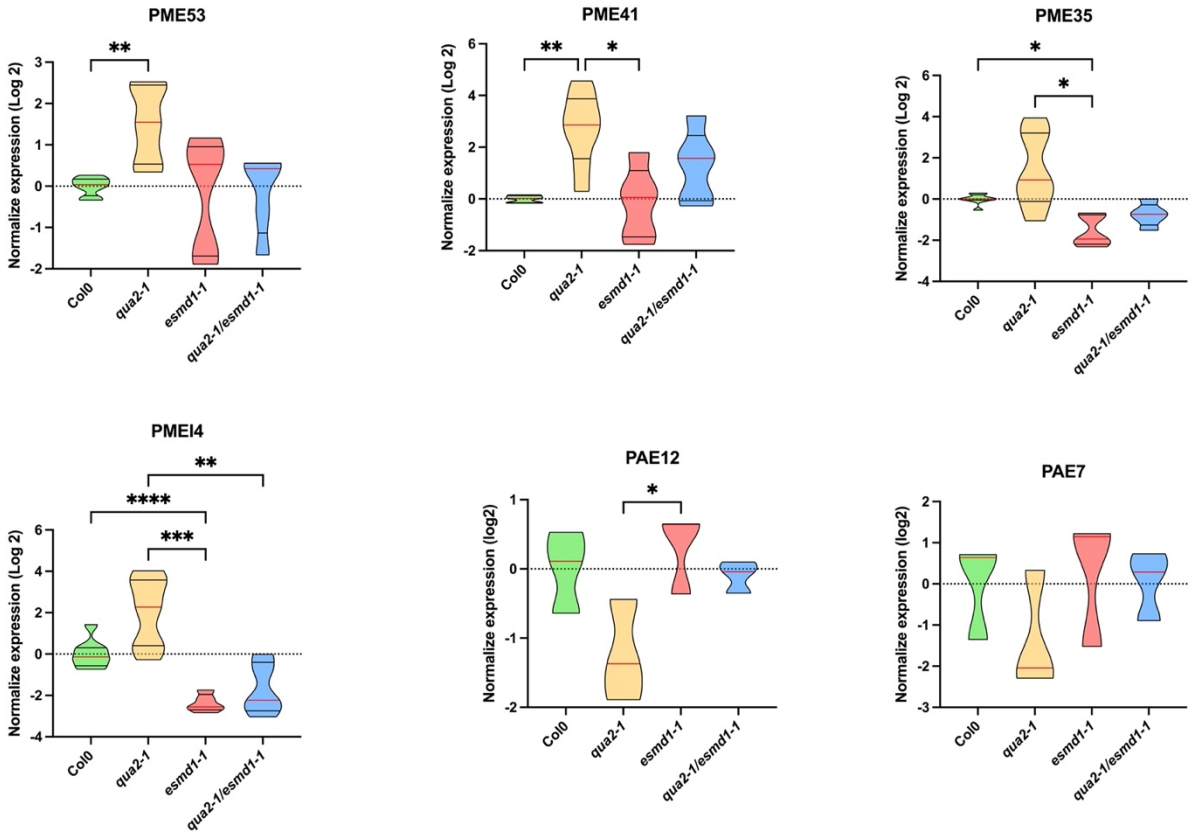

Figure A-5 **PME/PMEI and PAE expression.**

Truncated violin plot of Normalized expression levels (log2) of *PMEI4, PME, 35, 41, 53* and *PAE 7 and 12,* from 4-day-old, etiolated seedlings of Col, *qua2*, *esmd1 and qua2/esmd1* by qPCR. *APT1 & CLATHERINE* were amplified as internal controls. Normalized expression levels (log2) were calculated according to a normalization factor of 2 housekeeping genes and reported to the expression of the wild type (Taylor et al., 2019). *Red line represents the median, black line the quartiles (n ≥ 5 biological replicates per genotype for PME and PMEI) (n = 3 biological replicates per genotype for PAE).*

In (A) and (C), *, $P < 0.05$ and **, $P < 0.001$, ***, $P < 0.0001$, ****, $P < 0.00001$ Brown-Forsythe and Welch ANOVA tests (Dunn's multiple comparisons test).

CONCLUSION

Thus, in our study, we were able to suggest that the restoration of the cell adhesion phenotype in quasimodo by the *esmeralda* mutation may results from a combination of different phenomena. The first of them consists in the restoration of a quantity of endogenous OGs and not from a different signature. This amount of endogenous OGs restored is linked on the one hand to a partial restoration of the digestibility of HGs. This is translated by an increase in the proportions of methylated HGs fragments and a decrease in the proportions of, acetylated, acetylated methylated-H_2O and oxidized HGs compared to *qua2*. Finally, the *esmeralda* mutation seems to modulate and or control the expression of 3 PME, one PMEI and 2 PAE leading to the restoration of the pectic pattern in *qua2*. These genes are new actors of this pathway. Together these data suggest that the restoration of adhesion by the *esmeralda* mutation leads to a pectic pattern more appropriate for cross-linking, but also may generate a quantity pectic signal leading to the restoration of cell adhesion.

6) Supplemental Data

a) List of HGs fragments significantly different

qua2-1/esmd1-1 VS qua2-1	Col0 vs *qua2-1*	Legend
GalA13Me7	GalA14Me8-H2O	OGs specific of Col0 > *qua2-1*
GalA14Me8-H2O	GalA12Me5	OGs specific of *qua2-1/esmd1-1* > *qua2-1*
GalA13Me8	GalA11Me5Ac	OGs specific of *qua2-1* > qua2-1/esmd1-1
GalA12Me5	GalA10Me4	OGs specific of *qua2-1* > Col0
GalA12Me6	GalA10Me5	In common Ogs of *qua2-1* > Col0 & *qua2-1/esmd1-1*
GalA12Me7	GalA12Me9Ac3-H2O	In common OGs of Col0 & *qua2-1/esmd1-1* > *qua2-1*
GalA11Me4	GalA9Me3Ac	
GalA12Me6-H2O	GalA9Me3	
GalA11Me5	GalA12Me10Ac2-H2O	
GalA12Me7-H2O	GalA9Me4 Ac	
GalA10Me4	GalA9Me4	
GalA11Me6	GalA9Me5Ac	
GalA10Me5	GalA9Me5	
GalA12Me9Ac3-H2O	GalA8Me3Ac	
GalA9Me3	GalA8Me3	
GalA10Me6	GalA9Me4-H2O	
GalA12Me10Ac2-H2O	GalA10Me7Ac3-H2O	
GalA10Me5-H2O	GalA8Me4Ac	
GalA9Me4	GalA8Me4	
GalA10Me6-H2O	GalA10Me8Ac2-H2O	
GalA9Me5	GalA10Me8Ac-H2O	
GalA8Me3	GalA7Me2Ac	
GalA9Me4-H2O	GalA8Me5Ac	
GalA10Me7Ac3-H2O	GalA8Me5	
GalA8Me4	GalA8Me4Ac-H2O	
GalA9Me5-H2O	GalA7Me3Ac	
GalA10Me8Ac2-H2O	GalA8Me4-H2O	
GalA7Me2	GalA7Me3	
GalA8Me5	GalA7Me4	
GalA9Me6-H2O	GalA6Me2	
GalA8Me4-H2O	GalA6Me3	
GalA7Me3	GalA5Me	
GalA7Me4	GalA8Me7Ac-H2O	
GalA6Me2	GalA8Me7-H2O	
GalA8Me5-H2O	GalA7Me5Ac-H2O	
GalA8Me6Ac2-H2O	GalA6Me3-H2O	
GalA7Me4-H2O	GalA5Me2	
GalA6Me3	GalA7Me6Ac-H2O	
GalA5Me	GalA5Me3	
GalA8Me7Ac-H2O	GalA4Me	
GalA6Me3-H2O	GalA6Me5Ac-H2O	
GalA4Ac	GalA5Me4Ac-H2O	
GalA5Me2	GalA4Me2-H2O	
GalA7Me6Ac-H2O	GalA3Me	
GalA5Me3	GalA2ox	
GalA4Me	GalA8Me6Ac2-H2O	
GalA6Me5Ac-H2O		
GalA3Ac		
GalA5Me4Ac-H2O		
GalA3Me		
GalA2ox		

Figure A-6 **List of HG fragments released significantly different**

Between *qua2-1* and *qua2-1/esmd1-1* (51 rows) column A, between *qua2-1* and *Col0* (46 rows) column B. Column C correspond to the legend.

b) List of all OGs released and identified

Mass	Retention time	Formule	Type of Ogs
1201,2606	7,0422	GalA13Me7	OGMe
1287,2783	7,0804	GalA14Me8-H2O	OGMe-H2O
1208,2679	7,0979	GalA13Me8	OGMe
1099,2297	7,1001	GalA12Me5	OGMe
1106,2374	7,1372	GalA12Me6	OGMe
1113,2446	7,1886	GalA12Me7	OGMe
1011,2136	7,2421	GalA11Me4	OGMe
1097,2313	7,253	GalA12Me6-H2O	OGMe-H2O
1120,2515	7,2552	GalA12Me8	OGMe
1039,226	7,288	GalA11Me5Ac	OGMeAc
1018,2211	7,2978	GalA11Me5	OGMe
1104,2388	7,3	GalA12Me7-H2O	OGMe-H2O
916,19	7,3437	GalA10Me4	OGMe
1025,2288	7,3634	GalA11Me6	OGMe
1111,2467	7,3721	GalA12Me8-H2O	OGMe-H2O
923,1972	7,3962	GalA10Me5	OGMe
1181,2703	7,4093	GalA12Me9Ac3-H2O	OGMeAc-H2O
842,1715	7,442	GalA9Me3Ac	OGMeAc
821,1657	7,4508	GalA9Me3	OGMe
930,2048	7,4803	GalA10Me6	OGMe
1167,2719	7,4879	GalA12Me10Ac2-H2O	OGMeAc-H2O
849,1787	7,501	GalA9Me4 Ac	OGMeAc
914,1919	7,5087	GalA10Me5-H2O	OGMe-H2O
828,1734	7,5119	GalA9Me4	OGMe
937,2122	7,5502	GalA10Me7	OGMe
942,2038	7,5622	GalA10Me6Ac-H2O	OGMeAc-H2O
856,186	7,572	GalA9Me5Ac	OGMeAc
921,1993	7,5841	GalA10Me6-H2O	OGMe-H2O
835,1812	7,5906	GalA9Me5	OGMe
754,1545	7,6124	GalA8Me3Ac	OGMeAc
733,1497	7,6223	GalA8Me3	OGMe
819,168	7,6245	GalA9Me4-H2O	OGMe-H2O
991,223	7,6354	GalA10Me7Ac3-H2O	OGMeAc-H2O
863,1935	7,6605	GalA9Me6Ac	OGMeAc
842,1888	7,6725	GalA9Me6	OGMe
928,2073	7,6758	GalA10Me7-H2O	OGMe-H2O
761,162	7,6889	GalA8Me4Ac	OGMeAc
740,1572	7,6977	GalA8Me4	OGMe
826,176	7,7031	GalA9Me5-H2O	OGMe-H2O
977,2259	7,7326	GalA10Me8Ac2-H2O	OGMeAc-H2O
956,2201	7,7392	GalA10Me8Ac-H2O	OGMeAc-H2O
659,1311	7,7425	GalA7Me2Ac	OGMeAc
638,1259	7,7425	GalA7Me2	OGMe
854,1884	7,7807	GalA9Me6Ac-H2O	OGMeAc-H2O
773,1619	7,7818	GalA8Me4Ac2-H2O	OGMeAc-H2O
768,1701	7,7894	GalA8Me5Ac	OGMeAc
747,1649	7,7927	GalA8Me5	OGMe
833,1834	7,7949	GalA9Me6-H2O	OGMe
752,1562	7,8058	GalA8Me4Ac-H2O	OGMeAc-H2O
666,1383	7,8091	GalA7Me3Ac	OGMeAc
731,1516	7,8179	GalA8Me4-H2O	OGMe-H2O
645,1331	7,8255	GalA7Me3	OGMe
882,202	7,8583	GalA9Me7Ac2-H2O	OGMeAc-H2O
759,1641	7,8889	GalA8Me5Ac-H2O	OGMeAc-H2O
1305,2883	7,9194	GalA7Me4	OGMe
1101,2258	7,9555	GalA6Me2	OGMe
738,1591	7,9697	GalA8Me5-H2O	OGMe-H2O
939,1736	7,973	GalA5Ac	OGAc
1575,3615	8,0134	GalA8Me6Ac2-H2O	OGMeAc-H2O
1491,3399	8,033	GalA8Me6-H2O	OGMe-H2O
1287,2787	8,0581	GalA7Me4-H2O	OGMe-H2O
953,1888	8,0614	GalA5MeAc	OGMeAc
1115,2414	8,0702	GalA6Me3	OGMe
911,1781	8,0898	GalA5Me	OGMe
1547,3674	8,1117	GalA8Me7Ac-H2O	OGMeAc-H2O
1505,3567	8,1171	GalA8Me7-H2O	OGMe-H2O
1343,3042	8,1586	GalA7Me5Ac-H2O	OGMeAc-H2O
1129,257	8,1673	GalA6Me4	OGMe
1139,2417	8,175	GalA6Me3Ac-H2O	OGMeAc-H2O
1301,2938	8,1794	GalA7Me5-H2O	OGMe-H2O
1097,2307	8,1925	GalA6Me3-H2O	OGMe-H2O
721,1305	8,2187	GalA4	OG
763,1415	8,2012	GalA4Ac	OGAc
925,194	8,2023	GalA5Me2	OGMe
1357,3197	8,2678	GalA7Me6Ac-H2O	OGMeAc-H2O
1315,309	8,282	GalA7Me6-H2O	OGMe-H2O
1153,2567	8,3017	GalA6Me4Ac-H2O	OGMeAc-H2O
939,2094	8,3246	GalA5Me3	OGMe
1111,2465	8,3301	GalA6Me4-H2O	OGMe-H2O
777,157	8,3356	GalA4MeAc	OGMeAc
735,1463	8,3377	GalA4Me	OGMe
1167,2732	8,4317	GalA6Me5Ac-H2O	OGMeAc-H2O
1125,2621	8,4393	GalA6Me5-H2O	OGMe-H2O
717,1358	8,4535	GalA4Me-H2O	OGMe-H2O
587,1089	8,4546	GalA3Ac	OGAc
545,0984	8,4798	GalA3	OG
977,2255	8,6163	GalA5Me4Ac-H2O	OGMeAc-H2O
935,2149	8,6338	GalA5Me4-H2O	OGMe-H2O
731,1512	8,6371	GalA4Me2-H2O	OGMe-H2O
559,1141	8,6491	GalA3Me	OGMe
385,0612	8,7146	GalA2ox	OGOx
193,0339	9,228	GalA	OG

Figure A-7 **List of HGs fragment identified by LCHR/MS**.

Some of them are monocharged related to the mass detected (GalA-$GalA_7Me_4$) the others are dicharged ($GalA_8Me_5Ac$-H_2O- $GalA_{13}Me_7$ including the $GalA_8Me_5$-H_2O).

PART II

1) Additional work on the cell wall modifications induced by *esmeralda* and identification of new actor of cell adhesion

a) Cell wall monosaccharide modifications

To understand how *esmeralda1* can mediate cell adhesion in *quasimodo2*, we decided to dissect the cell wall and other components of the extracellular matrix. First, we chose to carry out an analysis of the various monosaccharides on seedlings grown in dark for 4 days in MilliQ water medium buffered at pH 5.7 (MES). This choice seems obvious since we know *qua2* has a defect in the carbon/nitrogen balance (Gao et al., 2008). Therefore, the use of a neutral medium such as deionized water limits the parasitic effects that can be caused by conventional culture media. We perform TFA hydrolysis on the washed, dried cell wall. GC / MS Analysis was used to quantify the different hydrolyzed monosaccharides.

According to the results representing the proportion in Mol% (**Figure A-8**), we were able to observe significant changes for 4 monosaccharides. The most affected monosaccharide is GalA. It presents a significant decrease of 1,4-fold in *qua2* compared to Col0 and *esmd1*. This result is consistent with those of previous studies showing a similar decrease compared to Col0 and /or *esmd1*, using other methods of extraction and analysis (Du et al., 2020; Mouille et al., 2007; Verger et al., 2016). The double mutant exhibits also a significant difference compared to Col0 and *esmd1*. This result correlates with the study carried out by (Verger et al., 2016) showing the double mutant significantly reduced the amount of GalA compared to Col0. Conversely, arabinose content is higher by 1,3-fold in *qua2* compared to wild type. Noted this content is consistent with the one observed by (Du et al., 2020) in *qua2* vs Col0. Moreover, this content is restored in the double mutant. Besides, the analysis also revealed a significant increase in the glucose content in *qua2* and the double mutant, probably an own feature of *quasimodo2* mutation. Finally, the significantly decreased xylose content about a 1,2-fold change in *qua2* is restored by the *esmeralda1* mutation. Together, these results highlight a defect in pectins and xyloglucans in *qua2*, appearing to be modulated by *esmd1* mutation. Pectin defect seems to be related to the HGs biosynthesis, according to (Du et al., 2020) showing downregulation of GAUT1, GAUT7, and GAUT15 in *qua2.* This mutation probably creates miss coordination of GAUT/PMT complexes occurring during HG biosynthesis (Atmodjo et al., 2013), and leading to pectin content defect. The decrease in xylose and glucose content can be assimilated to a difference in the xyloglucan pattern which could explain the slight modifications observed.

However, both changes may participate in polysaccharide cross-linkage occurring in the cell wall probably led to the restoration of cell adhesion and cell wall integrity.

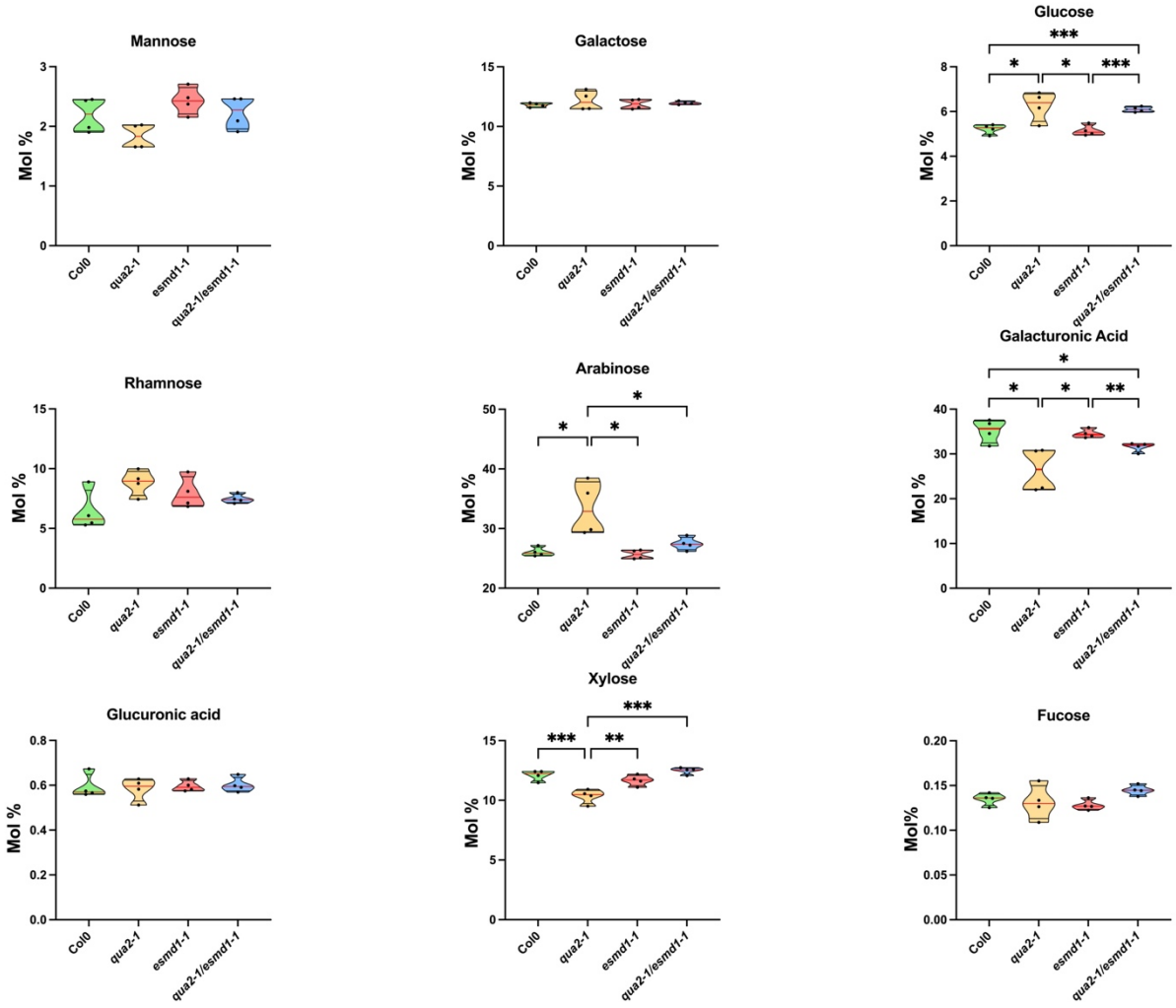

Figure A-8 **Cell wall monosaccharides composition.**

Truncated violin plot of Monosaccharides content in mol% quantifies by GC/MS on dried cell wall seedlings 4 days dark grown of Col-0, *qua2-1, qua2-1/esmd1-1 and esmd1-1. Red line represents the median, black line the quartiles, black dot represents biological replicate (n = 4 biological replicates per genotype).* *, $P < 0.05$, **, $P < 0.001$, ***, $P < 0.0001$, T-Test.

b) Does *esmeralda* affect the cuticle layer?

Recently it was demonstrated that the mutant *quasimodo* possesses a more permeable cuticle without any change in structure (Lorrai et al., 2021). Thus, we wanted to know if the *esmeralda* mutation causes changes at the level of this layer. To do this, we carried out a toluidine blue staining according to the protocol of Creff et al., (2019) on 4-day-old dark grown hypocotyls. Following staining, blue coloration is intense in *qua2* (**A-9B**) and absent in Col0 (**A-9A**). This suggests that *qua2* does have a permeable cuticle probably linked to its adhesion defect as described in (Lorrai et al., 2021) Besides, we can observe that *esmeralda* mutation in the double mutant (**Figure A-9C**) lead to change the coloration turning pink. This changement of stainning, can translate an uncomplete restoration of the cuticle permeability. We are not able to define which layer of the cuticle is modified by this mutation. Nonetheless, we can hypothesize that change in staining is probably related to the restoration of cell adhesion in *qua2/esmd1*. Thus, we can suggest the mutation *esmeralda* leads to different changes in the cell wall but also on another layer of the extra cellular matrix such as the cuticle.

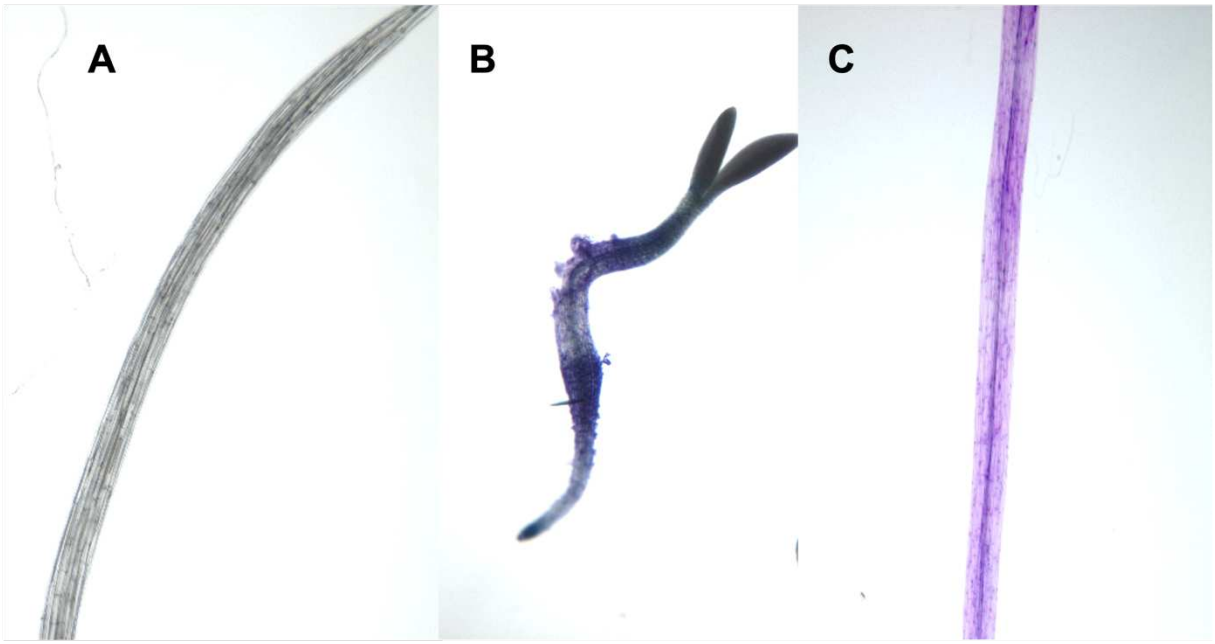

Figure A-9 **Cuticle permeability.**

(A) Picture of Col0 4-day-old dark grown hypocotyl, stained with toluidine bleu, (B) *qua2-1* and (C) *qua2-1/esmd1.*

c) Are xyloglucans implicated in cell adhesion?

We explored what could be the xyloglucans modifications mediated by *esmd1* that restore xylose content observed in q*uasimodo2* monosaccharide analysis. So, we decided to analyze the fine structure of the xyloglucan. To achieve this, we used a commercial endo-*cellulase* applied on dried cell wall of 4 days old dark grown seedlings. We performed a digestion for 24 hours and the fragments released were analyzed by LC-MS. According to the result (**Figure A-10**), we find only differences in quantity and not identity. Among the 6 fragments identified, only the relative amount of XXG and XXXG fragment was significantly reduced in *qua2* compared to all genotypes. These 2 changesets can correlate with the decrease of xylose content in *qua2* previously observed (**Figure A-8**). It cannot be overlooked that xyloglucans may participate in cell adhesion as demonstrated by immunolocalization in the carried out by study (Ordaz-Ortiz et al., 2009). Moreover, xyloglucans play an important role in the interlacing of cellulose microfibrils and have been strongly involved in the regulation of cell wall extension. Loss of xyloglucan affects, the mechanic and the stability of the microtubule cytoskeleton (Xiao et al., 2016b). However, the total sum of xyloglucan does not differ significantly (data not shown) and these structural changes are not as important as those observed on the pectic pattern. Thus, we need to investigate more to be able to conclude on this change of pattern.

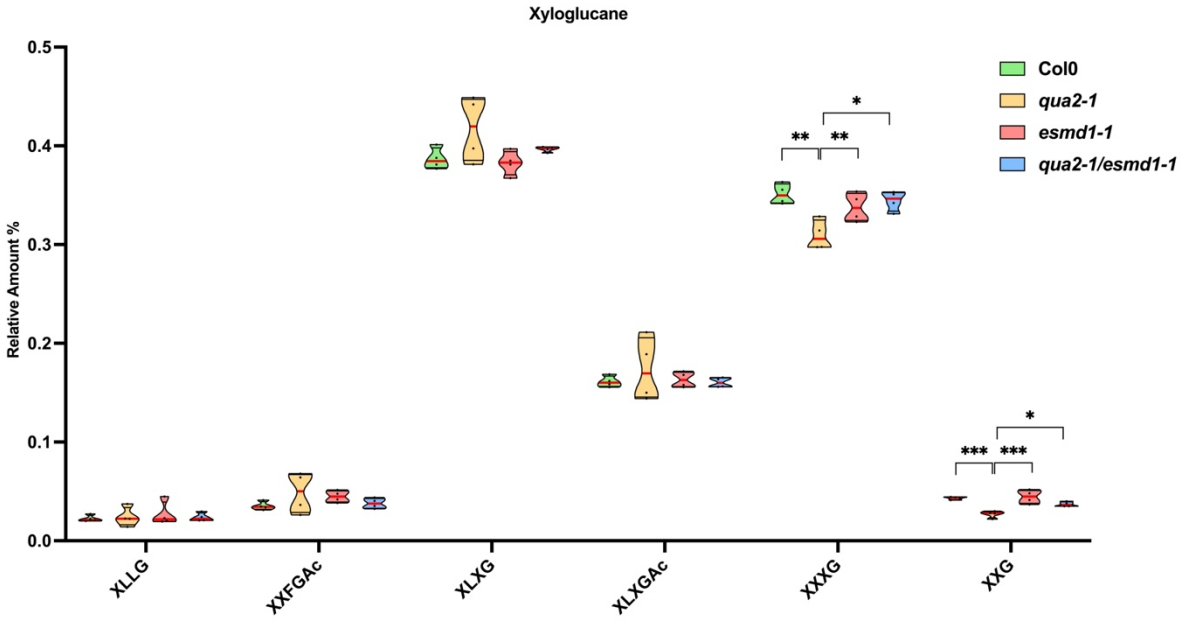

Figure A-10 **Fine structure of xyloglucans.**

Truncated violin plot of Xyloglucans fragment digested by *endo-cellulase* applied on dried cell wall seedlings 4 days dark grown of Col-0, *qua2-1, qua2-1/esmd1-1 and esmd1-1*. Fragments

were quantified by LC/MSMS according to (Voxeur et al., 2019). *Red line represents the median, black line the quartiles, black dot represents biological replicate (n = 4 biological replicates per genotype).*

*, $P < 0.05$ and **, $P < 0.001$, ***, $P < 0.0001$, Anova one-way (Tukey's multiple comparisons test).

d) Protein production in heterologous system

To characterize the different new actors PME/PMEI and PAE and to determine their impact on cell adhesion and on the homogalacturonans we have chosen to produce the proteins by heterologous system.

For PME53 the expected size is 39 Da, after PNgase digestion to eliminate potential glycosylation, a corresponding size is indeed found.

Concerning the 2 PAEs, the expected size of PAE12 corresponds to the observed one: 46 Da. For PAE7, the observed size is greater than expected. No potential glycosylation site is described on the UniProt site.

For PMEI4 the expected size was found to be 19 Da but not as the major band. The larger sizes may correspond to forms glycosylated by Pichia. The size of the full-length PME35 protein is the expected one: 55 Da but with a very low intensity. The lower band corresponds to the catalytic PME part without the pro domain 37 Da and the upper bands may correspond to glycosylated forms. For PME41 we observe a band at 61 Da and a lower band of 43Da corresponding to the PME catalytic domain without the pro domain. Finally, for Fadlox the expected size of 57 Da was detected but not as a major band. The major band is between 72 and 95 Da. It probably corresponds to a glycosylated form due to the number of glycosylation sites described by UniProt.

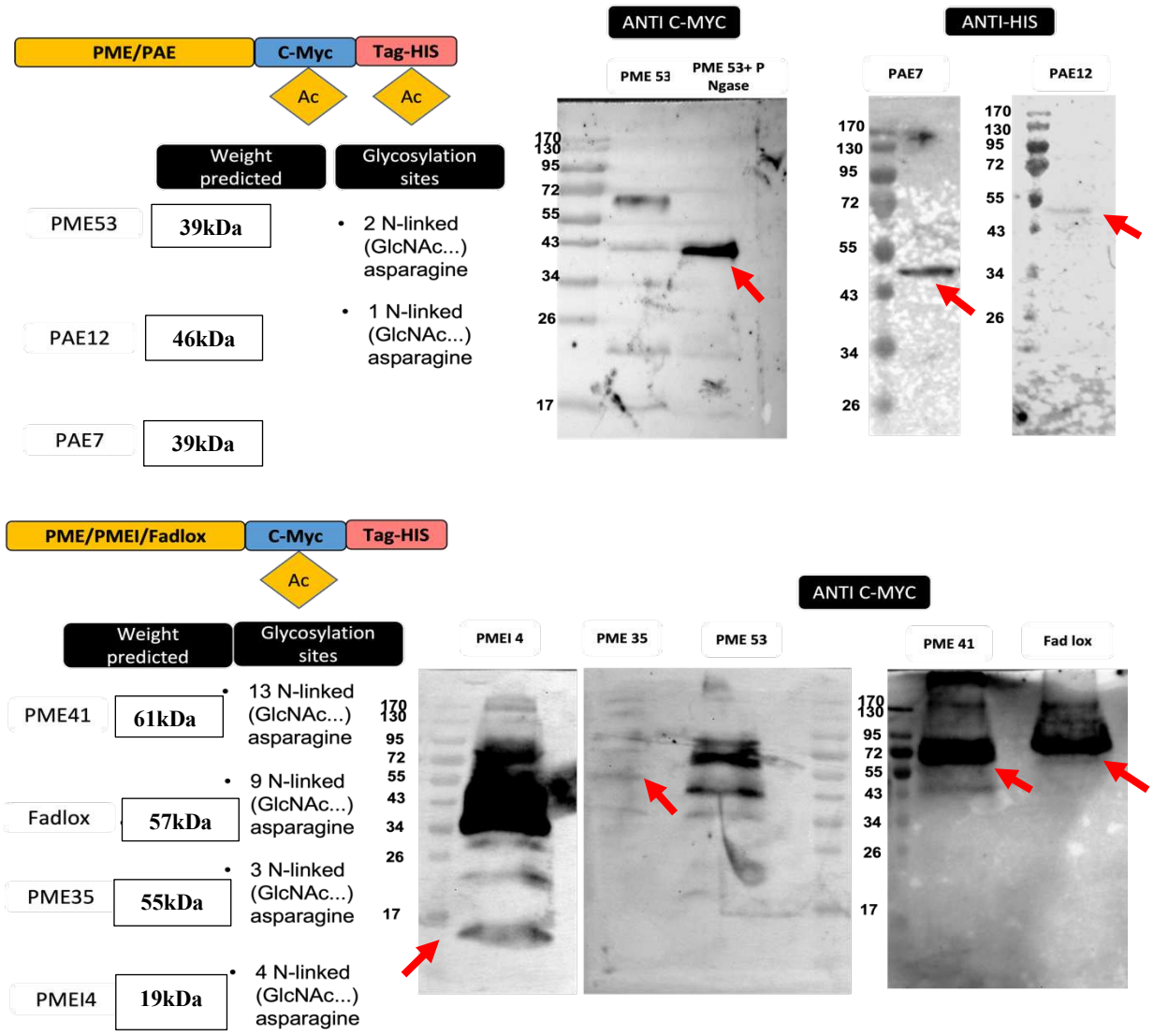

Figure A-11 **Western blot of different unpurified proteins produced in a heterologous system.**

The red arrows indicate the bands corresponding to the protein. Antibody used: anti-Histidine or anti-C-Myc.

e) Do pectin methylesterase and pectin methylesterase inhibitor candidates enzymes affect the cell adhesion?

After having produced some of our candidate proteins in a heterologous system, we applied them for 48 hours on 4-day-old dark grown hypocotyls (from day 2). Since we know that PMEI and PME candidates are transcriptionally regulated by the *esmd* mutation in *qua2*, they may participate in the restoration of cell adhesion. We performed a ruthenium red phenotyping to find out if our candidates cause cell adhesion defects on *qua2/esmd1* or Col0. Thus, according to (**Figure A-12**) (A-E) only PME35 (B), PME53 (D) and PMEI4 (E) seem to cause cell

adhesion defects on hypocotyl in the double mutant in comparison with the control condition (**Figure A-12A**). This correlates with the level of expression of the genes coding for these proteins, revealed previously. As a reminder, *qua2/esmd1* under-expressed *PME35* and *PMEi4* compared to *qua2* or Col0. For *PME53*, the level of expression in *qua2/esmd1* had returned to a level equivalent to wild type whereas *qua2* overexpressed it. Thus, it is therefore not surprising that the addition of these proteins in the medium induces a cell detachment. The effect of these enzymes on *qua2/esmd1* cell adhesion suggests that they may affect the pectic pattern leading to cell adhesion defects in the *qua2* context. This could be explained by the fact that *esmd* mutation controls *PME35* expression level. This control then may restore the methylated pectic pattern that mediates the restoration of cell adhesion in the double mutant. In Col0 (**Figure A-12 F-J)** no **PME and PMEi affect cell adhesion.** phenotypic effect was revealed after application of all enzymes.

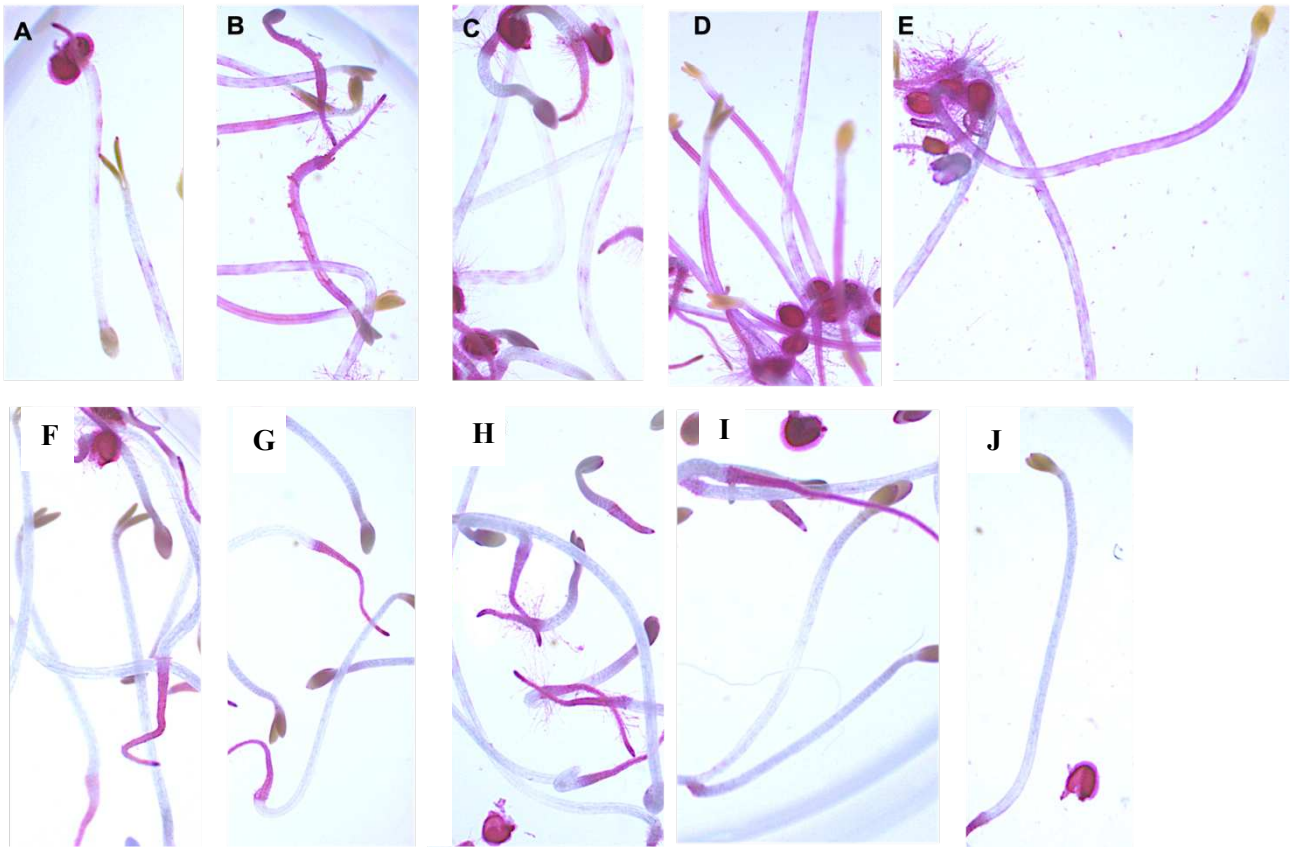

Figure A-12 **PME and PMEi affect cell adhesion.**

Ruthenium red staining of enzyme application on 4 d old dark grown hypocotyls (from day 2) on *qua2-1/esmd1-1* (A-E): (A) empty vector, (B) PME35, (C) PME41, (D) PME53, (E) PMEI4. Col0 (F-J), same order of protein.

f) How do PAE candidates affect the *quasimodo* pectic pattern?

According to our RTqPCR analysis, the PAE 7 and PAE12 genes are under-expressed in *qua2*. We observed previously (**see Chapter 1 Figure A-3**) the acetylated and acetylated methylated-H_2O pectic are more abundant in the pectin of *qua2* compared to *esmd1* and the double mutant. In this sense, after having produced the 2 candidate PAE proteins in a heterologous system, we applied them for 48 hours on living dark grown hypocotyls and we analyzed by LC/MS the acetylated and acetylated methylated-H_2O OGs released by the digestion with a commercial PG. We observed from (**Figure A-13A**) that the sum of acetylated OGs decrease when *qua2* is treated with the supernatant of Pichia expressing PAEs. PAE7 seems to have a stronger impact on this pattern compared to PAE12. When we look in detail at the different OGs identified (**Figure A-13B**), we observe that the 2 PAEs significantly reduce the $GalA_5Ac$. Furthermore, PAE 7 also significantly reduces the quantity of $GalA_3Ac$ and Gal_3Ac_2. Finally, no difference was observed in the methyl acetylated H_2O pattern (data not shown). Indeed, we have demonstrated that the $GalA_3Ac$ is significantly increased in *qua2* compared to *qua2/esmd1*. Thus, the observed restoration of the level of expression of PAE 7 and PAE 12 in the double mutant compared to *qua2* may be partly responsible for the restoration of the acetylated pattern. Together these results suggest that the 2 PAEs would have a preference for acetylated patterns.

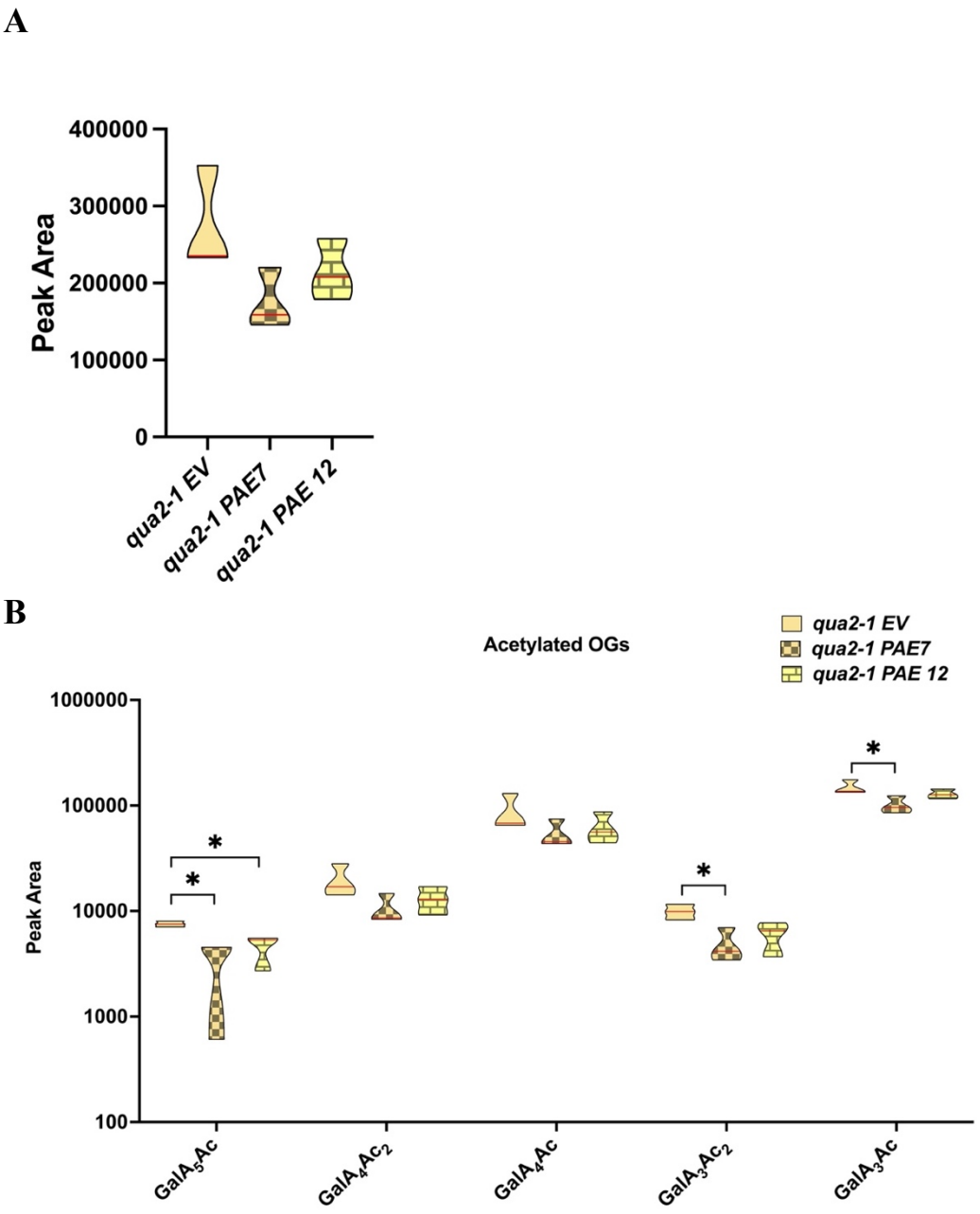

Figure A-13 **Pectic pattern affected by PAE7 and 12.**

Truncated violin plot of Sum of the quantity of Acetylated HGs fragments digested by PG *Aspergillus aculeatus* of dried cell wall of 4-day-old dark grown seedlings of *qua2-1* treated for 48h (first 48h in control medium and next 48h with the protein extract) with the secreted compounds of Pichia transformed with an empty vector or producing PAE7 or PAE12. *Red line represents the median, (n = 3 biological replicates per genotype).*

Truncated violin plot of acetylated HGs fragments released by PG *Aspergillus aculeatus* digestion of dried cell wall 4-day-old dark grown seedlings *qua2-1. (n = 3 biological replicates per genotype)* *, $p < 0.05$, T-Test.

g) How does PME41 affect the wild-type pectic pattern?

According to our RTqPCR analysis, the PME41 gene is over-expressed in *qua2* compared to Col0. We observed previously (**see Chapter 1 Figure A-2, A-3, A-4**) that the methylated and methylated-H_2O pectic are more abundant in the pectin of Col0 compared to *qua2*. In this sense, after having produced the PME41 proteins in a heterologous system, we applied them for 48 hours on living dark grown hypocotyls and we analyzed by LC/MS the methylated and methylated-H_2O OGs released by the digestion with a commercial PG. We observed from (**Figure A-14)** that the sum of methylated and methylated-H_2O OGs decreases when Col0 is treated with the "supernatant" PEM41. When we look in detail at the different OGs identified, we observed that the PME41 significantly reduce the $GalA_{12}Me_9$-H_2O, $GalA_{12}Me_8$-H_2O, $GalA_{10}Me_8$-H_2O consistently among the 3 replicates. PME41, seems to have a significant effect on methylated-dehydrated pattern. Since we know that PME41 protein is a PME Type I and may have a random action on homogalacturonan methyl esterification. It may explain why we observed only slight modifications on the global digestibility. However, we cannot omit that endogenous PMEI may also control the PME action. Together these results suggest that the PME41 may prefer the methylated dehydrated patterns.

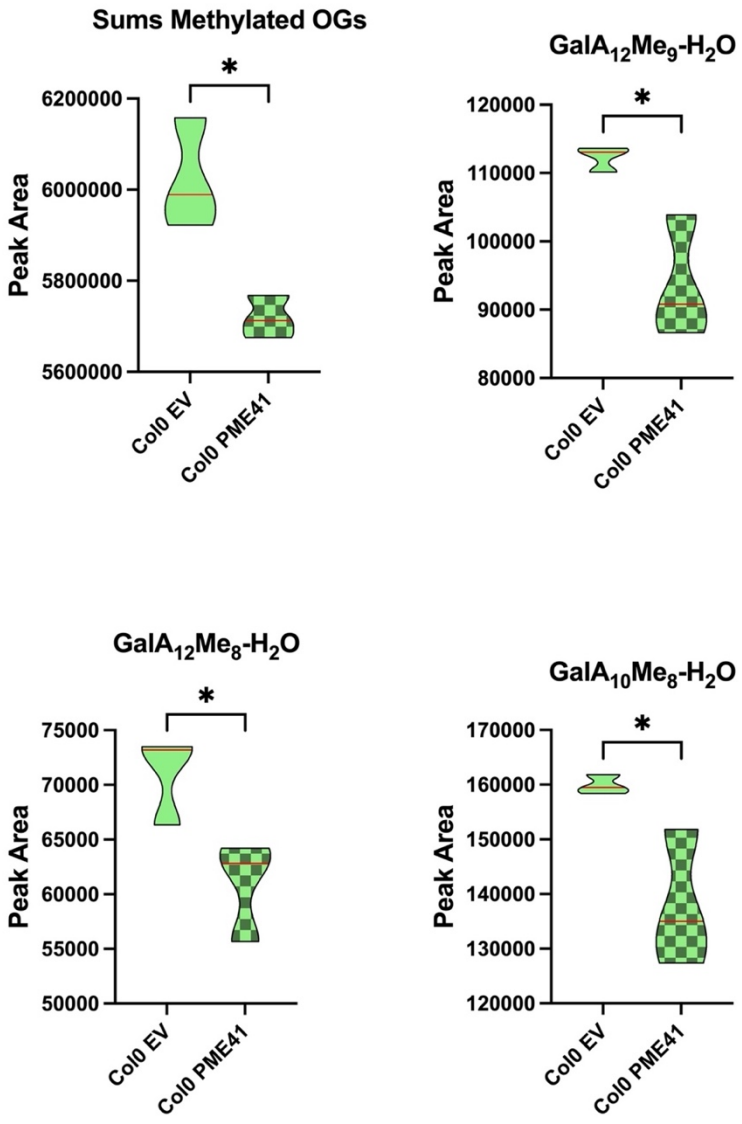

Figure A-14 **Pectic pattern affected by PME41.**

Truncated violin plot of the quantity of HGs fragments released by PG *Aspergillus aculeatus* digestion of dried cell wall of 4-day-old dark grown seedlings.

We present the Sum of the quantity of HGs methylated and methylated-H_2O and the HGs Fragments that are significantly differentially accumulated between the control condition and the treated condition Col0 was treated for 48h (first 48h in liquid medium and next 48h with the protein extract) with the secreted compounds of Pichia transformed with an empty vector (Col0 EV) or producing PME41 (Col0 PME41). *Red line represents the median (n = 3 biological replicates).* *$p < 0.05$, T-Test.

h) New actor of cell adhesion

To find a new actor involved in cell adhesion, we carried on a mutagenesis of 2500 seeds of the Col0 accession. The conditions of this experiment were carried out as described in the protocol of Verger et al. (2016). The screening approach was performed by a ruthenium red screening on 4-day-old dark grown hypocotyls. (**Figure A-15A)** show the results of the ruthenium red screening. We identified on mutant named 60. We can observe that this mutant displays a high permeability to ruthenium without necessarily presenting a clear cell detachment.

The homozygous plants were then backcrossed with Col0. Among the 400 plants resulting from the segregation of this backcross, 100 (no staining) and 100 plants displaying cell adhesion defect (stained) were identified by the same ruthenium red screening. The DNAs of the100 plants of each genotype were pooled and sequenced through NGS sequencing with an average depth of 6X.

The analysis of the sequencing results was carried out in the same way as the protocol of Verger et al. (2016). After alignment with Col0 reference genome. We compared the SNPs in our 2 pools of DNA. We identify 5 SNPs exclusively present in the DNA of the plants displaying loss of cell adhesion phenotype (**Figure A-15 B**). Five TDNA mutants in these genes are currently under genotyping and phenotyping to identify if the mutation of one of these genes is responsible for the cell adhesion phenotype of the mutant 60.

A

B

	Chromosome	Position	col0 nucléotide	60 nucleotide	read number		ID	Name
60	Chr 2	17946219	G	T	5	exon	AT2G43150	Extensin 21
60	Chr 2	17946252	C	T	5	exon	AT2G43150	Extensin 21
60	Chr 4	10025654	A	T	5	exon	AT4G18050	ABC transporter B family member 9
60	Chr 5	2906942	T	C	4	exon	AT5G09360	Laccase 14
60	Chr 5	5554232	C	T	26	exon	AT5G16890	Exostosin Family protein
60	Chr 5	6851842	C	T	22	exon	AT5G20290	Ribosomal protein S8e family protein

Figure A-15 **Identification of a new mutation involved in the control of cell adhesion.** Picture 4-day-old dark grown hypocotyl, stained with ruthenium red (A) new homozygous EMS mutant called "60" (B) List of candidate genes mutated the mutant 60.

i) Second feature of this new cell adhesion mutant

After sowing the seeds of the mutant 60, we noticed that they were floating even after 2 days in water. Thus, we performed ruthenium red staining of the adherent mucilage to assess whether the mutant showed any difference compared to the wild type. We can observe a net reduction of the adherent mucilage released in water in the mutant 60 (**Figure A-16 B, C**) compared to the wildtype (**Figure A-16 A**). Conversely, by using a chelating agent such as EDTA, forming a complex with the different polysaccharides and favoring the releases of the mucilage. We can observe that the mutant 60 (**Figure A-16 E, F**) releases as much mucilage as the wildtype (figure D). Such a phenotype in water has already been observed in the *mum5* mutant encoding the putative xylosyl transferase (Ralet et al., 2016). This protein is required to produce highly branched xylan in seed coat mucilage. Specifically, the binding affinity of xylose branches on RG-I to a cellulose scaffold is one of the factors involved in the formation of the adherent mucilage layer. Thus, we can suggest that mutant 60 has a polysaccharide defect which leads to a defect in releasing adherent mucilage.

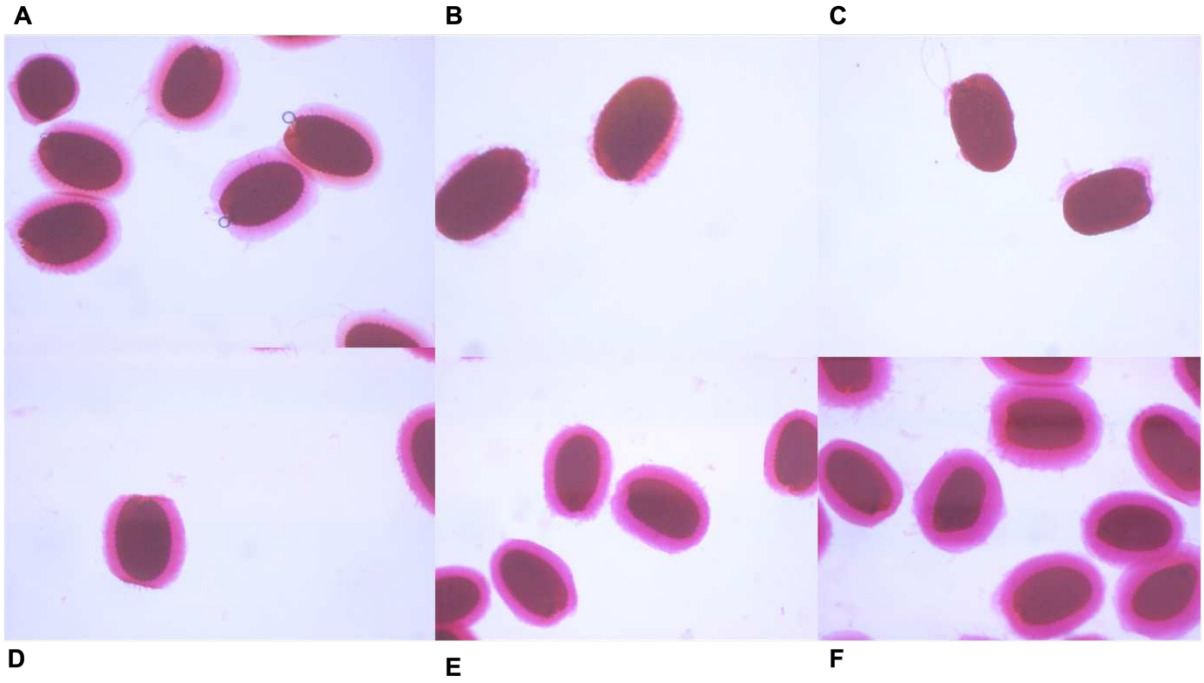

Figure A-16 **Visualization of the adherent mucilage layer by ruthenium red staining of seeds**.

(**A**) Col0, (**B**) mutant 60 homozygote plant A, (**C**) mutant 60 homozygote plant B after agitation in water. (**D**) Col0, (**E**) mutant 60 homozygote A, (**f**) mutant 60 homozygote B, in 0.05 M EDTA.

B) CHAPTER 2: GALACTURONIC ACID INDUCES THE RESTORATION OF CELL ADHESION THROUGH EXTENSINS CROSSLINK

PART I

The second part of my work consisted in identifying actors not necessarily linked to *Esmeralda1* "pathway" but involved in the control of cell adhesion. The approach presented below aims to identify signals that induce a signaling pathway that controls the cell adhesion, always using the etiolated hypocotyl model of *quasimodo*. We focus on the characterization of the endogenous OGs present in dark hypocotyl. It leads to the discovery of a molecule able to restore the cell adhesion defect occurring in *quasimodo*. Then we explored in details the effects of this compound on cell adhesion and demonstrate that adhesion can be controlled by direct mechanisms which are not necessarily going through signal transduction and/or *Esmeralda*1 pathway.

1) Does the pectic monomer balance are important in cell adhesion?

In the Arabidopsis cell adhesion model, OGs appeared to be the best candidates to mediate different signals via their perception by the cell wall receptor. This is because mutant *qua2* can be restored without modifying the pectin defect while repressing the expression of the pectin response gene (Verger et al., 2016; Denoux et al., 2008, Kohorn, 2016). Thus, deciphering the diversity of OGs produced in planta, also called endogenous OGs, and understanding their role in the context of cell adhesion seems necessary. We decided to perform an extraction with 70% ethanol, heated to 80 ° C during 1H, on fresh material of 150 dissected hypocotyls grown 4 days in the dark (4 biological replicates). Endogenous OGs were analyzed by high-performance size exclusion chromatography (HP-SEC) - MS-based (Voxeur et al., 2019). Each endogenous OGs identified by the simple MS method was fragmented to confirm their identity. By this extraction and analysis, we identified 9 different OGs between a DP 1 to 5 with different methylation or oxidation signatures. Among the various OGs identified (**Figure B-1**) we observed only a difference in quantity but not in identity between Col0 and *qua2*. Obviously, the esterification profile of the identified endogenous OGs implies that the esterification pattern and the susceptibility to the PGs that generate endogenous free compounds might be unchanged

between the 2 genotypes. Moreover, we must note that the ratio of each OGs of *qua2* compared to Col0 seems similar for most of the OGs (0,5 to 0,63 for the significant differences), except for the 2 monomers. The galacturonic acid GalA is the most affected and galactaric acid GalAOx the less. This larger difference of free galacturonic acid could be assimilated to the defect in pectin of *qua2*, while oxidized OGs are known to be implicated in pathology context (Voxeur et al., 2019) and their potential of elicitation is weaker (Benedetti et al., 2018). In conclusion, in *qua2* the balance between GalAOx and GalA is inverted compared to the wild type. Thus, it appears interesting to investigate the effect of exogenous Galacturonic acid on *qua2* to counter care this inverted balance.

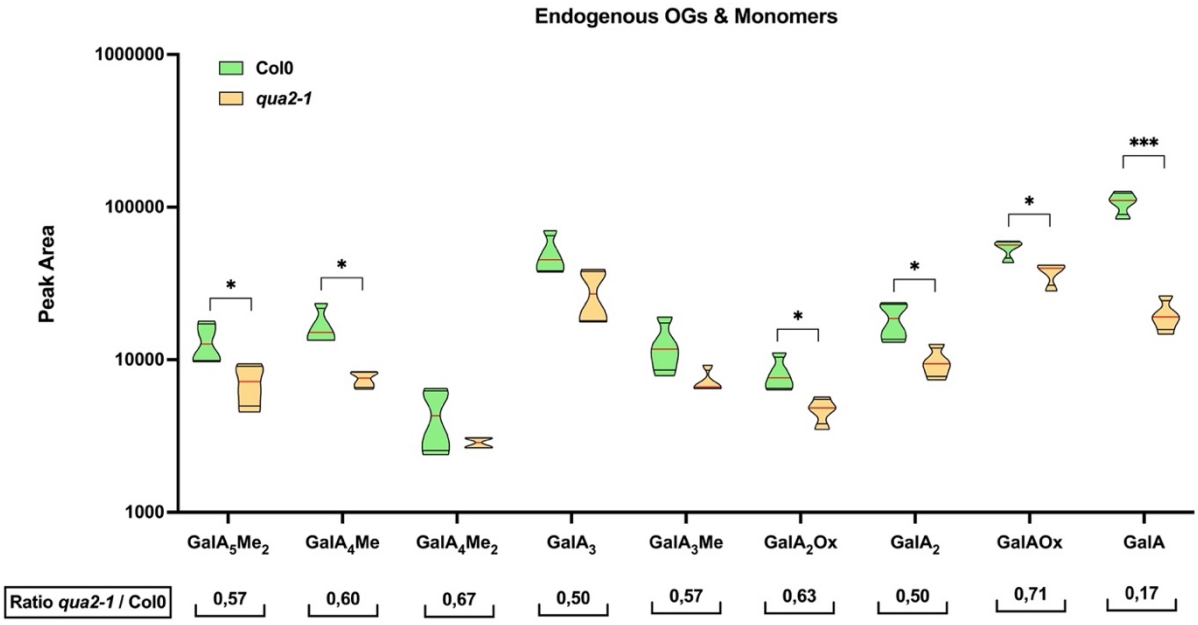

Figure B-1 **Endogenous OGs and monomers.**

Truncated violin plot of peak area of endogenous OGs for 150 4-day-old dark grown dissected hypocotyls of Col-0, *qua2-1*. Oligogalacturonides (OGs) are named as follow $GalA_xMe_y$. The number x in subscripts indicates the degree of polymerization, and y the number of methylation or oxidation. GalA: galacturonic acid; Me: methyl ester group Ox: oxidation.

Red line represents the median, black line the quartiles (n = 4 biological replicates per genotype). *, $P < 0.05$, Mann & Whitney test

2) What's happening when we try to counter care the inverted balance Gal<GalAOx in *quasimodo* by GalA application?

To study the effect of galacturonic acid, we decided to cultivate our plant in MilliQ water buffered at pH 5.7 with MES, with or without GalA. The phenotypic effects of GalA on *qua2* were observed on 4-day-old dark grown hypocotyls, stained with ruthenium red. The results observed (**Figure B-2A and B-2B**) demonstrate a decrease in the staining by ruthenium red of *qua2* treated with galacturonic acid (Fi**gure B-2B**) compared to the control condition (**Figure B-2A**). The second phenotypic effect that we can observe concerns the level of cell detachment, which is greatly reduced by the treatment, reflecting a restorative effect linked to the application of galacturonic acid (**Figure B-2B**). Finally, the basal zone of the hypocotyl (**Figure B-2B**) corresponding to the oldest part, is more strongly red than the rest of the hypocotyl and shows most of the time slight detachment suggesting a gradual restoration during the elongation of the hypocotyl. To ensure the restoration is induced by the unique effect of galacturonic acid and not a metabolic effect, we treated *qua2* with glucuronic acid, a GalA precursor, at the same concentration. The results (**Chapter 2 Supp data Figure B-10)** do not show any restorative effect linked to glucuronic acid, confirming a specific effect of galacturonic acid at the same concentration. Moreover, we suspected an increase in the length. To confirm it, we measured the length of 30 hypocotyls and performed a 2way-ANOVA to confirm an interaction between treatment and genotype (**Figure B-2C**). The interaction results between the 2 factors were significant and account for 1.779% of the total variance. Genotype Factor accounts for 70.31% of the total variance and treatment 2.781%. The multiple comparisons (**Figure B-2C**) revealed the length of Col0 is significantly higher compared to *qua2*. Besides, the GalA treatment increase significantly *qua2* length whereas it does not affect Col0. Furthermore, the GlcA treatment has no effect. This confirms those preliminary empiric observations.

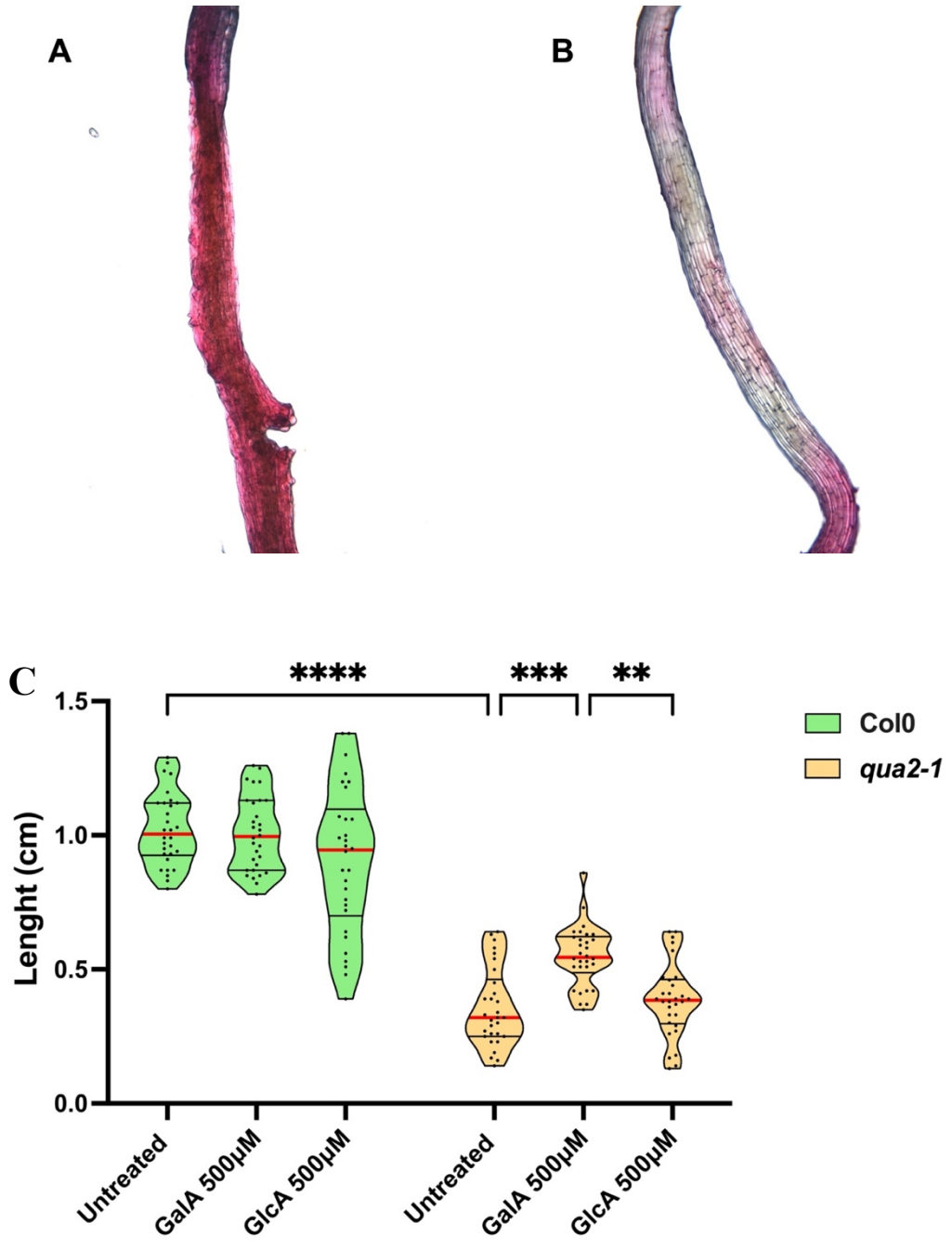

Figure B-2 **GalA restore cell adhesion and enhance length.**

Ruthenium red staining on 4-day-old dark grown hypocotyls of (A) *qua2-1* (B) *qua2-1 GalA 500µM.* (C) Truncated violin plot of the length of 30 4-day-old dark grown hypocotyls. *Red line represents the median, black line the quartiles, black dot represents biological replicate*. In (C) **, P < 0.001, ***, P < 0.0001, ****, P < 0.00001, 2way-ANOVA (Tukey's multiple comparisons test).

3) A new tool to evaluate cell adhesion

To confirm the observations relating to the restoration of cell detachment, we decided to use a new tool to assess the tortuosity of the 2D binary shape of the hypocotyls. Tortuosity is a property of a curve that is meandering around the shape. The MATLAB code we used, was created to determine the cell shape dynamic by measuring the boundaries curvature (Discroll et al., 2012). Thus, we thought that it might be interesting to see if this code can be adapted to our model, in order to highlight differences in tortuosity of the curvatures between the multiple boundaries defining the binary shape of our condition (**Figure B-3A**). From the result obtained after running the code, we observed (**Figure B-3B**) that the tortuosity of the 2D shape of *qua2* is significantly highest compared to the wild type straighter. It is interesting to note that the GalA treatment on *qua2* significantly restored tortuosity and does not show any significant difference with the wild type. To confirm what we observed previously with the staining, we also analyzed the GlcA treatment which does not restore the level of tortuosity in *qua2*. Thus, this new tool allows evaluating the tortuosity and cell detachment.

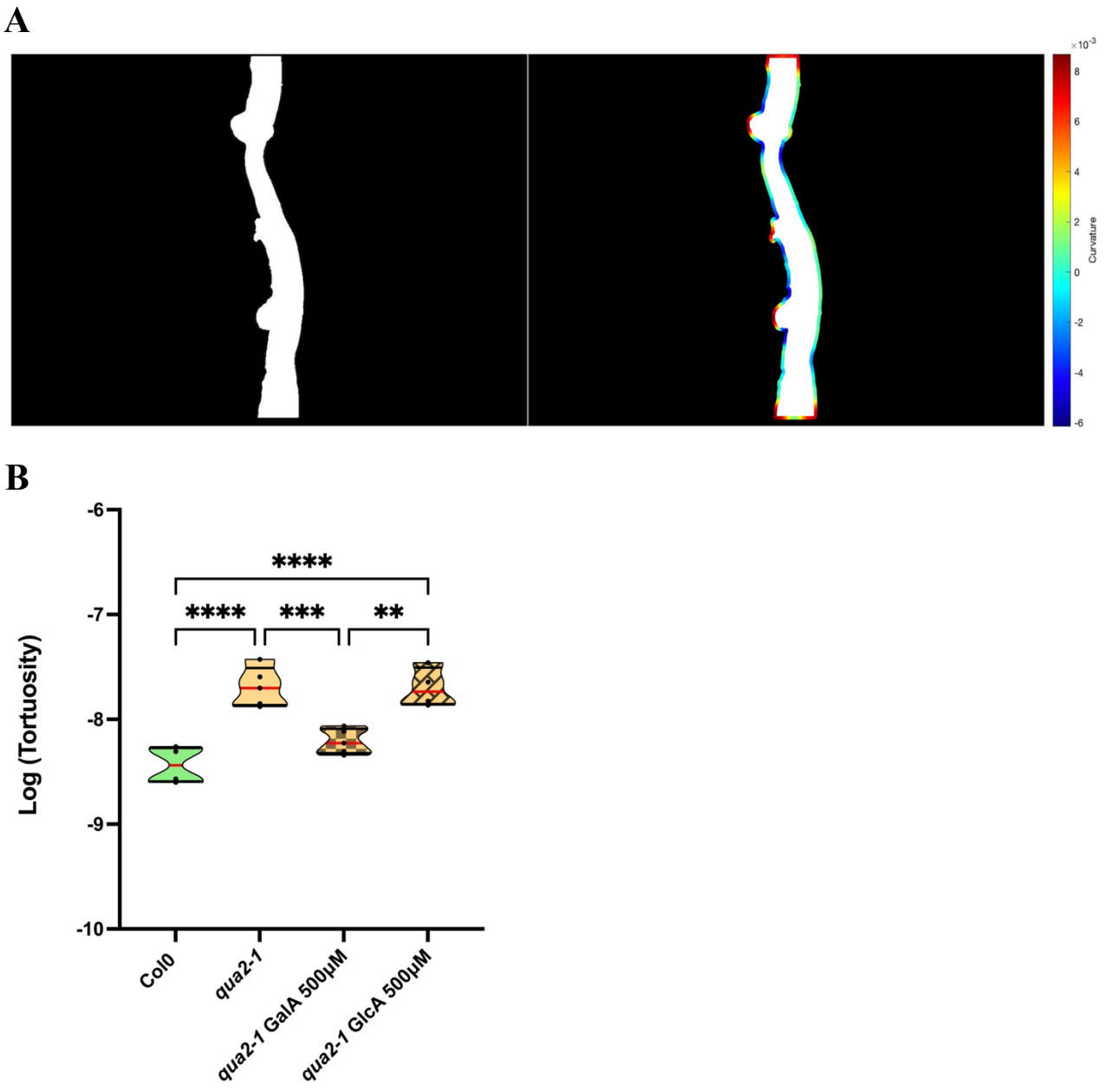

Figure B-3 **New tool to evaluate cell adhesion.**

(A) Binary picture of 4-day-old dark grown hypocotyls of *qua2-1* after running Matlab code. The second picture corresponds to the level of curvature around the shape.

(B) Truncated violin plot of the shape tortuosity of 4-day-old dark grown hypocotyls for the different conditions. *Red line represents the median, black line the quartiles, black dot represents biological replicate.* In (B) and (C), **, P < 0.001, ***, P < 0.0001, ****, P < 0.0000, 1-way-ANOVA (Tukey's multiple comparisons test) *(n ≥ 4 biological replicates per condition).*

4) GalA where are you going?

Then we try to elucidate what are the modifications generated by the treatment with galacturonic acid leading to the partial restoration of the phenotype *quasimodo2*. We decided to analyze the fine structure of the pectin to know if this treatment induces modifications of the pectic matrix. To achieve this, we used a commercial endo-PG A*spergillus aculeatus* applied on dried cell wall of 4 days dark grown hypocotyls and we performed a digestion for 24 hours to digest the pectic fraction as much as possible. The fragment released were analyzed by LC-HRMS. In this fraction, we identified 92 HGs fragments including 1 monomer and 4 Xylogalacturonans ranging from a DP1-13 with different signatures of methylation, acetylation, and oxidation (**Chapter 2 Supp data Figure-B-11**). The first thing observed is that the quantity of HGs fragments released (**Figure B-4A**) significantly reduced in the *qua2* mutant compared to the wild type. The treatment with galacturonic acid does not affect this difference compared to *qua2* untreated suggesting an effect of the treatment. This result can be explained by the fact that *qua2* has less pectin in general and this is also revealed in our analysis. The fragments identified were grouped and divided into 7 different classes to know if the pattern proportions are identical between the wild type and the mutant. According to the part of the whole (**Figure B-4B**), *quasimodo* has 1,3 times less methylated fragments compared to the wild type. Galacturonic acid causes an insignificant change of 0,05 times compared to not treated *qua2*. Globally, the patterns are very different between *qua2* and the wild-type, and thus may participate in its lack of adhesion. The treatment with galacturonic acid causes only a few insignificant changes in the *quasimodo* pattern. Additionally, the quantity of individual HG fragments or monomers and XGAs is not different between *qua2* treated and untreated. Some of them are just slightly up or down.

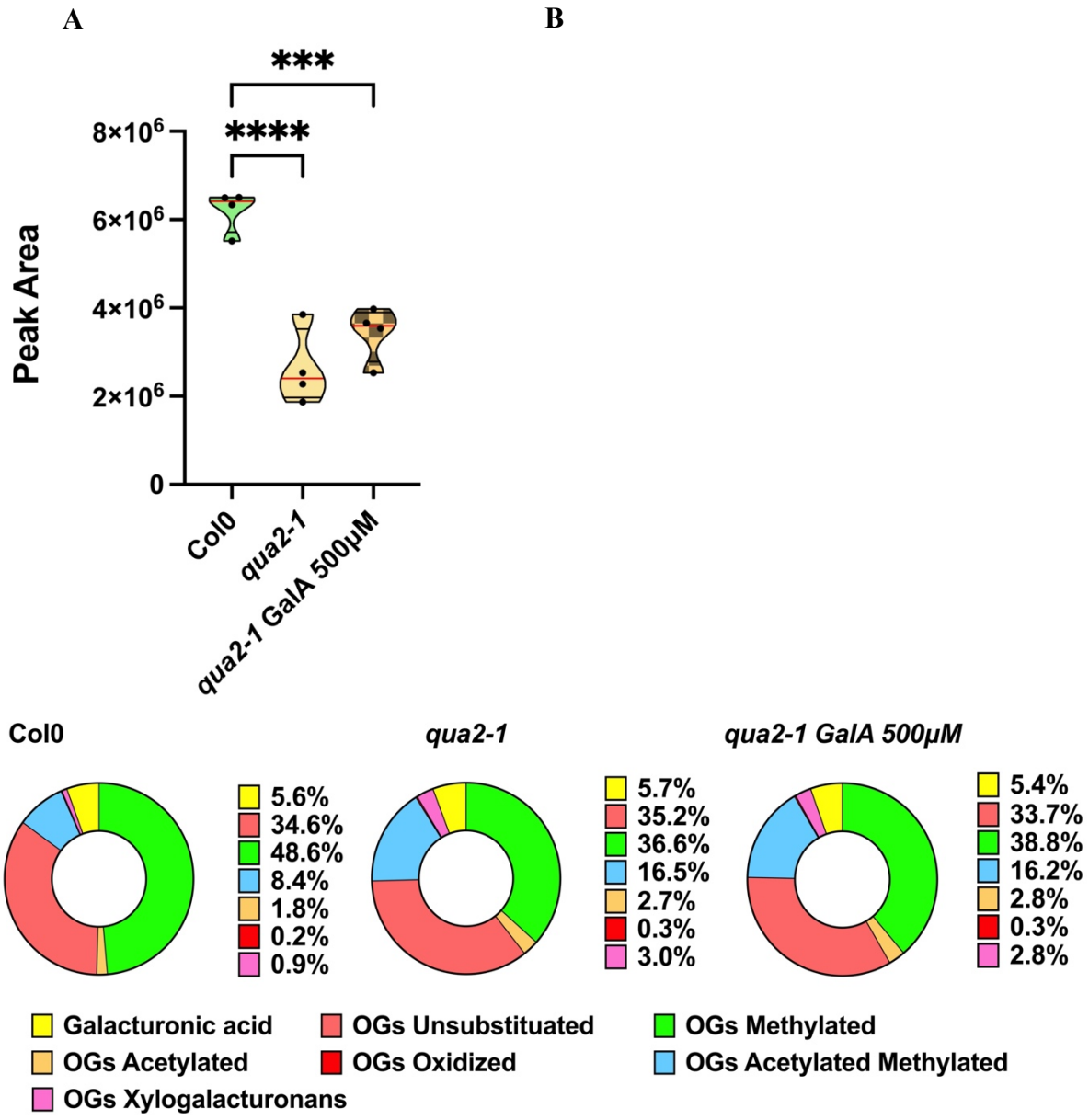

Figure B-4 **Fine structure of HGS fragment & monomer.**

(A)Truncated violin plot of the quantity of HGs fragments family released by PG *Aspergillus aculeatus* digestion of dried cell wall 4-day-old dark grown seedlings of Col-0, *qua2-1, qua2-1 GalA 500µM. Red line represents the median, black line the quartiles.* (B) (C) Relative content of HGS fragment & monomer family released by PG digestion of dried cell wall of 4-day-old dark grown of seedlings of Col-0, *qua2-1, qua2-1 GalA 500µM (n = 4 biological replicates).*

***, $P < 0.0001$, ****, $P < 0.00001$, T-Test.

5) Is GalAOx responsible for cell adhesion restoration in *quasimodo*?

As a control in our experiment, we used the same material with the inactivated enzyme buffered with ammonium acetate. It is interesting to note that this fraction also released OGs probably trapped in the cell wall by weak non-covalent binding. Among the 6 OGs and monomers (**Figure B-5A)** identified in this fraction, the 2 monomers were significantly increased. GalA treatment obviously increased the quantity of GalA trapped in the cell wall. Moreover, the most interesting and unexpected thing concerns the amount of GalAOx. The quantity of GalAOx is multiplied 30 times by the treatment in *qua2*. It suggests that the added GalA is oxidized. It also implies that oxidases participate in this conversion. In this way, we decided to study the effect of GalAox on *qua2* at the same concentration. As shown in the photo (**Figure B-5B**), GalAOx does not restore the cell adhesion phenotype in *quasimodo2*. We can therefore resume the phenomenon observed from the beginning (**Figure B-5C**). We add galacturonic acid which restores adhesion in *qua2,* but only subtly changes pectins pattern. This addition induces a strong accumulation of GalAOx and this conversion by oxidases also generates H_2O_2 so we decided to investigate its effect.

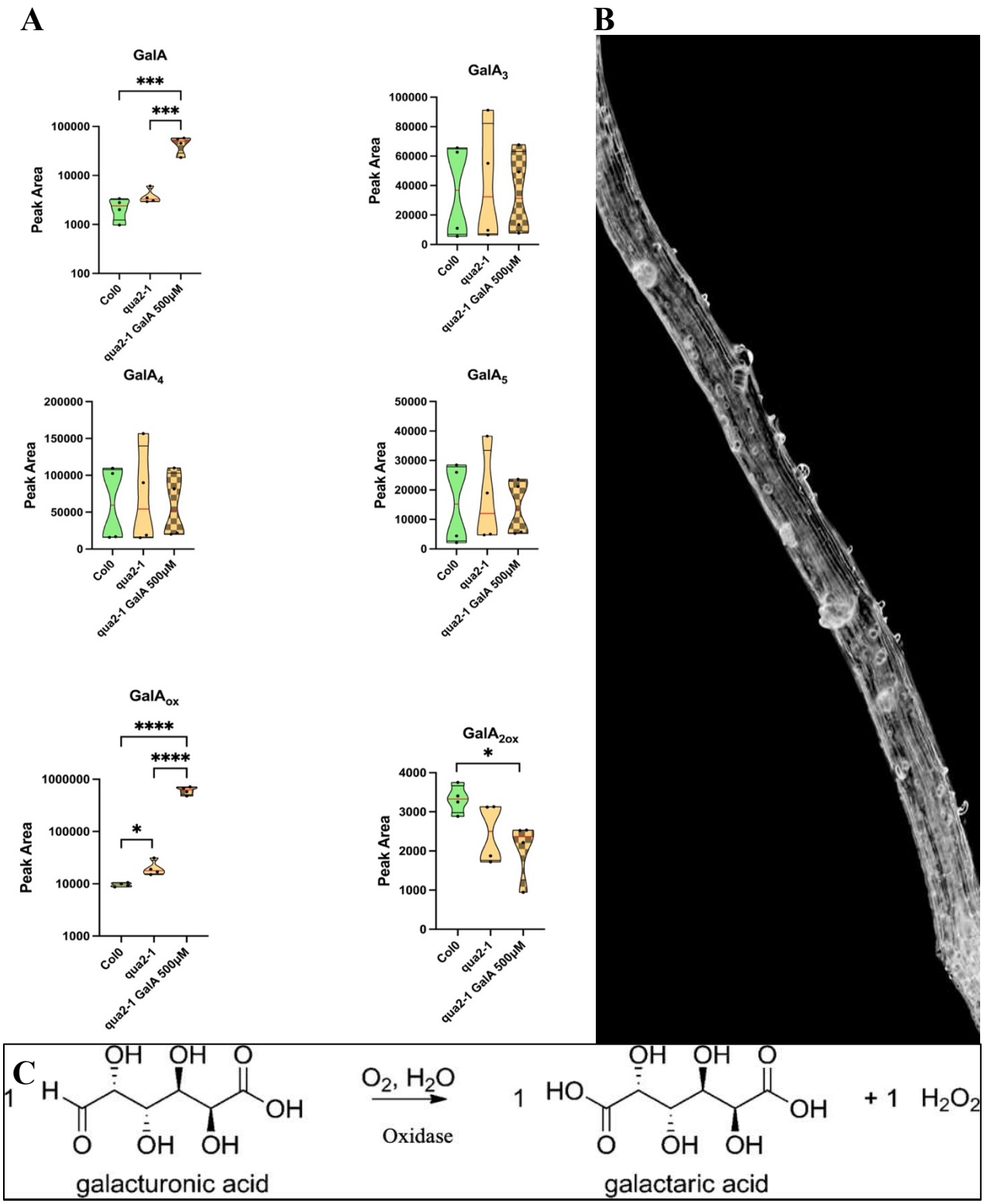

Figure B-5 **OGs bind to cell wall polymers.**

(A) OG released from the undigested fraction of dried cell wall of 4-day-old dark grown seedlings Col-0, qua2-1, qua2-1 GalA 500µM (n = 4 biological replicates per genotype). Red line represents the median, black line the quartiles, black dot represents biological replicate. (B)

Picture of GalAOx treatment on qua2-1. (C) Conversion reaction of GalA into GalAOx which generate H_2O_2. In (A) *, P < 0.01, ***, P < 0.0001, ****, P < 0.00001, T-Test.

6) What about the H_2O_2 effect?

To study the effect of H_2O_2, we cultivated our plant in the same condition as we used for the previous treatment on 4-day-old dark grown hypocotyls and stained with ruthenium red (**Figure B-6 A and B**). We, therefore, observe the restoration of the *qua2-1* phenotype by H_2O_2 (**Figure B-6B**) with a very weak ruthenium red staining compared to the control (**Figure B-6A**) condition. Moreover, cell detachment is also restored in this condition. We have also quantified the tortuosity of this treatment (**Figure B-6C**). H_2O_2 application restores the tortuosity, as well as the GalA treatment at the same concentration. This result allows us to establish that the 2 treatments are intimately linked to the common restoration mechanism.

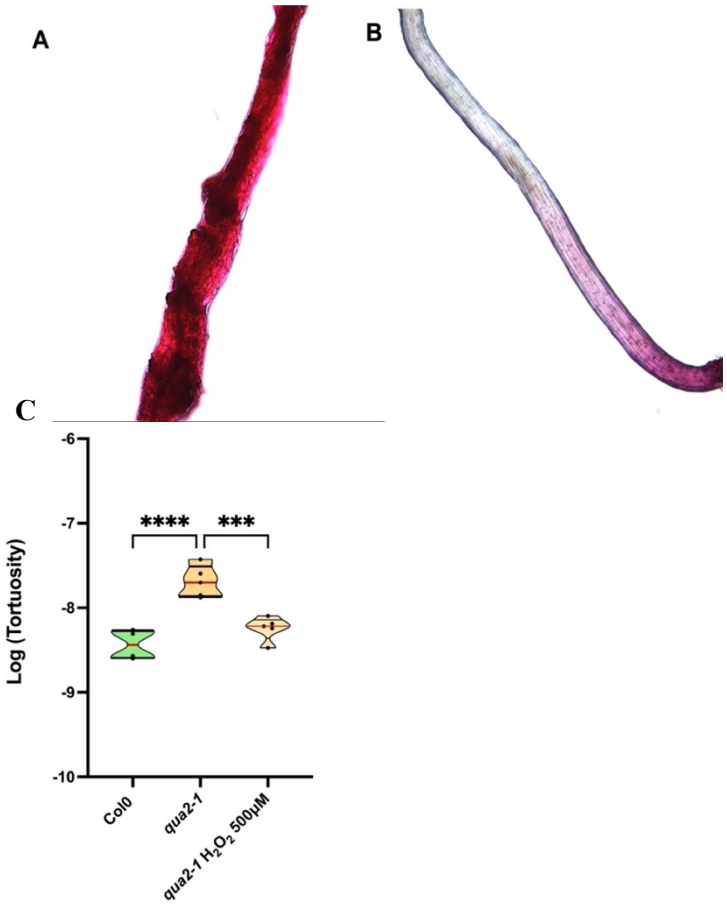

Figure B-6 **H_2O_2 restore cell adhesion.**

(A) Ruthenium red staining on 4-day-old dark grown hypocotyls of (A) *qua2-1* (B) *qua2-1 H_2O_2 500µM*. (B) Truncated violin plot of the shape tortuosity of 4-day-old dark grown hypocotyls for the different conditions. *Red line represents the median, black line the quartiles,*

black dot represents biological replicate. In (C), ***, P < 0.0001, ****, P < 0.00001 1way-ANOVA (Tukey's multiple comparisons test). *(n ≥ 4 biological replicates per condition).*

7) Is added or produced H_2O_2 allowing structural protein crosslink and mediate cell to cell adhesion in *quasimodo*?

The question now is how H_2O_2 can be used to mediate the restoration of cell adhesion. It has been demonstrated by several studies that this compound can enhance the crosslinking of extensin HRGPs through their tyrosine residue. So, the first thing that was essential to know, was how this phenomenon of crosslinking of proteins could be highlighted. We, therefore, used the protocol described by (Mellersh et al., 2002) & (Asselbergh et al., 2007) which consists in carrying out an SDS treatment at 80 ° C for 24 hours to eliminate the non-crosslinked proteins and keep only those crosslinked. The staining is carried out with Coomassie blue and makes it possible to reveal the crosslinked proteins. According to our results, we did not observe between the cells in Col0 (**Figure B-7A**) compared to *qua2* (**Figure B-7B**) showing staining between cells. This can be explained by the fact that *qua2* overexpresses some extensins and therefore potentially accumulates crosslinked proteins (Du et al., 2020). We observe much more intense and abundant labeling between the cells, after treatment with galacturonic acid (**Figure B-7C**) or H_2O_2 (**Figure B-7D**). This suggests an increase in crosslinked related to the treatment and therefore potentially mediated restoration of *qua2* phenotype by these crosslinks.

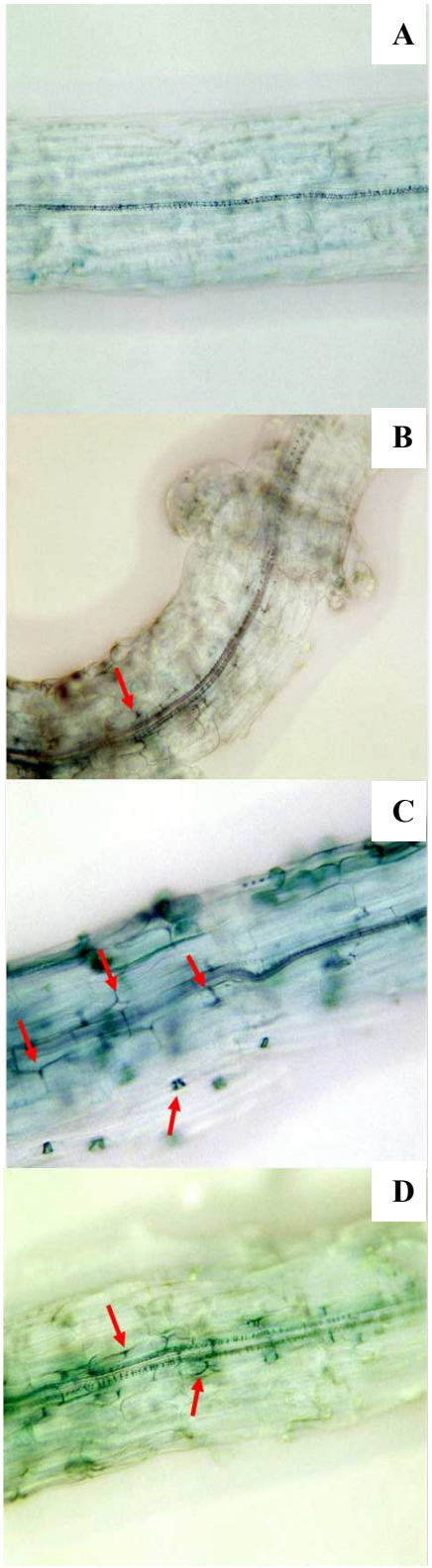

Figure B-7 **Crosslinked structural protein Coomassie blue staining**.

Picture of 4-day-old dark grown hypocotyl, (A) Col0 (B) *qua2-1* and (C) *qua2-1 GalA 500µM,* (D) *qua2-1* H_2O_2 *500µM*. Red arrow indicate the crosslinked proteins

8) What kind of structural protein crosslinked mediates cell to cell adhesion in *quasimodo*?

To confirm our staining, we sought to quantify dimeric, trimeric, and tetrameric tyrosine from 4-day-old seedlings grown in the dark. Thus, after a 6N HCL hydrolysis was carried out on the dry cell wall and we analyzed the hydrolysate by LC / MS. Each identified molecule was fragmented into MS / MS and subjected to a match formula and fragmentation profile, search with SIRIUS Web module. We were able to identify 6 different forms of tyrosine ranging from the single amino acid to the tetramer Di-isodityrosine. The isodityrosine is an intramolecular dimer, the five others of these cross-linked tyrosines reveal interchains cross-linking.

We observe a significant increase in the total amount of intermolecular linked tyrosine in *qua2* compared to the WT. This phenomenon is enhanced and becomes statistically significant after the treatment by GalA (**Figure B-8A**). It confirmed the enhanced protein crosslink observed visually (**Figure B-7**). The global higher content of intermolecular cross-link tyrosine observed in *quasimodo* (**Figure B-8A**) is due to a higher amount of all types of cross-linked tyrosine particularly the isodityrosine; the only statistically significant (**Figure B-8A**). The GalA treatment in *qua2* induces the same modification specifically via the significant enhancement of the quantity of Pulcherosine and Trityrosine. a non-significant increase compared to the wild type and a slight increase compared to its control. The most interesting facts concern the tetramer and the 2 trimers identified (**Figure B-8B**).

Finally, the significant increase in the relative amount of di-isodityrosine (intramolecular linked) observed in *qua2* treated or not compared to wild type probably reflects the overexpression of Extensin gene in *quasimodo* previously described (Du et al., 2020).

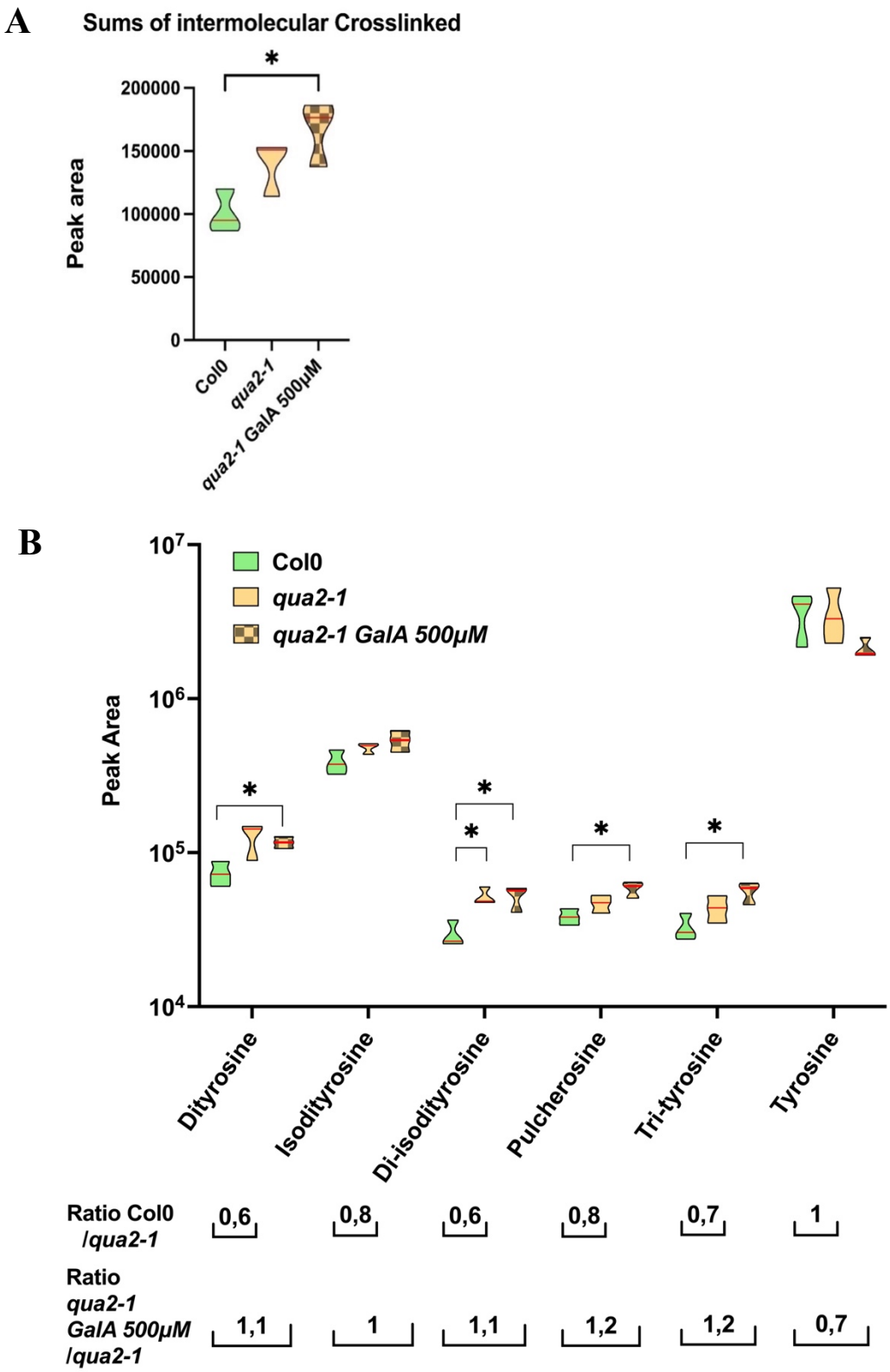

Figure B-8 **Extensins crosslinked.**

(A) Truncated violin plot of the sums of intermolecular crosslink including pulcherosine, di-isodityrosine and trityrosine of 4-day-old dark grown seedlings for the different conditions. (B)

Truncated violin plot of the quantity of the different intermolecular and intermolecular crosslink identified and fragmented of 4-day-old dark grown seedlings for the different conditions. *Red line represents the median (n = 3 biological replicates per genotype)*. In (A) and (B) *, $P < 0.05$, T-Test.

CONCLUSION

In conclusion, we observed that the GalA treatment in *qua2* significantly increased the number of intermolecular crosslinks of tyrosine regardless of the type of bond. The different types of intra or intermolecular crosslinks identified have already been described in different studies (Fry, 1982; Epstein and Lamport, 1984; Brady et al., 1998; Held et al., 2004; Cannon et al., 2007). These studies justify the iso-dityrosine, pulcherosine and di-isodityrosine bonds and therefore the C-O bond is catalyzed by peroxidase. In addition, a study shows that *qua2* overexpresses *peroxidase 71* in the apoplast (Raggi et al., 2015). We propose that this candidate peroxidase could be the one responsible for the crosslinking modification that is observed. Regarding C-C bond, no study has shown any influence of H_2O_2 on the formation of these bonds in the plant. On the other hand, a recent study in humans shows that H_2O_2 allows the crosslinking of dityrosine (Mukherjee et al., 2017). This could explain the increase of dityrosine and tri-tyrosine induced in *qua2* and/or by the GalA treatment. Finally, it remains to understand how the extensin would be a potential candidate in the restoration of the adhesion of the mutant *qua2*. Since the mechanism we have highlighted by the application of GalA or H_2O_2 is relatively fast. A study on the model of graft union in Arabidopsis may help to link between what we observed and the restoration of cell adhesion. Sala et al. (2019) demonstrate that 3 components of the cell wall were present in abundance in the material deposited extracellularly. This material includes weakly or unesterified HGs and extensins leading to the formation of a network allowing cell adhesion. We suggest that, here in the case of *qua2*, the extensins would form a network on their own and/or interact with the HGs of the weak middle lamella of *qua2* and enhance cell adhesion.

9) Supplemental Data

a) Does the GalA induce some hormonal pathway?

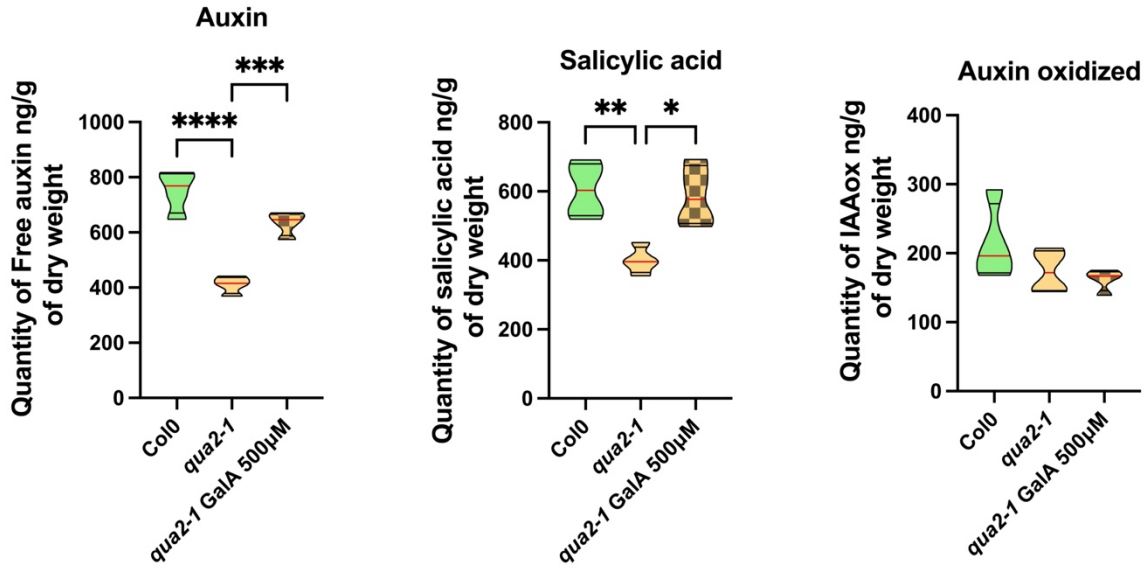

Figure B-9 **Hormone quantification**

Truncated violin plot of quantity of hormone, from dried pouder of 4-day-old, etiolated Col, *qua2*, *esmd1 and qua2/esmd1* seedlings. Quantification was performed by UPLC/MS. *Red line represents the median, black line the quartiles (n = 4 biological replicates per genotype).* *, P < 0.05, **, P < 0.001, ***, P < 0.0001, T-Test.

The quantity of free Auxin is significantly increased by the GalA treatment on *qua2* compared to *qua2* untreated as well as the quantity of salicylic acid.

b) Does the GlcA induce restoration of cell adhesion in *quasimodo*?

Figure B-10 **Picture of GlcA treatment on *qua2-1*.**

As described in (**Chapter 2: Figure B-2 and B-3**) no restoration of cell adhesion was observed with the GlcA on qua2-1.

c) List of all fragments released and identified

Mass	Retention time	Formule
1194,2544	7,0303	GalA13Me6
1201,2616	7,0827	GalA13Me7
1099,2312	7,121	GalA12Me5
1208,2694	7,1439	GalA13Me8
1106,2381	7,1789	GalA12Me6
1113,2458	7,2368	GalA12Me7
1011,2148	7,2751	GalA11Me4
1120,2523	7,3068	GalA12Me8
1104,2399	7,3385	GalA12Me7-H2O
1018,2221	7,3439	GalA11Me5
916,1908	7,3811	GalA10Me4
1111,2476	7,4237	GalA12Me8-H2O
923,1983	7,439	GalA10Me5
1181,2712	7,4532	GalA12Me9Ac3-H2O
1160,2656	7,4685	GalA12Me9Ac2-H2O
842,1734	7,4784	GalA9Me3Ac
1032,237	7,4794	GalA11Me7
1139,2604	7,4795	GalA12Me9Ac-H2O
1118,2558	7,4827	GalA12Me9-H2O
821,1666	7,486	GalA9Me3
1167,2732	7,5308	GalA12Me10Ac2-H2O
930,2061	7,5319	GalA10Me6
914,1928	7,5516	GalA10Me5-H2O
828,1745	7,5571	GalA9Me4
937,2135	7,5964	GalA10Me7
835,1823	7,639	GalA9Me5
921,2006	7,639	GalA10Me6-H2O
856,1871	7,6325	GalA9Me5Ac
754,1555	7,6522	GalA8Me3Ac
819,169	7,6675	GalA9Me4-H2O
991,2243	7,6838	GalA10Me7Ac3-H2O
1467,3055	7,6434	GalA8Me3
970,2186	7,6948	GalA10Me7Ac2-H2O
949,2132	7,7079	GalA10Me7Ac-H2O
842,1899	7,7232	GalA9Me6
928,2084	7,7265	GalA10Me7-H2O
847,1806	7,733	GalA9Me5Ac-H2O
826,1768	7,7483	GalA9Me5-H2O
1481,3215	7,7221	GalA8Me4
977,2267	7,78	GalA10Me8Ac2-H2O
956,2215	7,791	GalA10Me8Ac-H2O
638,127	7,7931	GalA7Me2
935,2161	7,8063	GalA10Me8-H2O
875,1951	7,8106	GalA9Me6Ac2-H2O
854,1899	7,8358	GalA9Me6Ac-H2O
833,1848	7,8456	GalA9Me6-H2O
752,1571	7,8489	GalA8Me4Ac-H2O
747,1658	7,8511	GalA8Me5
666,1396	7,862	GalA7Me3Ac
645,1344	7,8686	GalA7Me3
1463,3105	7,8751	GalA8Me4-H2O
882,2032	7,9145	GalA9Me7Ac2-H2O
861,1978	7,9155	GalA9Me7Ac-H2O
840,1925	7,9308	GalA9Me7-H2O
1477,3274	7,9855	GalA8Me5-H2O
1101,2274	8,0259	GalA6Me2
1575,363	8,0598	GalA8Me6Ac2-H2O
1491,3428	8,0882	GalA8Me6-H2O
953,1901	8,1134	GalA5MeAc
643,138	8,1166	GalA7Me4-H2O
1115,2423	8,1243	GalA6Me3
911,1793	8,1418	GalA5Me
1547,3688	8,1625	GalA8Me7Ac-H2O
1505,358	8,1746	GalA8Me7-H2O
1343,3053	8,2106	GalA7Me5Ac-H2O
1129,2584	8,227	GalA6Me4
1301,2948	8,2303	GalA7Me5-H2O
1097,2317	8,2434	GalA6Me3-H2O
763,1423	8,2511	GalA4Ac
925,1947	8,2565	GalA5Me2
721,1317	8,2631	GalA4
1357,3207	8,3221	GalA7Me6Ac-H2O
867,1894	8,3286	GalA4XylMe
1315,3102	8,3341	GalA7Me6-H2O
555,1206	8,3625	GalA6Me4-H2O
939,2104	8,3844	GalA5Me3
777,1574	8,3844	GalA4MeAc
735,1474	8,3953	GalA4Me
809,1845	8,4259	GalA3Xyl2
1167,2734	8,4838	GalA6Me5Ac-H2O
677,1418	8,4937	XylGalA3
1125,263	8,5046	GalA6Me5-H2O
587,1101	8,5144	GalA3Ac
717,1367	8,5166	GalA4Me-H2O
545,0995	8,5505	GalA3
691,1575	8,6237	GalA3XylMe
977,2264	8,6718	GalA5Me4Ac-H2O
935,2157	8,6849	GalA5Me4-H2O
731,1526	8,6991	GalA4Me2-H2O
559,1152	8,7089	GalA3Me
385,0623	8,7581	GalA2ox
193,0352	9,3023	GalA

Figure B-11 **List of fragments released and identified by LCHR/MS.**

PARTII

1) Additional work on the GalA effect

a) Does the GalA restore cell adhesion defect in other mutants?

To find out if GalA treatment is effective on other mutants with cell adhesion defects, we have grown *quasimodo1* (Bouton et al., 2002) in buffered water containing Uronic Acid *Quasimodo1* mutant has been described as having phenotypes similar to *qua2.* Indeed, *qua1* presents a dwarf phenotype, accompanied by a lack of cell adhesion, a reduction in the quantity of GalA and an abnormal release of "border like cells" (Bouton et al., 2002; Durand et al., 2009). According to our staining with ruthenium red, we can observe that untreated (**Figure B-12A**) and GlcA (**Figure B-12B**) treated *qua1* hypocotyl are red and present both cell adhesion defects. Conversely, the application of galacturonic acid (**Figure B-12C**), partially restores the adhesion defects with a reduction in labeling and probably a reduction in cell detachment. This result was already seen with *qua2*. Additional experiments on cell wall using FTIR and hypocotyl length measurement are in progress to confirm a potential link between the restoration of cell adhesion mediated by the application of GalA in *qua1* and *qua2*. Together these results reinforce the idea that QUA1/GAUT8 and QUA2 are involved in the same pathway and even could interact in the synthesis of HG (Mouille et al., 2007). (Verger et al., 2016). Finally, this gives a starting point for a common pathway of restoration by galacturonic acid for these 2 mutants.

Figure B-12 **Visualization of Cell adhesion defect by ruthenium red staining.**

Picture 4-day-old dark grown hypocotyl, stained with ruthenium red (A) of *qua1-1*, (B) *qua1-1 GlcA* 500µM *and* (C) *qua1-1 GalA* 500µM.

b) Does the GalA restore the cuticle?

Because *esmeralda* mutation causes changes at the level of the cuticle layer on *qua2*, we explored this feature on GalA treated *qua2* mutant. To do this, we carried out a toluidine blue staining according to the protocol of Creff et al. (2019) on 4-day-old dark grown hypocotyls. Following staining, blue coloration is intense in *qua2* (**Figure B-13B**) and absent in Col0 (**Figure B-13A**). Besides, we can observe that the GalA treatment clearly reduced the staining (**Figure B-13C**). The coloration of the cuticle turns white and pink in the middle of the hypocotyl. These results demonstrate that the GalA treatment partially restores the permeability of the cuticle in *qua2*. This probably means that the restoration of cell adhesion mediated by GalA causes weak penetration of the stain used. Given that *qua2* does not have any defects in the ultrastructure of the cuticle (Lorrai et al., 2021) our results do not allow us for the moment to define what are the real changes caused by GalA on the restoration of the cuticle.

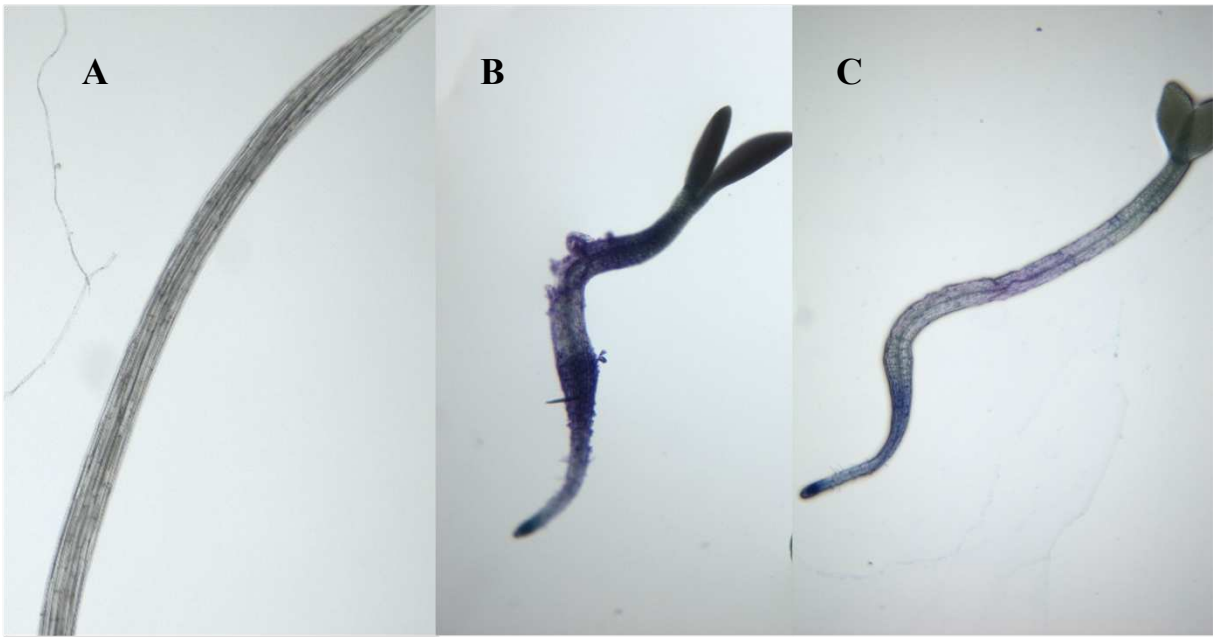

Figure B-13 **Cuticle permeability.**

(A) Picture of Col0 4-day-old dark grown hypocotyl, stained with toluidine bleu, (B) *qua2-1* and (C) *qua2-1 GalA 500µM.*

c) Who are the candidates genes for the GalA oxidation and the protein crosslink?

Due to the identification of a significant accumulation of GalAox linked to the application of GalA, we sought to identify the oxidases that may be responsible for this oxidation. Remember that some members of the FAD binding berberine family have been characterized as OG oxidases (Benedetti et al., 2018). Thus, by cross-checking the transcriptome data from (Verger, 2014) and the dark ground hypocotyl cell wall proteome data from (Jamet et al., 2006) we identified 8 candidates. According to the qPCR analysis (Figure B-14A) we can observe that 3 candidates, *OGOX4*, *OGOX3* and *BBE5* are more expressed in *qua2* treated or not with Gal A compared to Col0. OGOX4 and OGOX3 are described as oligogalacturonide oxidase that inactivates the elicitor-active oligogalacturonides OGs (Benedetti et al., 2018). No specific functional characterization has been demonstrated for BBE5. Thus, this confirms that the mechanism of oxidation of GalA to GalAox is already present in *qua2*. The application of GalA in *qua2* not changing the level of expression of these genes suggested that the activity of these proteins would be changed independently of their expression by post-transcriptional regulation. Nonetheless, *BBE3/Fadlox* seems to be overexpressed in *qua2* treated with GalA compared to

Col0. This gene is known to respond to the pectic signal (Denoux et al., 2008). The over expression of *BBE3* in response to GalA application demonstrates that the application of GalA is signaling as a pectic signal. However, it has been described that *qua2* overexpressed *BBE3* but under light conditions (Verger et al., 2016). Here, in the dark culture conditions, we observed that this gene is not overexpressed in *qua2*. This suggests the *BBE3* expression is differential depending on the culture conditions in *qua2*.

Recent studies demonstrated that *qua2* overexpressed 2 extensins compared to wild type (Du et al., 2020; Kohorn et al., 2021). We wanted to know what effect our treatments have on the expression of these 2 genes. According to RTqPCR analysis of the expression of these genes (**Figure B-14B**), we can confirm that *EXT4* is strongly overexpressed in *qua2* compared to Col0 and that the application of H_2O_2 or GalA does not change the level of expression. This confirms that EXT4 would be one of the candidates subject to the cross-linking of its tyrosines in the presence of H_2O_2 by the action of peroxidase and allowing the restoration of adhesion in *qua2*. As for oxidases, *EXT4* expression is not increased with GalA treatment. These results suggest that the treatment applied on *qua2* just makes it possible to increase the crosslinking yield of EXT4 without changing its level of expression. In addition, Transgenics over-expressing *EXT4* plants have stems of increased thickness (Roberts & Shirsat, 2006) correlating with our adhesion restoration results in *qua2*. Interestingly, we were able to observe a significant increase in the level of expression of *EXT3* by the application of GalA in *qua2* compared to Col0. This suggests that GalA induces additional expression of other extensins. Conversely, H_2O_2 is the product inducing/or enabling cross-linking not triggering this over-expression. This may suggest faster cross-linking by H_2O_2 which is not necessitating the EXT3 to mediate cell adhesion in *qua2*. The GalA requiring an intermediate conversion to GalAox would lead to a signal triggering the overexpression of EXT3.

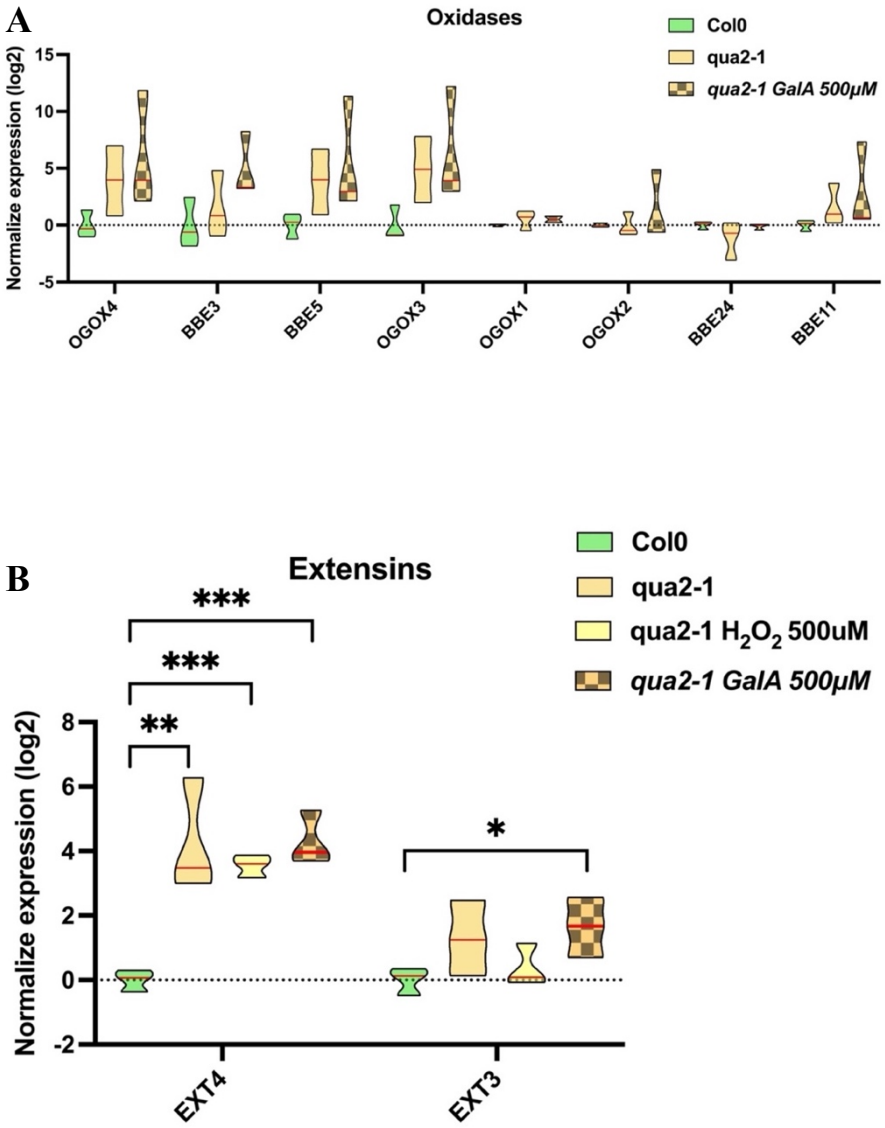

Figure B-14 **Oxidase and extensin expression.**

(A) Truncated violin plot of Normalized expression levels (log2) of 8 oxidases of the FAD Binding Berberine family, from 4-day-old, etiolated seedlings of Col0, *qua2*, *qua2-1* treated with GalA 500µM by qPCR. *APT1 & CLATHERINE* were amplified as internal controls. Normalized expression levels (log2) were calculated according to a normalization factor of 2 housekeeping genes and reported to the expression of the wild type (Taylor et al., 2019). (B) Truncated violin plot of Normalized expression levels (log2) of *EXT4 and EXT3*, from 4-day-old, etiolated Col0, *qua2*, *qua2-1 H_2O_2 500µM*, *qua2-1 GalA 500µM* seedlings by qPCR. *Red line represents the median (n = 3 biological replicates per condition). In (B)* *, $P < 0.05$, **, $P < 0.001$, ***, $P < 0.0001$, T-Test.

d) Does the GalA affect some *PME/PMEI* expression?

In order to identify the different signaling effects of GalA, we carried out an RtqPCR analysis of the *PME* and *PMEI* genes deregulated in *qua2*. Among these 4 genes (**Figure B-15**), we can observe that the expression of *PME 41* and *53* in treated conditions remains unchanged compared to *qua2* untreated. *PME41* is overexpressed in *qua2* and but also in *friable1* (Neumetzler et al., 2012). We have seen previously that the overexpression of *PME41* associated with that of *PME53* is probably responsible for the methylated pectic pattern less present in *qua2* compared to the wild type, and probably contributes to the lack of cell adhesion in *qua2*. We already showed that the methylated pattern of *qua2* was globally unchanged by the GalA treatment. This result fits with overexpression of *PME41* and 53 still present in GalA treated *qua2*. Nevertheless, this suggests that restoration of cell adhesion in *qua2* by GalA application bypass these *PME41* and *PME53* deregulations. However, we can observe that *PMEI4* and *PME35* genes are under-expressed by GalA treatment both in the wild type and *qua2*. We observed the same PME35 and PMEI4 under the mediation of expression by the *esmd* mutation (**see in Chapter 1 Figure A-5**). Thus, this result suggests that GalA has a signaling effect leading to a decrease in the expression of *PMEI4* and *PME35*. Furthermore, the *PMEI4* underexpression in the *qua2* treated can also be attributed to the restored elongation observed corresponding to a triggered growth (Pelletier et al., 2010). Together, these results suggest that GalA may have a signaling effect, implying a part of a common pathway with *esmeralda*.

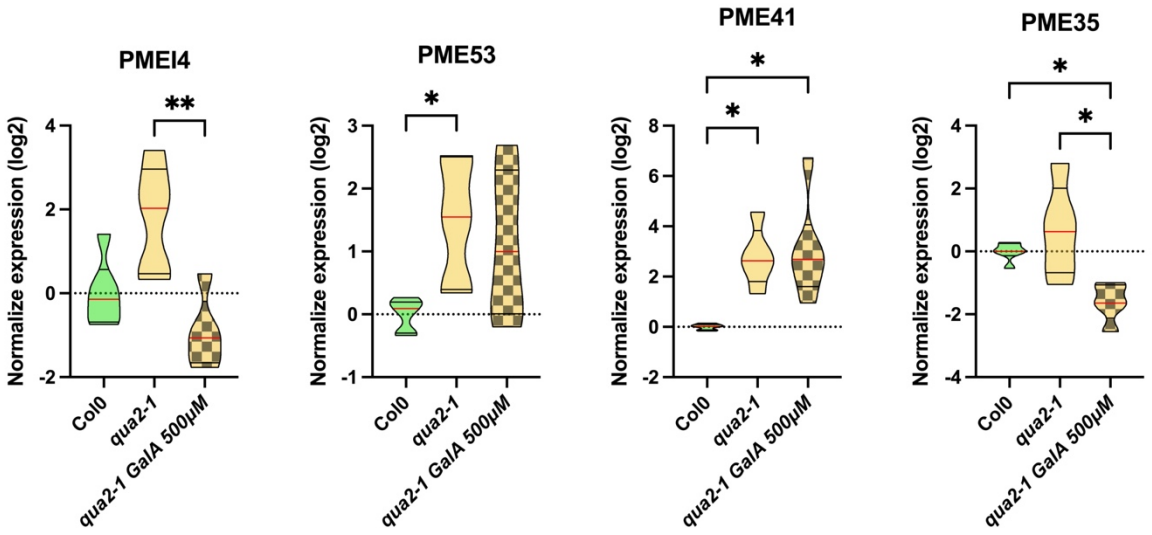

Figure B-15 **Level of expression of PME/PMEi**.

Truncated violin plot of Normalized expression levels (log2) of *PMEI4, PME, 35, 41, 53,* from 4-day-old etiolated seedlings Col, *qua2*, *qua2-1* grown in GalA 500µM measured by qPCR. *APT1 & CLATHERINE* were amplified as internal controls. Normalized expression levels (log2) were calculated according to a normalization factor of 2 housekeeping genes *APT1 & CLATHERINE* and reported to the expression of the wild type (Taylor et al., 2019). Red line represents the median, black line the quartiles (n ≥ 5 biological replicates per genotype for PME and PMEI)

For *, $P < 0.05$ and **, $P < 0.001$, Krustall Wallis ANOVA tests (Dunn's multiple comparisons test).

A) *ESMERALDA1* WHAT ARE YOU DOING?

Recent studies on ESMERALDA1 have demonstrated the importance of the mediation of the signal triggered by this putative O-fucosyltransferase in the context of cell adhesion. In animals, the O-fucosylation occurs on Epidermal Growth Factor domains of particular receptors. This O-Fucosylation mediates some protein-ligand/protein-protein interactions (Takeushi et al., 2014 ; Lei et al., 2003). Thus, a change in O-fucosylation can lead to defects in receptor interaction and trafficking. In plants, some receptors, such as Wall Associated Kinase or Leucine-Rich Repeat Receptor-Like Kinase, contain EGF domain showing some similarity to the animal one. Other receptors, such as WAK-Like, contain truncated EGF domains. Verger et coll (2016) suggested that some of these EGF could be targets of ESMERALDA. However, no O-fucolsyltransferase activity was demonstrated for ESMERALDA1. Nevertheless, ESMERALDA1 seems to be involved in different mechanisms that are still under study. If we refer to previous studies, a mutation in this gene allows the restoration of several cell adhesion defective mutants with (Verger et al., 2016). *esmd* appears to restore cell adhesion defects of several mutant, *qua1/gaut8* mutant affected in galacturonosyl transferase, *qua2* in pectin methyltransferase and *friable1* mutated in one isoform of ESMERALDA1. Thus, ESMERALDA1 seems to be a central and versatile element controlling cell adhesion (Verger et al., 2016).

The research on the mechanism leading to the restoration of cell adhesion in *qua2* by the *esmd1* mutation has been the subject of detailed studies. They brought various elements on the involvement of *esmd1* in cell adhesion but also the identification of new potential actors of this pathway. Indeed, in addition to restoring the *qua2* phenotype, the *esmd1* mutation leads to the decrease of the expression of the *FADlox* gene, known to respond to the pectic signal (Denoux et al., 2008), and this without restoring the defect in *qua2* pectin content (Verger et al. al., 2016). Moreover, in our lab, a new suppressor has been identified. *esmd4*; a mutant affected in a gene encoding another member of the O-fucosyltransferase family. This mutation does restore *qua2* cell adhesion phenotype (Mouille et al, unpublished).

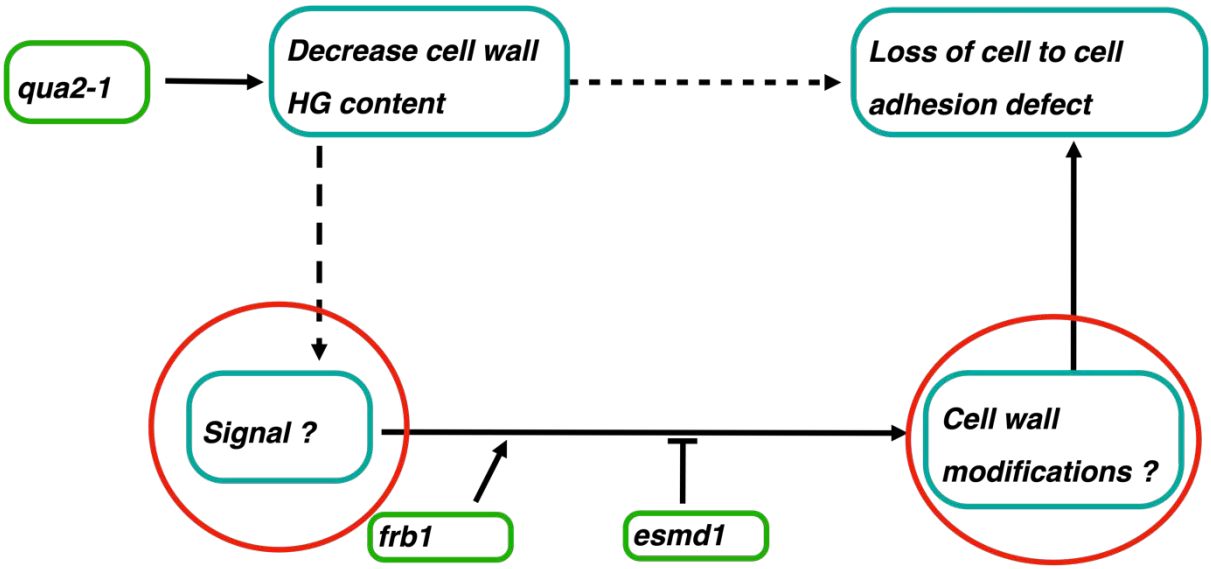

Figure A-1 **Cell adhesion current model (Verger et al., 2016)**

It was proposed that *qua2* pectin deficiency in not responsible for the loss of cell adhesion (dashed arrow), but instead creates a signal that activates a signaling pathway leading to the loss of cell adhesion. The *frb1* and *esmd1* mutations affect this pathway positively and negatively, respectively, thus triggering or suppressing the cell adhesion defect through as yet unidentified cell wall modifications.

Based on this knowledge, the first objective of this thesis was to understand what was the signal repressed by *esmd* allowing the restoration of adhesion in *qua2*. Thus, the first experiment consisted to identify endogenous OGs of dark-grown hypocotyls. The role of Oligosaccharides in plant development and response to its environment was mainly explored through the exogenous application of OGs provided by the enzymatic fingerprint of pectin (Safran et al., 2021; Voxeur et al., 2019; Hocq et al., 2017; Hocq et al., 2020) or PGA HG enriched fractions on plants or the use of pectin egg box (Korhorn et al 2009; Denoux et al., 2008; Voxeur et al., 2109; Sinclair et al., 2017; Davidson et al., 2017; Verger et al., 2014). In the literature only one endogenous OG was tested on etiolated seedlings by Sinclair and coll (2017), which was shown to induce cell elongation. So the challenge here was first to prove the presence of endogenous OGs in our plant material and determine what are the main OGs present. Thanks to the method developed by (Voxeur et al., 2019) we were able to identify and quantify 7 different OGs, thus proving the presence of endogenous OGs within our dark grown hypocotyls. Unfortunately, among the different mutants used we could not demonstrate the existence of specific OGs characteristic of one particular genotype. Globally, *esmd* restores the abundance of OGs in *qua2*

to an equivalent level as the wild type. Some of the OGs identified, have been characterized in other contexts. $GalA_3$, the most abundant OG seems logical since it is considered as a trigger signal for hypocotyl elongation in the dark (Sinclair et al., 2017). The higher quantity of $GalA_3$ observed in *esmd/qua2* double mutant could be assimilated to the restored elongation observed (Verger et al., 2016). Two methylated OGs, $GalA_4Me$ and $GalA_4Me_2$ seem to be specifically increased by the *esmd* mutation. These methylated OGs are considered to have a lower affinity to WAK receptors (Kohorn et al., 2009). Nevertheless, these OGs may constitute a signal in plant. Indeed, a recent study showed that a $GalA_4MeAc$-H_2O enriched fraction triggers plant defense mechanisms against the attack by *Botrytis cinerea* (Voxeur et al., 2019). So even if these OGs have a lower affinity with WAK-type receptors, they could constitute a specific signal through other receptors or be required in quantity to trigger a signal mediated by *esmd* mutation.

Together these different elements may also suggest that the overall amount of endogenous OGs restored by *esmd* in *qua2* corresponds to an eliciting amount required to restore or maintain cell adhesion. In another context Branca et coll. (1988) demonstrated an antagonistic response between OG and IAA. Furthermore, in some cases, the loosening of the cell wall is induced by auxin and leads to the formation of OGs (Sénéchal et al., 2014). So, the increase in the quantity of OGs, induced by *esmd* in *qua2*, could be antagonistic to auxin and prevent degradation of the middle lamella by a negative feedback loop. Then in *qua2* the quantity of OGs, not sufficient, would lead to a degradation of the middle lamella and cell adhesion loosening.

The second objective of our study was to identify what are the major modifications induced by *esmd* on the pectins of *qua2* and the responsible actors of these modifications. This could allow one to understand how *esmd* permits the increase of the amount of endogenous OGs. To do this, we chose to analyze the pectic patterns by enzymatic fingerprinting. Thus, we were able to reveal that *esmd* can restore the digestibility of pectin thanks to a modulation of the HGs pattern in *qua2*. This differential management of the pattern is attributed to the increase of the amount of methylated pattern revealing 39 methylated HGs fragments increased and 18 specific signatures. Furthermore, a decrease in the amount in the specific pattern of *qua2*, concerning highly methylated and acetylated HGs fragments, would seem to contribute to this restoration of digestibility. In addition, all these modifications are made without restoring a quantity of HGs (Verger et al., 2016). Together, these results offer several hypotheses. The double mutant pectic pattern similar to the wild type would probably allow a more appropriate pattern leading to more inter-spaced micro-domains crosslinking *via* Ca^{2+} on homogalacturonan (Grant et al.,

1973; Willats et al., 2001) and favorize the restoration of cell adhesion. The pectic pattern could contribute also to cross-linking with other cell wall polymers such as AGPs, extensins or cellulose (Nunes et al., 2012; Valentin et al., 2010; Sala et al., 2019; Hijazi et al., 2012; Hijazi et al., 2014). Finally, these observations correlate with the increase in endogenous OGs observed previously, emphasizing an essential role of ESMERALDA1 in the control of the pectic pattern.

Thanks to an analysis by RTqPCR of all *PME, PMEI* and *PAE* genes we were able to reveal that some of them are regulated transcriptionally by *esmd* in *qua2* background. *esmd* mutation led to the underexpression of *PMEi4*, implying an acceleration of the growth of the triggered hypocotyl (Pelletier et al., 2010) which happens to be untriggered in *qua2*. This would explain why the *esmd* mutation restores growth in *qua2*. Moreover, *esmd* restores the expression of *PME53* to a level equivalent to that of the wild type, decreases the expression of *PME41* and *PME35* in *qua2*. Interestingly *PME41* is overexpressed in *qua2* but also in *frb1* (Neumetzler et al., 2012). This suggests that this gene is probably responsible for an unstable pectic pattern contributing to cell adhesion defects. In addition, 2 *PAE* genes are restored to a level equivalent to the wild type by the *esmd*, whereas they are under-expressed in *qua2*. This confirms that the transcriptional regulation governs by the *esmd* contributes to the restoration of the pattern allowing to restore digestibility in *qua2*.

Together, these data suggest that the *esmd* mutation in *qua2* generates a loop bypassing the cell adhesion defect via the transcriptional modification of HGME, allowing an appropriate pattern to improve pectin digestibility or reticulation. This loop can prevent degradation of the middle lamella thanks to the accumulation of an eliciting quantity of endogenous OGs or a restored signal perceived by cell wall receptors.

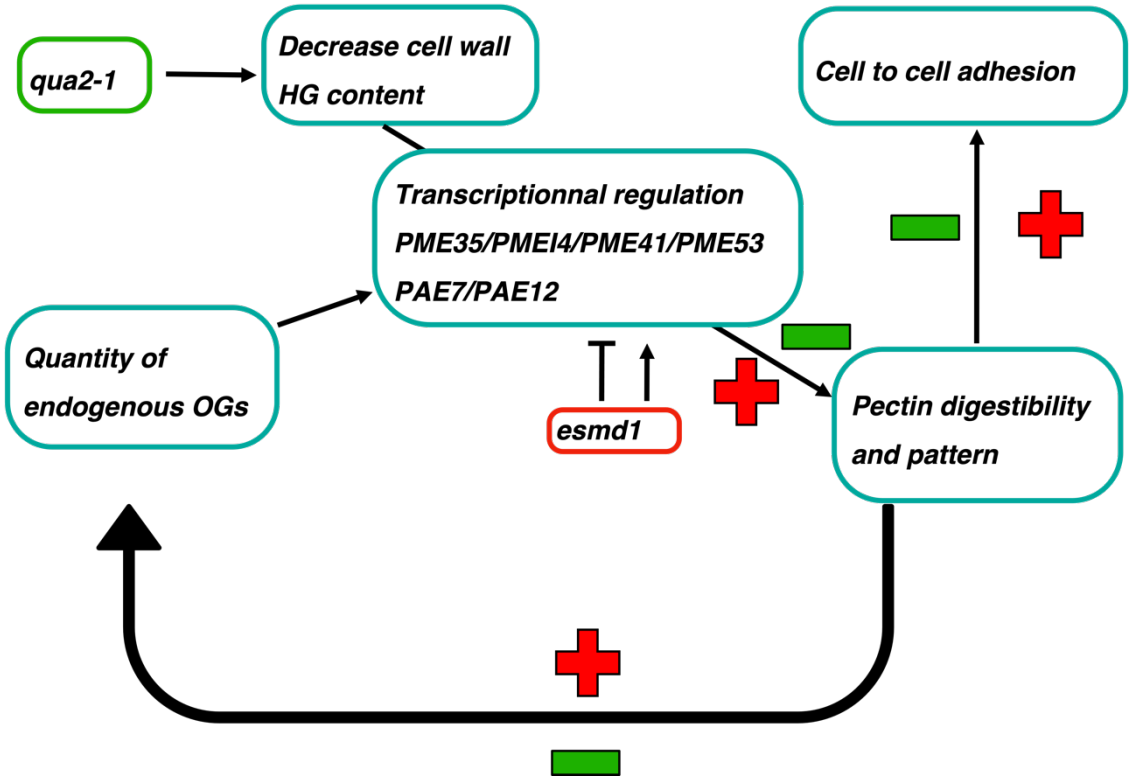

Figure A-2 **Cell adhesion feedback loop**

The cell adhesion feedback loop is positively regulated by *esmd (in red)* through transcriptional regulation of some HGMEs contributing to restoring digestibility and pectin pattern. This mediates to restore the cell adhesion but also creates another loop that restores the eliciting quantity of endogenous OGs. This restored quantity may contribute to the right signal through their perception. In the case of *qua2 (green),* the transcriptional regulation of HGMEs negatively affects the pectin digestibility and pattern. This led to cell-to-cell adhesion defect and reduced the eliciting quantity of endogenous OGs.

B) *QUASIMODO* TRY TO RESTORE HIS CELL ADHESION DEFECT ITSELF BUT HE CAN'T DO IT ALONE

From our analysis of endogenous free OGs, we also identified two monomers, GalA and GalAox (Chapter 2 Figure 1) in *qua2* and col0. We were able to demonstrate an inversion of the GalA/GalAox balance in *qua2* compared to the wild type. This is due to a higher quantity of GalAox than of GalA in this mutant. Thus, to restore the GalA/GalAox balance, we applied GalA to *qua2* seedlings. We were able to observe a specific action of the monosaccharide GalA leading to the restoration of cell adhesion and growth of the *qua2* hypocotyl. Since GlcA does

not induce the same effect as GalA, restoration of the *qua2* phenotype by GalA is probably a non-metabolic process. Furthermore, GalA induces various hormonal pathways including auxin, which could contribute to the restoration of hypocotyl growth in *qua2*. IAA response factors have previously been shown to be involved in hypocotyl growth (Reed et al., 2018). This also suggests that a single pectic monosaccharide may have an impact on development and cell adhesion. Since the enzymatic fingerprint showed no significant change in pectic pattern and digestibility related to the application, the salvage pathway process seems again to be excluded. Furthermore, we were able to identify that GalA activates an oxidation pathway to transform into GalAox. This also allows the production of H_2O_2. ROS such as H_2O_2 can induce the accumulation of salicylic acid (Chamnongpol et al., 1998) and participate in increasing its production. Thus, it is not surprising to observe the activation of the SA hormonal pathway that derives from this production of H_2O_2. Moreover, the effect of SA crosstalk and auxin on development has already been studied. A low concentration of SA would act as a developmental regulator by regulating auxin transport resulting in the accumulation of free auxin (Pasternak et al., 2019)). Besides, it has been demonstrated that the application of NPA (1-N-naphthylphthalamic), leads to restoring of cell adhesion on the *qua2* hypocotyl, in a dose-response manner (Verger, 2014). Thus, this suggests that the increase in SA linked to the production of H_2O_2 resulting from the oxidation of GalA may be antagonistic to the transport of auxin and prevent excessive degradation of the middle lamella by a negative feedback loop. This feedback loop may explain the accumulation of free auxin and contribute to the maintenance of adhesion. In untreated *qua2*, the quantity of SA may not be sufficient, and this led to a degradation of the middle lamella by the signal induced by auxin. Nevertheless, this phenomenon is only a hypothesis.

Thus, how the GalA oxidation mediate the restoration of cell adhesion and/or maintenance? In the same way as for GalA. We applied GalAox or H_2O_2 on *qua2* to determine if one of them is responsible of this restoration. Only H_2O_2 gives the same restoration phenotype on *qua2*. Thus, by carrying out some bibliographic research, we have identified that extensins proteins can be cross-linked together by their tyrosine residue thanks to the action of peroxidases in the presence of H_2O_2 (Fry, 1982; Epstein and Lamport, 1984; Brady et al., 1998; Held et al., 2004; Canon et al., 2008). Thanks to Coomassie blue staining and LC/MS analysis, we were able to demonstrate that GalA application led to an increase of inter-extensin crosslinks and in particular tyrosine trimers. In addition, 2 studies allow us to suggest that the extensins are the targeted polymer which allows the restoration. One study demonstrated that *qua2* overexpresses *peroxidase71* in the apoplast (Raggi et al., 2015). This peroxidase could be one of the candidates

implicated in extensins cross-linking. In addition, the study carried out by Du et al., (2020) showed that *qua2* overexpresses *EXT 3* and *EXT4* which code for extensin. This may explain the improved crosslinking in *qua2* following the application of GalA or H_2O_2.

Moreover, a recent study has isolated a new suppressor of another mutant *QUA2* allele, *qua2-4*, identified as SABRE (SAB). The *qua2/sab* double mutant seems to overexpress extensins without modifying the quantity of HGs (Kohorn et al., 2020). Thus, all these data suggest that the cell adhesion restoration pathway in *qua2* highlighted by the application of GalA or H_2O_2, could occur through extensin crosslinks. The question now is: how an extensin crosslinking network can contribute to the restoration of cell adhesion in *qua2?* Indeed, the mechanism that we have highlighted by the application of GalA or H_2O_2 is relatively fast. A study of the graft union model in Arabidopsis may explain what we observed. (Sala et al., 2019) demonstrated that 3 cell wall components were present in abundance in the material deposited in the extracellular layer. These included weakly or non-esterified HGs and extensins leading to the formation of a network allowing cell adhesion. We suggest here that in the case of *qua2* treated, the extensins after their crosslinked would form a network on their own and/or interact with the HGs of the middle lamella and allow cell adhesion. Moreover, such a network has already been demonstrated. Extensins and pectins have been used to build multi-layered structures *in vitro*. The AFM analysis of this final structure shows that the polymers are intimately mixed and confirms a rearrangement during the adsorption step. This interaction may be related to the balance of charges between the two polymers, the basic extensins forming an ionic bond with the acidic pectins (Valentin et al., 2010).

To conclude, we have highlighted a specific mechanism in *qua2* which consists in transforming GalA into GalAox. This oxidation allows the production of H_2O_2 in order to crosslink the extensins proteins through peroxidase action. However, due to the low pectin content of *qua2*, this mechanism is not sufficient to allow cell adhesion. The addition of GalA on *qua2* increases this mechanism and therefore allows the restoration of cell adhesion.

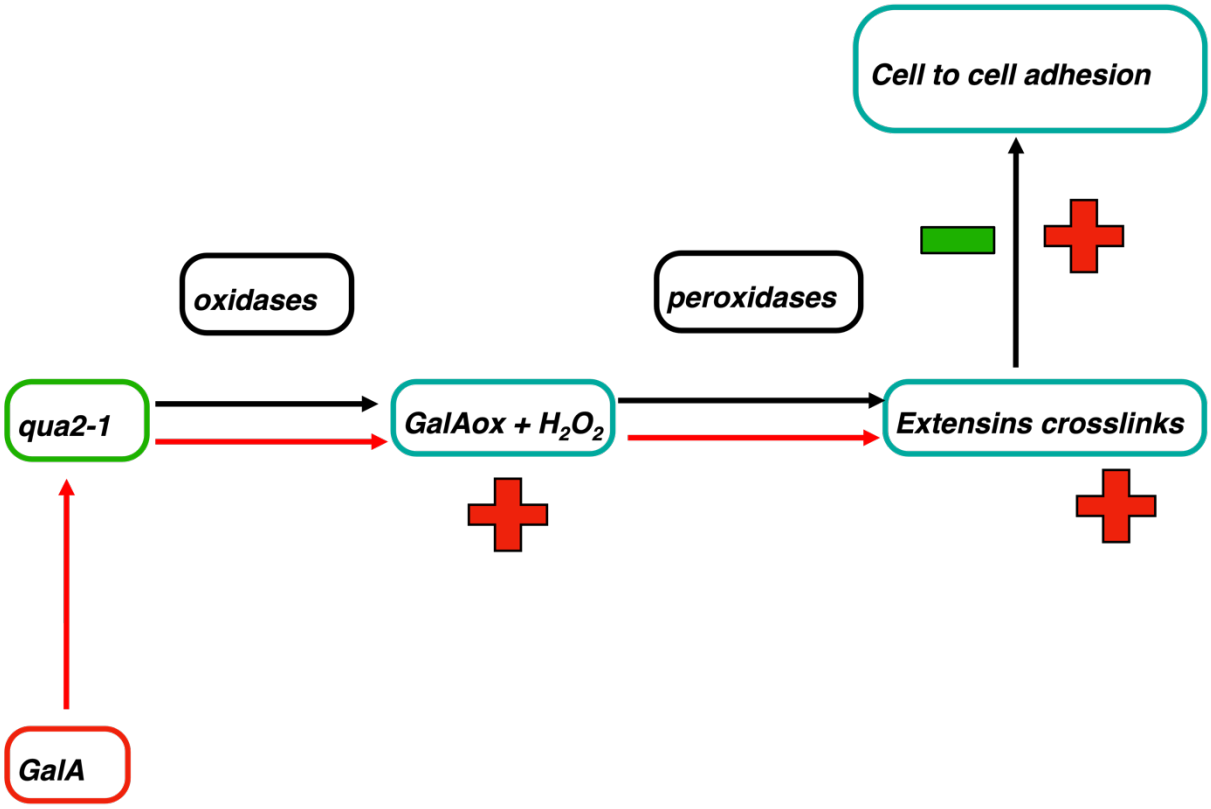

Figure B-1 **Mechanism to restore the cell adhesion by exogenous GalA**

This scheme represents an intrinsic qua2 pathway (Black arrow). This pathway involves the oxidation of endogenous GalA by cell wall oxidases. This oxidation leads to the production of H_2O_2 which will be used by the peroxidases to cross-link the extensins. But this is not enough to mediate cell adhesion. By adding exogenous GalA, we enhanced the production of GalAox and H_2O_2, without modifying the transcription of the oxidases. This allows more crosslinks through the extensins and mediates the cell adhesion.

PERSPECTIVES

Investigation of HGME's function and regulation in the control of cell adhesion

Through our study, we revealed that the *esmeralda* mutation in a *qua2* genetic background controls the expression of some pectin remodeling genes. This leads to the restoration of the pectic pattern that seems to lead to the restoration of an eliciting quantity of endogenous OGs. This confirms, among other things, the link between ESMERALDA and the pectic signature and/or endogenous OGs. Thus, different perspectives are offered to us to identify other actors of the signal transduction pathway mediated by ESMERALDA and leading to the control of HGMEs. To achieve this, I have built different *PME/PMEI/PAE*::*LUC* constructs that will be introduced in various genetic backgrounds (*emsd1; esmd1/qua2; qua2*) to follow luciferase expression driving by *PME/PMEI/PAE* promotors. Thus, we will carry out a mutagenesis of these lines and search for mutants whose expression has returned to the level of expression observed in the wild-type genetic background. This will be carried out thanks to a screening technique using a phenobox associated with a camera imagined chemiluminescence (by the action of luciferase on luciferin). This approach will reveal the actors involved in the signal transduction cascade mediated by ESMD or QUASIMODO. Furthermore, exogenous application of various HGME enzymes produced in a heterologous system will be used to determine the impact of these candidate proteins on the pectic pattern. I already introduced *P35S::PAE7* or *PAE12* constructs in a *qua2* background, to determine the impact of the over expression of *PAE* on the phenotype and the pectic pattern of *qua2.*
Finally, fractions enriched with identified endogenous OGs will be tested for their eliciting effects in the context of cell adhesion.

Investigation of the role of the GalA monomer in the maintenance of cell adhesion through cross-linking of HRGPs

Through our study, we also highlighted the specific action of the monosaccharide GalA able to restore the cell adhesion in *quasimodo* through a non-metabolic process. The oxidation of GalA to GalAox generates H_2O_2 used by peroxidases to cross-link cell wall proteins. This suggests that a pectic monosaccharide could affect cell adhesion during development. Confirming and/or understanding this phenomenon requires further investigation. We have identified candidate genes encoding oxidases. We have produced two proteins BBE3 and OGOX4 in a heterologous system. They will be soon tested for their ability to reduce GalA *in vitro*. In addition, the

generation of candidate *qua2/ogox or bbe* double mutants is in progress. These two strategies will confirm or not the role of these potential candidates in the oxidation of GalA in a *qua2*. In addition, *qua2/prx71* mutant plants are undergoing phenotypic analysis. This gene encoding the peroxidase *PRX71* is known to be overexpressed in *qua2* and could be the perfect candidate for the origin of increased extensin cross-linking observed in *qua2*.

Several studies showed that *qua2* overexpresses 2 extensins, *EXT3 and 4*. We will also investigate the double mutant *qua2/ext3* and/or *ext4* to confirm our different results concerning the role of these extensins in the restoration of cell adhesion through the GalA application. Moreover, an analysis of the transcriptome and the metabolism seems necessary to determine the other pathways involved in this restoration of adhesion in *qua2*. Finally, the GalA will be used on other mutants with adhesion defects to establish a solid link between the cross-linking of extensins resulting from an oxidation process and the restoration of adhesion. Preliminary results obtained on *quasimodo1* mutant seem to support this phenomenon.

GLOSSAIRE

ABA = Abscisic acid

ADPG = Arabidopsis dehiscence zone polygalacturonase

AFM = Atomic force microscopy

AGPs = Arabinogalactan proteins

APAP1 = Arabinoxylan pectin arabinogalactan protein1

Ara = Arabinose

ARAD = Arabinose deficient

BBE like = Berberine-bridge enzyme-like

BLC = Border-like cell

BR = Brassinosteroids

BLR = BELLRINGER

C= Carbon

CBF = Cold binding factor

CDS = Coding DNA sequence

CESA = Cellulose Synthases

CGR= Cotton Golgi-related

CSC = Cellulose Synthase Complex

DAMPS = damage associated molecular pattern

d-Gal = d-Galactose

d-GalA= d-Galacturonic Acid

DA = Degree of acetylation

DM = Degree of methylation

DP = Degree of polymerization

DP= Degree polymerization

ECM = Extra cellular matrix

EDTA = Ethylènediaminetétraacétique

EGF = Epidermal growth factor

ET = Ethylene

ETT= ETTIN

ExAD = Arabinose deficient

EXT = Extensin

FER= Feronia

FUT = Fucosyltransferase

GALS= Galactan synthase

GALT= Galactosyltransferase

GalA = Galacturonic Acid

GAUT = Galacturonosyltransferase

Glc= Glucose

GlcA= Gucuronic acid

GLCAT = Glucuronosyl transferases

GT = Glycosyltransferase

HERK= Herkule

HGME = HomoGalacturonan modifying enzyme

His = Histidine

HGs =Hhomogalacturonans

HPAT = Hydroxyproline O-β-arabinosyltransferases

HRGPs = Hydroxyproline-rich glycoproteins

Hyp = hydroxyproline

H_2O_2 = Hydrogen peroxyde

IAA = Indole-3-acetic acid

IDA = Inflorescence deficient in abscission

JA = Jasmonic Acid

KO = Knock-out

KOH = Potassium hydroxide

LC = Liquid chromatography

MALDI TOF = Matrix Assisted Laser Desorption Ionisation/Time Of Flight

ML =Middle Lamella

MPK = Map kinase

MS = Mass spectrometry

MT = Methyl transferase

MUM = Mucilage modified

NAA = Naphthaleneacetic acid

NaCl= Sodium chloride

NaOH = Sodium hydroxide

NMR = Nuclear magnetic resonance

NPA = 1-N-naphthylphthalamic acid

NPL = Nin-like protein

OG = Oligogalacturonid

OGOX= Oligogalacturonid oxidase

PAE = Pectin acetylesterase

PATAg = Periodic acid–thio carbohydrazide silver proteinate

PDF = Plantdefensin

PG= Polygalacturonase

PGIP = Polygalacturonase-inhibiting proteins

PGA = Polygalacturonic acid

PGLR= Polygalacturonase lateral root

PGX = Polygalacturonase involved in expansion

PLL = Pectate lyase-like

PME= Pectin methylesterase

PMEI = Pectin methylesterase inhibitor

Pro = Proline

PRPs = Proline-rich proteins

PRX= Peroxidase

QUA = Quasimodo

QRT = Quartet

RCPG = Root cap polygalacturonase

RGI= Rhamnogalacturonans I

RGII= Rhamnogalacturonans II

RGXT= Rhamnogalacturonans xylosylransferase

Rha= rhamnose

ROS = ROS = Reactive species oxygen

RRA = Reduced residual arabinose

RRT= Rhamnosyltransferase

SAM = S-adenosyl-methionine

SDS = Sodium dodecyl sulfate

SDS-PAGE = Sodium dodecyl sulfate - polyacrylamide gel electrophoresis

Ser= Serine

SGT = Serine galactosyltransferase

STORM = Stochastic Optical Reconstruction Microscopy

TF = Transcription factor

THE = Theseus

TLB = Trichome birefringence like

UDP = Uridine diphosphate-glucose

WAK = Wall associated kinase

XG = Xyloglucan

Xyl= Xylose

BIBLIOGRAPHY

Aeschbacher, R. A., Hauser, M.-T., Feldmann, K. A., & Benfey, P. N. (1995). The SABRE gene is required for normal cell expansion in Arabldopsls. *GENES & DEVELOPMENT*, *9*, 330–340.

Alessandro Raiola, Vincenzo Lionetti, Ibrahim Elmaghraby, Peter Immerzeel, Ewa J. Mellerowicz, Giovanni Salvi, Felice Cervone and, & Daniela Bellincamp. (2018). Pectin Methylesterase Is Induced in Arabidopsisupon Infection and Is Necessary for a Successful Colonization by Necrotrophic Pathogens. *Molecular Plant-Microbe Interactions*, *19*(5), 432–440. https://doi.org/10.1094/MPMI

An, S. H., Sohn, K. H., Choi, H. W., Hwang, I. S., Lee, S. C., & Hwang, B. K. (2008). Pepper pectin methylesterase inhibitor protein CaPMEI1 is required for antifungal activity, basal disease resistance and abiotic stress tolerance. *Planta*, *228*(1), 61–78. https://doi.org/10.1007/s00425-008-0719-z

Anderson, C. T. (2016). We be jammin': An update on pectin biosynthesis, trafficking and dynamics. In *Journal of Experimental Botany* (Vol. 67, Issue 2, pp. 495–502). Oxford University Press. https://doi.org/10.1093/jxb/erv501

Andres-Robin, A., Reymond, M. C., Dupire, A., Battu, V., Dubrulle, N., Mouille, G., Lefebvre, V., Pelloux, J., Boudaoud, A., Traas, J., Scutt, C. P., & Monéger, F. (2018). Evidence for the regulation of gynoecium morphogenesis by ETTIN via cell wall dynamics. *Plant Physiology*, *178*(3), 1222–1232. https://doi.org/10.1104/pp.18.00745

Aragunde, H., Biarnés, X., & Planas, A. (2018). Substrate recognition and specificity of chitin deacetylases and related family 4 carbohydrate esterases. In *International Journal of Molecular Sciences* (Vol. 19, Issue 2). MDPI AG. https://doi.org/10.3390/ijms19020412

Asselbergh, B., Curvers, K., França, S. C., Audenaert, K., Vuylsteke, M., van Breusegem, F., & Höfte, M. (2007). Resistance to Botrytis cinerea in sitiens, an abscisic acid-deficient tomato mutant, involves timely production of hydrogen peroxide and cell wall modifications in the epidermis. *Plant Physiology*, *144*(4), 1863–1877. https://doi.org/10.1104/pp.107.099226

Atkinson, R. G., Sutherland, P. W., Johnston, S. L., Gunaseelan, K., Hallett, I. C., Mitra, D., Brummell, D. A., Schröder, R., Johnston, J. W., & Schaffer, R. J. (2012). Down-regulation of POLYGALACTURONASE1 alters firmness, tensile strength and water loss in apple (Malus x domestica) fruit. *BMC Plant Biology*, *12*. https://doi.org/10.1186/1471-2229-12-129

Atmodjo, M. A., Hao, Z., & Mohnen, D. (2013). Evolving views of pectin biosynthesis. In *Annual Review of Plant Biology* (Vol. 64, pp. 747–779). https://doi.org/10.1146/annurev-arplant-042811-105534

Atmodjo, M. A., Sakuragi, Y., Zhu, X., Burrell, A. J., Mohanty, S. S., Atwood, J. A., Orlando, R., Scheller, H. v., & Mohnen, D. (2011). Galacturonosyltransferase (GAUT)1 and GAUT7 are the core of a plant cell wall pectin biosynthetic homogalacturonan: galacturonosyltransferase complex. *Proceedings of the National Academy of Sciences of the United States of America*, *108*(50), 20225–20230. https://doi.org/10.1073/pnas.1112816108

Bar-Peled, M., & O'Neill, M. A. (2011). Plant nucleotide sugar formation, interconversion, and salvage by sugar recycling. *Annual Review of Plant Biology*, *62*, 127–155. https://doi.org/10.1146/annurev-arplant-042110-103918

Bar-Peled, M., Urbanowicz, B. R., & O'Neill, M. A. (2012). The synthesis and origin of the pectic polysaccharide rhamnogalacturonan II - Insights from nucleotide sugar formation

and diversity. In *Frontiers in Plant Science* (Vol. 3, Issue MAY). Frontiers Research Foundation. https://doi.org/10.3389/fpls.2012.00092

Beldman, G., Vincken, J. P., Schols, H. A., Meeuwsen, P. J. A., Herweijer, M., & Voragen, A. G. J. (2003). Degradation of differently substituted xylogalacturonans by endoxylogalacturonan hydrolase and endopolygalacturonases. *Biocatalysis and Biotransformation*, *21*(4–5), 189–198. https://doi.org/10.1080/10242420310001618546

Benedetti, M., Verrascina, I., Pontiggia, D., Locci, F., Mattei, B., de Lorenzo, G., & Cervone, F. (2018). Four Arabidopsis berberine bridge enzyme-like proteins are specific oxidases that inactivate the elicitor-active oligogalacturonides. *Plant Journal*, *94*(2), 260–273. https://doi.org/10.1111/tpj.13852

Bonnin, E., le Goff, A., van Alebeek, G.-J. W. M., Voragen, A. G. J., & Thibault, J.-F. (2002). Mode of action of Fusarium moniliforme endopolygalacturonase towards acetylated pectin. *Carbohydrate Polymers*, *52*, 381–388.

Borner, G. H. H., Lilley, K. S., Stevens, T. J., & Dupree, P. (2003). Identification of glycosylphosphatidylinositol-anchored proteins in Arabidopsis. A proteomic and genomic analysis. *Plant Physiology*, *132*(2), 568–577. https://doi.org/10.1104/pp.103.021170

Bosh M, & Hepler P K. (2005). Pectin Methylesterases and Pectin Dynamics in Pollen Tubes. *The Plant Cell*, *17*, 3219–3226.

Bouton, S., Leboeuf, E., Mouille, G., Leydecker, M. T., Talbotec, J., Granier, F., Lahaye, M., Höfte, H., & Truong, H. N. (2002). Quasimodo1 encodes a putative membrane-bound glycosyltransferase required for normal pectin synthesis and cell adhesion in Arabidopsis. *Plant Cell*, *14*(10), 2577–2590. https://doi.org/10.1105/tpc.004259

Branca, C., de Lorenzo, G., Branca, F. C., Lorenzo, D., & Cervone, G. (1998). Competitive inhibition of the auxin-induced elongation by a-D-oligogalacturonides in pea stem segments. *PHYSIOLOGIA PLANTARUM*, *72*, 499–504.

Braybrook, S. A., & Peaucelle, A. (2013). Mechano-Chemical Aspects of Organ Formation in Arabidopsis thaliana: The Relationship between Auxin and Pectin. *PLoS ONE*, *8*(3). https://doi.org/10.1371/journal.pone.0057813

Brummell, D. A., & Harpster, M. H. (2001). Cell wall metabolism in fruit softening and quality and its manipulation in transgenic plants. In *Plant Molecular Biology* (Vol. 47).

Burlat, V., Kwon, M., Davin, L. B., & Lewis, N. G. (2001). Dirigent proteins and dirigent sites in lignifying tissues. *Phytochemistry* , *57*, 883–897.

Burton, R. A., Gidley, M. J., & Fincher, G. B. (2010). Heterogeneity in the chemistry, structure and function of plant cell walls. In *Nature Chemical Biology* (Vol. 6, Issue 10, pp. 724–732). Nature Publishing Group. https://doi.org/10.1038/nchembio.439

Cabrera, J. C., Boland, A., Cambier, P., Frettinger, P., & van Cutsem, P. (2010). Chitosan oligosaccharides modulate the supramolecular conformation and the biological activity of oligogalacturonides in Arabidopsis. *Glycobiology*, *20*(6), 775–786. https://doi.org/10.1093/glycob/cwq034

Cabrera, J. C., Boland, A., Messiaen, J., Cambier, P., & van Cutsem, P. (2008). Egg box conformation of oligogalacturonides: The time-dependent stabilization of the elicitor-active conformation increases its biological activity. *Glycobiology*, *18*(6), 473–482. https://doi.org/10.1093/glycob/cwn027

Caffall, K. H., & Mohnen, D. (2009). The structure, function, and biosynthesis of plant cell wall pectic polysaccharides. *Carbohydrate Research*, *344*(14), 1879–1900. https://doi.org/10.1016/j.carres.2009.05.021

Cannon, M. C., Terneus, K., Hall, Q., Tan, L., Wang, Y., Wegenhart, B. L., Chen, L., Lamport, D. T. A., Chen, Y., & Kieliszewski, M. J. (2007). Self-assembly of the plant cell wall requires an extensin scaffold. *PNAS*, *105*, 2226–2231.

Carpita, N. C., & Gibeaut, D. M. (1993). Structural models of primary cell walls in flowering plants: consistency of molecular structure with the physical properties of the walls during growth. *The Plant Journal*, *3*(1), 1–30.

Chambat, G., Karmous, M., Costes, M., Picard, M., & Joseleau, J. P. (2005). Variation of xyloglucan substitution pattern affects the sorption on celluloses with different degrees of crystallinity. In *Cellulose* (Vol. 12, Issue 2, pp. 117–125). https://doi.org/10.1007/s10570-004-1040-z

Chamnongpol, S., Willekens, H., Moeder, W., Langebartels, C., Sandermann, H., van Montagu, M., Inzé, D., & Camp, W. van. (1998). Defense activation and enhanced pathogen tolerance induced by H 2 O 2 in transgenic tobacco. In *Plant Biology* (Vol. 95).

Chen, Y., Dong, W., Tan, L., Held, M. A., & Kieliszewski, M. J. (2015). Arabinosylation Plays a Crucial Role in Extensin Cross-linking In Vitro . *Biochemistry Insights*, *8s2*, BCI.S31353. https://doi.org/10.4137/bci.s31353

Chen, Y. E., Mao, J. J., Sun, L. Q., Huang, B., Ding, C. B., Gu, Y., Liao, J. Q., Hu, C., Zhang, Z. W., Yuan, S., & Yuan, M. (2018). Exogenous melatonin enhances salt stress tolerance in maize seedlings by improving antioxidant and photosynthetic capacity. *Physiologia Plantarum*, *164*(3), 349–363. https://doi.org/10.1111/ppl.12737

Clement, G., Moison, M., Soulay, F., Reisdorf-Cren, M., & Masclaux-Daubresse, C. (2018). Metabolomics of laminae and midvein during leaf senescence and source-sink metabolite management in Brassica napus L. leaves. *Journal of Experimental Botany*, *69*(4), 891–903. https://doi.org/10.1093/jxb/erx253

Cocuron, J.-C., Lerouxel, O., Drakakaki, G., Alonso, A. P., Liepman, A. H., Keegstra, K., Raikhel, N., & Wilkerson, C. G. (2007). A gene from the cellulose synthase-like C family encodes a-1,4 glucan synthase. *PNAS*, *104*, 8550–8555.

Cornuault, V., Manfield, I. W., Ralet, M. C., & Paul Knox, J. (2014). Epitope detection chromatography: A method to dissect the structural heterogeneity and inter-connections of plant cell-wall matrix glycans. *Plant Journal*, *78*(4), 715–722. https://doi.org/10.1111/tpj.12504

Cosgrove, D. J. (1997). ASSEMBLY AND ENLARGEMENT OF THE PRIMARY CELL WALL IN PLANTS. In *Annu. Rev. Cell Dev. Biol* (Vol. 13).

Cosgrove, D. J. (2005). Growth of the plant cell wall. In *Nature Reviews Molecular Cell Biology* (Vol. 6, Issue 11, pp. 850–861). https://doi.org/10.1038/nrm1746

Creff, A., Brocard, L., Joubès, J., Taconnat, L., Doll, N. M., Marsollier, A. C., Pascal, S., Galletti, R., Boeuf, S., Moussu, S., Widiez, T., Domergue, F., & Ingram, G. (2019). A stress-response-related inter-compartmental signalling pathway regulates embryonic cuticle integrity in Arabidopsis. *PLoS Genetics*, *15*(4). https://doi.org/10.1371/journal.pgen.1007847

Curvers, K., Seifi, H., Mouille, G., de Rycke, R., Asselbergh, B., van Hecke, A., Vanderschaeghe, D., Höfte, H., Callewaert, N., van Breusegem, F., & Höfte, M. (2010). Abscisic acid deficiency causes changes in cuticle permeability and pectin composition that influence tomato resistance to Botrytis cinerea. *Plant Physiology*, *154*(2), 847–860. https://doi.org/10.1104/pp.110.158972

Daas, P. J. H., Boxma, B., Hopman, A. M. C. P., Voragen, A. G. J., & Schols, H. A. (2001). Nonesterified Galacturonic Acid Sequence Homology of Pectins. *Biopolymers*, *58*, 1–8.

Daher, F. B., & Braybrook, S. A. (2015). How to let go: Pectin and plant cell adhesion. In *Frontiers in Plant Science* (Vol. 6, Issue JULY). Frontiers Media S.A. https://doi.org/10.3389/fpls.2015.00523

Daniel, B., Wallner, S., Steiner, B., Oberdorfer, G., Kumar, P., van der Graaff, E., Roitsch, T., Sensen, C. W., Gruber, K., & Macheroux, P. (2016). Structure of a berberine bridge

enzyme-like enzyme with an active site specific to the plant family Brassicaceae. *PLoS ONE*, *11*(6). https://doi.org/10.1371/journal.pone.0156892
Davidsson, P., Broberg, M., Kariola, T., Sipari, N., Pirhonen, M., & Palva, E. T. (2017). Short oligogalacturonides induce pathogen resistance-associated gene expression in Arabidopsis thaliana. *BMC Plant Biology*, *17*(1). https://doi.org/10.1186/s12870-016-0959-1
de Lorenzo, G., & Ferrari, S. (2002). Polygalacturonase-inhibiting proteins in defense against phytopathogenic fungi. In *Current Opinion in Plant Biology* (Vol. 5, Issue 4, pp. 295–299). Elsevier Ltd. https://doi.org/10.1016/S1369-5266(02)00271-6
de Souza, A., Hull, P. A., Gille, S., & Pauly, M. (2014). Identification and functional characterization of the distinct plant pectin esterases PAE8 and PAE9 and their deletion mutants. *Planta*, *240*(5), 1123–1138. https://doi.org/10.1007/s00425-014-2139-6
del Corpo, D., Fullone, M. R., Miele, R., Lafond, M., Pontiggia, D., Grisel, S., Kieffer-Jaquinod, S., Giardina, T., Bellincampi, D., & Lionetti, V. (2020). AtPME17 is a functional Arabidopsis thaliana pectin methylesterase regulated by its PRO region that triggers PME activity in the resistance to Botrytis cinerea. *Molecular Plant Pathology*, *21*(12), 1620–1633. https://doi.org/10.1111/mpp.13002
Denoux, C., Galletti, R., Mammarella, N., Gopalan, S., Werck, D., de Lorenzo, G., Ferrari, S., Ausubel, F. M., & Dewdney, J. (2008). Activation of defense response pathways by OGs and Flg22 elicitors in Arabidopsis seedlings. *Molecular Plant*, *1*(3), 423–445. https://doi.org/10.1093/mp/ssn019
Dick-Pérez, M., Zhang, Y., Hayes, J., Salazar, A., Zabotina, O. A., & Hong, M. (2011). Structure and interactions of plant cell-wall polysaccharides by two- and three-dimensional magic-angle-spinning solid-state NMR. *Biochemistry*, *50*(6), 989–1000. https://doi.org/10.1021/bi101795q
Dilokpimol, A., & Geshi, N. (2014). Arabidopsis thaliana glucuronosyltransferase in family GT14. *Plant Signaling and Behavior*, *9*(6). https://doi.org/10.4161/psb.28891
Du, J., Kirui, A., Huang, S., Wang, L., Barnes, W. J., Kiemle, S. N., Zheng, Y., Rui, Y., Ruan, M., Qi, S., Kim, S. H., Wang, T., Cosgrove, D. J., Anderson, C. T., & Xiao, C. (2020). Mutations in the Pectin Methyltransferase QUASIMODO2 influence cellulose biosynthesis and wall integrity in arabidopsis. *Plant Cell*, *32*(11), 3576–3597. https://doi.org/10.1105/TPC.20.00252
Dührkop, K., Nothias, L. F., Fleischauer, M., Reher, R., Ludwig, M., Hoffmann, M. A., Petras, D., Gerwick, W. H., Rousu, J., Dorrestein, P. C., & Böcker, S. (2021). Systematic classification of unknown metabolites using high-resolution fragmentation mass spectra. *Nature Biotechnology*, *39*(4), 462–471. https://doi.org/10.1038/s41587-020-0740-8
Dumont, M., Lehner, A., Bouton, S., Kiefer-Meyer, M. C., Voxeur, A., Pelloux, J., Lerouge, P., & Mollet, J. C. (2014). The cell wall pectic polymer rhamnogalacturonan-II is required for proper pollen tube elongation: Implications of a putative sialyltransferase-like protein. *Annals of Botany*, *114*(6), 1177–1188. https://doi.org/10.1093/aob/mcu093
Dumont, M., Lehner, A., Vauzeilles, B., Malassis, J., Marchant, A., Smyth, K., Linclau, B., Baron, A., Mas Pons, J., Anderson, C. T., Schapman, D., Galas, L., Mollet, J. C., & Lerouge, P. (2016). Plant cell wall imaging by metabolic click-mediated labelling of rhamnogalacturonan II using azido 3-deoxy- d -manno-oct-2-ulosonic acid. *Plant Journal*, *85*(3), 437–447. https://doi.org/10.1111/tpj.13104
Durand, C., Vicré-Gibouin, M., Follet-Gueye, M. L., Duponchel, L., Moreau, M., Lerouge, P., & Driouich, A. (2009). The organization pattern of root border-like cells of Arabidopsis is dependent on cell wall homogalacturonan. *Plant Physiology*, *150*(3), 1411–1421. https://doi.org/10.1104/pp.109.136382
Egelund, J., Obel, N., Ulvskov, P., Geshi, N., Pauly, M., Bacic, A., & Petersen, B. L. (2007). Molecular characterization of two Arabidopsis thaliana glycosyltransferase mutants, rra1

and rra2, which have a reduced residual arabinose content in a polymer tightly associated with the cellulosic wall residue. *Plant Molecular Biology*, *64*(4), 439–451. https://doi.org/10.1007/s11103-007-9162-y

Egelund, J., Petersen, B. L., Motawia, M. S., Damager, I., Faik, A., Olsen, C. E., Ishii, T., Clausen, H., Ulvskov, P., & Geshi, N. (2006). Arabidopsis thaliana RGXT1 and RGXT2 encode golgi-localized (1,3)-α-D-xylosyltransferases involved in the synthesis of pectic rhamnogalacturonan-II. *Plant Cell*, *18*(10), 2593–2607. https://doi.org/10.1105/tpc.105.036566

Egelund, N. (2008). The value of international comparative studies of achievement–a Danish perspective. *Assessment in Education: Principles, Policy and Practice*, *15*(3), 245–251. https://doi.org/10.1080/09695940802417400

Epstein, L., & Lamport, D. T. A. (1984). AN INTRAMOLECULAR LINKAGE INVOLVING ISODITYROSINE IN EXTENSIN. *Phytochemistry* , *23*(6), 1241–1246.

Federici, L., Caprari, C., Mattei, B., Savino, C., Matteo, A. di, de Lorenzo, G., Cervone, F., & Tsernoglou, D. (2001). Structural requirements of endopolygalacturonase for the interaction with PGIP (polygalacturonase-inhibiting protein). *PNAS*, *98*(23), 13425–13430.

Fernández, V., Guzmán-Delgado, P., Graça, J., Santos, S., & Gil, L. (2016). Cuticle structure in relation to chemical composition: Re-assessing the prevailing model. In *Frontiers in Plant Science* (Vol. 7, Issue MAR2016). Frontiers Media S.A. https://doi.org/10.3389/fpls.2016.00427

Ferrari, S., Galletti, R., Denoux, C., de Lorenzo, G., Ausubel, F. M., & Dewdney, J. (2007). Resistance to Botrytis cinerea induced in arabidopsis by elicitors is independent of salicylic acid, ethylene, or jasmonate signaling but requires PHYTOALEXIN DEFICIENT3. *Plant Physiology*, *144*(1), 367–379. https://doi.org/10.1104/pp.107.095596

Ferrari, S., Savatin, D. v., Sicilia, F., Gramegna, G., Cervone, F., & de Lorenzo, G. (2013). Oligogalacturonides: Plant damage-associated molecular patterns and regulators of growth and development. In *Frontiers in Plant Science* (Vol. 4, Issue MAR). Frontiers Research Foundation. https://doi.org/10.3389/fpls.2013.00049

Francis, K. E., Lam, S. Y., & Copenhaver, G. P. (2006). Separation of Arabidopsis pollen tetrads is regulated by QUARTET1, a pectin methylesterase gene. *Plant Physiology*, *142*(3), 1004–1013. https://doi.org/10.1104/pp.106.085274

Fry, S. C. (1982). Isodityrosine, a new cross-linking amino acid from plant cell-wall glycoprotein. In *Biochem. J*, *204*(2), 449-455.

Fry, S. C. (2010). Cell Wall Polysaccharide Composition and Covalent Crosslinking. In *Annual Plant Reviews, Plant Polysaccharides: Biosynthesis and Bioengineering* (Vol. 41, pp. 1–42). Wiley Blackwell. https://doi.org/10.1002/9781444391015.ch1

Fry, S. C., York, W. S., Albersheim, P., Darvill, A., Hayashi, T., Joseleau, J.-P., Kato, Y., Perez Lorences, E., Maclachlan, G. A., McNeil, M., Mort, A. J., Grant Reid, J. S., Ulrich Seitz, H., Selvendran, R. R., J Voragen, A. G., White Fry, A. R., Darvill, P., L-p, J., P, L. E., … G Reid, J. S. (1993). An unambiguous nomenclature for xyloglucan-derived oligosaccharides. *PHYSIOLOGIA PLANTARUM* , *89*, 1–3.

G. Beldman, L.A.M. van den Broek, H.A. Schols, M.J.F Searle-van Leeuwen, K.M.J van Laere, & and A.G.J. Voragen. (1996). AN EXOGALACTURONASE FROM ASPERGILLUS ACULEATUS ABLE TO DEGRADE XYLOGALACTURONAN. *Biotechnology* , *18*(6), 707–712.

Gao, P., Xin, Z., & Zheng, Z. L. (2008). The OSU1/QUA2/TSD2-encoded putative methyltransferase is a critical modulator of carbon and nitrogen nutrient balance response in Arabidopsis. *PLoS ONE*, *3*(1). https://doi.org/10.1371/journal.pone.0001387

Geshi, N., Johansen, J. N., Dilokpimol, A., Rolland, A., Belcram, K., Verger, S., Kotake, T., Tsumuraya, Y., Kaneko, S., Tryfona, T., Dupree, P., Scheller, H. v., Höfte, H., & Mouille, G. (2013). A galactosyltransferase acting on arabinogalactan protein glycans is essential for embryo development in Arabidopsis. *Plant Journal*, *76*(1), 128–137. https://doi.org/10.1111/tpj.12281

Gille, S., de Souza, A., Xiong, G., Benz, M., Cheng, K., Schultink, A., Reca, I. B., & Pauly, M. (2011). O-acetylation of Arabidopsis hemicellulose xyloglucan requires AXY4 or AXY4L, proteins with a TBL an DUF231 domain. *Plant Cell*, *23*(11), 4041–4053. https://doi.org/10.1105/tpc.111.091728

Gille, S., Hä Nsel B, U., Ziemann, M., & Pauly, M. (2009). Identification of plant cell wall mutants by means of a forward chemical genetic approach using hydrolases. *PNAS*, *106*(34), 14699–14704. www.cazy.org/

Giovane, A., Servillo, L., Balestrieri, C., Raiola, A., D'Avino, R., Tamburrini, M., Ciardiello, M. A., & Camardella, L. (2004). Pectin methylesterase inhibitor. In *Biochimica et Biophysica Acta - Proteins and Proteomics* (Vol. 1696, Issue 2, pp. 245–252). Elsevier. https://doi.org/10.1016/j.bbapap.2003.08.011

Gou, J. Y., Miller, L. M., Hou, G., Yu, X. H., Chen, X. Y., & Liu, C. J. (2012). Acetylesterase-mediated deacetylation of pectin impairs cell elongation, pollen germination, and plant reproduction. *Plant Cell*, *24*(1), 50–65. https://doi.org/10.1105/tpc.111.092411

Grant, G. T., Mon, E. R., David REES, S. A., Jci Smiti-i, P., & Thom, id. (1973). BIOLOGICAL INTERACTIONS BETWEEN POLYSACCHARtDES AND DIVALENT CATIONS: THE EGG-BOX MODEL. *FEBS Letters*, *32*(1), 195–198.

Grandjean, C (2018) Role of pectin modification in response to stress. *Master report*

Guénin, S., Mareck, A., Rayon, C., Lamour, R., Assoumou Ndong, Y., Domon, J. M., Sénéchal, F., Fournet, F., Jamet, E., Canut, H., Percoco, G., Mouille, G., Rolland, A., Rustérucci, C., Guerineau, F., van Wuytswinkel, O., Gillet, F., Driouich, A., Lerouge, P., … Pelloux, J. (2011). Identification of pectin methylesterase 3 as a basic pectin methylesterase isoform involved in adventitious rooting in Arabidopsis thaliana. *New Phytologist*, *192*(1), 114–126. https://doi.org/10.1111/j.1469-8137.2011.03797.x

Guo, H., Li, L., Ye, H., Yu, X., Algreen, A., & Yin, Y. (2009). Three related receptor-like kinases are required for optimal cell elongation in Arabidopsis thaliana. *PNAS*, *106*(18), 7648–7653. www.pnas.org/cgi/content/full/

Haas, K. T., Wightman, R., Meyerowitz, E. M., & Peaucelle, A. (2020). Pectin homogalacturonan nanofilament expansion drives morphogenesis in plant epidermal cells. *Science*, *367*(6481), 1003–1007. http://science.sciencemag.org/

Hall, Q., & Cannon, M. C. (2002). The cell wall hydroxyproline-rich glycoprotein RSH is essential for normal embryo development in Arabidopsis. *Plant Cell*, *14*(5), 1161–1172. https://doi.org/10.1105/tpc.010477

Harholt, J., Jensen, J. K., Sørensen, S. O., Orfila, C., Pauly, M., & Scheller, H. V. (2006). ARABINAN DEFICIENT 1 is a putative arabinosyltransferase involved in biosynthesis of pectic arabinan in arabidopsis. *Plant Physiology*, *140*(1), 49–58. https://doi.org/10.1104/pp.105.072744

Harholt, J., Jensen, J. K., Verhertbruggen, Y., Søgaard, C., Bernard, S., Nafisi, M., Poulsen, C. P., Geshi, N., Sakuragi, Y., Driouich, A., Knox, J. P., & Scheller, H. V. (2012). ARAD proteins associated with pectic Arabinan biosynthesis form complexes when transiently overexpressed in planta. *Planta*, *236*(1), 115–128. https://doi.org/10.1007/s00425-012-1592-3

Harris, D., & DeBolt, S. (2008). Relative crystallinity of plant biomass: Studies on assembly, adaptation and acclimation. *PLoS ONE*, *3*(8). https://doi.org/10.1371/journal.pone.0002897

He, Z. H., Fujiki, M., & Kohorn, B. D. (1996). A cell wall-associated, receptor-like protein kinase. *Journal of Biological Chemistry*, *271*(33), 19789–19793. https://doi.org/10.1074/jbc.271.33.19789

Held, M. A., Be, E., Zemelis, S., Withers, S., Wilkerson, C., & Brandizzi, F. (2011). CGR3: A golgi-localized protein influencing homogalacturonan methylesterification. *Molecular Plant*, *4*(5), 832–844. https://doi.org/10.1093/mp/ssr012

Held, M. A., Tan, L., Kamyabi, A., Hare, M., Shpak, E., & Kieliszewski, M. J. (2004). Di-isodityrosine is the intermolecular cross-link of isodityrosine-rich extensin analogs cross-linked in vitro. *Journal of Biological Chemistry*, *279*(53), 55474–55482. https://doi.org/10.1074/jbc.M408396200

Hewezi, T., Howe, P., Maier, T. R., Hussey, R. S., Mitchum, M. G., Davis, E. L., & Baum, T. J. (2008). Cellulose binding protein from the parasitic nematode heterodera Schachtii interacts with arabidopsis pectin methylesterase: Cooperative cell wall modification during parasitism. *Plant Cell*, *20*(11), 3080–3093. https://doi.org/10.1105/tpc.108.063065

Hijazi, M., Durand, J., Pichereaux, C., Pont, F., Jamet, E., & Albenne, C. (2012). Characterization of the arabinogalactan protein 31 (AGP31) of Arabidopsis thaliana: New advances on the Hyp-O-glycosylation of the pro-rich domain. *Journal of Biological Chemistry*, *287*(12), 9623–9632. https://doi.org/10.1074/jbc.M111.247874

Hijazi, M., Roujol, D., Nguyen-Kim, H., del Rocio Cisneros Castillo, L., Saland, E., Jamet, E., & Albenne, C. (2014). Arabinogalactan protein 31 (AGP31), a putative network-forming protein in Arabidopsis thaliana cell walls? *Annals of Botany*, *114*(6), 1087–1097. https://doi.org/10.1093/aob/mcu038

Hocq, L., Habrylo, O., Voxeur, A., Pau-Roblot, C., Safran, J., Sénéchal, F., Fournet, F., Bassard, S., Battu, V., Demailly, H., Tovar, J. C., Pilard, S., Marcelo, P., Savary, B. J., Mercadante, D., Njo, F., Beeckman, T., Boudaoud, A., Pelloux, J., & Lefebvre, V. (2021). The pH-dependent processivity of Arabidopsis AtPME2 can control cell wall mechanical properties. *BioRxiv*. https://doi.org/10.1101/2021.03.03.433777

Hoffmann, N., King, S., Samuels, A. L., & McFarlane, H. E. (2021). Subcellular coordination of plant cell wall synthesis. In *Developmental Cell* (Vol. 56, Issue 7, pp. 933–948). Cell Press. https://doi.org/10.1016/j.devcel.2021.03.004

Höfte, H., & Voxeur, A. (2017). Plant cell walls. In *Current Biology* (Vol. 27, Issue 17, pp. R865–R870). Cell Press. https://doi.org/10.1016/j.cub.2017.05.025

Hongo, S., Sato, K., Yokoyama, R., & Nishitani, K. (2012). Demethylesterification of the primary wall by PECTIN METHYLESTERASE35 provides mechanical support to the Arabidopsis stem. *Plant Cell*, *24*(6), 2624–2634. https://doi.org/10.1105/tpc.112.099325

Huang, Y. C., Wu, H. C., Wang, Y. da, Liu, C. H., Lin, C. C., Luo, D. L., & Jinn, T. L. (2017). PECTIN METHYLESTERASE34 contributes to heat tolerance through its role in promoting stomatal movement. *Plant Physiology*, *174*(2), 748–763. https://doi.org/10.1104/pp.17.00335

Immerzeel, P., Eppink, M. M., de Vries, S. C., Schols, H. A., & Voragen, A. G. J. (2006). Carrot arabinogalactan proteins are interlinked with pectins. *Physiologia Plantarum*, *128*(1), 18–28. https://doi.org/10.1111/j.1399-3054.2006.00712.x

Ishii, T., Matsunaga, T., & Hayashi, N. (2001). Formation of Rhamnogalacturonan II-Borate Dimer in Pectin Determines Cell Wall Thickness of Pumpkin Tissue. *Plant Physiology* , *126*, 1698–1705.

Ishii, T., Matsunaga, T., Pellerin, P., O'Neill, M. A., Darvill, A., & Albersheim, P. (1999). The plant cell wall polysaccharide rhamnogalacturonan II self-assembles into a covalently cross-linked dimer. *Journal of Biological Chemistry*, *274*(19), 13098–13104. https://doi.org/10.1074/jbc.274.19.13098

Jamet, E., Canut, H., Boudart, G., & Pont-Lezica, R. F. (2006). Cell wall proteins: a new insight through proteomics. In *Trends in Plant Science* , *11*(1), 33-39.

Jarvis, M. C., Briggs, S. P. H., & Knox, J. P. (2003). Intercellular adhesion and cell separation in plants. In *Plant, Cell and Environment* , *11*(1), 33-39.

Jensen, J. K., Schultink, A., Keegstra, K., Wilkerson, C. G., & Pauly, M. (2012). RNA-seq analysis of developing nasturtium seeds (Tropaeolum majus): Identification and characterization of an additional galactosyltransferase involved in xyloglucan biosynthesis. *Molecular Plant*, *5*(5), 984–992. https://doi.org/10.1093/mp/sss032

Jensen, J. K., Sørensen, S. O., Harholt, J., Geshi, N., Sakuragi, Y., Møller, I., Zandleven, J., Bernal, A. J., Jensen, N. B., Sørensen, C., Pauly, M., Beldman, G., Willats, W. G. T., & Scheller, H. V. (2008). Identification of a xylogalacturonan xylosyltransferase involved in pectin biosynthesis in Arabidopsis. *Plant Cell*, *20*(5), 1289–1302. https://doi.org/10.1105/tpc.107.050906

Jones, L., Seymour, C. B., & Knox, J. P. (1997). Localization of Pectic Galactan in Tomato Cell Walls Using a Monoclonal Antibody Specific to (1-+4)-P-~-Galactan'. In *Plant Physiol* (Vol. 113).

Kamiya, M., Higashio, S. Y., Isomoto, A., Kim, J. M., Seki, M., Miyashima, S., & Nakajima, K. (2016). Control of root cap maturation and cell detachment by BEARSKIN transcription factors in Arabidopsis. *Development (Cambridge)*, *143*(21), 4063–4072. https://doi.org/10.1242/dev.142331

Karve, R., Suárez-Román, F., & Iyer-Pascuzzi, A. S. (2016). The transcription factor NIN-LIKE PROTEIN7 controls border-like cell release. *Plant Physiology*, *171*(3), 2101–2111. https://doi.org/10.1104/pp.16.00453

Keegstra, K. (2010). Plant cell walls. *Plant Physiology*, *154*(2), 483–486. https://doi.org/10.1104/pp.110.161240

Kirui, A., Du, J., Zhao, W., Barnes, W., Kang, X., Anderson, C. T., Xiao, C., & Wang, T. (2021). A pectin methyltransferase modulates polysaccharide dynamics and interactions in Arabidopsis primary cell walls: Evidence from solid-state NMR. *Carbohydrate Polymers*, *270*. https://doi.org/10.1016/j.carbpol.2021.118370

Knox, J. P. (1992). Cell adhesion, cell separation and plant morphogenesis. In *The Plant Journal* (Vol. 992, Issue 1).

Kohorn, B. D. (2016). Cell wall-associated kinases and pectin perception. In *Journal of Experimental Botany* (Vol. 67, Issue 2, pp. 489–494). Oxford University Press. https://doi.org/10.1093/jxb/erv467

Kohorn, B. D., Greed, B. E., Mouille, G., Verger, S., & Kohorn, S. L. (2021). Effects of Arabidopsis wall associated kinase mutations on ESMERALDA1 and elicitor induced ROS. *PLoS ONE*, *16*(5 May 2021). https://doi.org/10.1371/journal.pone.0251922

Kohorn, B. D., Johansen, S., Shishido, A., Todorova, T., Martinez, R., Defeo, E., & Obregon, P. (2009). Pectin activation of MAP kinase and gene expression is WAK2 dependent. *Plant Journal*, *60*(6), 974–982. https://doi.org/10.1111/j.1365-313X.2009.04016.x

Kohorn, B. D., & Kohorn, S. L. (2012). The cell wall-associated kinases, WAKs, as pectin receptors. *Frontiers in Plant Science*, *3*(May), 1–5. https://doi.org/10.3389/fpls.2012.00088

Kohorn, B. D., Kohorn, S. L., Saba, N. J., & Martinez, V. M. (2014). Requirement for pectin methyl esterase and preference for fragmented over native pectins for wall-associated kinase-activated, EDS1/PAD4-dependent stress response in arabidopsis. *Journal of Biological Chemistry*, *289*(27), 18978–18986. https://doi.org/10.1074/jbc.M114.567545

Kohorn, B. D., Zorensky, F. D. H., Dexter-Meldrum, J., Chabout, S., Mouille, G., & Kohorn, S. (2021). Mutation of an Arabidopsis Golgi membrane protein ELMO1 reduces cell adhesion. *Development (Cambridge)*, *148*(10). https://doi.org/10.1242/DEV.199420

Kohorn, B., Dexter-Meldrum, J., Zorensky, F., Chabout, S., Mouille, G., Kohorn, S., Kohorn, B. D., & Zorensky, F. D. H. (2021). Pectin Dependent Cell Adhesion Restored by a Mutant Microtubule Organizing Membrane Protein. *Plants*, *10*(4), 1–16. https://doi.org/10.3390/plants10040690ï

Kotchoni, S. O., Zakharova, T., Mallery, E. L., Le, J., El-Assal, S. E. D., & Szymanski, D. B. (2009). The association of the arabidopsis actin-related protein2/3 complex with cell membranes is linked to its assembly status but not its activation. *Plant Physiology*, *151*(4), 2095–2109. https://doi.org/10.1104/pp.109.143859

Krupková, E., Immerzeel, P., Pauly, M., & Schmülling, T. (2007). The Tumorous Shoot Development2 gene of Arabidopsis encoding a putative methyltransferase is required for cell adhesion and co-ordinated plant development. *Plant Journal*, *50*(4), 735–750. https://doi.org/10.1111/j.1365-313X.2007.03123.x

Kumpf, R. P., Shi, C.-L., Larrieu, A., Stø, I. M., Butenko, M. A., Péret, B., Riiser, E. S., Bennett, M. J., & Aalen, R. B. (2013). Floral organ abscission peptide IDA and its HAE/HSL2 receptors control cell separation during lateral root emergence. *Proceedings of the National Academy of Sciences*, *110*(13), 5235–5240. https://doi.org/10.1073/PNAS.1210835110

Laskowski, M., Biller, S., Stanley, K., Kajstura, T., & Prusty, R. (2006). Expression profiling of auxin-treated Arabidopsis roots: Toward a molecular analysis of lateral root emergence. *Plant and Cell Physiology*, *47*(6), 788–792. https://doi.org/10.1093/pcp/pcj043

Lathe, R. S., McFarlane, H. E., Abbas Khan, G., Ebert, B., Ramírez-Rodríguez, A., Noord, N., Bhalerao, R., & Persson, S. (2021). A DUF1068 protein acts as a pectin biosynthesis scaffold and maintains Golgi morphology 2 and cell adhesion in Arabidopsis. *BioXr*. https://doi.org/10.1101/2021.05.03.442108

le Gall, H., Philippe, F., Domon, J. M., Gillet, F., Pelloux, J., & Rayon, C. (2015). Cell wall metabolism in response to abiotic stress. In *Plants* (Vol. 4, Issue 1, pp. 112–166). MDPI AG. https://doi.org/10.3390/plants4010112

Lei, L., Xu, A., Panin, V. M., & Irvine, K. D. (2003). An O-fucose site in the ligand binding domain inhibits Notch activation. *Development*, *130*(26), 6411–6421. https://doi.org/10.1242/dev.00883

Levesque-Tremblay, G., Pelloux, J., Braybrook, S. A., & Müller, K. (2015). Tuning of pectin methylesterification: consequences for cell wall biomechanics and development. In *Planta* (Vol. 242, Issue 4, pp. 791–811). Springer Verlag. https://doi.org/10.1007/s00425-015-2358-5

Le Roux, C., Del Prete, S., Boutet-Mercey, S., Perreau, F., Balagué, C., Roby, D., Fagard, M. and Gaudin, V. (2014) The hnRNP-Q Protein LIF2 Participates in the Plant Immune Response. Plos One (6), e99343.

Li, L., Li, K., Ali, A., & Guo, Y. (2021). Atwakl10, a cell wall associated receptor-like kinase, negatively regulates leaf senescence in arabidopsis thaliana. *International Journal of Molecular Sciences*, *22*(9). https://doi.org/10.3390/ijms22094885

Li, S., Blanchoin, L., Yang, Z., & Lord, E. M. (2003). The putative arabidopsis Arp2/3 complex controls leaf cell morphogenesis. *Plant Physiology*, *132*(4), 2034–2044. https://doi.org/10.1104/pp.103.028563

Liang, Y., Basu, D., Pattathil, S., Xu, W. L., Venetos, A., Martin, S. L., Faik, A., Hahn, M. G., & Showalter, A. M. (2013). Biochemical and physiological characterization of fut4 and fut6 mutants defective in arabinogalactan-protein fucosylation in Arabidopsis. *Journal of Experimental Botany*, *64*(18), 5537–5551. https://doi.org/10.1093/jxb/ert321

Lionetti, V., Cervone, F., & Bellincampi, D. (2012). Methyl esterification of pectin plays a role during plant-pathogen interactions and affects plant resistance to diseases. *Journal of Plant Physiology*, *169*(16), 1623–1630. https://doi.org/10.1016/j.jplph.2012.05.006

Lionetti, V., Fabri, E., de Caroli, M., Hansen, A. R., Willats, W. G. T., Piro, G., & Bellincampi, D. (2017). Three pectin methylesterase inhibitors protect cell wall integrity for arabidopsis immunity to Botrytis. *Plant Physiology*, *173*(3), 1844–1863. https://doi.org/10.1104/pp.16.01185

Liu, H., Ma, Y., Chen, N., Guo, S., Liu, H., Guo, X., Chong, K., & Xu, Y. (2014). Overexpression of stress-inducible OsBURP16, the β subunit of polygalacturonase 1, decreases pectin content and cell adhesion and increases abiotic stress sensitivity in rice. *Plant, Cell and Environment*, *37*(5), 1144–1158. https://doi.org/10.1111/pce.12223

Liu, N., Zhang, X., Sun, Y., Wang, P., Li, X., Pei, Y., Li, F., & Hou, Y. (2017). Molecular evidence for the involvement of a polygalacturonase-inhibiting protein, GhPGIP1, in enhanced resistance to Verticillium and Fusarium wilts in cotton. *Scientific Reports*, *7*. https://doi.org/10.1038/srep39840

Liu, X. L., Liu, L., Niu, Q. K., Xia, C., Yang, K. Z., Li, R., Chen, L. Q., Zhang, X. Q., Zhou, Y., & Ye, D. (2011). MALE GAMETOPHYTE DEFECTIVE 4 encodes a rhamnogalacturonan II xylosyltransferase and is important for growth of pollen tubes and roots in Arabidopsis. *Plant Journal*, *65*(4), 647–660. https://doi.org/10.1111/j.1365-313X.2010.04452.x

Liu, X., Wolfe, R., Welch, L. R., Domozych, D. S., Popper, Z. A., & Showalter, A. M. (2016). Bioinformatic identification and analysis of extensins in the plant kingdom. *PLoS ONE*, *11*(2). https://doi.org/10.1371/journal.pone.0150177

Lopez-Hernandez, F., Tryfona, T., Rizza, A., Yu, X. L., Harris, M. O. B., Webb, A. A. R., Kotake, T., & Dupree, P. (2020). Calcium binding by arabinogalactan polysaccharides is important for normal plant development. *Plant Cell*, *32*(10), 3346–3369. https://doi.org/10.1105/tpc.20.00027

Lorrai, R., Francocci, F., Gully, K., Martens, H. J., de Lorenzo, G., Nawrath, C., & Ferrari, S. (2021). Impaired Cuticle Functionality and Robust Resistance to Botrytis cinerea in Arabidopsis thaliana Plants With Altered Homogalacturonan Integrity Are Dependent on the Class III Peroxidase AtPRX71. *Frontiers in Plant Science*, *12*. https://doi.org/10.3389/fpls.2021.696955

Losner-Goshen, D., Portnoy, V. H., Mayer, A. M., & Joel, D. M. (1997). Pectolytic Activity by the Haustorium of the Parasitic Plant Orobanche L. (Orobanchaceae) in Host Roots. *Annals of Botany*, *81*, 319–326.

Louvet, R., Rayon, C., Domon, J. M., Rusterucci, C., Fournet, F., Leaustic, A., Crépeau, M. J., Ralet, M. C., Rihouey, C., Bardor, M., Lerouge, P., Gillet, F., & Pelloux, J. (2011). Major changes in the cell wall during silique development in Arabidopsis thaliana. *Phytochemistry*, *72*(1), 59–67. https://doi.org/10.1016/j.phytochem.2010.10.008

Madrid Liwanag, A. J., Ebert, B., Verhertbruggen, Y., Rennie, E. A., Rautengarten, C., Oikawa, A., Andersen, M. C. F., Clausen, M. H., & Scheller, H. V. (2013). Pectin biosynthesis: GALS1 in Arabidopsis thaliana Is a β-1,4-Galactan β-1,4-Galactosyltransferase. *Plant Cell*, *24*(12), 5024–5036. https://doi.org/10.1105/tpc.112.106625

Madson, M., Dunand, C., Li, X., Verma, R., Vanzin, G. F., Caplan, J., Shoue, D. A., Carpita, N. C., & Reiter, W. D. (2003). The MUR3 gene of Arabidopsis encodes a xyloglucan galactosyltransferase that is evolutionarily related to animal exostosins. *Plant Cell*, *15*(7), 1662–1670. https://doi.org/10.1105/tpc.009837

Makarova, E. N., & Shakhmatov, E. G. (2021). Characterization of pectin-xylan-glucan-arabinogalactan proteins complex from Siberian fir Abies sibirica Ledeb. *Carbohydrate Polymers*, *260*. https://doi.org/10.1016/j.carbpol.2021.117825

Maria J. Peña, Yingzhen Kong, William S. York, & Malcolm A. O'Neill. (2012). A Galacturonic Acid–Containing Xyloglucan Is Involved inArabidopsisRoot Hair Tip Growth. *The Plant Cell*, *24*, 4511–4524.

Matar, D., & Catesson, A. M. (1988). Cell Plate Development and Delayed Formation of the Pectic Middle Lamella in Root Meristems. In *Protoplasma* (Vol. 146).

Mellersh, D. G., Foulds, I. v, Higgins, V. J., & Heath, M. C. (2002). H 2 O 2 plays different roles in determining penetration failure in three diverse plant±fungal interactions. *The Plant Journal*, *29*(3), 257–268.

Miao, Y., Li, H. Y., Shen, J., Wang, J., & Jiang, L. (2011). QUASIMODO 3 (QUA3) is a putative homogalacturonan methyltransferase regulating cell wall biosynthesis in Arabidopsis suspension-cultured cells. *Journal of Experimental Botany*, *62*(14), 5063–5078. https://doi.org/10.1093/jxb/err211

Mishler-Elmore, J. W., Zhou, Y., Sukul, A., Oblak, M., Tan, L., Faik, A., & Held, M. A. (2021). Extensins: Self-Assembly, Crosslinking, and the Role of Peroxidases. In *Frontiers in Plant Science* (Vol. 12). Frontiers Media S.A. https://doi.org/10.3389/fpls.2021.664738

Mitsumasu, K., Seto, Y., & Yoshida, S. (2015). Apoplastic interactions between plants and plant root intruders. In *Frontiers in Plant Science* (Vol. 6, Issue AUG). Frontiers Media S.A. https://doi.org/10.3389/fpls.2015.00617

Mohnen, D. (2008). Pectin structure and biosynthesis. In *Current Opinion in Plant Biology* (Vol. 11, Issue 3, pp. 266–277). https://doi.org/10.1016/j.pbi.2008.03.006

Moore, P. J., Darvill, A. G., Albersheim, P., & Staehelin, L. A. (1986). Immunogold Localization of Xyloglucan and Rhamnogalacturonan I in the Cell Walls of Suspension-Cultured Sycamore Cells'. In *Plant Physiol*, *82*(3), 787-794

Moore, P. J., & Staehelin, L. A. (1988). Immunogold localization of the cell-wall-matrix polysaccharides rhamnogalacturonan I and xyloglucan during cell expansion and cytokinesis in Trifolium pratense L.; implication for secretory pathways. In *Planta* (Vol. 174).

Mouille, G., Ralet, M. C., Cavelier, C., Eland, C., Effroy, D., Hématy, K., McCartney, L., Truong, H. N., Gaudon, V., Thibault, J. F., Marchant, A., & Höfte, H. (2007). Homogalacturonan synthesis in Arabidopsis thaliana requires a Golgi-localized protein with a putative methyltransferase domain. *Plant Journal*, *50*(4), 605–614. https://doi.org/10.1111/j.1365-313X.2007.03086.x

Mukherjee, S., Kapp, E. A., Lothian, A., Roberts, A. M., Vasilev, Y., Boughton, B., Barnham, K. J., Kok, W. M., Hutton, C. A., Masters, C. L., Bush, A., Beckman, J. S., Dey, S. G., & Roberts, B. R. (2017). Characterization and identification of dityrosine cross-linked peptides using tandem mass spectrometry. *Analytical Chemistry*, 1–26. http://pubs.acs.org

Negi, J., Moriwaki, K., Konishi, M., Yokoyama, R., Nakano, T., Kusumi, K., Hashimoto-Sugimoto, M., Schroeder, J. I., Nishitani, K., Yanagisawa, S., & Iba, K. (2013). A dof transcription factor, SCAP1, is essential for the development of functional stomata in arabidopsis. *Current Biology*, *23*(6), 479–484. https://doi.org/10.1016/j.cub.2013.02.001

Neumetzler, L., Humphrey, T., Lumba, S., Snyder, S., Yeats, T. H., Usadel, B., Vasilevski, A., Patel, J., Rose, J. K. C., Persson, S., & Bonetta, D. (2012). The FRIABLE1 gene product affects cell adhesion in arabidopsis. *PLoS ONE*, *7*(8). https://doi.org/10.1371/journal.pone.0042914

Nunes, C., Silva, L., Fernandes, A. P., Guiné, R. P. F., Rosário, M., Domingues, M., & Coimbra, M. A. (2012). Occurrence of cellobiose residues directly linked to galacturonic acid in pectic polysaccharides. *Carbohydrate Polymers*, *87*(1), 620–626.

Nunez, A., Fishman, M. L., Fortis, L. L., Cooke, P. H., & Hotchkiss, A. T. (2009). Identification of extensin protein associated with sugar beet pectin. *Journal of Agricultural and Food Chemistry*, *57*(22), 10951–10958. https://doi.org/10.1021/jf902162t

Nuss, L., Mahé, A., Clark, A. J., Grisvard, J., Dron, M., Cervone, F., & de Lorenzo, G. (1996). Differential accumulation of PGIP (polygalacturonase-inhibiting protein) mRNA in two

near-isogenic lines of Phaseolus vulgaris L. upon infection with Colletotrichum lindemuthianum. In *Physiological and Molecular Plant Pathology 48*(2), 83-89.

Ogawa-Ohnishi, M., Matsushita, W., & Matsubayashi, Y. (2013). Identification of three hydroxyproline O-arabinosyltransferases in Arabidopsis thaliana. *Nature Chemical Biology*, *9*(11), 726–730. https://doi.org/10.1038/nchembio.1351

O'neill, M. A., Eberhard, S., Albersheim, P., & Darvill, A. G. (2001). Requirement of Borate Cross-Linking of Cell Wall Rhamnogalacturonan II for Arabidopsis Growth. *Sciences*, *294*, 846–849. www.sciencemag.org/cgi/content/full/294/

O'Neill, M. A., & York, W. S. (2018). The Composition and Structure of Plant Primary Cell Walls. In *Annual Plant Reviews online* (pp. 1–54). John Wiley & Sons, Ltd. https://doi.org/10.1002/9781119312994.apr0067

Ordaz-Ortiz, J. J., Marcus, S. E., & Paul Knox, J. (2009). Cell wall microstructure analysis implicates hemicellulose polysaccharides in cell adhesion in tomato fruit pericarp parenchyma. *Molecular Plant*, *2*(5), 910–921. https://doi.org/10.1093/mp/ssp049

Orfila, C., Degan, F. D., Jørgensen, B., Scheller, H. V., Ray, P. M., & Ulvskov, P. (2012). Expression of mung bean pectin acetyl esterase in potato tubers: Effect on acetylation of cell wall polymers and tuber mechanical properties. *Planta*, *236*(1), 185–196. https://doi.org/10.1007/s00425-012-1596-z

Pasternak, T., Groot, E. P., Kazantsev, F. v., Teale, W., Omelyanchuk, N., Kovrizhnykh, V., Palme, K., & Mironova, V. v. (2019). Salicylic acid affects root meristem patterning via auxin distribution in a concentration-dependent manner. *Plant Physiology*, *180*(3), 1725–1739. https://doi.org/10.1104/pp.19.00130

Pauly, M., Albersheim, P., Darvill, A., & York, W. S. (1999). Molecular domains of the cellulose/xyloglucan network in the cell walls of higher plants. *The Plant Journal*, *20*(6), 629–639.

Pauly, M., Gille, S., Liu, L., Mansoori, N., de Souza, A., Schultink, A., & Xiong, G. (2013). Hemicellulose biosynthesis. In *Planta* (Vol. 238, Issue 4, pp. 627–642). https://doi.org/10.1007/s00425-013-1921-1

Peaucelle, A., Louvet, R., Johansen, J. N., Höfte, H., Laufs, P., Pelloux, J., & Mouille, G. (2008). Arabidopsis Phyllotaxis Is Controlled by the Methyl-Esterification Status of Cell-Wall Pectins. *Current Biology*, *18*(24), 1943–1948. https://doi.org/10.1016/j.cub.2008.10.065

Peaucelle, A., Wightman, R., & Höfte, H. (2015). The Control of Growth Symmetry Breaking in the Arabidopsis Hypocotyl. *Current Biology*, *25*(13), 1746–1752. https://doi.org/10.1016/j.cub.2015.05.022

Peaucelle, A., Louvet, R., Johansen, J. N., Salsac, F., Morin, H., Fournet, F., ... & Pelloux, J. (2011). The transcription factor BELLRINGER modulates phyllotaxis by regulating the expression of a pectin methylesterase in Arabidopsis. *Development*, *138*(21), 4733-4741 https://doi.org/10.1242/dev.072496

Pelletier, S., van Orden, J., Wolf, S., Vissenberg, K., Delacourt, J., Ndong, Y. A., Pelloux, J., Bischoff, V., Urbain, A., Mouille, G., Lemonnier, G., Renou, J. P., & Höfte, H. (2010). A role for pectin de-methylesterification in a developmentally regulated growth acceleration in dark-grown Arabidopsis hypocotyls. *New Phytologist*, *188*(3), 726–739. https://doi.org/10.1111/j.1469-8137.2010.03409.x

Pelloux, J., Rustérucci, C., & Mellerowicz, E. J. (2007). New insights into pectin methylesterase structure and function. *Trends in Plant Science*, *12*(6), 267–277. https://doi.org/10.1016/j.tplants.2007.04.001

Philippe, F., Pelloux, J., & Rayon, C. (2017). Plant pectin acetylesterase structure and function: New insights from bioinformatic analysis. *BMC Genomics*, *18*(1). https://doi.org/10.1186/s12864-017-3833-0

Pietra, S., Gustavsson, A., Kiefer, C., Kalmbach, L., Hörstedt, P., Ikeda, Y., Stepanova, A. N., Alonso, J. M., & Grebe, M. (2013). ArabidopsisSABRE and CLASP interact to stabilize cell division plane orientation and planar polarity. *Nature Communications*, *4*. https://doi.org/10.1038/ncomms3779

Pluskal, T., Castillo, S., Villar-Briones, A., & Orešič, M. (2010). MZmine 2: Modular framework for processing, visualizing, and analyzing mass spectrometry-based molecular profile data. *BMC Bioinformatics*, *11*. https://doi.org/10.1186/1471-2105-11-395

Popper, Z. A., & Fry, S. C. (2005). Widespread occurrence of a covalent linkage between xyloglucan and acidic polysaccharides in suspension-cultured angiosperm cells. *Annals of Botany*, *96*(1), 91–99. https://doi.org/10.1093/aob/mci153

Qu, T., Liu, R., Wang, W., An, L., Chen, T., Liu, G., & Zhao, Z. (2011). Brassinosteroids regulate pectin methylesterase activity and AtPME41 expression in Arabidopsis under chilling stress. *Cryobiology*, *63*(2), 111–117. https://doi.org/10.1016/j.cryobiol.2011.07.003

Raggi, S., Ferrarini, A., Delledonne, M., Dunand, C., Ranocha, P., de Lorenzo, G., Cervone, F., & Ferrari, S. (2015). The arabidopsis class III peroxidase AtPRX71 negatively regulates growth under physiological conditions and in response to cell wall damage. *Plant Physiology*, *169*(4), 2513–2525. https://doi.org/10.1104/pp.15.01464

Ralet, M. C., Cabrera, J. C., Bonnin, E., Quéméner, B., Hellìn, P., & Thibault, J. F. (2005). Mapping sugar beet pectin acetylation pattern. *Phytochemistry*, *66*(15), 1832–1843. https://doi.org/10.1016/j.phytochem.2005.06.003

Ralet, M. C., Crépeau, M. J., Buchholt, H. C., & Thibault, J. F. (2003). Polyelectrolyte behaviour and calcium binding properties of sugar beet pectins differing in their degrees of methylation and acetylation. *Biochemical Engineering Journal*, *16*(2), 191–201. https://doi.org/10.1016/S1369-703X(03)00037-8

Ralet, M. C., Crépeau, M. J., Vigouroux, J., Tran, J., Berger, A., Sallé, C., Granier, F., Botran, L., & North, H. M. (2016). Xylans provide the structural driving force for mucilage adhesion to the Arabidopsis seed coat. *Plant Physiology*, *171*(1), 165–178. https://doi.org/10.1104/pp.16.00211

Reed, J. W., Wu, M. F., Reeves, P. H., Hodgens, C., Yadav, V., Hayes, S., & Pierik, R. (2018). Three auxin response factors promote hypocotyl elongation. *Plant physiology*, *178*(2), 864-875.

Rhee, S. Y., Osborne, E., Poindexter, P. D., & Somerville, C. R. (2003). Microspore Separation in the quartet 3 Mutants of Arabidopsis Is Impaired by a Defect in a Developmentally Regulated Polygalacturonase Required for Pollen Mother Cell Wall Degradation. *Plant Physiology*, *133*(3), 1170–1180. https://doi.org/10.1104/pp.103.028266

Rhee, S. Y., & Somerville, C. R. (1998). Tetrad pollen formation in quartet mutants of Arabidopsis thaliana is associated with persistence of pectic polysaccharides of the pollen mother cell wall. In *The Plant Journal* (Vol. 15, Issue 1) p.79-88

Ridley, B. L., O'neill, M. A., & Mohnen, D. (2001). Pectins: structure, biosynthesis, and oligogalacturonide-related signaling. *Phytochemistry* , *57*, 929–967. www.elsevier.com/locate/phytochem

Roberts, K., & Shirsat, A. H. (2006). Increased extensin levels in Arabidopsis affect inflorescence stem thickening and height. *Journal of Experimental Botany*, *57*(3), 537–545. https://doi.org/10.1093/jxb/erj036

Robyn M. Perrin, Zhonghua Jia, Tanya A. Wagner, Malcolm A. O'Neill, Rodrigo Sarria, William S. York, Natasha V. Raikhel, & and Kenneth Keegstra*. (2003). Analysis of Xyloglucan Fucosylation in Arabidopsis. *Plant Physiology*, *132*, 768–778.

Rui, Y., Xiao, C., Yi, H., Kandemir, B., Wang, J. Z., Puri, V. M., & Anderson, C. T. (2017). POLYGALACTURONASE INVOLVED IN EXPANSION3 functions in seedling development, rosette growth, and stomatal dynamics in Arabidopsis thaliana. *Plant Cell*, *29*(10), 2413–2432. https://doi.org/10.1105/tpc.17.00568

Saez-Aguayo, S., Ralet, M. C., Berger, A., Botran, L., Ropartz, D., Marion-Poll, A., & Northa, H. M. (2013). PECTIN METHYLESTERASE INHIBITOR6 promotes Arabidopsis mucilage release by limiting methylesterification of homogalacturonan in seed coat epidermal cells. *The Plant Cell*, *25*(1), 308–323. https://doi.org/10.1105/tpc.112.106575

Saffer, A. M. (2018). Expanding roles for pectins in plant development. In *Journal of Integrative Plant Biology* (Vol. 60, Issue 10, pp. 910–923). Blackwell Publishing Ltd. https://doi.org/10.1111/jipb.12662

Saito, F., Suyama, A., Oka, T., Yoko-O, T., Matsuoka, K., Jigami, Y., & Shimma, Y. I. (2014). Identification of novel peptidyl serine α-galactosyltransferase gene family in plants. *Journal of Biological Chemistry*, *289*(30), 20405–20420. https://doi.org/10.1074/jbc.M114.553933

Sala, K., Karcz, J., Rypień, A., & Kurczyńska, E. U. (2019). Unmethyl-esterified homogalacturonan and extensins seal Arabidopsis graft union. *BMC Plant Biology*, *19*(1). https://doi.org/10.1186/s12870-019-1748-4

Sander, L., Child, R., Ulvskov, P., Albrechtsen, M., & Borkhardt, B. (2001). Analysis of a dehiscence zone endo-polygalacturonase in oilseed rape (Brassica napus) and Arabidopsis thaliana: evidence for roles in cell separation in dehiscence and abscission zones, and in stylar tissues during pollen tube growth. In *Plant Molecular Biology* (Vol. 46). http://rsb.info.nih.gov/nih-image/

Sechet, J., Htwe, S., Urbanowicz, B., Agyeman, A., Feng, W., Ishikawa, T., Colomes, M., Kumar, K. S., Kawai-Yamada, M., Dinneny, J. R., O'Neill, M. A., & Mortimer, J. C. (2018). Suppression of Arabidopsis GGLT1 affects growth by reducing the L-galactose content and borate cross-linking of rhamnogalacturonan-II. *Plant Journal*, *96*(5), 1036–1050. https://doi.org/10.1111/tpj.14088

Segado, P., Domínguez, E., & Heredia, A. (2016). Ultrastructure of the epidermal cell wall and cuticle of tomato fruit (Solanum lycopersicum L.) during development. *Plant Physiology*, *170*(2), 935–946. https://doi.org/10.1104/pp.15.01725

Seifert, G. J. (2020). On the Potential Function of Type II Arabinogalactan O-Glycosylation in Regulating the Fate of Plant Secretory Proteins. In *Frontiers in Plant Science* (Vol. 11). Frontiers Media S.A. https://doi.org/10.3389/fpls.2020.563735

Sénéchal, F., Mareck, A., Marcelo, P., Lerouge, P., & Pelloux, J. (2015). Arabidopsis PME17 activity can be controlled by pectin methylesterase inhibitor4. *Plant Signaling and Behavior*, *10*(2). https://doi.org/10.4161/15592324.2014.983351

Sénéchal, F., Wattier, C., Rustérucci, C., & Pelloux, J. (2014). Homogalacturonan-modifying enzymes: Structure, expression, and roles in plants. *Journal of Experimental Botany*, *65*(18), 5125–5160. https://doi.org/10.1093/jxb/eru272

Shi, D., Ren, A., Tang, X., Qi, G., Xu, Z., Chai, G., Hu, R., Zhou, G., & Kong, Y. (2018). MYB52 negatively regulates pectin demethylesterification in seed coat mucilage. *Plant Physiology*, *176*(4), 2737–2749. https://doi.org/10.1104/pp.17.01771

Showalter, A. M., & Basu, D. (2016). Extensin and arabinogalactan-protein biosynthesis: Glycosyltransferases, research challenges, and biosensors. In *Frontiers in Plant Science* (Vol. 7, Issue JUNE2016). Frontiers Research Foundation. https://doi.org/10.3389/fpls.2016.00814

Showalter, A. M., Keppler, B., Lichtenberg, J., Gu, D., & Welch, L. R. (2010). A bioinformatics approach to the identification, classification, and analysis of hydroxyproline-rich glycoproteins. *Plant Physiology*, *153*(2), 485–513. https://doi.org/10.1104/pp.110.156554

Silva-Sanzana, C., Celiz-Balboa, J., Garzo, E., Marcus, S. E., Parra-Rojas, J. P., Rojas, B., Olmedo, P., Rubilar, M. A., Rios, I., Chorbadjian, R. A., Fereres, A., Knox, P., Saez-Aguayo, S., & Blanco-Herrera, F. (2019). Pectin methylesterases modulate plant homogalacturonan status in defenses against the aphid myzus persicae. *Plant Cell*, *31*(8), 1913–1929. https://doi.org/10.1105/tpc.19.00136

Simonini, S., Bencivenga, S., Trick, M., & Østergaard, L. (2017). Auxin-induced modulation of ETTIN activity orchestrates gene expression in arabidopsis. *Plant Cell*, *29*(8), 1864–1882. https://doi.org/10.1105/tpc.17.00389

Simpson, S. D., Ashford, D. A., Harvey, D. J., & Bowles, D. J. (1998). Short chain oligogalacturonides induce ethylene production and expression of the gene encoding aminocyclopropane 1-carboxylic acid oxidase in tomato plants. In *Glycobiology* (Vol. 8, Issue 6). https://academic.oup.com/glycob/article/8/6/579/666736

Sinclair, S. A., Gille, S., Pauly, M., & Krämer, U. (2020). Regulation of acetylation of plant cell wall components is complex and responds to external stimuli. *Plant Signaling & Behavior*, *15*(1), 1687185. https://doi.org/10.1080/15592324.2019.1687185

Sinclair, S. A., Larue, C., Bonk, L., Khan, A., Castillo-Michel, H., Stein, R. J., Grolimund, D., Begerow, D., Neumann, U., Haydon, M. J., & Krämer, U. (2017). Etiolated Seedling Development Requires Repression of Photomorphogenesis by a Small Cell-Wall-Derived Dark Signal. *Current Biology*, *27*(22), 3403-3418.e7. https://doi.org/10.1016/j.cub.2017.09.063

Singh, S. K., Eland, C., Harholt, J., Scheller, H. V., & Marchant, A. (2005). Cell adhesion in Arabidopsis thaliana is mediated by ECTOPICALLY PARTING CELLS 1 - A glycosyltransferase (GT64) related to the animal exostosins. *Plant Journal*, *43*(3), 384–397. https://doi.org/10.1111/j.1365-313X.2005.02455.x

Sinitsyna, O. A., Fedorova, E. A., Semenova, M. v., Gusakov, A. v., Sokolova, L. M., Bubnova, T. M., Okunev, O. N., Chulkin, A. M., Vavilova, E. A., Vinetsky, Y. P., & Sinitsyn, A. P. (2007). Isolation and characterization of extracellular pectin lyase from Penicillium canescens. *Biochemistry (Moscow)*, *72*(5), 565–571. https://doi.org/10.1134/S0006297907050148

Smith, D. K., Harper, J. F., & Wallace, I. S. (2018). A potential role for protein O-fucosylation during pollen-pistil interactions. *Plant Signaling & Behavior*, *13*(5), e1467687. https://doi.org/10.1080/15592324.2018.1467687

Šola, K., Gilchrist, E. J., Ropartz, D., Wang, L., Feussner, I., Mansfield, S. D., Ralet, M. C., & Haughn, G. W. (2019). RUBY, a putative galactose oxidase, influences pectin properties and promotes cell-to-cell adhesion in the seed coat epidermis of arabidopsis. *Plant Cell*, *31*(4), 809–831. https://doi.org/10.1105/tpc.18.00954

Somerville, C. (2006). Cellulose synthesis in higher plants. In *Annual Review of Cell and Developmental Biology* (Vol. 22, pp. 53–78). https://doi.org/10.1146/annurev.cellbio.22.022206.160206

Spadoni, S., Zabotina, O., di Matteo, A., Mikkelsen, J. D., Cervone, F., de Lorenzo, G., Mattei, B., & Bellincampi, D. (2006). Polygalacturonase-inhibiting protein interacts with pectin through a binding site formed by four clustered residues of arginine and lysine. *Plant Physiology*, *141*(2), 557–564. https://doi.org/10.1104/pp.106.076950

Sterling, J. D., Atmodjo, M. A., Inwood, S. E., Kumar Kolli, V. S., Quigley, H. F., Hahn, M. G., & Mohnen, D. (2006). Functional identification of an Arabidopsis pectin biosynthetic homogalacturonan galacturonosyltransferase. *PNAS*, *103*(13), 5236–5241. www.pnas.orgcgidoi10.1073pnas.0600120103

Stranne, M., Ren, Y., Fimognari, L., Birdseye, D., Yan, J., Bardor, M., Mollet, J. C., Komatsu, T., Kikuchi, J., Scheller, H. v., & Sakuragi, Y. (2018). TBL10 is required for O-acetylation of pectic rhamnogalacturonan-I in Arabidopsis thaliana. *Plant Journal*, *96*(4), 772–785. https://doi.org/10.1111/tpj.14067

Sun, Y., Fan, X. Y., Cao, D. M., Tang, W., He, K., Zhu, J. Y., He, J. X., Bai, M. Y., Zhu, S., Oh, E., Patil, S., Kim, T. W., Ji, H., Wong, W. H., Rhee, S. Y., & Wang, Z. Y. (2010). Integration of Brassinosteroid Signal Transduction with the Transcription Network for Plant Growth Regulation in Arabidopsis. *Developmental Cell*, *19*(5), 765–777. https://doi.org/10.1016/j.devcel.2010.10.010

Suzuki, T., Tomita-Yokotani, K., Yoshida, S., Takase, Y., Kusakabe, I., & Hasegawa, K. (2002). Preparation and isolation of oligogalacturonic acids and their biological effects in cockscomb (Celosia argentea L.) seedlings. *Journal of Plant Growth Regulation*, *21*(3), 209–215. https://doi.org/10.1007/s003440010060

Swain, J. E., & Smith, G. D. (2011). Advances in embryo culture platforms: Novel approaches to improve preimplantation embryo development through modifications of the microenvironment. *Human Reproduction Update*, *17*(4), 541–557. https://doi.org/10.1093/humupd/dmr006

Tabi, W, Exogenous application of plant Polygalacturonase PGLR reveals the cross-talk between cell signaling, cell wall chemistry, and cell-to-cell adhesion (INRAE, BioEcoAgro, Université de Picardie, France)

Tacken, E., Ireland, H., Gunaseelan, K., Karunairetnam, S., Wang, D., Schultz, K., Bowen, J., Atkinson, R. G., Johnston, J. W., Putterill, J., Hellens, R. P., & Schaffer, R. J. (2010). The role of ethylene and cold temperature in the regulation of the apple POLYGALACTURONASE1 gene and fruit softening. *Plant Physiology*, *153*(1), 294–305. https://doi.org/10.1104/pp.109.151092

Takenaka, Y., Kato, K., Ogawa-Ohnishi, M., Tsuruhama, K., Kajiura, H., Yagyu, K., Takeda, A., Takeda, Y., Kunieda, T., Hara-Nishimura, I., Kuroha, T., Nishitani, K., Matsubayashi, Y., & Ishimizu, T. (2018). Pectin RG-I rhamnosyltransferases represent a novel plant-specific glycosyltransferase family. In *Nature Plants* (Vol. 4, Issue 9, pp. 669–676). Palgrave Macmillan Ltd. https://doi.org/10.1038/s41477-018-0217-7

Takeuchi, S., & Yano, S. (2014). Clinical significance of epidermal growth factor receptor tyrosine kinase inhibitors: Sensitivity and resistance. In *Respiratory Investigation* (Vol. 52, Issue 6, pp. 348–356). Elsevier B.V. https://doi.org/10.1016/j.resinv.2014.10.002

Tan, L., Eberhard, S., Pattathil, S., Warder, C., Glushka, J., Yuan, C., Hao, Z., Zhu, X., Avci, U., Miller, J. S., Baldwin, D., Pham, C., Orlando, R., Darvill, A., Hahn, M. G., Kieliszewski, M. J., & Mohnena, D. (2013). An Arabidopsis cell wall proteoglycan consists of pectin and arabinoxylan covalently linked to an arabinogalactan protein. *Plant Cell*, *25*(1), 270–287. https://doi.org/10.1105/tpc.112.107334

Tavares, E. Q. P., de Souza, A. P., Romim, G. H., Grandis, A., Plasencia, A., Gaiarsa, J. W., Grima-Pettenati, J., de Setta, N., van Sluys, M. A., & Buckeridge, M. S. (2019). The control of endopolygalacturonase expression by the sugarcane RAV transcription factor during aerenchyma formation. *Journal of Experimental Botany*, *70*(2), 497–506. https://doi.org/10.1093/jxb/ery362

Taylor, S. C., Nadeau, K., Abbasi, M., Lachance, C., Nguyen, M., & Fenrich, J. (2019). The Ultimate qPCR Experiment: Producing Publication Quality, Reproducible Data the First Time. In *Trends in Biotechnology* (Vol. 37, Issue 7, pp. 761–774). Elsevier Ltd. https://doi.org/10.1016/j.tibtech.2018.12.002

Tiainen, P., Myllyharju, J., & Koivunen, P. (2005). Characterization of a second Arabidopsis thaliana prolyl 4-hydroxylase with distinct substrate specificity. *Journal of Biological Chemistry*, *280*(2), 1142–1148. https://doi.org/10.1074/jbc.M411109200

Toyooka, K., Goto, Y., Asatsuma, S., Koizumi, M., Mitsui, T., & Matsuoka, K. (2009). A mobile secretory vesicle cluster involved in mass transport from the golgi to the plant cell exterior. *Plant Cell*, *21*(4), 1212–1229. https://doi.org/10.1105/tpc.108.058933

Tryfona, T., Theys, T. E., Wagner, T., Stott, K., Keegstra, K., & Dupree, P. (2014). Characterisation of FUT4 and FUT6 α-(1→2)-fucosyltransferases reveals that absence of root arabinogalactan fucosylation increases arabidopsis root growth salt sensitivity. *PLoS ONE*, *9*(3). https://doi.org/10.1371/journal.pone.0093291

Turbant, A., Fournet, F., Lequart, M., Zabijak, L., Pageau, K., Bouton, S., & van Wuytswinkel, O. (2016). PME58 plays a role in pectin distribution during seed coat mucilage extrusion through homogalacturonan modification. *Journal of Experimental Botany*, *67*(8), 2177–2190. https://doi.org/10.1093/jxb/erw025

Valent, B. S., & Albersheim, P. (1974). The Structure of Plant Cell Walls V. ON THE BINDING OF XYLOGLUCAN TO CELLULOSE FIBERS'. In *Plant Physiol* (Vol. 54).

Velasquez, S. M., Ricardi, M. M., Dorosz, J. G., Fernandez, P. v., Nadra, A. D., Pol-Fachin, L., Egelund, J., Gille, S., Harholt, J., Ciancia, M., Verli, H., Pauly, M., Bacic, A., Olsen, C. E., Ulvskov, P., Petersen, B. L., Somerville, C., Iusem, N. D., & Estevez, J. M. (2011). O-glycosylated cell wall proteins are essential in root hair growth. *Science*, *332*(6036), 1401–1403. https://doi.org/10.1126/science.1206657

Verger, S.(2014) Genetic and chemical genomic dissection of cell adhesion mechanisms in plant. *Thesis*

Verger, S., Chabout, S., Gineau, E., & Mouille, G. (2016). Cell adhesion in plants is under the control of putative O-fucosyltransferases. *Development (Cambridge)*, *143*(14), 2536–2540. https://doi.org/10.1242/dev.132308

Verger, S., Long, Y., Boudaoud, A., & Hamant, O. (2018). A tension-adhesion feedback loop in plant epidermis. *ELife*, *7*. https://doi.org/10.7554/eLife.34460

Verica, J. A., & He, Z. H. (2002). The cell wall-associated kinase (WAK) and WAK-like kinase gene family. *Plant Physiology*, *129*(2), 455–459. https://doi.org/10.1104/pp.011028

Verlent, I., Smout, C., Duvetter, T., Hendrickx, M. E., & van Loey, A. (2005). Effect of temperature and pressure on the activity of purified tomato polygalacturonase in the presence of pectins with different patterns of methyl esterification. *Innovative Food Science and Emerging Technologies*, *6*(3), 293–303. https://doi.org/10.1016/j.ifset.2005.02.003

Vincken, J.-P., Schols, H. A., Oomen, R. J. F. J., Mccann, M. C., Ulvskov, P., Voragen, A. G. J., & Visser, R. G. F. (2003). If Homogalacturonan Were a Side Chain of Rhamnogalacturonan I. Implications for Cell Wall Architecture. *Physiology*, *132*(4), 1781–1789. https://doi.org/10.1104/nnso

Voragen, A. G. J., Coenen, G. J., Verhoef, R. P., & Schols, H. A. (2009). Pectin, a versatile polysaccharide present in plant cell walls. *Structural Chemistry*, *20*(2), 263–275. https://doi.org/10.1007/s11224-009-9442-z

Voxeur, A., Gilbert, L., Rihouey, C., Driouich, A., Rothan, C., Baldet, P., & Lerouge, P. (2011). Silencing of the GDP-D-mannose 3,5-epimerase affects the structure and cross-linking of the pectic polysaccharide rhamnogalacturonan II and plant growth in tomato. *Journal of Biological Chemistry*, *286*(10), 8014–8020. https://doi.org/10.1074/jbc.M110.198614

Voxeur, A., Habrylo, O., Guénin, S., Miart, F., Soulié, M.-C., Rihouey, C., Pau-Roblot, C., Domon, J.-M., Gutierrez, L., Pelloux, J., Mouille, G., Fagard, M., Höfte, H., & Vernhettes, S. (2019). Oligogalacturonide production upon Arabidopsis thaliana–Botrytis cinerea interaction Proceedings of the National Academy of Sciences, 116(39), 19743 LP – 19752. https://doi.org/10.1073/pnas.1900317116

Vriesmann, L. C., & Petkowicz, C. L. O. (2013). Highly acetylated pectin from cacao pod husks (Theobroma cacao L.) forms gel. *Food Hydrocolloids*, *33*(1), 58–65. https://doi.org/10.1016/j.foodhyd.2013.02.010

Wachananawat, B., Kuroha, T., Takenaka, Y., Kajiura, H., Naramoto, S., Yokoyama, R., Ishizaki, K., Nishitani, K., & Ishimizu, T. (2020). Diversity of Pectin Rhamnogalacturonan I Rhamnosyltransferases in Glycosyltransferase Family 106. *Frontiers in Plant Science*, *11*. https://doi.org/10.3389/fpls.2020.00997

Waldron, K. W., & Brett, C. T. (2007). The role of polymer cross-linking in intercellular adhesion. *Plant Cell Separation and Adhesion*, 183–200.

Wang, T., Park, Y. B., Cosgrove, D. J., & Hong, M. (2015). Cellulose-pectin spatial contacts are Inherent to never-dried Arabidopsis primary cell walls: Evidence from solid-state nuclear magnetic resonance. *Plant Physiology*, *168*(3), 871–884. https://doi.org/10.1104/pp.15.00665

Wang, T., Zabotina, O., & Hong, M. (2012). Pectin-cellulose interactions in the arabidopsis primary cell wall from two-dimensional magic-angle-spinning solid-state nuclear magnetic resonance. *Biochemistry*, *51*(49), 9846–9856. https://doi.org/10.1021/bi3015532

Willats, W. G. T., Mccartney, L., Mackie, W., & Knox, J. P. (2001). Pectin: cell biology and prospects for functional analysis. In *Plant Molecular Biology* (Vol. 47).p 9-27

Willats, W. G. T., McCartney, L., Steele-King, C. G., Marcus, S. E., Mort, A., Huisman, M., van Alebeek, G. J., Schols, H. A., Voragen, A. G. J., le Goff, A., Bonnin, E., Thibault, J. F., & Knox, J. P. (2004). A xylogalacturonan epitope is specifically associated with plant cell detachment. *Planta*, *218*(4), 673–681. https://doi.org/10.1007/s00425-003-1147-8

Wolf, S., & Höfte, H. (2014). Growth control: A saga of cell walls, ROS, and peptide receptors. *Plant Cell*, *26*(5), 1848–1856. https://doi.org/10.1105/tpc.114.125518

Wolf, S., Mravec, J., Greiner, S., Mouille, G., & Höfte, H. (2012). Plant cell wall homeostasis is mediated by brassinosteroid feedback signaling. *Current Biology*, *22*(18), 1732–1737. https://doi.org/10.1016/j.cub.2012.07.036

Xiao, C., Barnes, W. J., Zamil, M. S., Yi, H., Puri, V. M., & Anderson, C. T. (2017). Activation tagging of Arabidopsis POLYGALACTURONASE INVOLVED IN EXPANSION2 promotes hypocotyl elongation, leaf expansion, stem lignification, mechanical stiffening, and lodging. *Plant Journal*, *89*(6), 1159–1173. https://doi.org/10.1111/tpj.13453

Xiao, C., Somerville, C., & Anderson, C. T. (2014). POLYGALACTURONASE INVOLVED IN EXPANSION1 functions in cell elongation and flower development in Arabidopsis. *Plant Cell*, *26*(3), 1018–1035. https://doi.org/10.1105/tpc.114.123968

Xiao, C., Zhang, T., Zheng, Y., Cosgrove, D. J., & Anderson, C. T. (2016). Xyloglucan deficiency disrupts microtubule stability and cellulose biosynthesis in arabidopsis, altering cell growth and morphogenesis1[OPEN]. *Plant Physiology*, *170*(1), 234–249. https://doi.org/10.1104/pp.15.01395

Xiong, J., Yang, Y., Fu, G., & Tao, L. (2015). Novel roles of hydrogen peroxide (H2O2) in regulating pectin synthesis and demethylesterification in the cell wall of rice (Oryza sativa) root tips. *New Phytologist*, *206*(1), 118–126. https://doi.org/10.1111/nph.13285

Xu, Y., Sechet, J., Wu, Y., Fu, Y., Zhu, L., Li, J., Zhang, Y., Gineau, E., Gaertner, C., Zhou, J., Fan, X., Liu, Y., Zhou, L., Mouille, G., & Lin, X. (2017). Rice sucrose partitioning mediated by a putative pectin methyltransferase and homogalacturonan methylesterification. *Plant Physiology*, *174*(3), 1595–1608. https://doi.org/10.1104/pp.16.01555

Yan, J., He, H., Fang, L., & Zhang, A. (2018). Pectin methylesterase31 positively regulates salt stress tolerance in Arabidopsis. *Biochemical and Biophysical Research Communications*, *496*(2), 497–501. https://doi.org/10.1016/j.bbrc.2018.01.025

Yang, S., Johnston, N., Talideh, E., Mitchell, S., Jeffree, C., Goodrich, J., & Ingram, G. (2008). The endosperm-specific ZHOUPI gene of Arabidopsis thaliana regulates endosperm breakdown and embryonicepidermal development. *Development*, *135*(21), 3501–3509. https://doi.org/10.1242/dev.026708

Yeats, T. H., & Rose, J. K. C. (2013). The formation and function of plant cuticles. In *Plant Physiology* (Vol. 163, Issue 1, pp. 5–20). American Society of Plant Biologists. https://doi.org/10.1104/pp.113.222737

Zeisler-Diehl, V., Müller, Y., & Schreiber, L. (2018). Epicuticular wax on leaf cuticles does not establish the transpiration barrier, which is essentially formed by intracuticular wax. *Journal of Plant Physiology*, *227*, 66–74. https://doi.org/10.1016/j.jplph.2018.03.018

Zhang, Y., Held, M. A., & Showalter, A. M. (2020). Elucidating the roles of three β-glucuronosyltransferases (GLCATs) acting on arabinogalactan-proteins using a CRISPR-Cas9 multiplexing approach in Arabidopsis. *BMC Plant Biology*, *20*(1). https://doi.org/10.1186/s12870-020-02420-5

Zhong, R., Cui, D., & Ye, Z. H. (2018). Members of the DUF231 Family are O-Acetyltransferases Catalyzing 2-O- and 3-O-Acetylation of Mannan. *Plant & Cell Physiology*, *59*(11), 2339–2349. https://doi.org/10.1093/pcp/pcy159

Zipfel, C., Robatzek, S., Navarro, L., Oakeley, E. J., Jones, J. D. G., Felix, G., & Boller, T. (2004). Bacterial disease resistance in Arabidopsis through flagellin perception. *Nature*, *428*, 764–767. http://mips.gsf.de/prog/thal/

Zykwinska, A., Thibault, J. F., & Ralet, M. C. (2007). Organization of pectic arabinan and galactan side chains in association with cellulose microfibrils in primary cell walls and related models envisaged. *Journal of Experimental Botany*, *58*(7), 1795–1802. https://doi.org/10.1093/jxb/erm037

Zykwinska, A., Thibault, J. F., & Ralet, M. C. (2008). Modelling of xyloglucan, pectins and pectic side chains binding onto cellulose microfibrils. *Carbohydrate Polymers*, *74*(1), 23–30. https://doi.org/10.1016/j.carbpol.2008.01.011

Zykwinska, A. W., Ralet, M. C. J., Garnier, C. D., & Thibault, J. F. J. (2005). Evidence for in vitro binding of pectin side chains to cellulose. In *Plant Physiology* (Vol. 139, Issue 1, pp. 397–407). American Society of Plant Biologists. https://doi.org/10.1104/pp.105.065912